Characterising the mechanisms through which the microbiota influences immune responses to vaccination in early life

Saoirse Clare Benson

The South Australian Health and Medical Research Institute

&

College of Medicine and Public Health, Flinders University

A thesis submitted to Flinders University for the degree of

Doctor of Philosophy

23rd August 2023

"Inspiration unlocks the future."

– The Wind Rises (2013)

"The earth is not dying. It is being killed, and the people killing it have names and addresses."

– Bruce Duncan Phillips

Abstract

Antibody-mediated responses play a critical role in vaccine-mediated immunity, however, for reasons that are poorly understood, responses are highly variable between individuals and different populations. In mice, antibiotic-driven dysbiosis in early-life leads to significantly dysregulated B and T cell responses to vaccines that are routinely administered to infants worldwide. To investigate whether this is also the case in infants we established the Antibiotics and Immune Responses (AIR) study, a clinical systems immunology study that assessed the effects of neonatal or intrapartum antibiotic exposure on the infant gut microbiota; blood gene expression; circulating immune cell populations; and antibody responses to multiple different infant vaccines in a cohort of 226 vaginally-born, healthy, term infants. Infants exposed to neonatal antibiotics had significantly lower antibody titres against multiple different vaccine antigens, most notably to polysaccharides in the 13-valent pneumococcal conjugate vaccine (PCV13) and altered transcriptional profiles pre- and post-vaccination. Multi-parameter immune profiling revealed that these transcriptional differences were not explained by differences in the frequency of major immune cell populations, though infants exposed to intrapartum antibiotics had a modest reduction in circulating CD45RA$^-$ iTregs compared to unexposed infants.

The mechanisms by which the gut microbiota influence vaccine responses remain poorly understood. I compared antibody responses to PCV13 in germ-free (GF) mice, in GF mice that were colonised at day 21 of life via fecal microbiota transplant (FMT), in mice that were born to GF dams that were recolonised prior to pregnancy (exGF) and in

conventionally colonised SPF mice. GF mice immunized at 3-4 weeks of age had impaired polysaccharide-specific and conjugate protein-specific antibody responses to the PCV13 vaccine compared to normally colonised SPF mice. Responses were restored to levels comparable to SPF mice in exGF but not in GF mice recolonised by FMT at day 21 of life. Comprehensive multi-parameter flow cytometry analysis of the spleen and draining lymph nodes revealed that GF mice had significantly impaired germinal centre B cells and Tfh cells after the second dose of PCV13. In addition, GF mice had significantly fewer innate-like B-1a and B-1b cells in the peritoneum following primary immunisation with PCV13. My findings indicate that both T-dependent and T-independent humoral responses to the PCV13 vaccine are dependent on signals from the gut microbiota and that there is a critical window of opportunity for those signals to be received.

I hypothesised that products from the microbiota could act as natural adjuvant and prime innate responses to vaccination via Toll-like receptor (TLRs) signalling. To investigate this, I assessed responses to PCV13 in *Myd88*$^{-/-}$ mice, a key adapter protein downstream of most TLRs, and found that *Myd88*$^{-/-}$ mice had significantly impaired humoral and germinal centre responses to the PCV13 vaccine. Further experiments in *Tlr2*$^{-/-}$ and *Tlr4*$^{-/-}$ mice revealed that TLR2 but not TLR4 signalling was necessary for primary antibody responses to PCV13. Surprisingly, antibiotic treatment in early life resulted in an apparent 'recovery' of the impaired humoral responses observed in *Myd88*$^{-/-}$ mice. My data suggest that microbiota-targeted inventions may be beneficial to support optimal responses to vaccination.

Table of Contents

List of Tables

List of Figures

Abbreviations

ABX – antibiotics/antibiotics treated

ADCC - antibody-dependent cellular cytotoxicity

AIR - Antibiotics and Immune Response Study

Alum – aluminium salt

APCs – antigen presenting cells

B. breve – Bifidobacterium breve

B. longum - Bifidobacterium longum

B. longum subspecies infantis – Bifidobacterium longum subspecies infantis

BCG – *Mycobacterium bovis* bacillus Calmette-Guérin

BCR – B cell receptor

cDCs - conventional DCs

CM – central memory

CoP – correlate of protection

CRM_{197} - cross reacting material

CTB - cholera toxin B subunit

D21 – day 21

D28 – day 28

D7 – day 7

DAMPs – damage-associated molecular patterns

DC – dendritic cell

dLN – draining lymph node

DTaP - diphtheria, tetanus, and acellular pertussis

DTP - Diphtheria Tetanus Pertussis

DTP-HepB-Hib – Diphtheria, tetanus, pertussis–hepatitis B virus–Haemophilus influenzae type B

DTwP - diphtheria, tetanus, whole cell pertussis

E14 – embryonic day 14

EBV - Epstein-Barr virus

EED – environmental enteric dysfunction

EM – effector memory

ExGF – ex-germ free

FcγR - Fcγ receptor

FHA - Filamentous haemagglutinin adhesion

FMT – faecal microbiome transplant

GAS - Group A *Streptococcus*

GC – germinal centre

GF – germ free

GPI - glycophosphatidyl inositol

HepB – hepatitis B

Hib - *Haemophilus influenzae* type B

HICs – High-income countries

HIV - human immunodeficiency virus

HMO – human milk oligosaccharide

HPV – human papillomavirus

HSA - human serum albumin

IFN – interferon

IFNγ – Interferon-γ

IgG – immunoglobulin G

IL-1, 4, 6, 8 or 10 – Interleukin - 1, 4, 6, 8 or 10

ILA - Indole-3-lactic acid

IPV - inactivated polio vaccine

iTreg – inducible T regularly cells

KO – knockout

LLPCs – long-lived plasma cells

LMICs – low middle income countries

LPG - *Lactobacillus plantarum*

LPS – lipopolysaccharide

MAMPs - microbial-associated molecular patterns

MAIT cells - mucosal associated invariant T cells

MDP - muramyl dipeptide

MenACWY - meningococcal vaccine

Men B – Meningococcal B

Men C - Meningococcal C

MHC - major histocompatibility complex

MMR - measles, mumps and rubella

MZ– marginal zone

Neo ABX - neonatally exposed to antibiotics

NK – natural killer

NLRs – NOD-like receptors

OCV - oral cholera vaccine

O.D. – optical density

OPV – Oral poliovirus vaccine

ORV - Oral Rotavirus vaccine

OSV – Oral shigella vaccine (candidate)

PAMPS – pathogen-associated molecular patterns

PBMC - Peripheral blood mononuclear cells

pDCs – plasmacytoid DCs

PCV7 - 7-valent pneumococcal polysaccharide vaccine

PCV13 - 13-valent pneumococcal polysaccharide vaccine

PPV23 - 23-valent pneumococcal polysaccharide vaccine

PPD – *Mycobacterium tuberculosis* purified protein derivative

PPS1 - polysaccharide antigens from serotype 1

PPS3 - polysaccharide antigens from serotype 3

PRN – Pertussis antigen pertactin

PRR – pattern recognition receptor

PSA - polysaccharide A

PT – Pertussis

QIV – Quadrivalent influenza vaccine

RCT – randomised control trial

RLRs – RIG-like receptors

RSV - respiratory syncytial virus

RV – Rotavirus

Sca-1 – Stem cell antigen-1

SCFAs – short chain fatty acids

SEM – standard error of mean

SPF – specific pathogen free

S. pneumoniae – Streptococcus pneumoniae

TCR – T cell receptor

Tfh cells - T follicular helper cells

Th1, Th2, Th17 - T helper cells

TIV - trivalent inactivated vaccine

TLRs – Toll-like receptors

Tregs - T regulatory cells

TT – Tetanus Toxoid

No ABX - Unexposed to antibiotics

V – time of vaccination

V+1, 2, 4, 6, 8 – time since vaccination in weeks

Wt – wild-type

YF-17D – Yellow fever 17D

Publications During Candidature

David J. Lynn, **Saoirse C. Benson**, Miriam A. Lynn, Bali Pulendran. **Modulation of immune responses to vaccination by the microbiota: implications and potential mechanisms.** *Nat Rev Immunol* (2021). https://doi.org/10.1038/s41577-021-00554-7

Ryan FJ, Norton TS, McCafferty C, Blake SJ, Stevens NE, James J, Eden GL, Tee YC, **Benson SC**, Masavuli MG, Yeow AEL, Abayasingam A, Agapiou D, Stevens H, Zecha J, Messina NL, Curtis N, Ignjatovic V, Monagle P, Tran H, McFadyen JD, Bull RA, Grubor-Bauk B, Lynn MA, Botten R, Barry SE, Lynn DJ. **A systems immunology study comparing innate and adaptive immune responses in adults to COVID-19 mRNA and adenovirus vectored vaccines.** Cell Rep Med. 2023 Mar 21;4(3):100971. doi: 10.1016/j.xcrm.2023.100971. Epub 2023 Feb 17. PMID: 36871558; PMCID: PMC9935276.

Miriam A. Lynn, Georgina Eden, Feargal J. Ryan, Julien Bensalem, Xuemin Wang, Stephen J. Blake, Jocelyn M. Choo, Yee Tee Chern, Anastasia Sribnaia, Jane James, **Saoirse C. Benson**, Lauren Sandeman, Jianling Xie, Sofia Hassiotis, Emily W. Sun, Alyce M. Martin, Marianne D. Keller, Damien J. Keating, Timothy J. Sargeant, Christopher G. Proud, Steve L. Wesselingh, Geraint B. Rogers, David J. Lynn. **The composition of the gut microbiota following early-life antibiotic exposure affects host health and longevity in later life**, *Cell Reports* (2021). 36(8); 109564. https://doi.org/10.1016/j.celrep.2021.109564.

Laure F. Pittet, Nicole L. Messina, Kaya Gardiner, Francesca Orsini, Veronica Abruzzo, Samantha Bannister, Marc Bonten, John Campbell, Julio Croda, Margareth Dalcolmo, Sonja Elia, Susie Germano, Casey Goodall, Amanda Gwee, Tenaya Jamieson, Bruno Jardim, Tobias R Kollman, Marcus VG Lacerda, Katherine J. Lee, Donna Legge, Michaela Lucas, David J. Lynn, Ellie McDonald, Laurens Manning, Craig F. Munns, Kirsten P. Perrett, Cristina Prat Aymerich, Peter Richmond, Frank Shann, Eva Sudbury, Paola Villanueva, Nicholas J. Wood, Katherine Lieschke, Kanta Subbarao, Andrew Davidson, Nigel Curtis & the **BRACE trial Consortium Group*** (2021). **BCG vaccination to reduce the impact of COVID-19 in healthcare workers: protocol for a randomised controlled trial (BRACE trial).** *BMJ Open* (In Press). * one of the authors listed as part of the BRACE Trial Consortium Group.

Stephen J. Blake, Jane James, Feargal J. Ryan, Jose Caparros-Martin, Georgina L. Eden, Yee C. Tee, John R. Salamon, **Saoirse C. Benson**, Damon J. Tumes, Anastasia Sribnaia, Natalie E. Stevens, John W. Finnie, Hiroki Kobayashi, Deborah L. White, Steve L. Wesselingh, Fergal O'Gara, Miriam A. Lynn, David J. Lynn. **The gut microbiota mediates the hepatoxicity and cytokine release syndrome induced by immune agonist antibody cancer immunotherapies.** Cell Reports Medicine (2021) DOI: 10.1016/j.xcrm.2021.100464

Declaration

I certify that this thesis: does not incorporate without acknowledgment any material previously submitted for a degree or diploma in any university and the research within will not be submitted for any other future degree or diploma without the permission of Flinders University; and to the best of my knowledge and belief, does not contain any material previously published or written by another person except where due reference is made in the text.

Saoirse Benson

May 2023

Acknowledgements

I wish to extend my deepest gratitude and respect to those who have made this research possible. First and foremost, I express my heartfelt thanks to my PhD supervisors, David, and Miriam Lynn, for their unwavering support throughout this journey. I am grateful to David for giving me the opportunity to join his research group five years ago. His guidance, encouragement, and practical support from the moment I stepped in the door have been invaluable. David has gone above and beyond his role as my supervisor, encouraging my participation in courses, conferences, and clinical projects, providing authorship opportunities, and being readily available for research discussions. I consider myself fortunate to have received such well-rounded support, and I am deeply appreciative.

On the lab side, Miriam's support has been indispensable for my research project. She has provided me with training, set up mouse cohorts, helped carry out long cull days, and even brought me food for them. The entire lab has been a supportive and collaborative team, allowing me to extend my research beyond its initial scope and participate in diverse projects. I express my heartfelt gratitude to Feargal, Natalie, Todd, Stephen, Georgina, and Alice, who have all contributed to cull days and research discussions, and to Feargal for his support and encouragement of early career researchers. I am equally thankful to Tee, Joyce, and Charne for their invaluable assistance with this project and for making the lab a fun and welcoming environment. I am excited to see what they all achieve in the future. I also recognize the contributions of past lab members who deserve special mention, including Damon and Jane. Damon taught me how to process samples for the AIR Study, helped me with initial data analysis stages and other aspects of data

handling. Jane became my best friend, providing me with a home when I needed one, and has always been there for me.

I extend my sincere appreciation to the South Australian Health and Medical Research Institute (SAHMRI) for providing me with a friendly and collaborative research space, and to the SAHMRI Student Association for organizing events and running the SAHMRI Ball. I am also grateful to Flinders University for supporting me, including their sponsorship of my international student fees. I express my gratitude to Jill Carr, my external reviewer, for her feedback throughout my candidature milestones. I appreciate the support of EMBL Australia during my thesis, including opportunities such as the EMBL PhD program in Tasmania, the EMBL Australia postgraduate symposium, and the EMBL PLN Student group. I acknowledge with gratitude the Women and Children's Hospital for their collaboration on the AIR study, the other authors, and the enrolled infants and their parents. I also thank Hey Bianca for providing over 50 pizzas during my candidature.

I wish to acknowledge my SAHMRI Student peers, particularly Natalya, Caleb, Emma, Laura, Maya, Alanah, Georgette, Justine, Jacqui, Jvaughan, Nick, Connor, Hayley, Julia, Clara, Najma, and Tim, for their moral support during the past few years. They have been a source of emotional support, advice, and companionship, helping me through the lonely and isolating aspects of candidature. I will miss them when I leave SAHMRI, and I hope that our friendship will continue wherever we end up. I especially thank Natalya for being a listening ear during tough times, supporting me through two breakups and other life challenges.

I would like to express my heartfelt gratitude to my housemates, Lydia and Elaine. Lydia, your kindness and support have been invaluable throughout my journey, and I am grateful for the many wonderful films and artists you have introduced me to. Elaine, thank you for being a reliable friend who has always been there for me, through both the ups and downs. I would also like to acknowledge the contributions of other dear friends, including Cian, whose friendship has been a source of inspiration and joy. Hetti, your camaraderie and PhD chats have been a wonderful reminder that I am not alone in this journey. Elliott, I am so grateful for your friendship, the wine celebrations after published papers, the walks in the botanic gardens, and your unwavering support, which has helped me stay grounded and focused. I would also like to extend my heartfelt appreciation to Chelsea and Macey, whose friendship has enriched my life with their creativity, Ancient World nights, and meaningful conversations.

Finally, I am deeply indebted to my family. Your love and support have been my greatest source of strength and motivation. It has not been easy for any of us to be separated over the course of the last few years, especially during the pandemic. Dad, thank you for always being there to chat, give advice, and book flights for me to come home to Dublin and spend Christmas with you all. Mum, your recipes, chats and books have been a constant source of comfort and inspiration. Oisin and Joe, your unwavering support and encouragement have been truly invaluable.

Finally, I would like to express my gratitude to my Grannies, Marilyn and Eileen, whose love and support have been a constant source of joy and inspiration. I would also like to remember my late grandfathers, Grandpa Bill and Des, who are dearly missed.

1 Introduction

Sections of this chapter are excerpts from:

Lynn, D.J., **Benson, S.C.**, Lynn, M.A. *et al.* Modulation of immune responses to vaccination by the microbiota: implications and potential mechanisms. *Nat Rev Immunol* (2021).

1.1 Vaccines

The need for highly effective vaccines that induce robust and long-lasting immunity has never been more apparent. The COVID-19 vaccination program alone is responsible for preventing more than 20 million deaths so far (Watson et al., 2022). Vaccines protect individuals from infectious diseases by eliciting a systemic immune response involving humoral, innate, and cell-mediated immunity (Mohr & Siegrist, 2016). As well as protecting individuals, vaccines can also protect populations by reducing transmission and limiting exposure risks (Turnbaugh et al., 2007). The estimated number of vaccinated individuals required to stop the spread of disease, a concept called herd immunity, is 90%-96%. However, this varies from disease to disease depending on its transmissibility (R. M. Anderson & May, 1985). In addition, variation in vaccine immune responses between individuals means that achieving herd immunity is not always possible. Therefore strategies that improve the effectiveness of existing vaccines are essential for improved population health globally (Grassly, Kang, & Kampmann, 2015).

Table 1.1 Immunogenicity of oral and parenteral vaccines in high-income countries compared with low- and middle-income countries

Vaccine	Populations compared	Differences observed in vaccine immunogenicity	Vaccine immunogenicity (HICs versus LMICs)	Head to head comparison?	Same vaccine schedule	Reference
ORV	HICs versus LMICs	IgA titres to ORV four-fold lower in infants from LMICs	+	No; review of multiple different studies.	Yes	(Patel et al., 2013)
ORV	HICs versus LMICs	Meta-analysis of RCTs of ORV: vaccine efficacy in HICs 94% (after 12 months) compared with 44% in LMICs	+	No; meta-analysis	Yes	(Clark et al., 2019)
OCV	Sweden versus Nicaragua	Mean IgA titres to CTB 1.6–1.9-fold lower in children from Nicaragua compared with children from Sweden; vibriocidal antibody concentrations also much higher in Swedish children	+	Yes	Yes	(Hallander et al., 2002)
OPV	HICs versus LMICs	~100% of individuals in HICs seroconvert following OPV compared with ~70% in LMICs	+	No; review of multiple different studies	No	(Patriarca, Wright, & John, 1991)
OSV	United States versus Bangladesh	High levels of immunogenicity in adults in US but little or no immunogenicity in Bangladeshi infants	+	No	No	(Levine, Kotloff, Barry, Pasetti, & Sztein, 2007)
DTP–HepB–Hib	HICs versus Indonesia	Similar levels of immunogenicity for infants in HICs and in Indonesia	=	No	Yes	(Rusmil et al., 2015)
QIV	Europe/Mediterranean, Asia-Pacific and Central America	Higher efficacy in children from HICs (73.4%) with lowest efficacy in LMICs (30.3%)	+	Yes	Yes, but some vaccine strain differences in different regions.	(Dbaibo et al., 2020)
RTS,S (malaria)	Burkina Faso, Ghana, Gabon, Kenya, Tanzania, Malawi and Mozambique	Efficacy after 3 doses from 40% to 77% at 11 different trial sites across 7 African countries	n/a	Yes	Yes	(Agnandji et al., 2014)

YF-17D	Switzerland versus Uganda	Antigen-specific T cell and neutralising antibody responses 3-fold and 2-fold lower, respectively, in vaccine recipients from Uganda compared with Switzerland	+	Yes	Yes	(Muyanja et al., 2014)
Ebola	UK versus Tanzania, Kenya and Uganda	23% higher antibody titres in vaccine recipients in UK compared with 3 East African countries	+	No; post-hoc analysis of data from three EBOVAC1 consortium phase 1 trials	Yes	(Pasin et al., 2019)
PCV7, PCV10 and PCV13	HICs and LMICs	Meta-analysis: higher mean antibody titres in Africa, South East Asia and the Western Pacific compared with Europe and the Americas	-	No; meta-analysis	Yes	(Choe, Blatt, Lee, & Choi, 2020)
BCG	UK versus Malawi	3 months after BCG vaccination: 100% of infants in UK had IFNγ response to PPD compared with 53% of infants in Malawi	+	Yes	Yes	(Lalor et al., 2009)
HIV	United States versus Kenya, Rwanda and South Africa	Significantly lower T cell responses in vaccine recipients in East Africa compared with South Africa or the United states	+	Yes	Yes	(Baden et al., 2016)

BCG, *Mycobacterium bovis* bacillus Calmette-Guérin; CTB, cholera toxin B subunit; DTP–HepB–Hib, diphtheria tetanus pertussis–hepatitis B–*Haemophilus influenzae* type B; HIC, high-income country; IFNγ, interferon-γ; LMIC, low- and middle-income country; OCV, oral cholera vaccine; OPV, oral poliovirus vaccine; ORV, oral rotavirus vaccine; OSV, oral shigella vaccine (candidate); PCV, pneumococcal conjugate vaccine; PPD, *Mycobacterium tuberculosis* purified protein derivative; QIV, quadrivalent influenza vaccine; RCT, randomised control trial; YF-17D, yellow fever 17D.

1.1.1 Vaccine types

Vaccines have had an unprecedented impact on human health. Vaccine programs have led to the eradication or near eradication of diseases such as smallpox and polio, reduce the need for antibiotics by preventing infections, reduce disease severity when an infection does occur, and can prevent the development of certain cancers, such as cervical

cancer, by targeting the causative infectious agent (e.g. human papilloma virus) (Mendonça, Lorincz, Boucher, & Curiel, 2021; The Lancet, 2022; Yousefi et al., 2022). There are several types of vaccines in use today. These include live attenuated, inactivated, subunit, mRNA and adenoviral-vectored vaccines, which vary in the level of immunogenicity and the type of immune response induced. Live-attenuated vaccines use a weakened form of the pathogenic virus or bacteria and promote a robust, long-lasting response. Vaccines of this nature include the combined measles, mumps and rubella (MMR) vaccine, the *Bacillus Calmette-Guérin* (BCG) vaccine, the oral rotavirus vaccine (ORV), the oral polio vaccine (OPV) and the yellow fever vaccine (Hajj Hussein et al., 2015). Despite their effectiveness, live vaccines have been associated with a higher frequency of adverse events and live attenuated vaccines are not recommended for use in immunocompromised individuals (Levitz & Golenbock, 2012). Consequently, most current vaccines are non-live, comprised of antigenic polysaccharides, proteins, glycoconjugates, or inactivated microorganisms (Van Duin, Medzhitov, & Shaw, 2006). Non-live vaccines that contain killed whole organisms or purified antigens are intrinsically safer but less immunogenic than live vaccines, meaning booster shots are required to boost responses to protective levels (Strugnell, Zepp, Cunningham, & Tantawichien, 2011). Inactivated vaccines include those for hepatitis A, influenza and the inactivated polio vaccine (IPV). Subunit, recombinant, polysaccharide and conjugate vaccines include vaccines against *Haemophilus influenzae* type b (Hib), hepatitis B, pertussis (DTaP combined vaccine), pneumococcal disease (PCV7, PCV13 and PPV23 vaccines) and meningococcal disease (MenACWY, Hib/MenC) (Assaf-Casals & Dbaibo, 2016, C. A. Siegrist, 2008). mRNA vaccines are a novel vaccine type composed of RNA packaged in a vector such as lipid nanoparticles. These vaccines received rapid approval to combat the COVID-19 pandemic and have demonstrated high efficacy (Polack et al.,

2020). Furthermore, additional mRNA vaccines are in the development pipeline for other viral diseases such as Epstein-Barr virus (EBV), respiratory syncytial virus (RSV), influenza, human immunodeficiency virus (HIV), and even to treat cancers such as melanoma (Barbier, Jiang, Zhang, Wooster, & Anderson, 2022; Graham, 2023). Adenovirus-vectored vaccines, such as the AstraZeneca ChadOx-1 vaccine, have also successfully been employed to tackle the COVID-19 pandemic (Ryan et al., 2023). Adenovirus-vectored vaccines are non-enveloped double-stranded DNA viruses that have the viral genes enabling replication deleted and replaced with transgenes that evade the antigen of interest e.g. spike protein (Mendonça et al., 2021).

1.1.2 The immune response to vaccination

Vaccine-mediated protection against the targeted infectious diseases is primarily mediated by antibodies (Siegrist, 2008). Antibodies have three main functions: neutralising pathogens, opsonising cells for phagocytosis and activating the complement system (Subramanian et al., 2014). Antibody-secreting cells (ASCs) are primarily formed in specialised microstructures called germinal centres (GCs) in secondary lymphoid organs. These GCs play a crucial role in vaccine-induced immunity by supporting the production of short-lived plasma cells and memory B cells (**Fig. 1.1**) (Stebegg et al., 2018). The initial response to vaccination begins at the injection site, where immature dendritic cells (DCs) mature and become activated (Palucka, Banchereau, & Mellman, 2010). For most vaccines, intramuscular injections are the preferred route of administration due to the extensive vascular network containing a high number of patrolling DCs (Guilliams Hervé Luche et al., 2012). Exceptions to this include the BCG vaccine, which is given intradermally. Activated DCs then migrate to draining lymph nodes (dLNs), where they present the antigen via their MHC class II molecules to engage

naïve $CD4^+$ T cells. This triggers the proliferation and differentiation of $CD4^+$ T cells into various effector T-helper cells, including T helper 1 (Th1), T helper 2 (Th2), T helper 17 (Th17) and T regulatory cells (Tregs). Some of these primed $CD4^+$ T cells differentiate into T follicular helper (Tfh) cells, which relocate to the B-T cell border within the GC. Tfh cells provide survival and co-stimulatory signals, leading to the differentiation of B cells into GC B cells, short-lived plasma cells, and memory B cells and initiate the GC response (N. S. De Silva & Klein, 2015; Liu, Zhao, & Qi, 2022; Waide et al., 2020; X Zhang et al., 2001). The plasma cells that exit the lymphoid follicle provide the first wave in the antibody response after vaccination. B cells then undergo a process of affinity maturation, where they are selected based on the affinity of their B cell receptor (BCR) for the antigen (Mesin, Ersching, & Victora, 2016). In Goldilocks fashion, B cells with affinity that is too high or too low will undergo apoptosis. Selected B cells whose affinity is 'just right' differentiate into long-lived plasma cells, some of which accumulate steadily in the bone marrow niche (M. J. Robinson et al., 2022). Long-lived plasma cells (LLPCs) that reach these survival niches in the bone marrow can survive for decades and provide long-lasting humoral protection (Slifka, Antia, Whitmire, & Ahmed, 1998; Zehentmeier et al., 2014). Vaccines can also illicit T-independent responses to vaccination. This response can be mediated by innate-like B cells such as B-1 cells and marginal zone (MZ) B cells. B-1 cells are important for responses to polysaccharide vaccines in mice (New, Dizon, Fucile, Rosenberg, Kearney, & King, 2020).

In addition to the need for boosting, inactivated vaccines often require adjuvants (e.g. aluminium salts or Alum) that accelerate, prolong and enhance immunity. Adjuvants recruit antigen-presenting cells (APCs) such as DCs and macrophages that express pattern recognition receptors (PRRs) both on their surface (Toll-like receptors (TLRs))

and intracellularly (NOD-like receptors (NLRs)) and RIG-like receptors (RLRs)) (Awate, Babiuk, & Mutwiri, 2013). Recognition of adjuvants via these receptors activates APCs, leading to maturation and migration to the draining LNs, where they activate B cells and $CD8^+$ T cells, enhancing immune responses to the vaccine. For example, the adjuvant AS04, a combination of TLR4 agonist MPL (3-O-desacyl-4'-monophosphoryl lipid A) and Alum, induces maturation and trafficking of DCs to the dLN to activate antigen-specific T cells (Didierlaurent et al., 2009). Another study found that AS04 can induce significantly higher antibody responses than with antigen alone, with 3-8 fold higher anti-human papillomavirus (HPV) antibody titres observed following vaccination with the AS04 adjuvanted HPV vaccine compared to alum-adjuvanted HPV vaccine (Einstein et al., 2014).

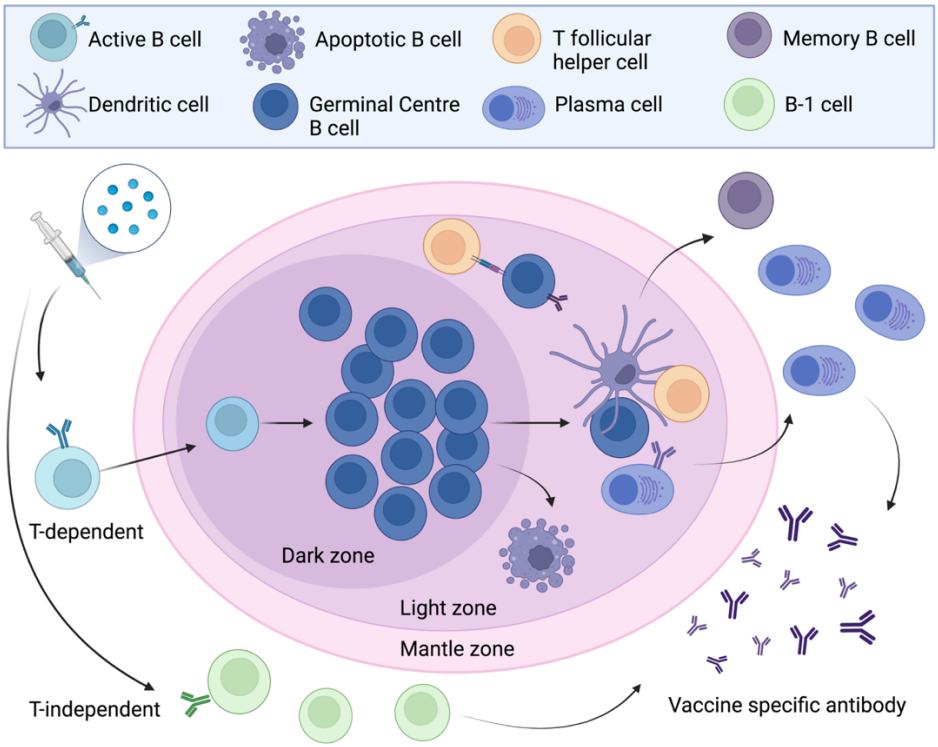

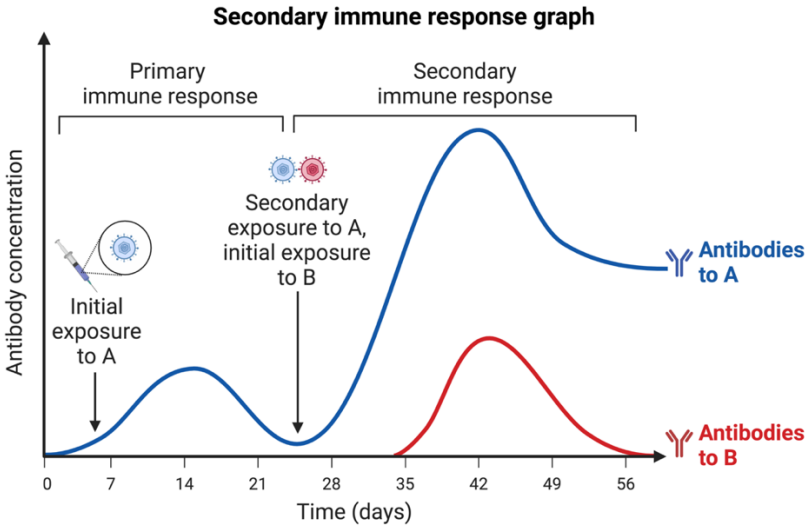

Figure 1.1| The immune response to vaccination involves both T-dependent and T-independent pathways. During the T-dependent response, antigen-presenting cells present vaccine antigens to T cells in lymph nodes, contributing to the formation of GCs where B cells undergo affinity maturation, somatic hypermutation, class switching, and differentiation into plasma cells that produce high-affinity antibodies. Memory B cells are also generated to provide long-term immunity. The T-independent response, which occurs mainly in response to certain types of antigens such as polysaccharides, involves activating innate-like B cells (such as B-1 cells) that produce antibodies without T cell help. However, the resulting antibody response is weaker and shorter-lived than the T-dependent response and does not lead to the generation of memory B cells. Boosting with a second dose of the vaccine is often necessary to achieve optimal immunity, and different types of vaccines can elicit different types and strengths of immune responses.

1.1.3 Suboptimal responses to vaccination in vulnerable populations

Despite the ongoing advancements in vaccine design, many challenges still lead to suboptimal vaccine effectiveness. Dramatic inter-individual and population differences in vaccine immunogenicity continue to be observed, especially in LMICs (**Fig. 1.2; Table 1**). Recent vaccine coverage analyses estimate that 4-19 million children are born each year who, despite receiving routine childhood vaccines against pertussis, tetanus, measles, diphtheria and pneumococcal disease, are not protected against these diseases due to suboptimal vaccine effectiveness (Grassly et al., 2015). For example, vaccine-type pneumococcal infection and carriage in Malawi children between the ages of 1 and 4 remained high three years post-vaccine introduction, with 17% testing positive despite being vaccinated. Similar results were found in Kenya, Gambia and South Africa (Heinsbroek et al., 2018; Hammitt et al., 2014; Nzenze et al., 2013; Roca et al., 2015). These estimates of pneumococcal carriage in low and middle-income countries are much higher than the 1-4% carriage in vaccinated children observed after PCV introduction in high-income countries (Dunais et al., 2015; Grant et al., 2016; Van Hoek et al., 2014). A significantly poorer efficacy of ORVs has also been reported in low- and middle-income countries. Vaccine efficacy for ORV was reported at only 76.9% in South Africa and even lower in Malawi at 49.4% (Madhi et al., 2010), levels of protection far lower than the >90% protection achieved in HICs such as the Netherlands (Vesikari et al., 2007; Clark et al., 2019). Extensive work has been carried out to characterise the various factors that could affect the immune response to vaccination (Zimmermann & Curtis, 2019).

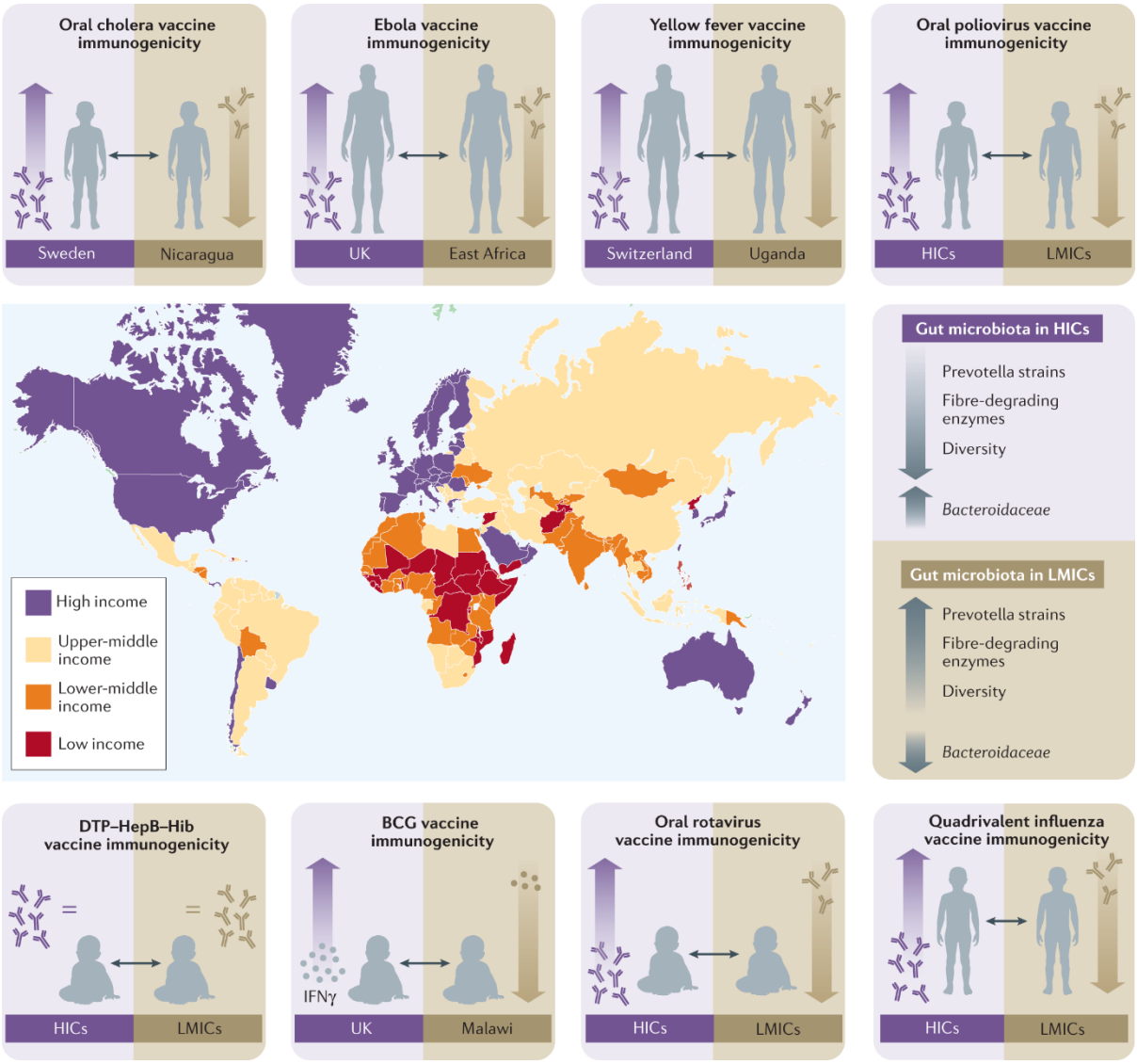

Figure 1.2| Differences in the composition and functional capacity of the gut microbiota between low-income and high-income countries correlate with differences in vaccine immunogenicity. Highlighted are example studies that have compared vaccine immunogenicity in individuals from low-income and middle-income countries (LMICs; red, orange and yellow) to those living in high-income countries (HICs; purple); see Table 1 for further details. The data for oral vaccines having reduced immunogenicity in LMICs are particularly convincing but further work is required to confirm whether responses to parenteral vaccines are impaired in LMICs as many of the reports so far are based on post hoc analyses of independent cohorts. Intriguingly, reported differences in vaccine immunogenicity correlate with differences in the composition and functional capacity of the gut microbiota between these populations. Classifications of income status are based on data from the World Bank, which within the broad category of LMICs, classifies countries as low income (red), lower-middle-income (orange) and upper-middle income (yellow). BCG, Bacillus Calmette-Guérin; DTP–HepB–Hib, diphtheria, tetanus, pertussis–hepatitis B virus–*Haemophilus influenzae* type B; IFNγ, interferon-γ.

1.1.4 Factors affecting vaccine immunogenicity

Specific host factors, such as age, sex and genetics, as well as perinatal, nutritional, behavioural and environmental factors, have been shown to significantly influence vaccine immunogenicity and efficacy (**Fig. 1.3**). For example, the age at which immunisations are administered can be an important factor limiting vaccine efficacy, especially in infancy. Antibody titres induced by vaccination are generally lower, subside more rapidly, and have significantly lower avidity when administered in the first months of life (N. Nair et al., 2007). Maternal antibodies may also interfere with vaccine responses (Halsey & Galazka, 1985; di Sant'Agnese, 1950; Nic Lochlainn et al., 2019). The risks of delaying vaccination in high infection areas could be fatal; therefore, finding ways to overcome lower vaccine immunogenicity in infants is essential. Poorer vaccine immunogenicity in infants may be due to the distinct properties of the neonatal immune system, which favours a tolerogenic environment of anti-inflammatory signals and a Th2 rather than a Th1 phenotype, as well as poorer plasma cell and germinal centre B cell responses (Olin et al., 2018; Zaghouani, Hoeman, & Adkins, 2009). There remains inadequate availability of vaccine formulas that circumvent the intrinsic properties of the neonatal immune system (Mohr & Siegrist, 2016).

Vaccine hypo-responsiveness in the elderly is a well-documented barrier to achieving herd immunity (J. Le Lee & Linterman, 2022). Several factors contribute to this, and associations have previously been made to the microbiota and immune senescence. A systems vaccinology approach using transcriptional and cytometric profiling approach predicted high and low responders to the HBV vaccine in an elderly cohort and found that

poorer antibody responses were driven by age-related inflammation (Fourati et al., 2016).

Genetic factors can also contribute to vaccine effectiveness, with variation in humoral and cellular responses to vaccination associated with polymorphisms in MHC genes (Zimmermann & Curtis, 2019). Other genetic factors associated with vaccine immunogenicity include polymorphisms in PRRs, such as TLRs or RLR genes, most likely due to their important role in recognising vaccine adjuvants, as well as pathogen-associated molecular patterns (PAMPs) and damage-associated molecular patterns (DAMPs) that may act as natural adjuvants. (Dhiman et al., 2008; Moore et al., 2012; Ovsyannikova et al., 2010; Randhawa et al., 2011). The microbiota is also sensed by innate immune cells via these pathways, and increasing evidence suggests the microbiota has an essential role in vaccine efficacy (Valdez, Brown, & Finlay, 2014; Ciabattini, Olivieri, Lazzeri, & Medaglini, 2019)

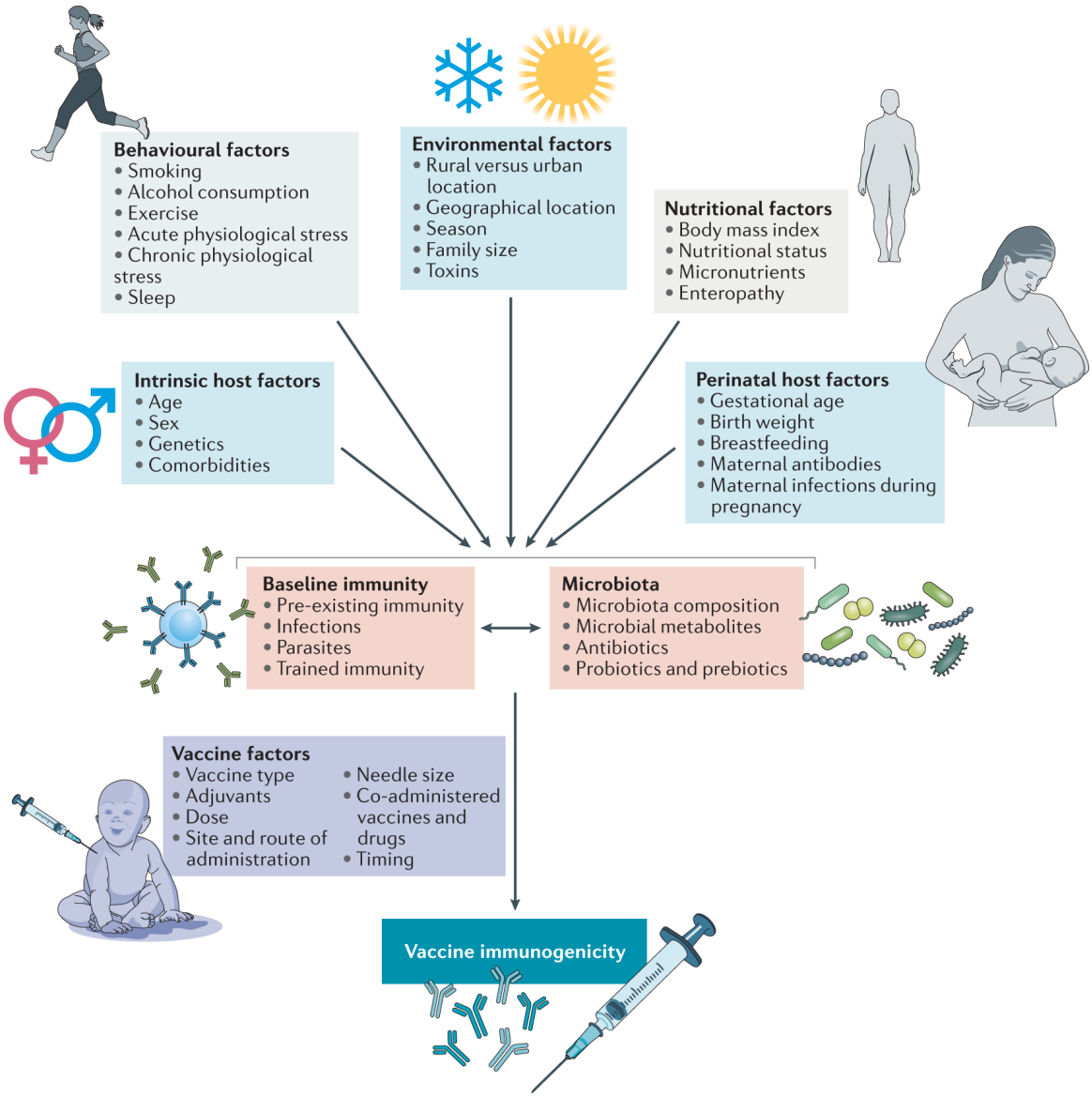

Figure 1.3| Factors with the potential to influence vaccine immunogenicity and/or efficacy. A range of intrinsic host factors (such as age, sex, genetics and comorbidities) and extrinsic factors (such as perinatal, nutritional, environmental and behavioural factors) have been suggested to influence vaccine immunogenicity and/or efficacy. The influence of these factors on vaccine immunogenicity is likely mediated indirectly via the effects of these factors on baseline immunity and/or the composition of the microbiota. Vaccine immunogenicity is also, of course, dependent on vaccine-intrinsic factors such as the adjuvant used, and vaccine efficacy may be influenced by factors other than vaccine immunogenicity, such as the degree of match between the vaccine and the strains circulating at the time.

1.2 The Human Microbiome

The human microbiome comprises the entire ecosystem of microorganisms (bacteria, fungi, viruses and protozoa), their genomes, and the surrounding environmental conditions which colonise niches within and on the human body (Dominguez-Bello, Godoy-Vitorino, Knight, & Blaser, 2019). This assemblage of archaea, bacteria, eukarya and viruses undergo temporal (Lai, Tan, & Pavelka, 2018) development in early life and the composition of the microbiome is largely unstable until the age of 2 - 3 years (Yatsunenko et al., 2012). Of these microorganisms, the bacteria residing in the intestinal compartment are found at the highest density in the human body and are the most extensively studied members of the human microbiota (Donaldson, Lee, & Mazmanian, 2015; Turnbaugh et al., 2007). The composition of the gut microbiome varies significantly throughout life and between individuals living in countries with different socio-economic conditions (Yatsunenko et al., 2012, Lin et al., 2013). In healthy infants, the gut microbiota supports a state of homeostasis. The microbiome does this by promoting immune tolerance, supporting optimal immune development, limiting the overgrowth of potential pathogens and producing a plethora of immunomodulatory metabolites, including shorts chained fatty acids (SCFAs) (Lai et al., 2018, Lynch & Pedersen, 2016). **Human infants are rapidly colonised upon birth**, and the consensus is that before birth, the neonate and its in-utero environment remain sterile, though recent work controversially suggests otherwise (Perez-Muñoz, Arrieta, Ramer-Tait, & Walter, 2017; Younge et al., 2019). Disruption of this microbial community, a process termed 'dysbiosis', in the first months of life can perturb the microbial signals that the infant receives, potentially affecting development. Therefore, it is essential to understand the factors that contribute to the development of the microbiota in early life.

1.2.1 Factors affecting infant gut microbiome composition

The establishment of the gut microbiota at birth is a highly dynamic process that is influenced by various host factors that contribute to the healthy development of the infant. Infants born via caesarean section are often colonised by a dysbiotic microbiota which can include opportunistic pathogens found in the hospital environment. In contrast, vaginally born infants follow what is considered a 'normal' path of development (Shao et al., 2019). In the first days of life, aerobic bacteria and facultative anaerobes, such as *Enterobacteria* and *Streptococci*, dominate the infant gut microbiota of vaginally born infants. The gut microbiota of breastfed infants is soon taken over by a restricted intestinal microbiota dominated by bifidobacteria, which can account for up to 60% of the total bacteria in the infant gut (Korpela & de Vos, 2018b; Huda et al., 2014). Microbiome maturation is driven by the cessation of breastfeeding rather than the introduction of solid foods and is associated with colonisation by members of the phylum Firmicutes, such as Clostridia (Stewart et al., 2018). Bacteria in the gut depend on the host's diet, and undernourishment can impair gut microbiota development (Subramanian et al., 2014). Disturbances in nutritional status, such as protein deprivation, can lead to intestinal dysbiosis, epithelial breaches, immune deficiencies, environmental enteric dysfunction, and altered metabolism in malnourished children (Guerrant, Oriá, Moore, Oriá, & Lima, 2008; Prendergast & Kelly, 2016).

Antibiotic exposure is a significant factor leading to long-term dysbiosis of the intestinal microbiome. Overuse of antibiotics is rife, and up to 50% of infants in Australia and other developed countries are exposed to antibiotics (H. Anderson et al., 2017). The dysbiosis caused by intrapartum antibiotic prophylaxis can persist up to 3 months, and antibiotic

exposure in early life has been associated with aberrant immune responses that increase the risk of allergies, inflammatory bowel disease (IBD), excessive weight gain, asthma and autoimmune diseases (Neuman, Forsythe, Uzan, Avni, & Koren, 2018; Subramanian et al., 2014). In addition, studies have shown an increased risk of infection-related hospitalisation for both mothers and infants that have been exposed to antibiotics during pregnancy and that preterm infants that have been directly exposed to antibiotics have increased susceptibility to late-onset sepsis (Miller et al., 2018, Kuppala, Meinzen-Derr, Morrow, & Schibler, 2011). Alterations in microbiome composition caused by these disturbances usually include increased enterobacteria, a reduced abundance of bifidobacteria, and a sustained lack of *Bacteroides* (Korpela & de Vos, 2018). Increasing evidence suggests that dysregulation of the gut microbiota during this critical developmental window could also influence the immune response to vaccination .

1.2.2 Evidence the microbiota may influence the immune responses to vaccination.

In recent years, the relationship between vaccine immunogenicity and the microbiota has been a topic of increasing interest, leading to several observational clinical studies (**Table 2**). One such study found a correlation between cultivable Bifidobacterium species, specifically *B. longum* subspecies *infantis* and *B. breve*, and anti-Polio virus IgA titres in infants who received prebiotics and were vaccinated against poliovirus (Mullié et al., 2004). A decade later, the relative abundance of bifidobacteria, assessed through sequencing of the 16S rRNA gene V4 segment, was positively correlated to $CD4^+$ T cell responses to tetanus toxoid (TT), BCG, and hepatitis B virus vaccines in Bangladeshi infants at 15 weeks of age (Huda et al., 2014). The relationship between bifidobacteria relative abundance and vaccine responses to BCG, TT, OPV, and HBV in infants persisted

into early childhood. The study also revealed the specific strains of bifidobacteria have either a positive or negative correlation with vaccine responses. For instance, *B. longum* and *B. longum infantis* colonisation at six weeks of age was linked to $CD4^+$ T cell responses to BCG, TT, and HBV at 15 months, while *B. longum* longum was negatively associated responses to with OPV at 15 weeks and *B. breve* at 2 years. A high relative abundance of *Bifidobacterium* and *E. coli* spp. in the first week of life has also been associated with higher saliva antibody responses to PCV10 at 12 months of age (de Koff et al., 2022). The authors of this paper also found that an increased relative abundance of *E. coli* was correlated with higher antibody responses to the meningococcal C (MenC) vaccine at 18 months of age.

Although most studies have focused on the gut microbiota, members of the respiratory microbiota, such as *Streptococcus infantis*, *Bacteroides ovatus*, *Veillonella dispar*, *Lactobacillus helveticus*, and *Prevotella melaninogenica*, have also been associated with influenza-specific IgA levels in nasal washes after intranasal vaccination with live attenuated influenza virus (Salk et al., 2016). However, further research is needed to determine if any of the associations identified in any of these studies represent causal relationships and to understand the mechanisms involved.

There is conflicting evidence for an association between the gut microbiota and responses to the OPV vaccine. For example, a study of responses to OPV in 107 infants in China found that the relative abundance of bifidobacteria in the infant faecal microbiota was correlated with increased poliovirus-specific IgA responses (Zhao et al., 2020a). In contrast, another study on infants in India found no significant differences in the relative abundances of specific taxa between responders and non-responders to OPV (Praharaj

et al., 2019). However, in both studies, higher microbiota diversity was associated with poorer responses to vaccination, similar to the findings of Parker *et al.* in the context of ORV vaccination (E. P. K. Parker et al., 2021).

Antibiotic exposure has also been shown to affect vaccine responses in specific contexts. A prospective cohort study found recent antibiotic exposure was associated with a trend towards lower seroconversion at 21 days after the first dose of COVID-19 vaccination (BNT162B2) but not at the later timepoints assessed at days 56 or 180 (Cheung et al., 2022). A low number of antibiotic-exposed participants (9.2% of 316 participants) means this study may be underpowered to see the effects of antibiotics in this population. A recent retrospective study found a deleterious effect of antibiotics on antibody responses to vaccines, including DTaP, IPV and Hib, in 560 young children (Chapman, Pham, Bajorski, & Pichichero, 2022). Each course of antibiotics up to booster resulted in a steady drop in induced antibody levels. After vaccine boosting, children exposed to antibiotics had 10-20% lower antibody levels compared to those unexposed.

Unfortunately, although most vaccines are administered to newborns and very young infants, limited clinical studies to date have focused on this high-risk group and the least is known about their vaccine responses. There is a need for systems biology approaches, measuring multiple parameters of the host response in this critical period of development (Amenyogbe, Levy, & Kollmann, 2015).

Table 2 | Clinical cohort and interventional studies assessing links between the microbiota and vaccine responses.

Vaccine	Samples size (enrolled)	Population	Method used to profile the composition of the microbiota	Study outcomes	Reference
Clinical cohort studies					
ORV	n = 39-154	Ghanaian (n = 39) and Dutch (n = 154) infants	Human Intestinal Tract Chip (HITChip)	The fecal microbiota of vaccine responder infants in Ghana was more similar to that of age-matched Dutch infants (assumed to be responders). Rel. abundance of *Bacteroides* and *Prevotella* species correlated with a lack of response to ORV. Rel. abundance of *Streptococcus bovis* positively correlated with response to ORV. Enterobacteria-Bacteroides ratio was significantly higher in responders.	(V. C. Harris et al., 2016)
ORV	n = 10 per group	Pakistani vs Dutch infants	Human Intestinal Tract Chip (HITChip)	Increased rel. abundance of Gram-negative bacteria notably *Serratia* and *E. coli* in vaccine responders. At a phylum level vaccine responders had significantly higher levels of Firmicutes (*Clostridium* cluster XI and Proteobacteria).	(V. Harris et al., 2018)
ORV	n = 170	Indian infants	16S rRNA amplicon sequencing	No significant associations between the composition of the fecal microbiota and responses to ORV were identified.	(E. P. K. Parker et al., 2018)
ORV	n = 50	Nicaraguan infants	16S rRNA amplicon sequencing	Prior to correction for multiple statistical comparisons the authors found significant associations between the rel. abundance of *Enterobacteriaceae* and *Eggerthella* and ORV seroconversion.	(Fix et al., 2020)
OPV	n = 107	Chinese infants	16S rRNA amplicon sequencing	The rel. abundance of Bifidobacteria in the infant fecal microbiota was correlated with increased poliovirus-specific IgA responses. Higher microbiota diversity was associated with poorer responses to vaccination. Rel. abundance of *Firmicutes* class *Clostridia* was significantly higher in OPV IgA negative infants.	(Zhao et al., 2020a)
OPV	n = 114-704	Indian infants	TaqMan array cards (n=704); 16S rRNA amplicon	No significant differences were found in the rel. abundance of specific taxa between responders and non-responders to OPV but	(Praharaj et al., 2019)

			sequencing (n=114)	higher microbiota diversity was associated with poorer responses to vaccination. Non-polio enteroviruses were significantly associated with reduced OPV seroconversion.	
BCG, OPV, TT, HepB	n = 291	Bangladeshi infants	16S rRNA amplicon sequencing	*Bifidobacterium* rel. abundance in early infancy was significantly positively associated with $CD4^+$ T cell response to BCG, TT, and HepB at 15 weeks; $CD4^+$ T cell response to BCG and TT at 2 years; and TT-specific IgG in plasma and OPV-specific IgA in stool at 2 years.	(Huda et al., 2019)
DTP-HepB-Hib, Polio, PCV13	n = 29-278	Antibiotic exposed (n=29) and unexposed (n=87-278) Australian infants enrolled in the MIS-BAIR study.	Not profiled	No significant differences in seroprotection rates or antibody responses to infant immunisations in infants exposed to antibiotics at 7 or 13 months of age.	(Zimmermann et al., 2020)
Interventional clinical studies					
OPV	n = 348-357	Indian infants randomised to receive azithromycin (n=348) or placebo (n=357)	qPCR and TaqMan array cards	Antibiotics did not improve OPV immunogenicity despite reducing biomarkers of environmental enteropathy and the prevalence of pathogenic intestinal bacteria.	(Grassly et al., 2016a)
ORV	n = 21 per group	Healthy Dutch adults randomised to receive a broad-spectrum cocktail of antibiotics; vancomycin or no antibiotics.	16S rRNA amplicon sequencing	Antibiotics did not alter absolute anti-ORV IgA titres. An increase in anti-RV IgA boosting was observed in adults treated with vancomycin. An increased ratio of *Enterobacteriaceae* to *Bacteroides* species was associated with enhanced boosting.	(V. C. Harris et al., 2018)
TIV	Cohort 1 n = 11 per group Cohort 2 (with low baseline immunity) n=17 controls; n=15 antibiotics exposed.	Healthy American adults randomised to receive a 5-day broad-spectrum cocktail of antibiotics or not.	16S rRNA amplicon sequencing	There was a significant impairment in H1N1-specific neutralization and IgG1 and IgA binding antibody titres in subjects from cohort 2 with low baseline antibody titres against influenza.	(Hagan et al., 2019)

BCG, *Mycobacterium bovis* bacillus Calmette-Guérin; DTP–HepB–Hib, diphtheria tetanus pertussis–hepatitis B–*Haemophilus influenzae* type B; OPV, oral poliovirus vaccine; ORV, oral rotavirus vaccine; PCV, pneumococcal conjugate vaccine; rel., relative; TIV, trivalent influenza vaccine; TT, tetanus toxoid.

1.2.3 Evidence the microbiota may influence rotavirus vaccine immune responses.

Given the limited efficacy of ORVs in countries with high mortality, there has been a growing interest in identifying factors, including differences in the microbiota, that may contribute to poorer immunogenicity in these settings (Clark et al., 2019). Two studies, one conducted in rural Ghana and the other in Pakistan, found that the microbiota of responders to the live-attenuated ORV, Rotarix, was more similar to that of age-matched Dutch infants (who respond effectively to the vaccine) compared to non-responders (V. Harris et al., 2018; V. C. Harris et al., 2017). In Ghanaian infants, ORV responders correlated with a low relative abundance of Bacteroidetes and a high relative abundance of *Streptococcus bovis* (V. C. Harris et al., 2017). On the other hand, ORV immunogenicity in Pakistani infants was correlated with an increased abundance of Proteobacteria, including *E. coli* and *Serratia* (V. Harris et al., 2018). There was a correlation between immunostimulatory bacteria, such as Gammaproteobacteria in Pakistan, enteropathogens in India, and bacteria related to *Streptococcus bovis* (which is known to have pathogenic potential) with vaccine immunogenicity across different regions (V. C. Harris, 2018). These results illustrate the geographic dependence of responses to vaccination, and how that is intrinsically linked to differences in the microbiota.

In contrast, another study examining rotavirus immunogenicity in a cohort of infants in South India did not find significant differences in microbiota composition between infants according to rotavirus seroconversion (E. P. K. Parker et al., 2018). The authors suggest that one possibility could be that all infants in this study harboured microbiota

that was inhibitory to rotavirus replication. Differences in methodology may also explain why this study did not find associations uncovered in the two other studies discussed above. For example, a higher relative abundance of Bacteroides at ten weeks of age amongst rotavirus shedders was observed in this study, in contrast to a lower relative abundance amongst seroconverters in the Ghana study, which were attributed to differences in methodology (V. C. Harris et al., 2017). More recent studies of infants in India and Nicaragua also did not find any significant associations between the faecal microbiota and responses to ORVs (Parker et al., 2018, Fix et al., 2020). Interestingly, however, before correction for multiple statistical comparisons, the Nicaraguan study, which was likely to be significantly underpowered with only 25 infants seroconverting, did identify significant associations between the relative abundances of several genera in the faecal microbiota (including *Enterobacteriaceae*) and ORV seroconversion.

Another study comparing responses to the ORV in Malawi (n=119) and India (n=60) and the UK (n=60) found that maternal antibodies and higher microbiota diversity was negatively associated with ORV immunogenicity (E. P. K. Parker et al., 2021). There was no relationship between environmental enteric dysfunction (EED), an incompletely defined syndrome of inflammation, reduced absorptive capacity, and reduced barrier function in the small intestine, and ORV responses. Therefore, EED was unlikely to be responsible for the poorer immunogenicity observed in LMICs (E. P. K. Parker et al., 2021). Interestingly, there was a high relative abundance of *Bifidobacterium* found in the Indian infants and a much lower of *Bifidobacterium* abundance in the UK cohort, in contrast to the literature suggesting that *Bifidobacterium* may have a positive role in vaccine responsiveness (Huda et al., 2019; Kandasamy, Chattha, Vlasova, Rajashekara, &

Saif, 2015; Mullié et al., 2004; Ng et al., 2022a). The authors suggest that the high viral and microbial burden in LMICs may induce a state of hyporesponsiveness.

Whole metagenome shotgun sequencing assessing the faecal microbiota of 158 Zimbabwean infants with low seroconversion found no distinct microbiome signature aligning with ORV immunogenicity (R. C. Robertson et al., 2021). This study took advantage of a broader clinical study, The Sanitation Hygiene Infant Nutrition Efficacy (SHINE) trial, which introduced potential confounding factors, such as an emphasis on breastfeeding within the cohort (>80%) which may have obscured microbiome-vaccine related effects. In addition, stool samples were collected from infants within a 30-day window of the time of vaccination, at a period of life that sees significant instability of the microbiota. The key outcome of this trial was a 50% improvement in ORV immunogenicity (Church et al., 2019), though no microbiome link was found to explain this improvement. In addition, there was no reduction in the incidence of diarrhea (Humphrey et al., 2019) or the burden of enteropathogen carriage (McQuade et al., 2020) that could explain this.

1.2.4 Evidence from interventional studies

Several observational and interventional studies have investigated whether antibiotic-driven perturbations of the gut microbiota led to altered responses to vaccination. In one of the first studies investigating antibiotics' effect on vaccine responses in humans, Harris *et al.* examined ORV efficacy in adults randomised to receive either broad or narrow spectrum antibiotics. Antibiotics did not affect absolute anti-rotavirus IgA titres, but participants receiving narrow-spectrum antibiotics had higher ORV shedding and slight

boosting (V. C. Harris et al., 2018). Furthermore, independently of the treatment groups they were placed in, rotavirus shedding and boosting was associated with a higher abundance of *Enterobacteriaceae* (Proteobacteria) and a lower abundance of *Prevotellaceae (*Bacteriodetes*)* (V. C. Harris et al., 2018). These results suggest that specific taxa and not microbiota depletion alone could influence ORV immunogenicity.

A study analysing a subset of infants enrolled in the Melbourne Infant Study: BCG for Allergy and Infection Reduction (MIS BAIR) (Zimmermann et al., 2020) found that seroprotection rates or antibody concentrations (assessed at 7 and 13 months of age) in response to routine infant immunizations (DTP, HepB, Hib, poliovirus and PCV13 vaccines) were not significantly different in infants exposed to antibiotics before vaccination (the majority of infants received antibiotics in the first week of life). However, the sample size of infants exposed to antibiotics in this study was modest ($n = 29$). A randomised controlled trial (RCT) investigating the effect of azithromycin on the immunogenicity of OPV in healthy infants found that azithromycin, administered once daily for 3 days before vaccination 11 days later, did not improve vaccine immunogenicity despite reducing biomarkers of EED and the prevalence of pathogenic intestinal bacteria (Grassly et al., 2016b). EED, or environmental entropy, is a poorly defined state of intestinal inflammation that is often accompanied by bacterial overgrowth in the small intestine, which has been suggested to lead to impaired oral vaccine immunogenicity (Gilmartin & Petri, 2015)

Recently, a systems vaccinology approach was used to comprehensively assess the impact of broad-spectrum antibiotics on innate and adaptive immune responses to influenza vaccination (Hagan et al., 2019). Broad-spectrum antibiotics (vancomycin,

neomycin and metronidazole) were administered to healthy young adults (n = 11) before and after vaccination. Antibiotic treatment resulted in a 10,000-fold, although transient, reduction in gut bacterial load and a marked and long-lasting reduction in bacterial diversity. However, there was no significant impact on neutralising or antigen-binding antibody responses induced by vaccination. To determine whether this was owing to pre-existing immunity, the experiment was repeated with individuals with low baseline antibody titres against the influenza virus. Interestingly, antibiotic treatment markedly reduced H1N1-specific neutralization in these participants and IgG1 and IgA binding antibody titres. In addition, in both study groups, antibiotic treatment resulted in increased transcriptional signatures of inflammation, which were similarly increased in healthy elderly subjects immunized with seasonal influenza vaccine (Nakaya et al., 2015) and divergent metabolic trajectories. There was a 1,000-fold reduction in serum levels of secondary bile acids after antibiotic treatment, which was highly correlated with transcriptional signatures of inflammation, suggesting a role for secondary bile acids in suppressing inflammation. Integrative modelling of the multi-omics datasets revealed significant associations between particular bacterial species and metabolic phenotypes. Taken together, these results suggest that antibiotic-driven changes to the gut microbiota can induce significant changes in the metabolome, alter inflammatory responses and impair antibody responses to vaccination.

In summary, studies carried out so far suggest that antibiotic-driven changes to the gut microbiota can influence responses to influenza, DTaP, IPV, Hib and possibly to ORV vaccination, although all of the studies are limited by a small sample size and by the fact that antibiotics were typically administered shortly before immunisation. Interestingly, antibiotic treatment did not affect responses to the influenza vaccine in recipients with

high levels of pre-existing immunity, which is consistent with the limited effect of antibiotics on responses to ORVs in individuals who had high levels of baseline seropositivity (V. C. Harris et al., 2018). It is therefore possible that the microbiota has a more marked effect on primary responses to vaccination than on secondary immune responses. Another limitation is that several of the studies conducted to date have assessed the impact of antibiotics on vaccine responses in adults. In mice (see next section), it has been shown that antibiotic exposure in infancy but not in adulthood leads to impaired responses to five parenteral vaccines licenced for infants (Lynn et al., 2018), which suggests that alterations to the microbiota in early life may have more significant effects on responses to vaccination than alterations in adulthood.

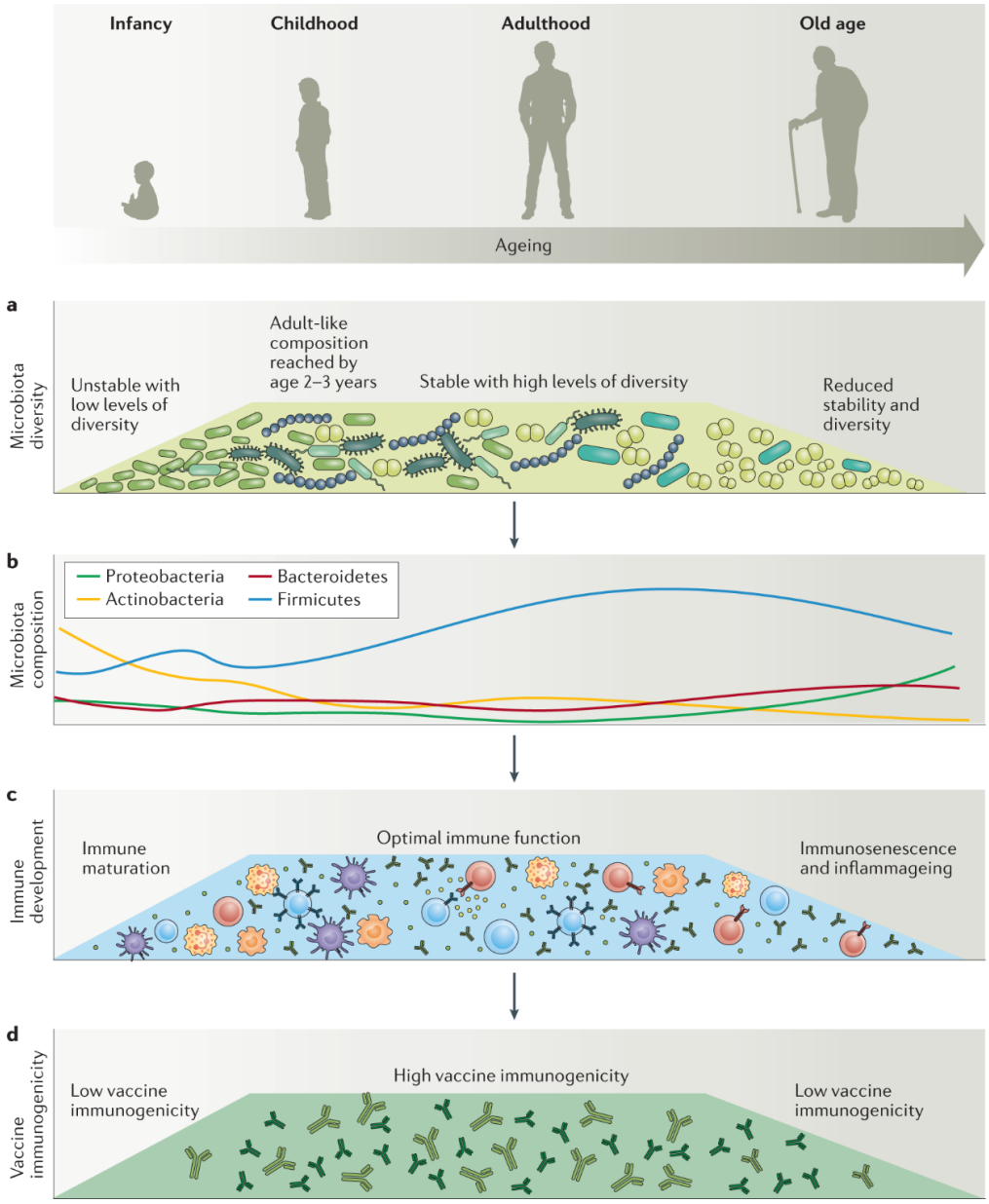

Figure 1.4| Differences in the gut microbiota of infants and the elderly compared with that of young adults correlate with altered immune status and suboptimal vaccine immunogenicity. a | The composition of the gut microbiota in early life is unstable and has low levels of diversity, with a small number of bacterial families tending to dominate. Over time, the diversity of the gut microbiota increases until an adult-like composition is reached between 2 and 3 years of age. The adult gut microbiota is more complex than in infancy (higher levels of diversity) but is also more homogeneous between individuals and, in the absence of external perturbations (such as antibiotics), is generally quite stable. **b** | As people age, the diversity and stability of the gut microbiota decline. There is also an increased relative abundance of inflammation-associated Proteobacteria and a decrease in Actinobacteria. **c** | The composition of the gut microbiota can strongly influence immune function and the baseline status of the immune system at the time of vaccination. Baseline immune status has been shown to be predictive of responses to vaccination in several studies. **d** | Compared with healthy adults, vaccine immunogenicity is poorer in infants and in the elderly. Increasing data suggest causal links between these phenomena.

1.2.5 Evidence from mice that the microbiota influences vaccine responses.

As previously discussed, the microbiota produces a range of immunomodulatory molecules that are recognised by the host's innate immune system. PRRs recognise some of these molecules that may then be able to act as a natural source of adjuvants (D. J. Lynn & Pulendran, 2017). These include flagellin, which is recognised by TLR5. TLR5-sensing of flagellin has been found to be necessary for antibody responses in mice to the non-adjuvanted seasonal flu vaccine, trivalent inactivated vaccine (TIV) (Oh et al., 2014). Antibody responses were reduced in *Tlr5*$^{-/-}$ mice and germ-free mice but could be restored by orally reintroducing the flagellated strain of *Escherichia coli,* but not an aflagellated strain. While these differences were observed for TIV, a non-adjuvanted vaccine, there were no differences in response to adjuvanted or live vaccines, suggesting the microbiota is not essential for optimal responses to these vaccine types.

Experimental evidence also suggests that NLRs may have a role in sensing molecules from the microbiota that can adjuvant immune responses to vaccination. NOD2 stimulation with the peptidoglycan component muramyl dipeptide (MDP) was essential for the mucosal adjuvant activity of intranasal cholera toxin activity in mice immunised with the model antigen human serum albumin (HSA) (Kim et al., 2016). Germ free (GF), antibiotic-treated (ABX), or mice deficient in NOD2 or receptor-interacting serine/threonine kinase, an adaptor protein downstream of NOD2, had significantly impaired IgG responses to HSA compared to wildtype mice.

Bacterial LPS signals through TLR4 to promote inflammatory responses and has the potential to act as a vaccine adjuvant. Mice immunised with synthetic nanoparticles containing antigens and TLR4 ligands enhanced neutralising antibodies (Kasturi et al.,

2011a). Different gut microbiota species produce different types of LPS, which can have varying effects on T helper responses (Pulendran et al., 2001) either through interaction with local immune cells or via translocation out of the gut to the liver, bloodstream or lymphoid organs. Systemic recognition of LPS by TLR4 on B cells was essential in the generation of microbiota-specific IgG, which provides evidence that LPS influences adaptive immune responses systemically (Melody Y. Zeng et al., 2016).

Previously, our laboratory has shown that the microbiota can modulate immune responses to vaccination in a murine model (Lynn et al., 2018). Mice treated with antibiotics (ampicillin and neomycin) in early life had significantly impaired antibody responses to 5 vaccines routinely administered to infants worldwide: BCG, the adjuvanted Bexsero meningococcal serogroup B (Men b), the NeisVac-C meningococcal serogroup C (Men C), PCV13 and the INFRANRIX hexa vaccine (Lynn et al., 2018). Impaired antibody responses could be restored in these mice following a faecal microbiome transplant (FMT) from untreated mice, suggesting that it is the species that colonise after antibiotic exposure and not the antibiotic exposure per se, which influence subsequent responses to vaccination. This result was exclusive to early life, as the same impairment was not observed in adult mice that underwent the same antibiotics treatment. This suggests that there is a potential 'window of opportunity' in early life, during which the microbiota may have a more marked influence on immune responses to vaccination. This is consistent with other studies that have highlighted a similar 'window' for the microbiota to imprint on the immune system in different contexts. For example, in mice, the intestinal microbiota induces a strong immune response at weaning that, if inhibited, can lead to pathological imprinting that drives disease susceptibility in later life (Al Nabhani et al., 2019).

In contrast to the impaired antibody responses observed in mice treated with antibiotics in early life, mice had exacerbated IFNγ production by T cells re-stimulated in culture with vaccine antigen. Interestingly, *Lynn et. al.* could not reproduce the findings in *Tlr5*$^{-/-}$ littermate mice for the influenza vaccine reported by Oh *et. al,* or in further maternal vaccination experiments investigating PCV13, suggesting the microbiota present in transgenic mice could have been mediating the differences seen between groups. More recently, broad-spectrum antibiotics were shown to significantly blunt T cell activation in response to BCG vaccination, which was accompanied by a decline in the T cell memory response (Nadeem, Maurya, Das, Khan, & Agrewala, 2020). This had negative consequences for *Mycobacterium tuberculosis* clearance in a challenge model as vaccinated ABX animals had poorer clearance than unexposed animals. Differences in the gut microbiota in mice also led to differences in the capacity to mount a GC response against *Plasmodium yoelii* (Waide et al., 2020). *Plasmodium yoelii* resistant mice had a higher diversity in their BCR repertoire and better GC structure maintenance in their spleens compared to susceptible mice.

Colonisation with *Bifidobacterium* has been associated with increased numbers of CD27^{+} memory B cells (Lundell et al., 2012, Rabe et al., 2020), IgA-secreting plasma cells (Gronlund, Arvilommi, Kero, Lehtonen, & Isolauri, 2000), and salivary IgA (Sjögren et al., 2009). Additionally, the relative abundance of several strains of bifidobacteria has been associated with improved CD4^{+} T cell vaccine responses in infants (Huda et al., 2019; Rabe et al., 2020). *Bifidobacterium* at 1 week of life was also associated with higher cytokine production, including IL-6, IL-1B, and TNF after T cell mitogen PHA stimulation, at 36 months of age in a study assessing responses in 65 Swedish infants (Rabe et al.,

2020). Moroishi *et al* found associations between the microbiota at 6 weeks of age and pneumococcal and tetanus antibody responses in these infants at 1 year (Moroishi et al., 2022). In contrast to Huda et al (Huda et al., 2014; Huda et al., 2019), they found an inverse association between tetanus antibody responses and a member of the *Bifidobacteriaceae* family, *Aerisacardovia aeriphila*. Therefore, further investigation into the effects that bifidobacteria isolated from infants has on immune responses to vaccination may be essential to determining the mechanism by which these important components of the infant microbiota have on the immune response to both oral and parenteral vaccines, particularly infant vaccines.

1.2.6 Microbiota and lymphocyte responses

Aside from studies that have directly investigated the role of the microbiota in responses to vaccination, several other studies have highlighted important roles for the gut microbiota in modulating B cell and T cell responses that likely have important implications for the effects of the microbiota on vaccine immunogenicity. For example, two recent preclinical studies have shown that mucosal or systemic microbiota exposure shapes B cell repertoires, which has important implications for antigen-specific vaccine responses (New et al., 2020; Li et al., 2020). In the first study, adult germ-free mice immunized with Group A *Streptococcus* (GAS) had significantly reduced B-1 cell clonotypes and serum antibodies specific for an immunodominant cell-wall polysaccharide of GAS (New, Dizon, Fucile, Rosenberg, Kearney, & King, 2020). Colonizing germ-free mice with a conventional microbiota restored these responses. These data could have important implications for infant polysaccharide conjugate vaccines such as PCV13. The second study showed that sequential exposure to different microorganisms in the intestine of adult germ-free mice led to the attenuation of pre-existing IgA

responses to microorganisms encountered previously (Li et al., 2020). This contrasted with sequential systemic microbial exposures, which led to a diverse IgG repertoire that could efficiently respond to these different encounters. These data may partially explain poor responses to oral vaccines observed in LMICs, particularly in settings where there is a high burden of environmental microorganisms in the gut.

It is crucial to prioritize the improvement of current vaccines in LMICs, where vaccine immunogenicity is notably lower compared to HICs. LMICs often face numerous challenges, such as high pathogen burden, micronutrient deficiencies, and exposure to pollution, resulting in a high prevalence of EED. A recent study demonstrated in a mouse model of EED regulatory T cells suppress $CD4^+$ T cell responses in the small intestine leading to impaired oral vaccine efficacy (Bhattacharjee et al., 2021). Mice were orally immunised with an attenuated labile toxin derived from enterotoxigenic *E. coli* (ETEC) and EED mice were unable to mount a vaccine specific $CD4^+$ T cell in their intestines. Instead, EED mice showed an increase of intestinal $ROR\gamma T^+$ Tregs. Targeted depletion of these Tregs could restore vaccine responsiveness in EED mice and protection against challenge.

1.2.7 The relationship between vaccination against SARS-CoV-2 and the microbiome

Responses to SARS-CoV-2 vaccines have been shown to be highly variable, and increasing data suggest that this variation can at least in part be explained by differences in the gut microbiota. Two recent studies found that baseline gut microbiota (pre-immunisation) is associated with responses to the SARS-CoV2 mRNA vaccine, BNT162b2 (Ng et al., 2022,

Healey et al., 2023). Healey *et al*. also found greater antibody avidity after BNT162b2 in people who consumed a high-fibre diet. High fibre intake results in increased SCFA production, so it is notable that Tang *et al*. found a link between SCFA production and increased antibody production in response to the inactivated SARS-CoV2 vaccine, BBIBP-CorV (Tang et al., 2022). Associations between microbiome-mediated SCFA production and antibody responses to influenza vaccination have also been reported (Cait et al., 2021). There were significant changes to the microbiota after the Sinovac SARS-CoV-2 vaccine was administered to young adults, as well as significant associations between the gut microbiota and SARS-CoV-2-specific antibody production (Han et al., 2022).

Nearly every study assessing associations between the gut microbiota and responses to vaccination against SARS-CoV-2 has found an altered microbiome profile after immunisation, and in many cases, these profiles can be used to predict vaccine responsiveness (Ng et al., 2022, Healey et al., 2023, Han et al., 2022, Tang et al., 2022). Lastly, BNT162b2 antibody responses positively correlated with the AP-1 transcription factor network and the gut microbial fucose/rhamnose degradation pathway (Hirota et al., 2022). Both were negatively correlated with T cell responses, showing another potential link between immune responses to the BNT162b2 SARS-CoV-2 vaccine and the gut microbiome.

1.2.8 Potential mechanisms

The mechanisms by which the microbiota might modulate immune responses to vaccination are currently incompletely understood. Several potential mechanisms have been proposed, including the natural adjuvant hypothesis, the modulation of B cell

responses by microbial metabolites and microbiota-encoded epitopes that are cross-reactive with vaccine antigens. Here, the evidence for and against these potential mechanisms is discussed. Most likely, the microbiota can influence vaccine responses in multiple ways. Potential redundancies between the different pathways involved and a dependency on the specific composition of the microbiota in different contexts may explain why it has so far been challenging to fully decipher these mechanisms.

1.2.9 Innate sensing of the microbiota by pattern recognition receptors

One potential way in which the microbiota is likely to modulate vaccine responses is by providing natural adjuvants that enhance responses to vaccination (**Fig. 1.5a**). Adjuvants are pharmacological or immunological agents, such as aluminium salts (alum), that function to accelerate, prolong or enhance antigen-specific immune responses. Commonly used vaccine adjuvants directly or indirectly activate antigen-presenting cells, such as dendritic cells (DCs), via pattern recognition receptors (PRRs) such as TLRs or NOD-like receptors (NLRs), which also detect microbial molecules, including those produced by the microbiota (Georg & Sander, 2019). For example, TLR5-mediated sensing of flagellin produced by the gut microbiota was required for optimal antibody responses to the non-adjuvanted influenza vaccine (Oh et al., 2014). Consistent with these data, the expression level of TLR5 on human peripheral blood mononuclear cells correlated with the magnitude of antibody titres assessed via a haemagglutination inhibition assay (Nakaya et al., 2011). However, in contrast to these data, another study did not find a strong dependency on TLR5 for antibody responses to influenza vaccine or PCV13 in young mice (Lynn et al., 2018). The reasons for these different results are not entirely clear but differences in the composition of the microbiota may play a role. Compared with non-littermate wild-type mice, which had a significantly different gut

microbiota, *Tlr5*$^{-/-}$ mice did have substantially impaired antibody responses to PCV13. Conversely, compared with littermate wild-type mice, which had a similar gut microbiota, antibody responses to PCV13 were not impaired (Lynn et al., 2018).

The activation of alternative PRR signalling pathways sensing microbial products other than flagellin might also provide similar adjuvant signals. Consistent with this possibility, the sensing of microbiota-produced peptidoglycan by NOD2 has been shown to be required for optimal responses to intranasal immunization with the model antigen human serum albumin and cholera toxin (Kim et al., 2016). Furthermore, the influence of the microbiota on B-1 cell responses to GAS has been found to depend on MYD88, a key adaptor protein downstream of multiple TLRs (New, Dizon, Fucile, Rosenberg, Kearney, King, et al., 2020). Further work is needed to assess whether other PRRs can also mediate the influence of the microbiota on vaccine responses. For example, although it is well established that bacterial LPS (sensed via TLR4) can have an adjuvant effect on responses to vaccination(Georg & Sander, 2019; Kasturi et al., 2011b), it remains to be shown whether TLR4-mediated sensing of LPS produced by the gut microbiota can modulate vaccine immune responses. This may be further complicated by the fact that different bacterial taxa in the microbiota produce different types of LPS that have varying degrees of immunogenicity (Vatanen et al., 2016).

The ability of the microbiota to provide natural vaccine adjuvants is likely also dependent on other factors, including the amount of specific immunomodulatory products that are produced and whether these products are confined to the gut or escape into the periphery. Blooms of specific pathobionts, such as members of the LPS-producing *Enterobacteriaceae*, which frequently overgrow when the gut is inflamed or following

antibiotic exposure, may lead to increased levels of LPS in the gut and the periphery (M. Y. Zeng, Inohara, & Nuñez, 2017), thereby influencing responses to vaccines that are administered concurrently with these blooms. The ability of the microbiota to influence the responses to parenteral vaccines is also likely dependent on gut barrier integrity. When the gut epithelial barrier is compromised, for example owing to gut inflammation, malnutrition or antibiotic exposure, increased levels of antigens and immunomodulatory products produced by the gut microbiota are readily detected in the periphery, where they can modulate systemic immune responses (Mu, Kirby, Reilly, & Luo, 2017). Furthermore, metabolites produced by specific taxa in the gut microbiota can support gut barrier integrity by upregulating epithelial tight junction proteins (Singh et al., 2019), which suggests that the abundance of specific taxa in the gut microbiota may alter the degree of gut 'leakiness' and therefore the amount of microbiota-produced natural adjuvants in the periphery.

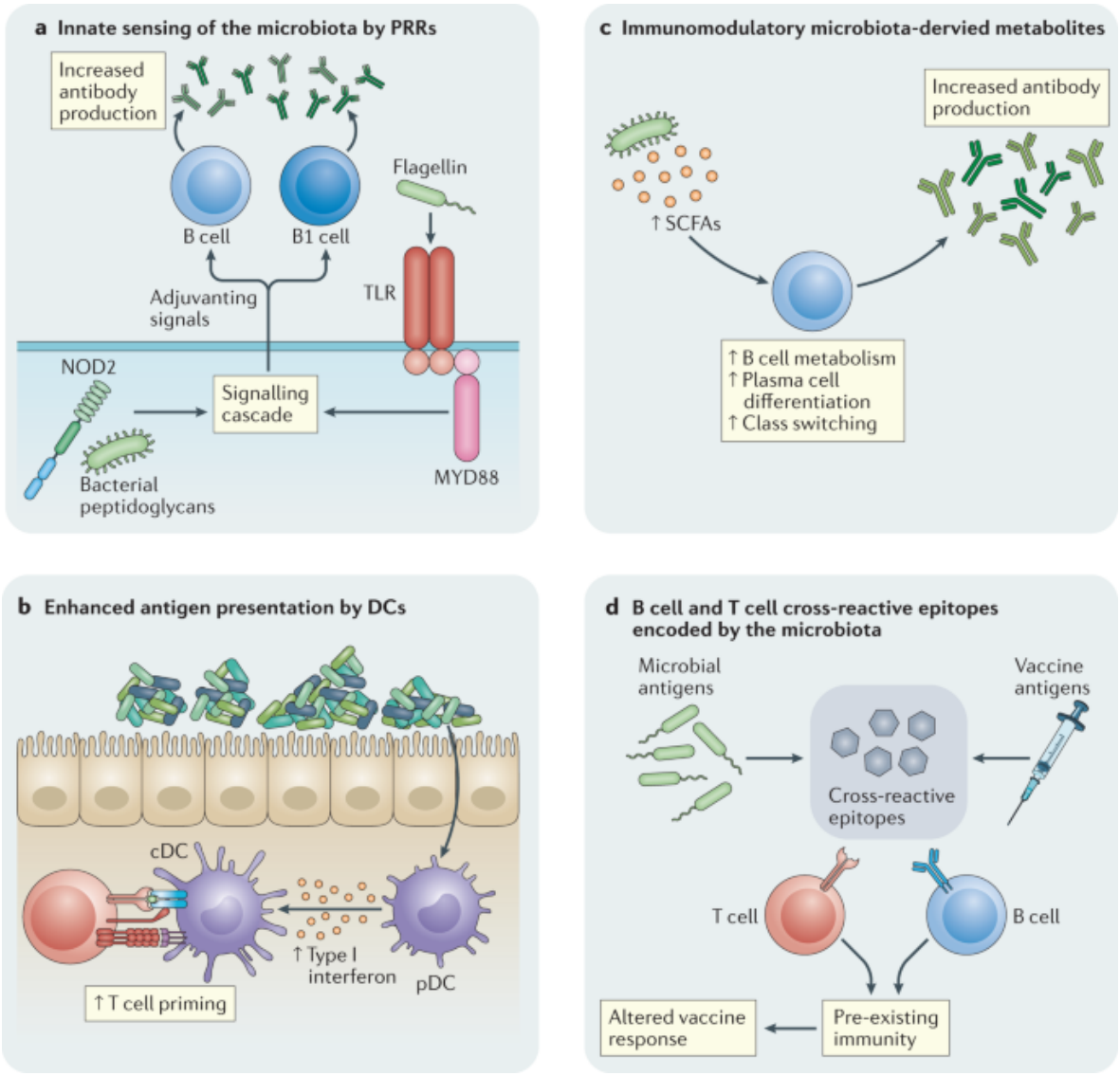

Figure 1.5| Potential mechanisms by which the microbiota could modulate vaccine immunogenicity and efficacy. a | Immunomodulatory molecules produced by the microbiota, such as flagellin and peptidoglycan, have been shown in animal models to modulate vaccine responses by providing natural adjuvants that are sensed by pattern recognition receptors (PRRs), such as Toll-like receptors (TLRs) and NOD2, expressed by antigen-presenting cells. Other immunomodulatory molecules, such as lipopolysaccharide, may also similarly modulate responses. PRRs expressed by T cells and B cells may also sense these molecules directly. **b |** Dendritic cells (DCs) have a crucial role in immune responses to vaccination by presenting vaccine antigens to T cells and secreting immunomodulatory cytokines. The microbiota regulates the production of type I interferons by plasmacytoid DCs (pDCs), which in turn instruct a specific metabolic and epigenomic state in conventional DCs (cDCs) that enhances T cell priming. **c |** Immunomodulatory metabolites produced by the microbiota, such as SCFAs, can enhance B cell metabolism to support the energy demands of antibody production and can increase the expression of genes involved in plasma cell differentiation and class switching, potentially altering responses to vaccination. **d |** Increasing data suggest that the microbiota can encode epitopes that are cross-reactive with pathogen-encoded or vaccine-encoded epitopes. The presence of cross-reactive B cells or T cells could potentially alter the responses to vaccination.

1.2.10 Microbiota-mediated reprogramming of antigen-presenting cells

Antigen-presenting cells, such as DCs, play a crucial role in presenting vaccine antigens to T cells and controlling the magnitude, quality and durability of the ensuing immune response. PRRs control the key functions of these cells (Georg & Sander, 2019) and increasing data indicate that the microbiota can potently modulate DC function, suggesting a potential way in which the microbiota could act as a natural adjuvant to vaccination (**Fig. 1.5b**). After intranasal immunization with inactive cholera toxin, TLR-mediated sensing of the microbiota by lung DCs led to the upregulation of the gut-homing receptors α4β7 integrin and CC-chemokine receptor 9 on IgA^+ B cells. The migration of these cells from the lung to the gut resulted in protection against oral challenge with cholera toxin (Ruane et al., 2016). In germ-free mice receiving intranasal immunization with inactive cholera toxin, the levels of antigen-specific IgA in the gut were significantly reduced. Furthermore, depletion of the microbiota by broad-spectrum antibiotics has been shown to inhibit the TLR-dependent production of total IgA in the lungs of mice and humans in intensive care units, contributing to increased susceptibility to *Pseudomonas aeruginosa* infection (Robak et al., 2018).

Recently, the microbiota has also been shown to regulate the constitutive production of type I interferon by plasmacytoid DCs (Schaupp et al., 2020). Type I interferon production by plasmacytoid DCs induces a specific epigenomic and metabolic state in conventional DCs such that they more efficiently prime antigen-specific T cell responses. The microbiota may also have an adjuvant effect on vaccine responses through effects on other antigen-presenting cells. For example, DCs were found to be dispensable for the ability of microbiota-produced flagellin to enhance the antibody responses to the non-adjuvanted influenza vaccine (Oh et al., 2014). Instead, these effects were dependent on

macrophages, as macrophage-depleted mice failed to mount a detectable antibody response to the vaccine at 7 days after immunization. The microbiota has also been shown to modulate antigen presentation by intestinal epithelial cells (Koyama et al., 2019), which could have implications for immune responses to oral vaccines and, as discussed in more detail below, the microbiota can also exert direct effects on B cells and T cells. More recently, *B. bifidum* has been shown to induce immunosuppressive Foxp3$^+$ Tregs through cell surface expression of ß-glucan/galactin (Verma et al., 2018). These tolerance signals were partially mediated through TLR2 on regulatory DCs sensing of these polysaccharides, leading to the production of IL-10 and TGF-ß1 and subsequent induction of Tregs.

1.2.11 Immunomodulation by microbiota-derived metabolites

In addition to molecules sensed by PRRs, the gut microbiota also produces a large number of metabolites that have the potential to modulate immune responses (**Fig. 1.5C**) (Bittinger et al., 2020). Amongst the best studied of these are SCFAs, such as acetate, butyrate and propionate, which are the main metabolic end products of bacterial fermentation in the colon. SCFAs have been shown to increase oxidative phosphorylation, glycolysis and fatty acid synthesis in B cells to support the energy demands of optimal homeostatic (non-pathogen-specific) antibody responses and antibody responses to *Citrobacter rodentium* infection (M. Kim, Qie, Park, & Kim, 2016). This study also showed that SCFAs enhanced the expression of genes involved in plasma cell differentiation and class switching. However, a more recent study reported that SCFAs inhibit rather than enhance antibody responses to intragastrically administered ovalbumin as well as inhibiting autoantibody responses (Sanchez et al., 2020). Given

these conflicting reports, further work is needed to assess the impact of SCFAs on antibody responses to oral and parenteral vaccines.

Aside from SCFAs, the immunomodulatory properties of many other microbiota-derived metabolites, including secondary bile acids and tryptophan metabolites, are increasingly being uncovered. For example, antibiotic treatment has been shown to significantly reduce levels of secondary bile acids, the reduction of which correlated with enhanced inflammatory signatures in humans immunized with the influenza vaccine (Hagan et al., 2019). As mentioned earlier, microbiota-derived metabolites may also indirectly regulate immune responses to vaccination by enhancing gut barrier integrity (Scott, Fu, & Chang, 2020), thus potentially reducing the escape of microbial molecules that enhance parenteral vaccine responses. Further work is also needed to assess the immunomodulatory effects of these metabolites on other immune cell populations that regulate responses to vaccination such as T cells and DCs. SCFAs have potent effects on T cells in other contexts (Garrett, 2019) but whether SCFAs can regulate vaccine-induced T cell-mediated immunity remains to be investigated.

Recently it was also reported that metabolites produced by the microbiota could also influence numbers of thymic mucosal-associated invariant T cells (MAIT) cells, a cell subset with a functional role in maintaining mucosal homeostasis. The microbiota controls the thymic development of MAIT cells through the production of vitamin B2 metabolites which are directly transferred to the thymus and presented by the MHC to thymocytes, driving their expansion (Legoux et al., 2019). Induction of MAIT cells only occurs during a limited early-life window, therefore disruption of these cells due to dysbiosis in early life could lead to dysregulation of mucosal homeostasis (Constantinides

et al., 2019a). MAIT cells have previously been shown to be important for responses to adenovirus-vectored vaccines, so this may be another plausible mechanism through which the microbiota may influence immune responses to these vaccines.

It is challenging to prove a causative role or the mechanisms behind how specific bacteria in the microbiome influence the immune system. It has been shown that infants colonised with *Bifidobacterium* species in early life have a reduced risk of developing immune-mediated diseases (Arrieta et al., 2018; Vatanen et al., 2016). In addition to this, there is a link between the loss of bifidobacteria in early life and enteric inflammation (Henrick et al., 2019). The authors followed up this study by assessing why the absence of bifidobacteria is associated with systemic inflammation and immune dysregulation in early life (Henrick et al., 2021). The authors found supplementing breastfed infants with a human milk oligosaccharide (HMO)-utilising commensal, *Bifidobacterium infantis* EVC001, skewed the immune system from an allergy-associated Th2 state towards a Th1 state. The metabolite Indole-3-lactic acid (ILA) was 10-fold more abundant in the faecal water of supplemented infants. ILA assessed *in vitro* also upregulated immunoregulatory galectin -1 in Th2 and Th17 cells. This could be one mechanism by which a healthy microbiome primes the immune system towards more controlled responses to vaccination.

1.2.12 Microbiota-encoded cross-reactive antigens

Previous studies in humans have identified $CD4^+$ memory T cells specific for pathogen-encoded antigens in individuals who were not previously infected with those pathogens (Su, Kidd, Han, Kotzin, & Davis, 2013). A potential explanation is T cell receptor (TCR) cross-reactivity to environmental antigens, particularly antigens and epitopes encoded

by the gut microbiota (**Fig. 1.5D**). Circulating and tissue-resident $CD4^+$ T cells with reactivity to the intestinal microbiota are abundant in healthy individuals (Hegazy et al., 2017) and bioinformatic predictions suggest that there is extensive sharing of the TCR epitope repertoire between the human proteome, the gut microbiota and pathogenic bacteria (Hegazy et al., 2017) and therefore, presumably, with vaccine-encoded pathogen antigens. Increasing data suggest that the presence of these cross-reactive T cells (and, in some cases, cross-reactive B cells (Williams et al., 2015)) can modulate immune responses to pathogens by either dampening or enhancing the immunogenicity of pathogen-associated antigenic epitopes (Pro et al., 2018; Williams et al., 2015). The presence of cross-reactive T cells at baseline has also been shown to positively correlate with immune responses to the influenza vaccine (Wilkinson et al., 2012). The origin of the cross-reactive T cells was not identified in these studies. Still, other studies have identified T cells that cross-react with both influenza virus-derived peptides and epitopes encoded by taxa in the microbiota (Su et al., 2013). Another study found cross-reactivity between MHC class I-restricted tumour antigens and epitopes of a bacteriophage protein encoded in the genome of *Enterococcus hirae*. Mice colonized with *E. hirae* harbouring this bacteriophage had improved responses to immunotherapy (Fluckiger et al., 2020). The most conclusive evidence for this hypothesis comes from a recent clinical study in 6 humans which found that marginal zone B cells that were pre-diversified by cross-reactive glycans from the microbiome were the main contributors to a T-independent response elicited by the 23-valent pneumococcal vaccine, Pneumovax (Weller et al., 2023). Therefore, this potential mechanism by which the gut microbiota could influence vaccine responses is worthy of further investigation.

Further work must be carried out to elucidate the mechanisms through which the microbiota can influence vaccine immunogenicity. While numerous studies have presented associations between the microbiota and vaccine responses, further work must be carried out to prove causative links using both clinical and pre-clinical models in humans, specifically infants, and in GF animals.

1.2.13 Targeting the microbiota

Microbiota-targeted interventions, including prebiotics, probiotics, synbiotics, FMT and small-molecule drugs that inhibit specific microbial processes, are being extensively investigated in many contexts (Cully, 2019; Wargo, 2020). Whereas some of these, such as FMT, are unlikely to be feasible at a population scale or are at very early stages of development, such as microbiota-targeted drugs, others such as probiotics (with or without prebiotics or other dietary interventions) are potentially more attractive interventions to improve vaccine efficacy owing to their safety, cost-effectiveness and scalability (Sanders, Merenstein, Reid, Gibson, & Rastall, 2019). For example, probiotics are already proving effective interventions to prevent necrotising enterocolitis, acute diarrhoea and sepsis (Alfaleh & Anabrees, 2014). Furthermore, a recent preclinical study has shown that synbiotics can enhance responses to the oral cholera vaccine in mice colonized with the microbiota of non-responder infants (Di Luccia et al., 2020).

A recent systematic review (Zimmermann & Curtis, 2018) reported that only ~50% of the 26 RCTs carried out so far have found a beneficial effect of probiotics on vaccine responses (Table 3). However, these trials had several limitations, including small sample sizes (n <50 per group in many studies). Furthermore, differences in the probiotic strains

investigated, including their purity and viability, and the timing, duration and dose of administration make these studies difficult to compare directly. Perhaps more importantly, none of these trials specifically recruited participants with a disrupted microbiota (for example, those exposed to antibiotics). Twelve of the 26 RCTs did not report whether or not participants were exposed to antibiotics; 9 expressly excluded these participants and in those studies that included antibiotic-exposed participants, the sample size was very small. It is highly unlikely that administering probiotics to already well-colonized, healthy infants would significantly affect the immune response to vaccination. Well-powered RCTs that assess the beneficial effects of microbiota-targeted interventions in infants with disrupted microbiota are therefore warranted.

More recently, the use of probiotics to improve responses to SARS-CoV-2 vaccination has been investigated. Mice administered with the probiotic *Lactobacillus plantarum (*LPG*)* after a course of antibiotics had improved SARS-CoV-2 neutralising antibody responses up to 6 months after COVID vaccination (primed DNA- S and boosted AdC68 CoV/Flu). RNA sequencing revealed that the effect of LPG colonisation on response to vaccination appears to be mediated by enhanced IFN signalling and a reduction of apoptotic and inflammatory pathways (Xu et al., 2021). There have also been promising results from large animal trials investigating the potential of probiotics to improve ORV responses. For examole, *E. coli* Nissle given to pigs led to improved responses to human rotavirus infection (Michael et al., 2021) and could prove to be a promising candidate to improve vaccine responses.

Trials investigating the impact of microbiota-targeted interventions, such as prebiotics and probiotics, on vaccine responses in the elderly have mostly examined responses to

the influenza vaccine. These studies found little to no improvement in vaccine responses in elderly individuals supplemented with probiotics (Akatsu et al., 2013; Boge et al., 2009a; Bunout et al., 2004a; Maruyama et al., 2015); however, the number of participants was small and these studies mostly used probiotics containing *Lactobacillus* strains, which are not commonly found in the adult gut. Further research is needed to identify adult-adapted strains of probiotics that might be more beneficial as interventions in the elderly. Some studies have suggested that probiotics can unexpectedly delay the re-establishment of a diverse microbiota following antibiotic exposure (Kotler et al., 2018). However, normal recolonization may not be required for a beneficial effect. For example, administering *Bifidobacterium bifidum*-based probiotics to antibiotic-treated mice prevented colonisation by pathobionts and suppressed inflammation without fully restoring a diverse gut microbiota (Ojima et al., 2020). Another study found *B. breve* probiotic supplementation to reduce oral cholera vaccine-specific IgA responses in children under 5 in Bangladesh (Matsuda et al., 2011). Given the potential effects of compromised gut barrier integrity and the translocation of microbial products on responses to vaccination, microbiota-targeted interventions may not need to fully restore the gut microbiota to a 'healthy' state to be of benefit.

Table 3 | Summary of randomised controlled trials assessing the effects of probiotics on vaccine responses in infants or the elderly

Probiotic	Age of participants (sample size)	Country	Antibiotic exposure	Effects on vaccine responses	Overall effect	Reference
Lactobacillus rhamnosus strain GG	6–10-week-old infants (n=135–143 per group)	India	Not recorded	Modest increase in seroconversion rate (+7.5%) in response to ORV in infants receiving the probiotic	+	(Lazarus et al., 2018)
Lactobacillus casei strain GG	2–5-month-old infants (n=30 per group)	Finland	Not recorded	Increased IgM (+11%) and IgA (+19%) seroconversion in response to ORV in the probiotic group	+	(Isolauri, Joensuu, Suomalainen, Luomala, &

						Vesikari, 1995)
Bifidobacterium breve strain Bbi99, *Propionibacterium freudenreichii* ssp. *shermanii* strain JS, *L. rhamnosus* strain GG and *L. rhamnosus* strain LC705	Neonates (n=40–47 per group)	Finland	12 antibiotic-exposed infants in probiotic arm	Protective antibody titres to Hib more frequent in the probiotic group (50% compared with 21%); IgG titres to diphtheria and tetanus vaccines comparable	+	(Kukkonen, Nieminen, Poussa, Savilahti, & Kuitunen, 2006)
Lactobacillus paracasei ssp. *paracasei* strain LF19	4–13-month-old infants (n=89–90 per group)	Sweden	Antibiotic-exposed infants not excluded	After adjusting for breastfeeding duration, diphtheria toxoid-specific IgG titres were significantly higher in the probiotic group after DTaP–IPV–Hib vaccination	+	(West et al., 2008)
Bifidobacterium longum strain BL999 and *L. rhamnosus* strain LPR	Neonates (n=28–29 per group)	Singapore	Not recorded	Trend (P=0.07) towards increased HepB virus surface IgG responses in the probiotic group in neonates receiving monovalent doses of HepB vaccine at birth and at 1 month of age and a DTaP–HepB combination vaccine at 6 months	~+	(Soh et al., 2010)
B. longum strain BB536	Neonates (n=148–152 per group)	China	Not recorded	No increase in antibody responses to DTP, polio or HepB vaccines in the probiotic group	=	(Wu, Yang, Xu, & Wang, 2016)
Bifidobacterium bifidum strain DSMZ20082, *B. longum* strain ATCC157078, *Bifidobacterium infantis* strain ATCC15697 and *Lactobacillus acidophilus* strain ATCC4356	8–10-month-old infants (n=27–29 per group)	Israel	Not recorded	No significant difference in the number of infants achieving protective titres of antibodies against any of the four MMR vaccine components	=	(Youngster, Kozer, Lazarovitch, Broide, & Goldman, 2011)
L. paracasei strain MCC1849 (heat-killed)	≥65-year-old old adults (n=22–23 per group)	Japan	Not recorded	No significant differences in antibody responses to TIV in the probiotic group	=	(Maruyama et al., 2016)
L. paracasei strain MoLac-1 (heat-killed)	68-83-year-old adults (n=7–8 per group)	Japan	Not recorded	No increase in antibody or T cell responses to TIV in the probiotic group	=	(Akatsu et al., 2013)
L. paracasei strain NCC 2461	≥70-year-old adults (n=30 per group)	Chile	Antibiotic-exposed adults excluded	No improvement in antibody responses to any serotypes of TIV or PPV23 in the probiotic group.	=	(Bunout et al., 2004)

L. paracasei strain DN-114 001, *Lactobacillus bulgaricus* and *Streptococcus thermophilus*	≥70-year-old adults (n=109–113 per group)	France	Antibiotic-exposed adults not excluded; no antibiotic use recorded	Significantly higher proportion seroprotected against the influenza virus B strain in the probiotic group following TIV immunisation	+	(Boge et al., 2009b)
Lactobacillus plantarum strain CECT7315/7316	65–85-year-old adults (n=14–19 per group)	Spain	Antibiotic-exposed adults excluded	Increased TIV-specific IgG and IgA titres and a trend towards increased IgM titre in the probiotic group	+	(Bosch et al., 2012)
B. longum strain BB536	≥65-year-old adults (n=18–19 per group)	Japan	2 antibiotic-exposed adults in probiotic arm	No difference in TIV-specific antibody titres or the proportion seroprotected in the probiotic group	=	(Maruyama et al., 2016)
L. casei strain Shirota	≥65-year-old adults (n=362–375 per group)	Belgium	Antibiotic-exposed adults excluded	No significant difference in mean TIV-specific antibody titre, seroconversion or seroprotection rates in the probiotic group	=	(Van Puyenbroeck et al., 2012)

DTaP, diphtheria, tetanus, acellular pertussis; DTwP, diphtheria, tetanus, whole cell pertussis; HepB, hepatitis B; Hib, *Haemophilus influenzae* type B; IPV, inactivated poliovirus vaccine; MMR, measles, mumps, rubella; ORV, oral rotavirus vaccine; PPV23, 23-valent pneumococcal polysaccharide vaccine; TIV, trivalent influenza vaccine.

1.3 Addressing the gaps

The studies discussed above support the idea that the gut microbiota modulates both B cell and T cell responses to vaccination, although much further work is required. In this thesis, I will investigate the influence of the microbiota on the immune response to vaccination in pre-clinical and clinical studies. While we know that mice exposed to antibiotics in early life have impaired antibody responses to several live and adjuvanted vaccines (Lynn et al., 2018), it is not yet known whether this is also the case in human infants and what effects this may have on circulating immune cell populations. Therefore, the effect of early life antibiotic exposure on the immune response to vaccination was investigated in a cohort of infants from the Antibiotics and Immune Response (AIR) Study. The AIR study collected metagenomic, RNA sequencing, antibody response and flow cytometry data from over 255 healthy, vaginally born infants that were divided into

groups based on their antibiotic exposure status. Subsequently, I investigated the influence of antibiotic exposure on circulating immune cell populations in these infants at seven weeks of life.

While we know that the microbiome is associated with differences in antibody responses, there have been few studies assessing the mechanisms by which the microbiome influences the immune response to vaccination in early life. Therefore, preclinical work in mice was carried out focusing on the infant pneumococcal vaccine, PCV13 which was previously shown to be impaired after early life antibiotics exposure in mice. I addressed the mechanisms through which the microbiota influences cellular responses, specifically the GC response, to vaccination using a GF mouse model.

As discussed previously, the microbiota can act as a natural adjuvant to certain vaccines via PRR signalling. It is not yet known if the microbiota can adjuvant immune responses to the PCV13 vaccine via TLR pathways. Therefore, I also investigated the role of microbiota signalling through TLRs, specifically TLR2 and TLR4, in addition to the critical adaptor protein MYD88 by employing the use of knockout mouse models.

2 Methods

2.1 Antibiotics Immune Response (AIR) protocols

2.1.1 Study design

The infants in this study were recruited as part of the Antibiotics and Immune Responses Clinic study. Infants were recruited at the Women's and Children's Hospital (WCH) Adelaide, Australia between April 2017 and March 2021. Ethics approval was obtained from Human Research Ethics Committee of the Women's and Children's Health Network (approval number HREC/17/WCHN/19). Exclusion criteria was maternal Body Mass Index (BMI) of >30 (at first trimester antenatal visit), mother had confirmed sepsis (defined by laboratory confirmed bacterial infection in blood cultures or CSF) during pregnancy, infant delivered by caesarean section, infant has a confirmed sepsis (defined by laboratory confirmed bacterial infection in blood cultures or CSF), a known or suspected disorder of the immune system that would prevent an immune response to the vaccines, such as participant with congenital or acquired immunodeficiency or those receiving systemic immunosuppressive therapy, infant has suspected or confirmed HIV, major congenital abnormality or serious illness, maternal or infant participation in a clinical study that may interfere with participation in this study, anything that would place the individual at increased risk or preclude the individual's full compliance with or completion of the study. For immunogenicity analyses, only participants who received at least one vaccine at study visit 1 will be included. Participants' allocation to an antibiotic exposure group for immunogenicity analyses was based on medical record review and discussion with the mother to ascertain any antibiotic exposure prior to vaccination at study visit 1 (approx. 6 weeks of age). Antibiotic exposure groups were defined as infants with no direct or maternal antibiotic exposure (control), infants, with documented direct

antibiotic exposure (defined as having received at least 48h of antibiotic treatment in the neonatal period with or without maternal antibiotic exposure, Neo-ABX), mothers having received antibiotics within 28 days prior to, or during delivery with no direct infant antibiotic exposure up to 6 weeks of age (IP-ABX), and infants with antibiotic exposure which did not meet either of the above criteria including maternal antibiotics while breastfeeding or the infant receiving less than 48 hours of antibiotics (PN-ABX).

Exposure groups will be classified as group 1): control (no exposure) or group 2): exposed to antibiotics, with the exposure group further classified into exposure types to allow for sensitivity analyses for various exposures.

2.1.2 AIR blood receipt

Blood samples were drawn from enrolled infants and collected in EDTA tubes (BD Vacutainer Plastic K_3EDTA Tube 2 mL) at the WCH and processed within 1-4 h of collection.

2.1.3 Infant blood preparation for flow cytometry

Upon arrival, 450 µl of infant blood was transferred into a sterile 10 mL tube. Red blood cells were lysed by adding 4.5 mL of 1x RBC lysis buffer (BD Pharm Lyse, BD) diluted in sterile MilliQ water and incubating for 15 min at RT. After centrifugation (10 min, 200 x *g*), the supernatant was aspirated and the cell pellet was washed in 10 mL of flow cytometry buffer (as described above). Live cells were counted using a hemocytometer and the number of cells were recorded.

2.1.4 Flow cytometry analysis of fresh blood samples

Infant blood cells prepared using method described section **2.1.3** was separated into 3 x 500 µl Eppendorf tubes. The tubes were centrifuged at 300 x g for 5 min and 50 µl of pre-stain Fc-block solution was added to each sample (Human Trustain FCX (Biolegend) diluted 1/20 in Brilliant Stain Buffer (BD Biosciences)) for 10 min. The three antibody cocktails listed in **Tables 2.1, 2.2 and 2.3** were prepared and added to one of each of the tubes. Samples were incubated in the dark and on ice for 30 min before being washed and resuspended in 300 µl of flow cytometry buffer. The B and T cell and extended T cell panels were transferred to round bottomed FACS tubes while the PAN panel was transferred to a Trucount FACS tube (BD Biosciences). 10 µl of flow-count beads were added to the B and T cell panel FACS tube. Before running, 10 µl DAPI was added to each sample to 3 µg/µl concentration. Cell populations were assessed using a BD FACSymphony™ flow cytometer (BD Biosciences) and final populations were analysed and manually gated using FlowJo™ (v10.6.1). The Spectre R package was used to undertake exploratory analysis (Ashhurst et al., 2022). The data was first clustered using FlowSOM, then down-sampling and UMAP dimensionality reduction was performed to enable visualization of the data and identification of clusters present in the dataset. Expression levels of each marker were represented as a heatmap overlaid on each cluster.

Table 2.1 Antibody cocktail 1, Pan-leukocyte panel

no.		Cat. No	Antibody name	Flurophore	Volume/test
-	BD	566349	BV stain BUFFER		25 ul
1	BD	561802	CD3	FITC	5 uL
2	BD	560999	CD11 c	PE	5 uL
3	BD	561358	HLA-DR	APC-H7	2.5 uL
4	Biolegend	362509	CD56	PE Cy7	2.5 uL
5	Biolegend	302243	CD19	BV605	1.25 ul
6	Biolegend	302355	CD20	BV786	1.25 ul
7	BD	561585	CD15	V500	1.25 ul
8	Biolegend	334621	FcεRI	PerCP Cy5.5	1.25 ul
9	BD	563791	CD45	BUV395	1.25 ul
10	BD	562878	CD16	BV421	0.7 uL
11	Biolegend	347109	Siglec8	PE Dazzle	0.7 uL
12	BD	562690	CD14	A647	0.7 uL
13	BD	563161	CD123	BV711	0.7 uL
Total					~50 uL

Table 2.2 Antibody cocktail 2, B and T cell panel

no	Supplier	Cat. No	Antibody name	Flurophore	Volume/test
-	BD	566347	BV BUFFER		13 ul
1	BD	555413	CD 19	PE	10 uL
2	BD	560816	CCR7/CD197	A647	10 uL
3	BD	351309	CD127	BV421	2.5 uL
4	BD	563251	CD38	BV510	2.5 uL
5	BD	561358	HLADR	APC H7	2.5 uL
6	BD	563548	CD3	BUV395	2.5 uL
7	BD	562659	CD4	BV605	1.25 uL
8	BD	560917	CD8	PE Cy7	1.25 uL
9	Biolegend	356125	CD25	PE-dazzle	1.25 uL
10	BD	561315	IgD	PerCP Cy5.5	1.25 uL
11	Biolegend	302355	CD20	BV786	1.25 uL
12	BD	563167	CD27	BV711	0.7 uL
13	Biolegend	304105	CD45RA	FITC	0.7 uL
Total					~50 uL

Table 2.3 Antibody cocktail 3, Extended T cell panel

no	Supplier	Cat. No	Antibody name	Flurophore	Volume/test
-	BD	566347	BV BUFFER		36 ul
1	BD	563548	CD3	BUV395	2 uL
2	Biolegend	304105	CD45RA	FITC	1 uL
3	BD	562659	CD4	BV605	1 uL
4	BD	560917	CD8	PE Cy7	1 uL
5	BD	562558	Cxcr3	BV421	1 uL
6	BD	564771	Ccr10	APC	2 uL
7	BD	563923	Ccr6	BV711	2 uL
8	BD	565391	Ccr4	PECF594	2 uL
9	NIH	561315	CD1d-Tet PBS57 (1/50 stock)	PE	1 uL
Total					~50 uL

2.1.5 AIR blood cell cryopreservation

To prepare infant blood for cryopreservation, 400 µl of infant blood was diluted 1:1 with PBS and gently overlayed over 600 µl of Ficoll-Paque PLUS (Merck) in a round bottom 5 mL tube. Ficoll preparations were centrifugated at 400 x *g* for 25 min with no brake at RT. Peripheral blood mononuclear cells (PBMCs) were isolated from the cloudy plasma:ficoll interface as shown in **Figure 2.1,** placed in a 10 mL tube and washed with flow cytometry buffer (PBS) with 0.1% bovine serum albumin (BSA Cat # PBSA-250G; Ausgenex, Molendinar, Australia,) and 2 mM EDTA (Life Tech Cat # 15575-038)). PBMCs were counted and resuspended at $2x10^6$ cells/mL in cell culture freezing medium. Cells were divided between 2 mL ampoules and frozen in a controlled rate freezer for 90 min to -80°C. Frozen samples were transferred for long-term storage at -80°C.

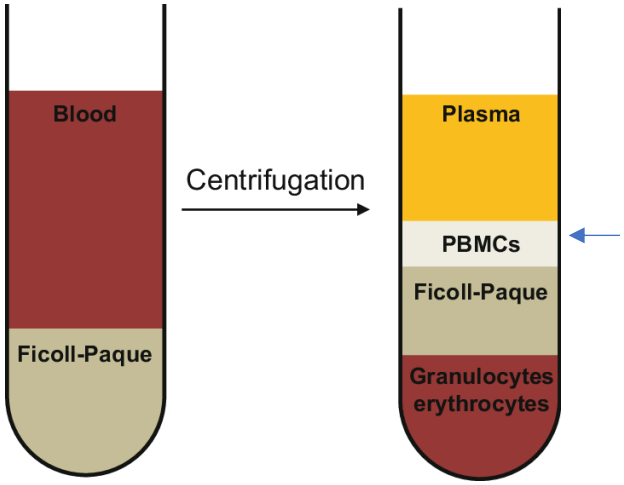

Figure 2.1| Principle of density centrifugation separation of blood using Ficoll-Paque. Adapted from (Julla et al., 2019).

2.2 Mice

SPF mice used in this project were C57BL/6J mice. Myd88 deficient (*Myd88*$^{-/-}$), *Tlr2*$^{-/-}$, *Tlr4*$^{-/-}$ and wildtype mice have been used in this project (The Jackson Laboratory, ME, USA). Mice were bred and maintained in opportunistic pathogen-free conditions at the South Australian Health and Medical Research Institute (SAHMRI). Littermate wildtype and genetically-deficient mice were obtained by backcrossing heterozygotes. Offspring were genotyped (Garvan Institute, Sydney) using gene-specific primers provided by The Jackson Laboratory. Mice were housed in cages with free access to commercial pelleted food and water under standardized conditions of temperature, daylight and humidity. Dams were selected from the same breeding colony and assigned to groups at random.

Germ free (GF) C57BL/6 mice were purchased from the Translational Research Institute, Brisbane. GF mice were housed at the SAHMRI PIRL facility in positively pressurised, high-efficiency particulate air (HEPA) filtered isolators with regulated humidity, temperature and daylight. GF mice had access to autoclaved commercially pelleted food and sterilised water. GF isolators and ISO-P cages were routinely tested for sterility, swabs from soiled nesting material, bedding and faeces were aerobically and anaerobically cultured (ComPath, Gilles Plains, Australia) to test for bacterial growth. Bacterial load in faecal samples was also assessed by 16S rRNA gene qPCR for sterility. A subset of GF dams were colonised with an FMT and their progeny (exGF mice) were transported to the SPF facility at SAHMRI. All experiments were carried out in accordance with protocols approved by the SAHMRI Animal Ethics Committee.

2.3 Antibiotic Treatment

Pairs of heterozygous (het) *Myd88*$^{+/-}$, *Tlr2*$^{+/-}$ and *Tlr4*$^{+/-}$ dams (8-12 weeks of age) were bred with het studs, with expected genotypes of 25% hom, 25% wt and 50% het offspring. Pregnant dams were treated with antibiotics from embryonic day 14 (E14; 14 days post – coitus) until weaning of their pups at day 21 post birth (D21). Neomycin (0.5g/L; Merck, St Louis, USA) and ampicillin (1g/L; Merck) were provided to antibiotic treated dams in sterile drinking water. Antibiotic water was replaced every 3 days for the duration of exposure.

2.4 Faecal sampling

Faecal samples were collected from dams prior to commencement of antibiotic treatment at E14, two days post-birth (D2) and at the end of antibiotic treatment, D21, to assess bacterial load prior to and after exposure to antibiotics. Dams in the untreated control groups also had faecal samples collected at the same timepoints. Faecal samples were also collected from the offspring at D28 and at 1,2, 4, 6, 8 and 10 weeks post vaccination. Briefly, mice were removed from their cages and separated into sterile containers. A tail-lift was performed, and faecal samples were aseptically collected. Dry ice was used to snap freeze the samples and samples stored at -80°C until processing.

2.5 Immunisations

To assess the mechanisms by which the microbiota influences immune responses to vaccination, mice were immunised 1-week post-cessation of antibiotics/after FMT administration (D28). Mice were immunised intraperitoneally with 100 µl of 13-Valent Pneumococcal Conjugate Vaccine (Prevnar13 ®, PCV13, Pfizer, New York, USA) diluted

1:2 in phosphate buffered saline (PBS, Merck). A control group of mice were mock immunized with 100 µl of PBS. A second booster dose of vaccine or control PBS was administered 2 weeks after the initial vaccination. The optimal route of administration was determined based on previous studies carried out within the research group. Intramuscular (i.m) administration of PCV13 was found to be poorly immunogenic. Serum was collected via lateral tail vein or superficial facial vein at the time of vaccination (V) and at V+ 2, 4, 6, 8 and 10 weeks post-vaccination, unless otherwise indicated. At V+2, 4, 10 or 12 weeks post-vaccination, mice were humanely killed and spleens, bone marrow and lymph nodes (mediastinal or inguinal) were harvested for immune assays.

2.6 Monoculture preparation

Monocultures were used to inoculate GF animals in several of experiments. *Enterobacter cloacae* monocultures were prepared by plating out serial dilutions of the caecal contents of mice with high levels of *Enterobacter cloacae* under anaerobic conditions. Single colonies of *Enterobacter cloacae* were identified using a Matrix-assisted laser desorption/ionization time-of-flight (MALDI-TOF) (Bruker Daltonik, Billerica, USA). Whole genome sequencing was performed to verify the bacterial strain using the Kraken tool (D. E. Wood & Salzberg, 2014). *Enterobacter cloacae* monocultures were cultured on brain and heart infusion culture overnight (Thermo Fisher Scientific, Waltham, USA) and CFU were calculated using serial dilutions. Bacterial monocultures were washed twice with 1X PBS and resuspended at 1 x 10^8 CFU/mL for oral gavage.

Bifidobacteria (Bifidobacterium longum subsp. Longum - DSM 20219, Bifidobacterium breve - DSM 20213, Braunschweig, Germany) were grown up in BHI + Mucin and were

cultured in the anaerobic chamber (Coy Lab Products, Grass Lake, USA). The anaerobic chamber was supplied with a gas mixture containing 10% CO_2, 10% H_2, and 80% N_2.

2.7 Faecal microbiota transplant (FMT) preparation

The cecal contents age-matched (day 21), untreated, healthy control SPF mice were extracted under anaerobic conditions, pooled and diluted 3X in sterile anaerobic PBS. The caecal suspension was then filtered through a 100 μM strainer and resuspended in 15% glycerol in a sterile Hungate tubes and stored at −80°C until use. The composition of cecal contents from the age-matched SPF mice was determined by 16S rRNA gene sequencing.

2.8 Oral gavage

Briefly, mice were placed under anaesthetic using isoflurane (2-5% isoflurane, 1 L oxygen/min) and administered 100 μl of monoculture preparation at 10^8 CFU/mL or FMT preparation via oral gavage in accordance with approved SAHMRI AEC- SOPs. GF monoculture, exGF and FMT experimental groups also received 100 μl of gavage material using these conditions at least twice.

2.9 DNA extraction from faecal samples

Single faecal pellet samples were weighed and resuspended in PBS and DNA extraction was performed using the DNeasy PoweLyzer PowerSoil Kit (Qiagen, Hilden, Germany) in accordance with the manufacturer's protocol with the following modifications: the faecal pellets were resuspended in 750 μl of Powersoil® bead solution and 60 μL solution C1. A 10 min heating step at 65°C prior to bead beating (Precellys 24 Tissue Homogenizer, Montigny-le-Bretonneux, France) was also included.

2.10 Splenocyte processing and takedown assays

2.10.1 Splenocyte and lymph node processing

Single cell suspensions of spleen cells were prepared by mechanical dissociation and filtration through a sterile 80 µm nylon filter (Merck Millipore, Darmstadt, Germany). Red blood cells were lysed with BD Pharm Lyse (BD Biosciences, San Jose, USA) prior to enumeration via manual counting. Lymph nodes were mechanically dissociated through a 40 µm nylon filter (Merck).

2.10.2 Bone marrow processing

One femur from each mouse was removed and flushed with PBS using a 1 mL 25 G x5/8 syringe. Red blood cells were lysed with BD Pharm Lyse (BD Biosciences) prior to enumeration via manual counting.

2.10.3 Splenocyte stimulation Assay

Splenocytes ($1x10^6$ /100 µl) were plated in 96-well flat bottom tissue culture plates (Corning, Corning City, USA) in complete culture media consisting of RPMI1640 (Merck) supplemented with GIBCO minimal essential media amino acids, GlutaMAX L-glutamine (Thermo Fisher Scientific), 10% fetal calf serum (FCS; Assay Matrix, Melbourne, Australia) and 55 nM 2-Mercaptoethanol (Life Technologies, Carlsbad, USA). Cells were stimulated with equal volume of a 136-fold dilution of PCV13 vaccine (Pfizer) in culture media, which equates to 0.5 µg/mL of the Diphtheria CRM_{197} protein (Wyeth Pharmaceuticals, Dallas, USA) in a final volume of 200 µL/well. Cells were cultured at

37°C, 5% CO_2 for 72 h. Supernatants were collected from unstimulated or stimulated wells and stored at -80°C until use.

2.10.4 Measurement of cytokines

Total IFNγ production was measured using a commercial ELISA (eBioscience,). Assay was performed with the manufacturers specifications and the results were analysed using GraphPad Prism 8.2.1 (GraphPad Software Inc., La Jolla, USA).

2.10.5 Flow cytometry

Prepared single cell suspensions of splenocytes (100-250 µL/5 mL preparation (2-5 % of organ)), lymph nodes (25-50% of organ) or bone marrow were added to a U bottomed 96-well plate. Cells were stained for 30 min with appropriate antibody panels (**Table 2.4 - 2.7**) in a volume of 30 µl, before being washed with 200 µL of flow cytometry (FACS) buffer (Merck) with 0.1% bovine serum albumin (BSA) (Ausgenex, Queensland, Australia) and 2 mM EDTA (Thermo Fisher Scientific). To assess CRM_{197}-specific B cells, cells were incubated with a biotinylated CRM_{197} probe (Fina Biosolutions, Rockville, USA) and the primary antibody stain. A secondary fluorescent streptavidin conjugated antibody to bind to biotinylated CRM_{197} was used.

After primary antibody staining, cells were prepared for panels containing intracellular markers (**Table 2.8**). Cells were resuspended in 80uL per well of eBioscience™ Foxp3 / Transcription Factor Staining Buffer Set (Thermo Fisher Scientific) fixing solution diluted 1 in 4 in diluent. Cells were then incubated for 30 min on ice before they were resuspended in 180 µL 1X Perm buffer (BD), diluted 1 in 10 with milliQ water. Cells were

spun 400 x *g* for 5 min at 4°C and incubated with 30 µl/well of the secondary stain diluted in perm buffer for 30 min.

For panels that were not fixed, 10 µl of DAPI was added to each sample before running. Cell populations were assessed using a FACSymphony™ (BD) flow cytometer and final populations were analysed using FlowJo™ (BD, v10.6.1). Gating strategies can be found in the results section.

Table 2.4 T-cell effector/memory panel

no.	Source	Antibody	Fluorophore	Dilution
1	BD	CD8	APC-Cy7	1:200
2	BD	TCRB	FITC	1:400
3	Biolegend	CD4	PE-cy7	1:400
4	BD	FCblock	-	1:200
5	BD	CD44	APC	1:200
6	Miltenyi	CD62L	PE	1:60
7	BD (Add just before running)	DAPI	DAPI	10uL of 1:1000 working solution

Table 2.5 GC B cell and plasma cell panel

no.	Source	Antibody	Fluorophore	Dilution
1	BD (dump channel)	CD3	Percp 5.5	1:100
2	BD	CD19	BV515	1:300
3	BD	B220	PEcSf594	1:300
4	BD	GL7	HI647	1:200
5	BD	IgD	BV510	1:200
6	BD	CD138	PE	1:200
7	BD	FC block	-	1:200
8	BD	DAPI	DAPI	10uL of 1:1000 working solution

Table 2.6 Extended GC, plasma cell and B1 panel

no.	Source	Antibody	Fluorophore	Dilution
1	BD	CD19	PerCP/Cy5.5	1:200
2	BD	IgM	BUV395	1:100
3	BD	CD11b	BV421	1:400
5	BD	Fas (CD95)	BV750	1:50
6	BD	B220	PECF594	1:3000

7	BD	GL7	Alexa-647	1:200
8	BD	CD138	PE	1:200
9	Biolegend	IgD	BV510	1:200
10	Thermo Fisher	CD5	PE-Cy7	1:100
11	BD	CD43	BB515	1:200
12	BD	FC block	-	1:200

Table 2.7 Antigen-specific GC B cell panel

no.	Source	Antibody	Fluorophore	Dilution
1	BD	CD19	PerCP/Cy5.5	1:200
2	BD	IgM	BUV395	1:100
3		CD38	PE Cy7	1:300
5	BD	Fas (CD95)	BV750	1:50
6	BD	B220	FITC	1:3000
7	BD	GL7	Alexa-647	1:200
8	BD	CD138	PE	1:200
9	Biolegend	IgD	BV510	1:200
10	BD	CD27	BV421	1:300
11	BD	Sca-1	APC Cy7	1:200
12	Fina Biosolutions	CRM_{197}-biotin	-	1:100
13	BD	Steptavidin	PE-CF594	1:400
14	BD	FC block	-	1:200

Table 2.8 Tfh panel

no.	Source	Antibody	Fluorophore	Dilution
1	BD	CXCR5	Biotin	1:100
2	BD	CD3	BV421	1:200
3	BD	CD19	PerCP/Cy5.5	1:200
4	BD	CD4	BV510	1:200
5	BD	PD-1	BUV737	1:100
6	BD	CD44	APC	1:200
7	BD	CD62L	BV395	1:400
8	Biolegend	ICOS	AF488	1:400
9	BD	FC block	-	1:200
10	BD	Fixable viability stain	FVS 700	1:1000

11	BD	Bcl6	PE	1:20

2.10.6 Intracellular staining (ICS) of stimulated splenocytes

After stimulation with 0.5 µg of PCV13 vaccine for 72 h, Brefeldin A (BD Biosciences) was added (**2.8.2**) and splenocytes were cultured for a further 3 h. Following centrifugation at 350 x *g* at 4°C for 5 min and washing with cold FACS buffer, cells were stained with the Surface Stain Panel (**Table 2.9)** for 30 min at 4°C. Cells were washed and incubated in neat BD Fixation buffer (BD Biosciences). Samples were washed in 1X BD Perm buffer and stained for 30 min with Intracellular Cytokine Stain (**Table 2.10)** in BD Cytofix/Cytoperm (BD Biosciences). Cells were washed once with 200 µL BD perm buffer and then resuspended in 200 µL FACS buffer. Resuspended cells were transferred to FACS tubes. All antibodies were titrated for optimal dilution. Cell populations were assessed using a BD FACSymphony™ flow cytometer and final populations were analysed using FlowJo™ (BD, v10.6.1).

Table 2.9 Surface stain panel

no.	Source	Antibody	Fluorophore	Dilution
1	Biolegend	Live/dead	Zombie Aqua	1:500
2	BD	FC block	-	1:200
3	BD	CD8	APC Cy7	1:200
4	BD	CD3	BV421	1:200
5	Biolegend	CD4	PE-Cy7	1:400
6	Biolegend	CD44	APC	1:400

Table 2.10 Intracellular cytokine stain

no.	Source	Antibody	Fluorophore	Dilution
7	Miltenyi	IFNγ	FITC	1:500

8	Miltenyi	TNFα	PE	1:50

2.10.7 ELISPOT Assay

To measure total IgG production by B cells, the ELISPOT plate was first coated with 5 µg/mL of antigen (1:10 dilution of PCV13 vaccine) diluted in PBS and incubated at 4°C overnight. After 24 h, the wells of the tray were washed with sterile PBS 5 times with the bottom tray removed. Wells were blocked with 100 µl RPMI (Merck) + 20% FCS (Assay Matrix) per well for 30 min. Wells were washed five times with sterile PBS before addition of 2 x 10^6 splenocytes or 2x10^5 bone marrow cells resuspended in complete culture media consisting of RPMI1640 (Merck) supplemented with GIBCO minimal essential media amino acids, GlutaMAX L-glutamine (Thermo Fisher Scientific), 10% FCS (Assay Matrix) and 55 nM 2-Mercaptoethanol (Life Technologies). 200 µl per well in duplicate was used. Cells were incubated for 16-24 h at 37°C, 5% $C0_2$. After this incubation was complete, cells were washed with sterile PBS with the bottom tray removed and 75 µl of 1:2000 horseradish peroxidase (HRP) conjugated anti-mouse IgG (AbCam, Cambridge, UK) and incubate for 1 h at room temperature (RT). Cells were then washed 5 times with PBS. To develop the plates, 75 µl of ELISPOT TMB reagent (BD) was added until spots were clearly visible. Membranes was washed in H_2O and dried and spots were counted via ELISPOT plate reader (ImmunoSpot, Shaker Heights, USA).

2.11 DNA and RNA procedures

2.11.1 RNA extraction

500 µl – 1 mL TRIzol (Thermo Fisher Scientific) was added to 10^7 pelleted splenocytes and samples were frozen at -80°C until processing. To extract RNA, samples were thawed

and 100 µL of chloroform (Merck) was added to each tube before shaking vigorously for 15 s. Samples were then incubated for 5 min at RT and centrifuged at 12,000 x *g* for 15 min at 4°C. The aqueous layer of the sample was removed and placed into a new tube with 0.5µl of glycogen (Thermo Fisher Scientific). 250 µl of 100% isopropanol (Merck) was added and tubes were inverted before a 10 min incubation at RT (20°C). Samples were then spun for 10 min at 12,000 x *g* at 4°C, supernatant was removed, and the remaining pellet was washed with 1 mL of freshly prepared 75% ethanol. Samples were centrifuged (10 min;15,000 x *g* at 4°C) and the ethanol wash step was repeated once more before air drying the pellet for 5 min and resuspending the RNA in RNase-free water.

2.11.2 Nano Drop

RNA quantity was measured with the NanoDrop 8000 Microvolume UV-Vis spectrophotometer (Thermo Fisher Scentific). 260/280 and 260/230 ratios of 1.8 or higher were consider of sufficient quality.

2.11.3 cDNA synthesis

cDNA was synthesized from purified RNA. A preparation of 1 µg of RNA, 10 mM dNTP's (Thermo Fisher Scientific) and 1µl 0.5 µg/µl Oligo dT's (Life Technologies) was brought up to a final volume of 10 µl with RNase-free water. The RNA preparation was then denatured using a 65°C heat block for 5 min. Following denaturation Protoscript II Reverse Transciptase (200U/µl), 0.1M DTT and 5X First Strand Buffer (New England Biolabs, Ipswich, USA) were added to the samples and solution was brought up to a final volume of 20 µl using RNase-free water. Samples were incubated at 42°C for 60 min with

a subsequent 20 min incubation at 65°C for enzyme inactivation. cDNA was stored at -20°C.

2.11.4 Quantitative real-time PCR analysis to determine bacterial load

The bacterial load in faecal samples was assessed by measuring the 16S rRNA gene using quantitative real-time PCR analysis. Primers for the conserved 16S rRNA gene were used to assess bacterial load (**Table 2.11**) (Nadkarni et al, 2002). Each reaction was loaded into optimal grade 384 well plates and real-time PCR was performed on a Quant Studio™ 7 Flex Real –time PCR system (Thermo Fisher Scientific). **Table 2.12** lists the composition of each reaction. No template controls and reagent only samples were included in each run, with 3 µl of sterile water substituted for DNA. Each sample was run in duplicate. The PCR amplification program ran as follows: 50°C for 2 min, followed by 95°C for 10 min, then 40 cycles of 95°C for 15 s and 60°C for 1 min. After the 40 cycles, a melting curve analysis was performed. The bacterial load for each sample was quantified against a standard curve of serial dilutions of *E. coli* genomic DNA, which was performed in the same PCR run and is detectable within a range of 3 to 3 x 10^6 equivalent *E. coli* cells. The bacterial load of *Enterobacter cloacae* was quantitated against a standard curve of serial dilutions of *Enterobacter cloacae* cells. The final number of cells were then normalised relative to the faecal weight of each sample.

Table 2.11 Table of bacterial primers.

16S Forward	5-TCCTACGGGAGGCAGCAGT-3
16S Reverse	5-GGACTACCAGGGTATCTAATCCTGTT-3

Table 2.12 Composition of Bacterial load qPCR.

Platinum®SYBR®Green qPCR SuperMix- UDG	5 µl
0.2 µM Forward Primer	1 µl
0.2 µM Reverse Primer	1 µl

DNA template + Sterile Water	3 µl
Total	10 µl/well

2.11.5 Quantitative real-time PCR for gene expression analysis

Real-time qPCR was carried out on a Quant Studio™ 7 Flex Real –time PCR system (Thermo Fisher Scientific), using optical grade 384 well plates. The expression of the housekeeping genes, Beta Actin and GAPDH (listed in **Table 2.13**), were used as reference genes for normalisation. The targeted genes and primers used are shown in **Table 2.13** and the composition of each well is shown in **Table 2.14**. A no template control was run alongside the samples, where DNA was substituted for 1 µl of sterile water. The PCR program ran as follows: 50°C for 2 min, followed by 95°C for 10 min, then 40 cycles of 95°C for 15 s and 60°C for 1 min. After program completion, a melting curve analysis was performed.

Table 2.13 Table of mouse primers.

Beta Actin Forward	5-TTGCTGACAGGATGCAGAAG-3
Beta Actin Reverse	5-AAGGGTGTAAAACGCAGCTC-3
Cxcl10 Forward	5-TATCCTGCCCACGTGTTGAG-3
Cxcl 10 Reverse	5-TGGTCTTAGATTCCGGATTCAGA-3
Ifih1 Forward	5-GCACAGCAGTGAAGTCAAGC-3
Ifih 1 Reverse	5-ACCGTCGTAGCGATAAGCAG-3
Il1b Forward	GTGCTGTCGGACCCATATGA
Il1b Reverse	TTGTCGTTGCTTGGTTCTCC
Il12a Forward	CAGTCCCGAAACCTGCTGAA
Il12a Reverse	TGTCTTCAGTGCAGGAA
Il12b Forward	CCAACTGCCGAGGAGACC
Il12b Reverse	CTTGGGCGGGTCTGGTTT
Il6 Forward	TCTGGGAAATCGTGGAAATGAC
Il6 Reverse	CAAGTGCATCATCGTTGTTCA
Ifny Forward	GAGGTCAACAACCCACAGGT
Ifny Reverse	GGGACAATCTCTTCCCCACC

Tnfa forward	CCAGACCCTCACACTCAGATCA
Tnfa Reverse	GTTTGCTACGACGTGGGCT
Gapdh F	GGGTCCCAGCTTAGGTTCAT
Gapdh R	TACGGCCAAATCCGTTCACA
Mcp1 F	AAGTCCCTGTCATGCTTCTG
Mcp1 R	TCTGGACCCATTCCTTCTTG
Mcp1 Forward	TGATCCCAATGAGTAGGCTGGAG
Mcp1 Reverse	ATGTCTGGACCCATTCCTTCTTG
Mip1alpha Forward	CAGCGAGTACCAGTCCCTTTT
Mip1alpha 39 Reverse	CCTCGCTGCCTCCAAGA

Table 2.14 Composition of gene expression qPCR.

Platinum®SYBR®Green qPCR SuperMix- UDG	5 µl
0.2 µM Forward Primer	0.725 µl
0.2 µM Reverse Primer	0.725 µl
DNA template + Sterile Water	3.5 µl
Sterile water	0.05 µl
Total	10 µl/well

2.11.6 16S rRNA gene sequencing analysis

16S rRNA gene sequencing was undertaken by the SA Genomics Centre on DNA extracted from faecal samples collected from individual mice at the V timepoint. DNA extracted from faecal samples was used to generate amplicons of the V4 hypervariable region of the 16S rRNA gene as described previously (Lynn et al., 2018). The amplicon library sequencing was performed using an Illumina Miseq system (2 × 300bp run). Paired end 16S rRNA gene sequences were demultiplexed and imported into QIIME2 (release

2019.9) for processing (Bolyen et al., 2019). Sequences were error corrected, and the counts of error-corrected reads per sample were generated with DADA2 version 1.8 (Callahan et al., 2016). A phylogenetic tree of error-corrected sequences was constructed with FastTree (Price, Dehal, & Arkin, 2010). Taxonomy was paired to sequences with the sklearn plugin for QIIME2 to which an 80% confidence threshold was applied, using the GreenGenes 13.8 database (DeSantis et al., 2006). The MetaCyc pathway relative abundance was predicted the PICRUSt2 plugin (Douglas et al., 2020). Statistical analysis was carried out in R version 3.6.3. Graphs were generated using ggplot2 (Wickham, 2016). Alpha and Beta diversity values were produced using PhyloSeq version 1.3 (McMurdie & Holmes, 2013). Shannon diversity, which takes evenness into account, was also used to assess differences between the groups. For example, if there is 10 species present, each is at 10% abundance.

2.11.7 Vaccine specific antibody ELISA

ELISAs against PCV13, the polysaccharides PPS1 and PPS3 and the conjugate protein CRM_{197} specific were carried out using Nunc MaxiSorp® ELISA plates (Merck). Concentrations of each were optimised using serial dilutions of both the coating buffer and serum. Plates were coated with 50 µl of either 0.05 µg/mL PCV13 vaccine, 1.25 ng/mL CRM_{197} protein, 5 ng/mL PPS1 or 5 ng/mL PPS3 and incubated overnight at 4°C. Plates were washed with 100 µl 0.5% Tween-20/PBS and blocked for 2 h at RT with 0.5x ELISA buffer (eBioscience, Waltham, USA). Serum samples collected from mice were diluted in 0.5x ELISA buffer and pipetted onto blocked plates. After overnight incubation at 4°C, antigen-specific antibodies were measured using HRP conjugated anti-mouse IgG (Novex, Lake Oswego, USA), IgG1, IgG3, IgG2b, IgA or IgM (all from AbCam, Cambridge, UK)(**Table 2.15 – 2.18**). The activity of HRP was measured using tetramethylbenzidine

(TMB) substrate (Thermo Fisher Scientific) and the reaction was stopped using 2N H_2SO_4. Plates were analysed using an EnVision microplate absorbance reader (PerkinElmer, Waltham, USA) at 450 nm adjusted by subtraction at 595 nm.

Table 2.15 Serum concentrations for ELISAs at V+1

Antigen	IgG_{total}
PCV13	1/100 - 1/250
PPS1	1/100
PPS3	1/250
CRM_{197}	1/500

Table 2.16 Serum concentrations for ELISAs at V+2

Antigen	IgG_{total}	IgM
PCV13	1/100 - 1/250	1/250
PPS1	1/100 - 1/250	1/100 - 1/2501``
PPS3	1/100 - 1/250	1/250
CRM_{197}	1/250	1/500

Table 2.17 Serum concentrations for ELISAs at V+4 – V+10

Antigen	IgG_{total}	IgM	IgG1	IgG3	IgG2b	IgA
PCV13	1/2000 - 1/4000	1/1000	1/2000	1/500 - 1/1000	1/1000	1/100
PPS1	1/500	1/500 - 1/1000	1/500	1/500	1/500	-
PPS3	1/1000 - 1/2000	1/1000	1/1000 - 1 in 2000	1/500	1/500	-
CRM_{197}	1/500 - 1/3000	1/1000	1/1000	1/500	1/500	-

Table 2.18 Antibody concentrations

Antibody	Concentration
IgG_{total}	1/2000
IgG1	1/10,000
IgG2b	1/2000
IgG3	1/1000
IgM	1/500 – 1/1000
IgA	1/100

2.12 Confocal microscopy of germinal centres.

2.12.1 Fixation, embedding and cryosectioning

Half of the collected spleen was fixed in fixation buffer (4% PFA- source in PBS) for 4-5 h. Spleens were then incubated with 1-2 mL of 30% sucrose solution for 12-16 h at 4°C until the tissue sinks (left up to 5 days). Sucrose solution was removed from the samples and dabbed dry with a paper tissue. Tissue was transferred into a cryomold containing OCT so it was fully immersed without bubbles surrounding it. Cryomolds were placed into an esky of dry ice for rapid freezing. The tissue block was wrapped with tinfoil and stored at -80°C. Samples were sent for cryosectioning at the Adelaide Health and Medical School (AHMS) and cut into 10µm sections on glass slides.

2.12.2 Immunofluoresence staining

Slides were removed from -80°C and air-dryed under airflow for 30 min at RT. An unbroken circle was drawn around tissue sections with a PAP pen to create a hydrophobic barrier, and left for 15-30 min until the wax had completely dried. The slides were transferred to a staining jar and washed 3 times for 5 min with Wash Buffer at RT. The slides were kept hydrated using a humidified chamber. Slides were blocked in blocking buffer (normal goat serum 4% (v/v), normal donkey serum 4% (v/v), bovine serum albumin 15% (v/v) in PBS) (Merck) for 120 min at RT. Slides were washed 3 times for 5 min with Wash Buffer at RT. Permeabilization buffer was added (Triton X-100 2% (v/v) in 1x PBS) for 30 min at RT. Slides were washed again 3 times at RT and 100ul of antibody cocktail (**Table 2.19**) made up in blocking buffer was added to slide, covering entire section (40-100 µl per slide). The covered slide was incubated in a dark humidified

chamber overnight at 4°C. The next day, slides were washed with Wash Buffer 3 times for 5 min at RT. Slides were then rinsed with 1X PBS and dried without disrupting the tissue. The tissue was mounted with Vector shield mounting medium and dried at RT until mounting medium has set. Slides were sealed with nail polish and stored at 4°C for imaging.

2.12.3 Confocal imaging acquisition

Sections were visualised using a Leica TCS SP8X confocal microscope. Tile scan images were acquired with a 10X magnification lens, which had a 10% overlap, while enlarged images were captured using a 20X magnification lens. Subsequently, the acquired images were processed and analysed using Fiji and ImageJ.

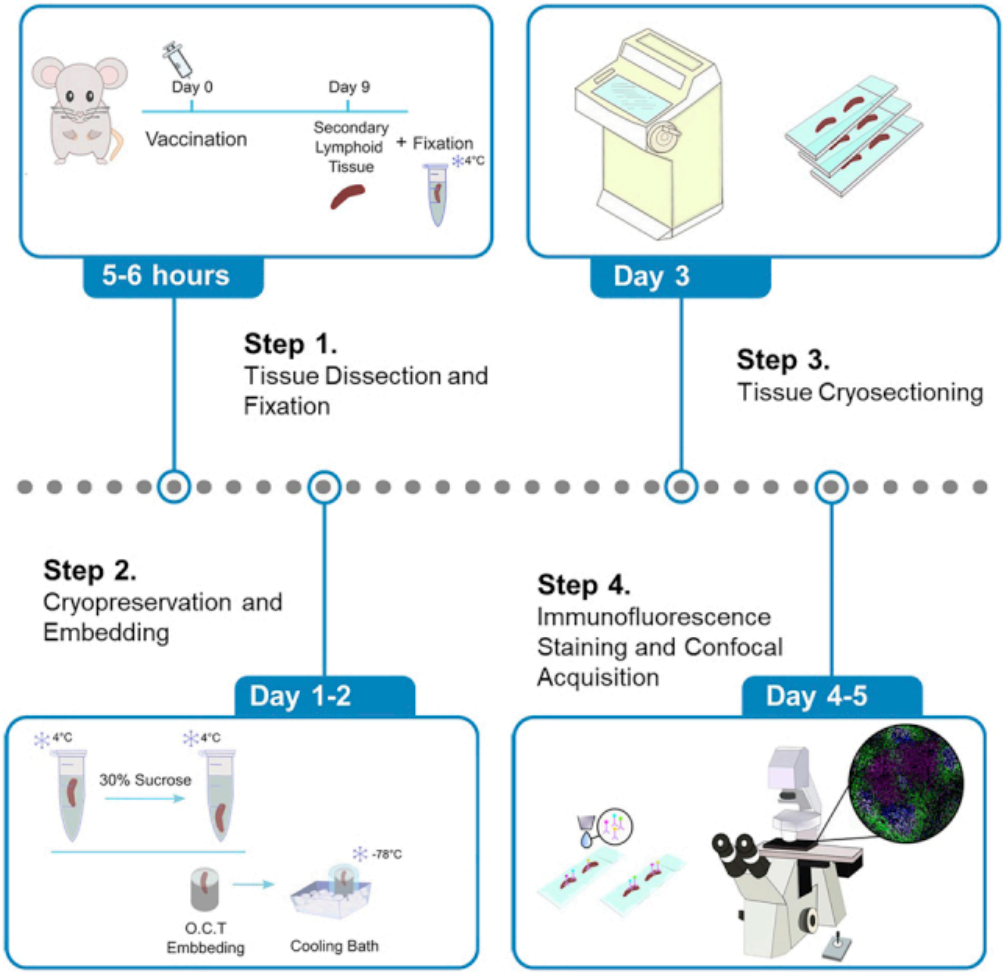

Figure 2.2| Immunofluorescence staining protocol for imaging germinal centres in spleens and draining lymph nodes of immunised mice. Figure from STAR methods protocol (Fra-Bido, Walker, Innocentin, & Linterman, 2021).

Table 2.19 Immunofluorescence staining antibody panel

Antibody	Conjugation	Dilution factor	Clone	Company
CD16/CD32 Purified	Purified	1:200	2.4G2	BD
CD21/35	BV421	1:200	7E9	Biolegend
GL7	AF488	1:100	GL7	Biolegend
CD3	AF594	1:200	17A2	Biolegend
IgD	AF647	1:200	11-26c	Biolegend

3 Assessing the impact of antibiotic exposure on peripheral blood immune cell populations in infants post-vaccination.

*This chapter includes data from The Antibiotics and Immune Response (AIR) Study. The full manuscript is in preparation for publication and can be found in the appendix of this thesis.

A systems immunology study to assess the impact of early-life antibiotic exposure on infant vaccine immune responses. Feargal J. Ryan[1,2†], Michelle Clarke[3,4†], A. Lynn[1,2], Saoirse C. Benson[1,2], Sonia McAlister[5,6], Lynne C. Giles[7], Jocelyn M. Choo[2], Alyson Richard[2], Lex Leong[2], Stephen J. Blake[1,2], Mary Walker[3], Steve L. Wesselingh[1,2], Damon J. Tumes[1,6], Peter Richmond[5,6,9], Geraint B. Rogers[1,2], Helen S. Marshall [3,4,7††], and David J. Lynn[1,2††]

3.1 Introduction

After clean water, vaccination is the most effective public health intervention we have to protect against infectious disease, with global immunisation programs preventing millions of deaths per year. However, even for licensed vaccines, there is room for improvement. For reasons that are poorly understood, antibody titres (the primary correlate of protection for most vaccines) can vary up to 100-fold between healthy individuals. My colleagues have previously shown in mice that early-life antibiotic-driven dysbiosis can impair antibody responses to live and adjuvanted infant vaccines (Lynn et al., 2018). These data suggest that the gut microbiota is an important regulator of immune responses to vaccination. These data are supported by clinical observational studies that have reported significant correlations between the composition of the gut microbiota and vaccine responses (Ng et al., 2022;V. Harris et al., 2018; V. C. Harris et al., 2017). Of particular note, Hagan and colleagues conducted a systems vaccinology study in which

adults were randomised to receive antibiotics or a placebo prior to influenza vaccination and found that in those participants with low pre-existing immunity, antibiotic exposure led to impaired IgG responses to vaccination, although the sample size was modest (n=11/group) (Hagan et al., 2019). In contrast, a recent epidemiological study evaluated the impact of antibiotic exposure on the seropositivity of oral rotavirus vaccine (ORV) in 537 infants from LMICs and found that those exposed to antibiotics from birth up to 7 days after vaccination had higher rates of seropositivity (St Jean et al., 2022).

To assess the gap in our understanding of how the microbiota may impact vaccine immunogenicity in infants, we established the Antibiotics & Immune Response (AIR) Study. The primary aim of this study was to assess the influence of antibiotic exposure on PCV13-specific antibody titres in infants, with secondary objectives including the assessment of the impact on responses to other infant vaccines. Over 1,000 blood and stool samples were collected from 224 healthy, full-term, vaginally delivered infants born at the Women's and Children's Hospital in Adelaide, Australia, between 2017 and 2019. I assessed more than 30 different immune cell populations via flow cytometry analysis of 156 fresh blood samples collected from these infants at 7 weeks of life (1 week after most primary immunisations were administered). I compared these immune cell population data to the other data gathered from this study. These included comparisons of circulating cell populations when grouped by sex, antibiotic exposure type and antibody response.

3.2 Study Design

The AIR Study was a clinical observational study that aimed to determine whether responses to vaccination are impaired in infants exposed to either maternal or direct

antibiotics in the neonatal period. Using a systems vaccinology approach, the study aimed to identify the key taxa and metagenomically-encoded processes in the infant gut microbiota associated with vaccine-specific antibody responses**.** Preterm infants, infants born by C-section, and infants born to mothers with a maternal BMI > 30 in the first trimester were excluded from the study. Additionally, infants were excluded where they or their mothers had sepsis, allergy to a vaccine component, major congenital abnormality, gastrointestinal or other severe disease, or with immunodeficiency or immunosuppression. Recruitment for the AIR study ended early in 2020. 255 healthy, vaginally born, term infants that were either exposed or unexposed to antibiotics were enrolled in the study. Antibiotic exposure groups were defined as unexposed infants (No ABX), direct antibiotic-treated in the neonatal period (Neo ABX), intrapartum exposed with no direct exposure (IP ABX) or post-natal maternal antibiotic exposed (PN ABX). A total of 81 infants were subsequently withdrawn, mostly citing concerns over multiple blood draws and the logistics of attending multiple appointments at the Women's and Children's Hospital. The sample collection timeline for the AIR study is illustrated in **Figure 3.1**. Faecal samples were collected for shotgun metagenomic sequencing to profile the microbiota composition in the neonatal period (~day 7 of life) and again immediately before primary vaccinations at week 6 of life (~day 45 of life). Blood samples were collected at weeks 6 and 7 for Total RNASeq. Flow cytometry analysis was performed on samples collected at week 7. Serum was collected at baseline (6 weeks) and then at 7 and 15 months to measure antibody responses. Serum IgG responses to 20 different vaccine antigens in the Hepatitis B (HepB), Infanrix hexa 6-in-1 vaccine (containing Diphtheria Tetanus Pertussis (DTP), Hepatitis B (Hep B), Polio, and Haemophilus influenzae type B (Hep B) vaccines) and the 13-valent Pneumococcal Conjugate Vaccine (PCV13) was assessed at the Telethon Kids Institute in Perth, Western

Australia using in-house multiplex fluorescent bead-based immunoassays. Serum IgA responses to the oral rotavirus vaccine (ORV) were also assessed. Data on possible confounders such as birth weight, type of antibiotics and feeding type were also collected, as well as summary data from the cohort (**Table 3.1**).

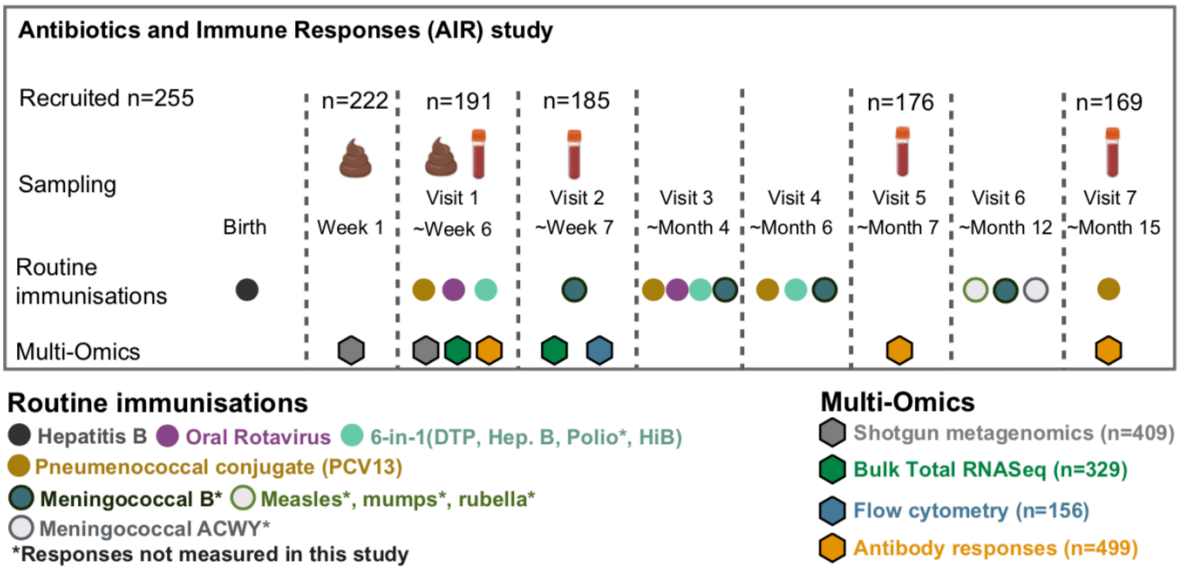

Figure 3.1| The Antibiotics and Immune Responses (AIR) Study was an observational clinical study that aimed to identify the key taxa and pathways in the infant gut microbiota associated with vaccine antibody responses. As part of the AIR study, we recruited a cohort of 255 vaginally born, healthy, term infants that were either unexposed (No ABX) or exposed to direct (Neo ABX), intrapartum (IP ABX) or postnatal maternal antibiotics (PN ABX). Faecal samples were collected for shotgun metagenomics in the first week of life and at week 6 (when the majority of primary immunisations were administered). Blood samples were collected at week 6, week 7, 7 months and 15 months for serology, flow cytometry and RNA sequencing. Serum IgG titres to 20+ vaccine antigens were assessed. Serum IgA responses to ORV were also assessed.

Table 3.1 Key demographics of the AIR study infants.

Vaccinated cohort (n=191)		Antibiotic exposed			Non Exposed
		Neo-ABX (n=32)	IP-ABX (n=49)	PN-ABX (n=30)	Control (n=80)
Mother	**Age at delivery** (Mean years, SD)	31 (5)	32 (4)	33 (4)	32 (4)
	BMI (mean kg/m2, SD)	24 (3)	24 (3)	23 (3)	24 (3)
	Pertussis vaccine during pregnancy (n, %)	31 (97%)	47 (96%)	30 (100%)	73 (94%)
Infant	**Birthweight** (mean kg, SD)	3.5 (0.5)	3.3 (0.4)	3.3 (0.4)	3.2 (0.5)
	Gestation at delivery (mean weeks, SD)	39 (1)	39 (1)	39 (1)	39 (1)
	Sex (n, % male)	17 (53%)	30 (61%)	15 (50%)	41/80 (51%)
	Apgar at 5 min (mean, SD)	8.6 (0.8)	8.9 (0.5)	8.9 (0.5)	8.9 (0.4)
	Breastfed (n, %)	32 (100%)	49 (100%)	30 (100%)	79 (99%)
	Received any formula (n, %)	5 (16%)	7 (14%)	5 (15%)	15 (19%)
	Probiotics during study (n, %)	6 (19%)	7 (14%)	5 (15%)	3 (2.5%)

*The Apgar test is performed on newborns soon after birth to check the infants **A**ppearance (skin colour), **P**ulse (heart rate), **G**rimace response (reflexes), **A**ctivity (muscle tone) and **R**espiration (breathing rate and effort). Scores are between 0 and 10.

3.2.1 Summary of key findings from the AIR Study

Analysis of the RNAseq, metagenomic and serology data in the AIR study was performed by others in the laboratory. Briefly, we found that neonates directly exposed to antibiotics had altered transcriptional profiles pre- and post-vaccination and significantly lower antibody titres against multiple vaccine antigens at 7 months, most notably in response to polysaccharides in the PCV13 pneumococcal vaccine. Consistent with data from previous studies (Neuman et al., 2018), we also found that both direct and intrapartum antibiotic exposure led to a significant reduction in the relative abundance of *Bifidobacterium* spp. in the infant microbiota prior to vaccination. Furthermore, these differences in the composition of the microbiota correlated with vaccine serological responses. Overall, these findings illustrate the profound effect on that ABX exposure has on the composition of the infant microbiota and suggest that a reduced relative abundance of *Bifidobacterium* spp. in antibiotic-exposed infants leads to impaired responses to vaccination. A more thorough presentation of these data can be found in the Appendix of this thesis (Ryan *et al.*, manuscript in preparation).*

*Removed due to copyright restriction.

3.2.2 Multiparameter flow cytometry analysis to characterise peripheral blood immune cell populations in the AIR infants

One way ABX in early life might affect responses to vaccination is by altering the frequency of different immune cell populations. In addition, it is important to examine differences in immune cell populations as they could confound RNA sequencing analysis. To determine whether there were any differences in the number or frequency of circulating immune cell populations in antibiotic-exposed infants, I performed flow cytometry analysis of fresh peripheral blood samples collected at approximately week 7 of life, one week after the infants received their first routine immunisations. A total of 156 infants (67 female, 89 male) had blood drawn at this time point and were assessed. Three multi-parameter flow cytometry panels were optimised to comprehensively phenotype immune cell populations in peripheral blood samples from the infants. The flow cytometry panels were developed in reference to those used in the Human Immunology Project (Maecker, McCoy, & Nussenblatt, 2012). Panel 1 can identify ~17 different cell types, including neutrophils, eosinophils, basophils, T cells, B cells, NK cells ($CD16^{+}CD56^{-}$, $CD16^{-}CD56^{+}$ subsets), NKT-like cells ($CD3^{+}CD56^{+}$), monocytes (classical, intermediate and nonclassical), and DCs (conventional and plasmacytoid subsets) (**Table 3.2, Fig. 3.2**). Panel 2 enabled the characterisation of ~18 functional subsets of B and T cells including naïve, central memory and effector memory $CD4^{+}$ and $CD8^{+}$ T cells; regulatory T cells; and naïve and memory B cells, as well as plasma cells (**Table 3.2, Fig. 3.3**) (Weller et al., 2004). A third panel which to assessed specific T helper subsets, including Th1, Th2, Th17, and Th22 cells, in addition to their memory subsets, was used to analyse a subset of infants (51 female, 67 male) (**Table 3.2, Fig. 3.4**). Blood samples were couriered immediately from WCH to SAHMRI for analysis of fresh, not frozen, samples. Processing

was carried out within 3 hours of the blood draw. This prevented the potential loss of cell populations sensitive to freeze-thaw cycles.

Table 3.2 Immune cell populations assessed via flow cytometry analysis in the AIR study.

Pan-leukocyte panel	
Immune cell subset	**Markers**
Eosinophils	$CD45^+SSC^{hi}CD16^-Siglec8^+$
$Fc\varepsilon RI^+$ eosinophils	$CD45^+SSC^{hi}CD16^-Siglec8^+Fc\varepsilon RI^+$
Basophils	$CD45^+SSC^{lo}CD3^-CD56^-CD14^-CD16^-CD19^-HLA\text{-}DR^-CD123^+$
$Fc\varepsilon RI^+$ basophils	$CD45^+SSC^{lo}CD3^-CD56^-CD14^-CD16^-CD19^-HLA\text{-}DR^-CD123^+Fc\varepsilon RI^+$
Neutrophils	$CD45^+SSC^{hi}CD16^+$
Classical Monocytes	$CD45^+SSC^{lo}CD3^-CD56^-CD14^{++}CD16^-$
Nonclassical Monocytes	$CD45^+SSC^{lo}CD3^-CD56^-CD14^-CD16^+$
Intermediate Monocytes	$CD45^+SSC^{lo}CD3^-CD56^-CD14^+CD16^+$
Conventional DCs (cDC)	$CD45^+SSC^{lo}CD3^-CD56^-CD14^-CD16^-CD19^-HLA\text{-}DR^+CD11c^+$
Plasmacytoid DCs (pDC)	$CD45^+SSC^{lo}CD3^-CD56^-CD14^-CD16^-CD19^-HLA\text{-}DR^+CD11c^-CD123^+$
$Fc\varepsilon RI^+$ cDCs	$CD45^+SSC^{lo}CD3^-CD56^-CD14^-CD16^-CD19^-HLA\text{-}DR^+CD11c^+Fc\varepsilon RI^+$
Lymphocytes	$FSC^{lo}SSC^{lo}$doublet discriminated
$CD16^-$ NK cells	$CD45^+SSC^{lo}CD3^-CD19^-CD56^+CD56^{++}CD16^-$
$CD16^+$ NK cells	$CD45^+SSC^{lo}CD3^-CD19^-CD56^+CD56^+CD16^+$
$CD3^+$ cells	$CD45^+SSC^{lo}CD3^+$
B and T cell panel markers	
Immune cell subset	**Markers**
$CD4^+$ T cells	$CD3^+CD56^-CD4^+$
$CD4^+CCR7^+$ T cells	$CD3^+CD56^-CD4^+CCR7^+$
$CD4^+CXCR5^-HLADR^+$ T cells	$CD3^+CD56^-CD4^+CXCR5^-HLA\text{-}DR^+$
Naïve $CD4^+$ T cells	$CD3^+CD56^-CD4^+CD45RA^+CCR7^+$
Central memory $CD4^+$ T cells	$CD3^+CD56^-CD4^+CD45RA^-CCR7^+$
Effector memory $CD4^+$ T cells	$CD3^+CD56^-CD4^+CD45RA^-CCR7^-$
Effector Memory cells re-expressing CD45RA (TemRA) $CD4^+$ T cells	$CD3^+CD56^-CD4^+CD45RA^+CCR7^-$
B cells	$CD3^-CD56^-CD19^+$
Naïve B cells	$CD3^-CD56^-CD19^+CD27^-$
IgD^+CD27^+ non-switched memory B cells/marginal zone B cells	$CD3^-CD56^-CD19^+IgD^+CD27^+$
Memory B cells	$CD3^-CD56^-CD19^+IgD^-CD27^+$
Plasmablasts	$CD3^-CD56^-CD19^{+/-}CD20^-CD27^{++}CD38^{++}$
iTreg cells	$CD3^+CD4^+CD127^-CD25^+$
$HLADR^+$ iTreg cells	$CD3^+CD4^+CD127^-CD25^+CD45RA^-HLADR^+$
$CD45RA^-$ iTreg cells	$CD3^+CD4^+CD127\text{-}CD25^+CD45RA^-$
$CD8^+$ T cells	$CD3^+CD56^-CD8^+$
Naïve $CD8^+$ T cells	$CD3^+CD56^-CD8^+CD45RA^+CD27^+$
Central memory $CD8^+$ T cells	$CD3^+CD56\text{-}CD8^+CD45RA^-CD27^+$
Effector memory $CD8^+$ T cells	$CD3^+CD56^-CD8^+CD45RA^-CD27^-$
Effector Memory cells re-expressing CD45RA (TemRA) $CD8^+$ T cells	$CD3^+CD56^-CD8^+CD45RA^+CCR7^-$
$CD8^+$ Tregs	$CD8^+CD25^+CD127^+$

Extended T cell panel markers	
Immune cell subset	**Markers**
Th1 cells	$CD3^+CD4^+CCR4^+CCR3^+$
Th2 cells	$CD3^+CD4^+CCR4^+CCR6^-$
Th17 cells	$CD3^+CD4^+CCR4^+CCR6^+CCR10^-CXCR3^-$
Th22 cells	$CD3^+CD4^+CCR4^+CCR6^+CCR10^+$
NKT cells	$CD3^+CD1d\text{-}tet^+$
$CD45RA^-$ $CD4^+$ T cells	$CD3^+CD4^+CD45RA^-$
Th1 memory cells (mTh1)	$CD3^+CD4^+CD45RA^-CCR4^-CXCR3^+$
Th2 memory cells (mTh2)	$CD3^+CD4^+CD45RA^-CCR4^-CXCR3^+CCR4^+CCR6^-$
$CD45RA^-$ $CD8^+$ T cells	$CD3^+CD8^+CD45RA^-$
$CD45RA^-$ $CD8^+$ Tc1 cells	$CD3^+CD8^+CD45RA^-CCR4^-CCR10^+$
$CCR6^+CCR10^-$ $mCD8^+$ T cells	$CD3^+CD8^+CD45RA^-CCR6^+CCR10^-$

The Spectre R package was used to undertake an initial exploratory analysis of the pan-leukocyte flow cytometry panel data (Ashhurst et al., 2022). The analysis began with clustering the data using FlowSOM, a scalable and efficient method for clustering large datasets. The resulting clustered data was then down-sampled, and UMAP dimensionality reduction was performed to enable visualisation of the data and identification of clusters present in the dataset (**Appendix Fig. S2.1**). Expression levels of each marker are represented as a heatmap overlaid on each cluster. For instance, distinct $CD3^+$ and $CD19^+$ clusters were observed that corresponded to T and B cell populations and CD15 and CD16 were co-expressed on the neutrophil cluster.

*Removed due to copyright restriction.

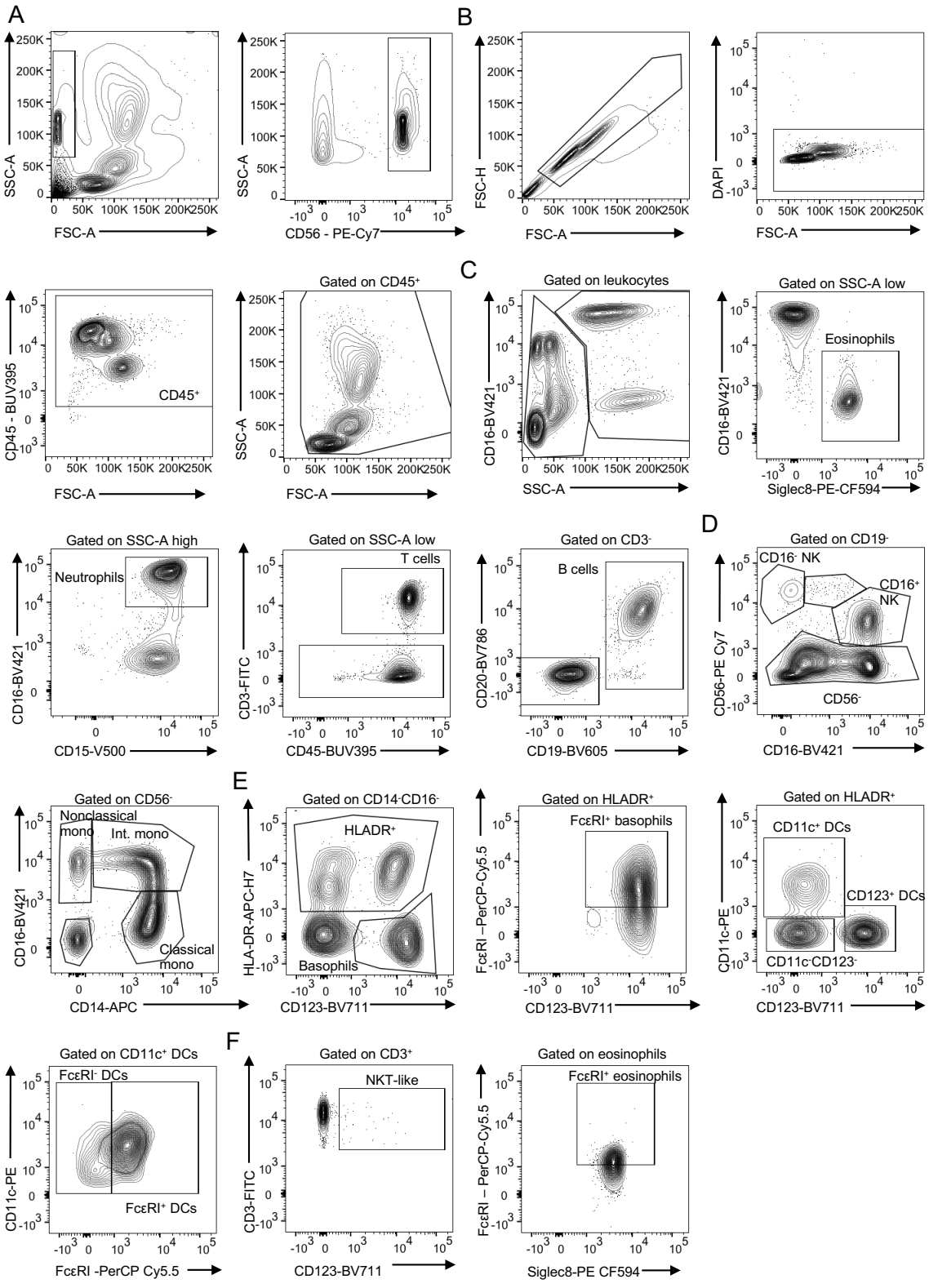

Figure 3.2| Pan-leukocyte panel gating strategy. A| Beads from each Trucount tube were recorded from the FSCxSSC gate and then the PE^{hi} population. **B|** For all pan-leukocyte panel analyses, cells were gated by singlet discrimination, followed by live ($DAPI^-$), $CD45^+$ and $CD45^+$ leukocytes. **C|** Leukocytes were split into SSC high and low populations. Eosinophils and neutrophils were gated on SSC low and high populations, respectively. T cells were gated on SSC low $CD3^{hi}$ and $CD3^-$ cells were further defined as $CD19^+CD20^+$ B cells. **D|** The $CD19^-$

population was gated on to define $CD16^{-}CD56^{+}$ NK cells. $CD56^{-}$ cells were further gated on CD16 and CD14 expression identifying monocyte populations. **E|** Remaining $CD14^{-}CD16^{-}$ cells were further gated on HLA-DR and CD123 expression to identify $CD123^{+}HLA\text{-}DR^{-}$ basophils. Basophils were further gated based on the positive expression of FcεRI. $HLA\text{-}DR^{+}$ cells were gated on CD11c and CD123 to identify various DC populations. Conventional $CD11c^{+}$ DCs were further gated based on their expression of FcεRI. **F|** $CD3^{+}$ T cells were gated further on their CD56 expression to identify $CD56^{+}CD3^{+}$ NKT-like cells. An additional $Fc\varepsilon RI^{+}$ population was also gated from the eosinophil gate.

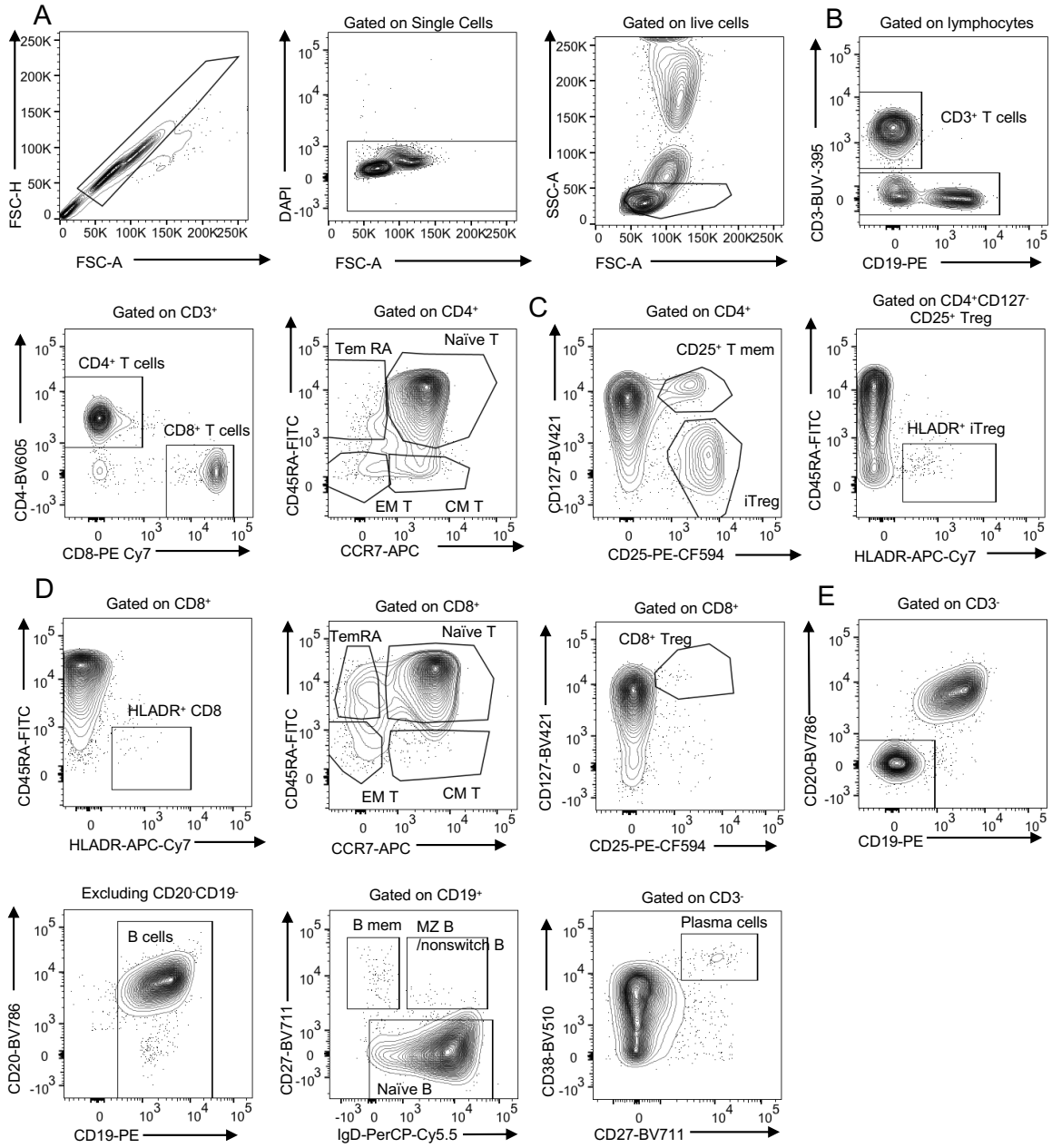

Figure 3.3| B and T cell panel gating strategy. A| For all B and T cell panel analyses, cells were gated by singlet discrimination, live ($DAPI^-$) and for leukocytes ($SSC\text{-}A^{lo}$) **B|** $CD3^+$ T cells were gated on $CD4^+$ and $CD8^+$ expression. $CD4^+$ T cells were then defined as $CD45RA^+HLADR^-$ TemRA $CD4^+$ T cells, $CCR7^+CD45RA^+$ Naïve $CD4^+$ T cells (naïve T), $CCR7^+CD45RA^-$ CD4 central memory T cells (T_{CM}), $CCR7^-CD45RA^-$ $CD4^+$ effector memory T cells (T_{EM}). **C|** $CD4^+$ T cells were also gated on CD127 and CD25 expression to identify $CD127^-CD25^+$ iTregs, further gated for CD45RA and HLADR expression to identify $CD45RA^-$ $HLADR^+$ iTregs. **D|** $CD8^+$ T cells were then defined as $CD45RA^+HLADR^-$ $CD8^+$ TemRA T cells, $CCR7^+CD45RA^+$ Naïve CD8 T cells (naïve T), $CCR7^+CD45RA^-$ $CD8^+$ central memory T cells (T_{CM}), $CCR7^-CD45RA^-$ $CD8^+$ effector memory T cells (T_{EM}). A population of $CD8^+CD25^+CD127^+$ Tregs was also identified from the $CD8^+$ T cell gate. **E|** The $CD3^-$ population from B| was gated further on CD20 and CD19 so that $CD20^-CD19^-$ cells could be gated out and $CD19^+$ B cells could then be identified. These were further divided into a CD38 and CD20 gate to identify $CD38^+CD20^-$ plasma cells and an IgD and CD27 gate was applied to identify IgD^-CD27^+ Memory B cells, IgD^+CD27^+ non-switched memory B cells/marginal zone-like B cells and IgD^- naïve B cells.

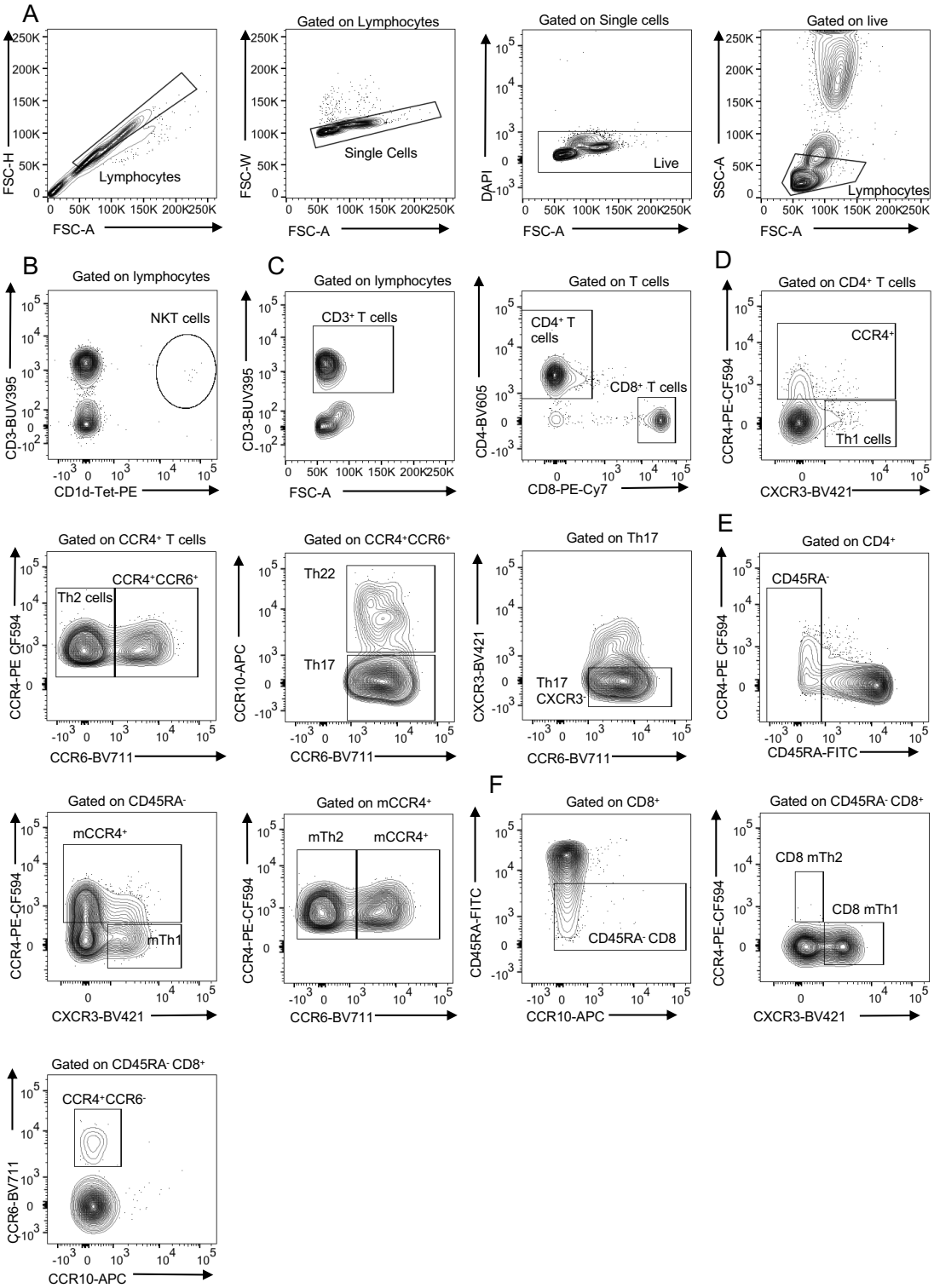

Figure 3.4| Extended T cell panel gating strategy. A| For all extended T cell panel analyses, cells were gated by singlet discrimination, live ($DAPI^-$) and leukocytes ($SSC\text{-}A^{lo}$). **B|** NKT cells were identified using a tetramer specific for CD1d. **C|** $CD3^+$ T cells were gated on $CD4^+$ and $CD8^+$ expression. **D|** $CD4^+$ T cells were then defined as $CCR4^+$ $CCR3^+$ Th1 cells and $CCR4^+$ $CD4^+$ T cells. This $CCR4^+$ gate was used to define $CCR4^+CCR6^-$ Th2 cells and $CCR4^+CCR6^+$ cells. The $CCR4^+CCR6^+$ cells were further gated to identify $CCR10^+CCR6^+$ Th22 cells and $CCR10^-CCR6^+$ Th17 cells. Th17 cells could be further distinguished by identifying the $CXCR3^-$ population of Th17 cells. **E|** $CD45^-$ T cells were identified using the $CD4^+$ T cell gate. This $CD45^-$ T cell gate was used to identify $CCR4^-CXCR3^+$ Th1 memory cells (mTh1) and a $CCR4^+$

memory population that was further gated to identify $CCR4^{+}CCR6^{-}$ Th2 memory cells (mTh2). **F|** Finally the $CD8^{+}$ T cell gate was further gated on the $CD45^{-}$ population to identify $CD45RA^{-}$ $CD8^{+}$ cells. This population was further gated to identify $CCR4^{+}CCR10^{-}$ $CD8^{+}$ mTh2 cells and $CCR10^{+}CCR4^{-}$ $CD8^{+}$ mTh1 cells. Finally, the $CD45RA^{-}$ $CD8^{+}$ population was also gated on to identify a $CCR6^{+}CCR10^{-}$ population.

3.2.3 Differences in immune cell populations due to biological sex

The AIR study collected comprehensive data on the demographics of enrolled infants, including information on sex, gestational age, breastfeeding, probiotic usage, etc. (**Table 3.1**). Many immunological factors are known to vary between the sexes throughout life (Klein & Flanagan, 2016), and consistent with this one of the most discernible differences in immune cell populations in the peripheral blood was sex (**Fig. 3.5)**. For example, female infants had significantly (P = 0.0078) higher numbers of $CD4^+$ T cells compared to male infants (**Fig. 3.5A**). Female infants also had significantly (P = 0.0077) higher numbers of naïve $CD4^+$ T cells compared to male infants, probably driving these overall differences in $CD4^+$ T cells (**Fig. 3.5B**). Similar sex differences were reported previously in another cohort of Australian infants (Collier et al., 2015). Significantly higher (P = 0.0363) numbers of Th1 cells were also observed in female infants (**Fig. 3.5C**). Previous studies have shown that female cord blood contains higher numbers of $CD4^+$ T cells and a higher ratio of $CD4^+/CD8^+$ T cells (van Gent et al., 2009). Male infants in the AIR study, however, did not have significantly lower numbers of total $CD8^+$ T cells or NK cells (**Appendix Fig. S2.3**), as has been reported in some other studies (Lee et al., 1996, Lisse et al., 1997, Uppal, Verma, & Dhot, 2003). Male infants in the AIR study did, however have lower effector memory (EM) $CD8^+$ T cells compared to female infants (**Fig. 3.5D**). The differences between studies may be due to population-specific effects as the two studies referenced above involved Asian and West African infants (Lee et al., 1996, Lisse et al., 1997), whereas the AIR study was conducted in South Australia.

Female infants also had significantly higher numbers of iTregs than male infants (**Fig. 3.5E**). iTregs play a crucial role in the regulation of Th1 and Th2 responses and are

critical for regulating autoimmunity and allergic responses (Lu et al., 2008; Wei et al., 2008). Female infants also had a modestly higher number of CD45RA$^-$ iTreg cells compared to male infants (**Fig. 3.5F)**. CD45RA$^-$ Tregs are a highly immunosuppressive cell type often referred to as effector Tregs that have been found at a higher frequency in infants that were predominantly colonised with Firmicutes compared to those predominantly colonised with *E.coli* (Silva-Neta et al., 2018; Ihara et al., 2017). As they are a CD4$^+$ T cell population, differences in this population may also contribute to overall differences in CD4$^+$ T cells between males and females. Previous studies have not reported differences in Treg populations between male and female Australian infants, but these studies assessed the proportion of resting naïve T regulatory cells (rTreg; CD4$^+$CD45RA$^+$FoxP3$^+$) and activated Tregs (aTreg, CD4$^+$CD45RA$^-$FoxP3^{high}) using the FoxP3 marker instead of CD127 and CD25 (Collier et al., 2015).

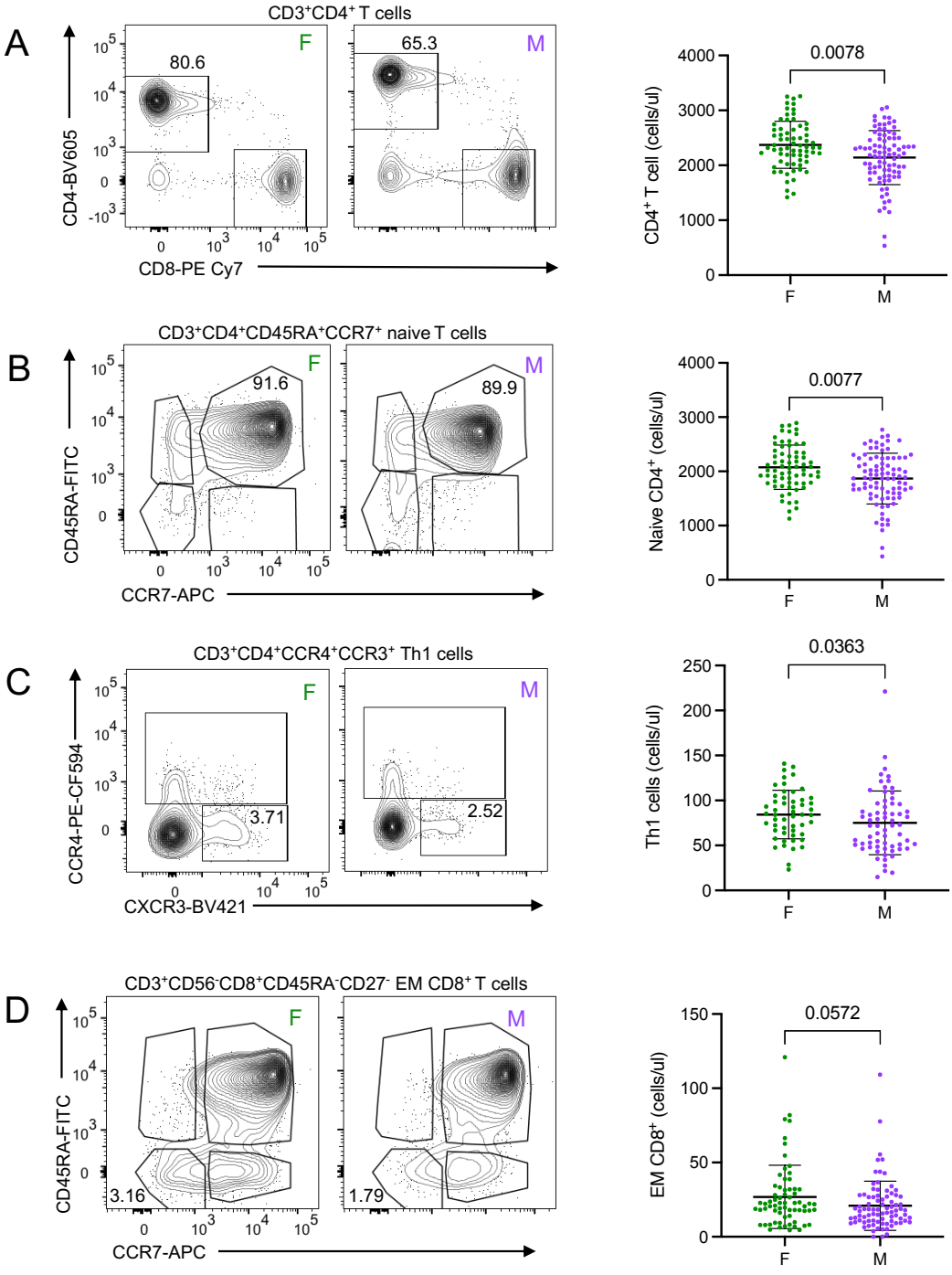
A
CD3+CD4+ T cells
F
M
80.6
65.3
CD4-BV605
CD8-PE Cy7
CD4+ T cell (cells/ul)
0.0078
B
CD3+CD4+CD45RA+CCR7+ naive T cells
91.6
89.9
CD45RA-FITC
CCR7-APC
Naive CD4+ (cells/ul)
0.0077
C
CD3+CD4+CCR4+CCR3+ Th1 cells
3.71
2.52
CCR4-PE-CF594
CXCR3-BV421
Th1 cells (cells/ul)
0.0363
D
CD3+CD56-CD8+CD45RA-CD27- EM CD8+ T cells
3.16
1.79
CD45RA-FITC
CCR7-APC
EM CD8+ (cells/ul)
0.0572

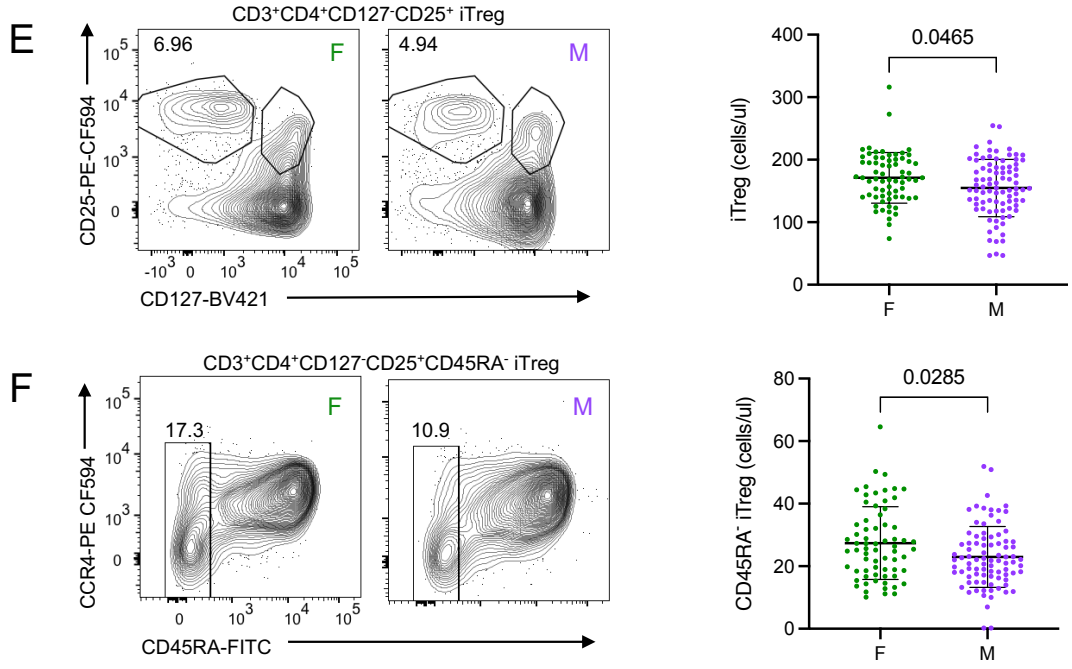

Figure 3.5| Sex-specific differences in infant peripheral blood T cell populations. Representative gating and the absolute number of **A|** $CD4^+$ T cells ($CD3^+CD4^+$), **B|** Naïve $CD4^+$ T cells ($CD3^+CD4^+CD45RA^+CCR7^+$), **C|** Th1 cells ($CD3^+CD4^+CCR4^+CCR3^+$), **D|** Effector Memory $CD8^+$ T cells ($CD3^+CD8^+CD45RA^-CCR7^-$), **E|** Tregs ($CD3^+CD4^+CD127^-CD25^+$) and **F|** $CD45RA^-$ Tregs ($CD3^+CD4^+CD127^-CD25^+CD45RA^-$) grouped by sex. Data are represented as the mean ± SEM. Statistical significance was assessed using a Mann-Whitney test as data were not normally distributed. F = Female, M= Male.

3.2.4 Infant circulating immune cell population counts were not significantly different between antibiotic exposure groups

Next, I assessed the differences in immune cell populations in infants based on their antibiotic exposure status. Each exposure group was assessed in comparison to the unexposed (no ABX) infants. No significant differences in immune cell populations were observed in any pan-leukocyte or B and T cell panel population when grouped by antibiotic exposure (**Fig. 3.6-7**). In addition, there were no differences in antibiotics-exposed infants in the subset of infants assessed in the extended T cell panel compared to unexposed infants (**Fig. 3.8**).

To assess differences in immune cell populations according to their frequencies, immune cell populations from each panel were graphed according to frequency of their parent populations. Differences were assessed in each exposure group compared to unexposed infants. Immune cell populations from the pan-leukocyte panel were also assessed as a frequency of $CD45^+$ cells (**Appendix Fig. S2.5**). The populations from the B and T cell and extended T cell panels were additional assessed by exposure group as a frequency of $CD4^+$, $CD8^+$ or $CD19^+$ cells. No significant differences were found (**Appendix Fig. S2.6-S2.7**).

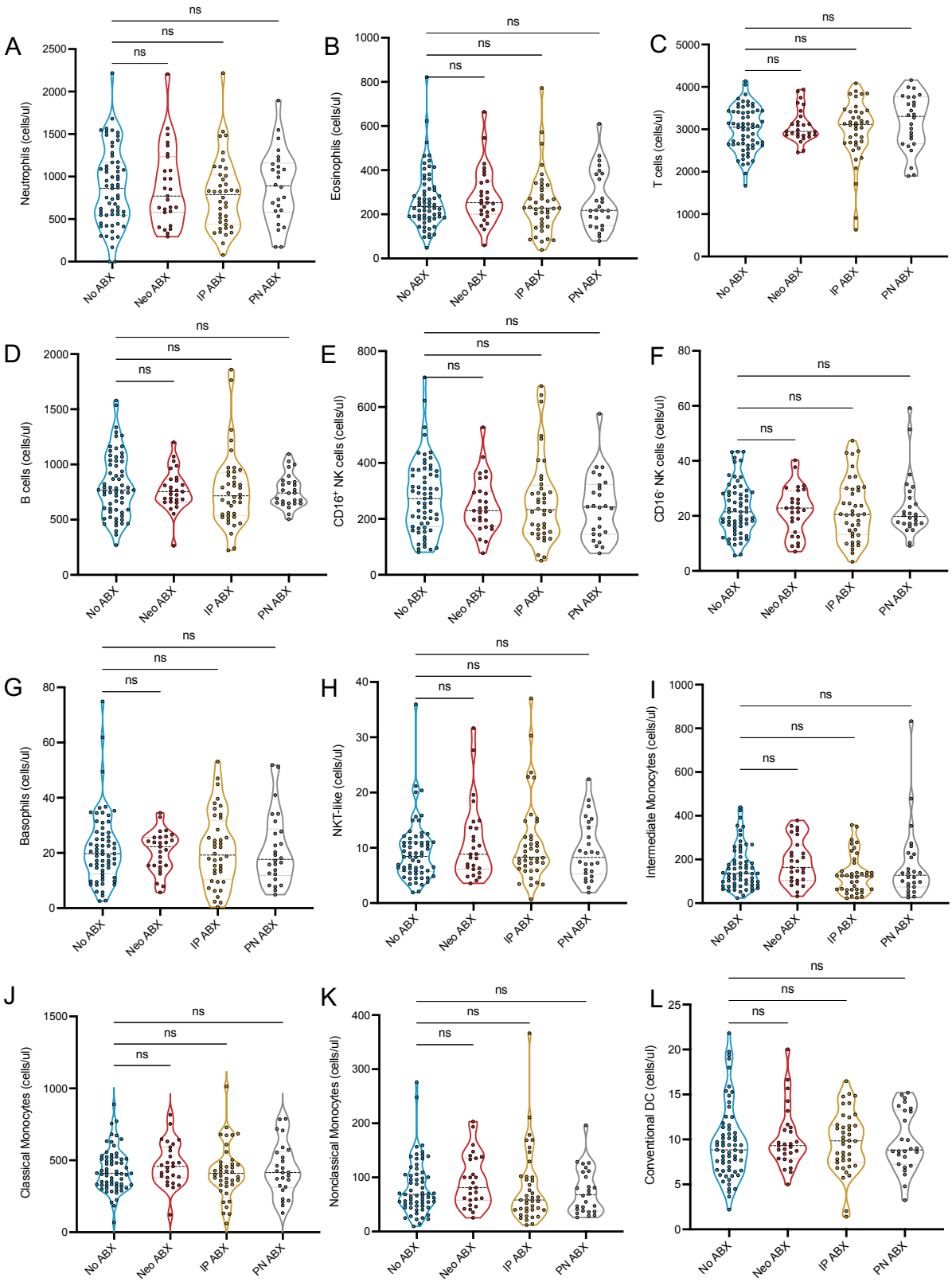
A
Neutrophils (cells/ul)
B
Eosinophils (cells/ul)
C
T cells (cells/ul)
D
B cells (cells/ul)
E
CD16+ NK cells (cells/ul)
F
CD16- NK cells (cells/ul)
G
Basophils (cells/ul)
H
NKT-like (cells/ul)
I
Intermediate Monocytes (cells/ul)
J
Classical Monocytes (cells/ul)
K
Nonclassical Monocytes (cells/ul)
L
Conventional DC (cells/ul)
ns
No ABX
Neo ABX
IP ABX
PN ABX

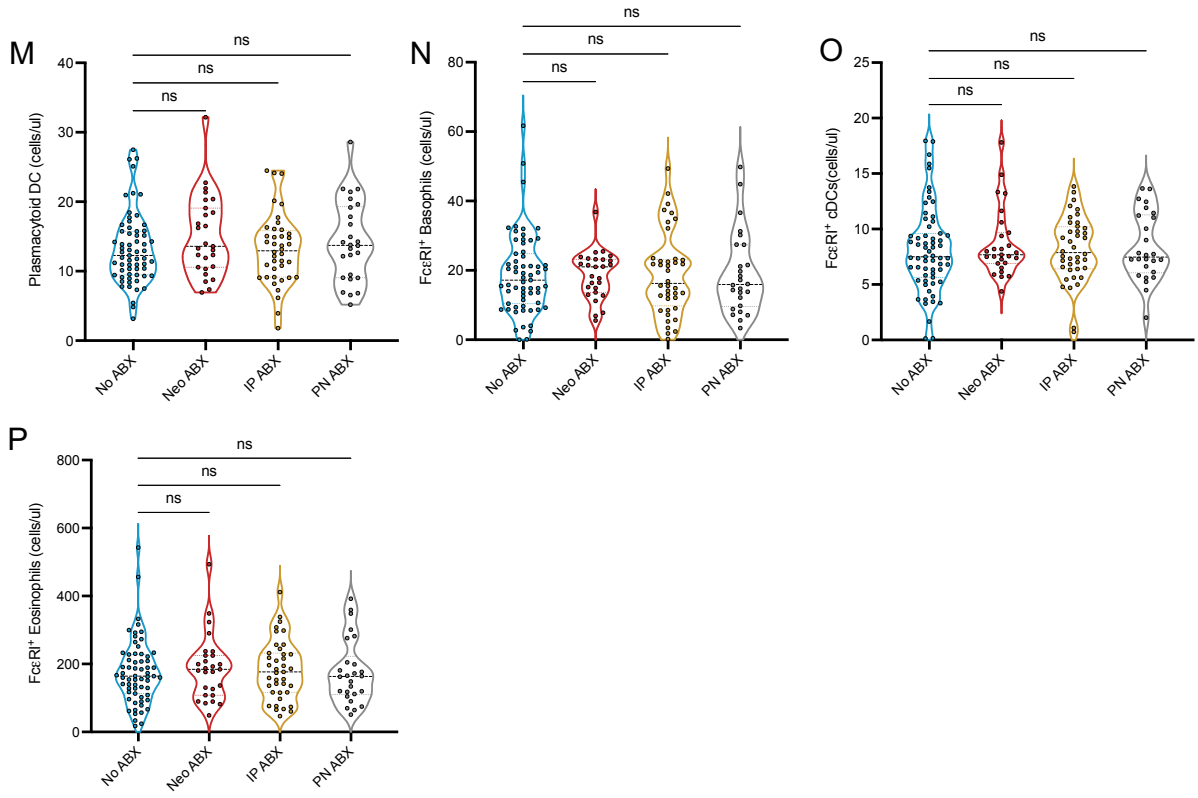

Figure 3.6| No significant differences in the circulating immune cell populations defined using the pan-leukocyte panel when assessed by antibiotic exposure group. The absolute number of **A|** Neutrophils ($SSC^{hi}CD16^{+}$), **B|** Eosinophils ($SSC^{hi}CD16^{-}Siglec8^{+}$), **C|** T cells ($SSC^{lo}CD3^{+}$), **D|** B cells ($CD3^{-}CD56^{-}CD19^{+}$), **E|** $CD16^{+}$ NK cells ($SSC^{lo}CD3^{-}CD19^{-}CD56^{+}CD56^{+}CD16^{+}$), **F|** $CD16^{-}$ NK cells ($SSC^{lo}CD3^{-}CD19^{-}CD56^{+}CD56^{++}CD16^{-}$), **G|** Basophils ($SSC^{lo}CD3^{-}CD56^{-}CD14^{-}CD16^{-}CD19^{-}HLA\text{-}DR^{-}CD123^{+}$), **H|** NKT-like cells ($CD3^{+}CD56^{+}$), **I|** Intermediate Monocytes ($SSC^{lo}CD3^{-}CD56^{-}CD14^{+}CD16^{+}$), **J|** Classical Monocytes ($SSC^{lo}CD3^{-}CD56^{-}CD14^{++}CD16^{-}$), **K|** Nonclassical Monocytes ($SSC^{lo}CD3^{-}CD56^{-}CD14^{-}CD16^{+}$), **L|** Conventional DCs ($SSC^{lo}CD3^{-}CD56^{-}CD14^{-}CD16^{-}CD19^{-}HLA\text{-}DR^{+}CD11c^{+}$), **M|** Plasmacytoid DC ($SSC^{lo}CD3^{-}CD56^{-}CD14^{-}CD16^{-}CD19^{-}HLA\text{-}DR^{+}CD11c^{-}CD123^{+}$), **N|** $FcεRI^{+}$ basophils ($SSC^{lo}CD3^{-}CD56^{-}CD14^{-}CD16^{-}CD19^{-}HLA\text{-}DR^{-}CD123^{+}FcεRI^{+}$) **O|** $FcεRI^{+}$ cDCs ($SSC^{lo}CD3^{-}CD56^{-}CD14^{-}CD16^{-}CD19^{-}HLA\text{-}DR^{+}CD11c^{+}FcεRI^{+}$) and **P|** $FcεRI^{+}$ eosinophils ($SSC^{hi}CD16^{-}Siglec8^{+}FcεRI^{+}$). All cell populations are $CD45^{+}$. Kruskal-Wallis tests were used to assess statistical significance. Dunn's multiple comparison tests was used to correct for multiple comparisons within each graph. Data are represented as a Violin plot, with the thick dashed representing the median and thinner dashed lines representing the quartiles. ns = not significant.

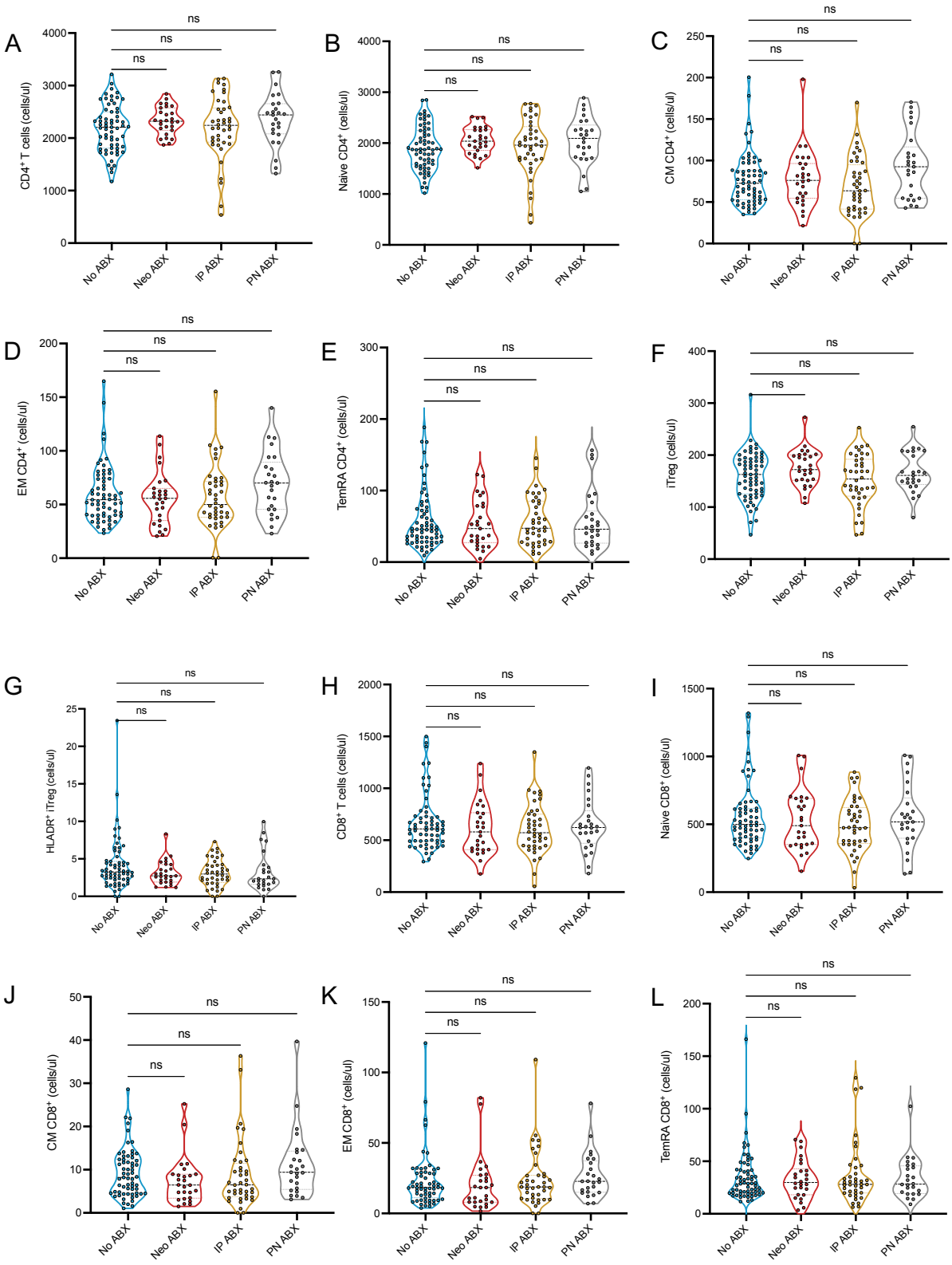
A
CD4+ T cells (cells/ul)
B
Naive CD4+ (cells/ul)
C
CM CD4+ (cells/ul)
D
EM CD4+ (cells/ul)
E
TemRA CD4+ (cells/ul)
F
iTreg (cells/ul)
G
HLADR+ iTreg (cells/ul)
H
CD8+ T cells (cells/ul)
I
Naive CD8+ (cells/ul)
J
CM CD8+ (cells/ul)
K
EM CD8+ (cells/ul)
L
TemRA CD8+ (cells/ul)
ns
No ABX
Neo ABX
IP ABX
PN ABX

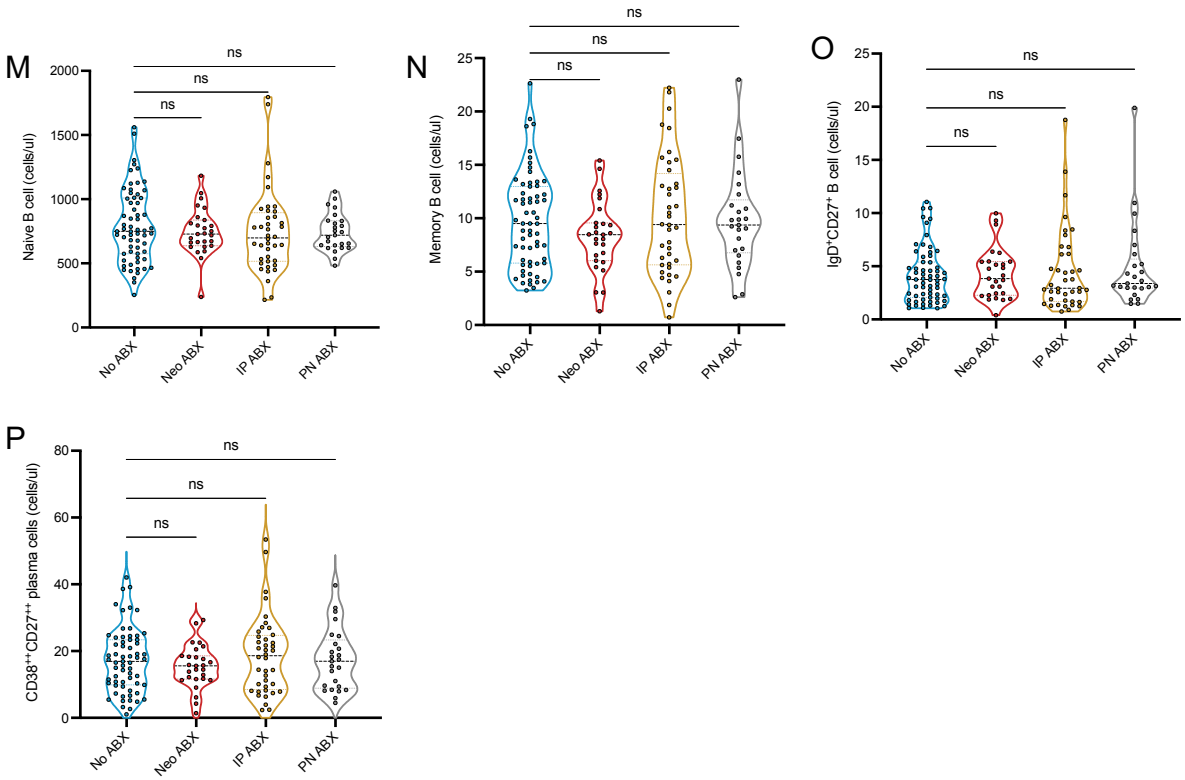

Figure 3.7| No significant differences in the majority of circulating B and T cell populations when assessed by antibiotic exposure group. The absolute number of **A|** $CD4^+$ T cells ($CD3^+CD56^-CD4^+$), **B|** Naïve $CD4^+$ T cells ($CD3^+CD56^-CD4^+CD45RA^+CCR7^+$), **C|** Central Memory $CD4^+$ T cell (T_{CM}) ($CD3^+CD56^-CD4^+CD45RA^-CCR7^+$), **D|** Effector Memory $CD4^+$ T (T_{EM}) cell ($CD3^+CD56^-CD4^+CD45RA^-CCR7^-$), **E|** TemRA $CD4^+$ T cells **(**$CD3^+CD56^-CD4^+CD45RA^+CCR7^-$) **F|** iTreg cells ($CD3^+CD4^+CD127^-CD25^+$) **G|** $HLADR^+CD45RA^-$ $CD4^+$ T cells. **H|** $CD8^+$ T cells **I|** Naïve $CD8^+$ T cells ($CD3^+CD56^-CD8^+CD45RA^+CD27^+$) **J|** Central memory $CD8^+$ T cells ($CD3^+CD56$-$CD8^+CD45RA^-CD27^+$), **K|** Effector Memory $CD8^+$ T cells ($CD3^+CD56^-CD8^+CD45RA^-CD27^-$), **L|** TemRA $CD8^+$ T cells ($CD3^+CD56^-CD8^+CD45RA^+CCR7^-$) **M|** Naïve B cells ($CD3^-CD56^-CD19^+CD27^-$), **N|** Memory B cells ($CD3^-CD56^-CD19^+IgD^-CD27^+$) **O|** IgD^+CD27^+ non-switched memory B cells/marginal zone B cells ($CD3^-CD56^-CD19^+IgD^+CD27^+$) and **P|** $CD38^{++}CD27^{++}$ plasma cells ($CD3^-CD56^-CD19^{+/-}CD20^-CD27^{++}CD38^{++}$). Kruskal-Wallis tests were used to assess statistical significance. Dunn's multiple comparison test was used to correct for multiple comparisons within each graph. Data are represented as a Violin plot, with the thick dashed representing the median and thinner dashed lines representing the quartiles. ns = not significant.

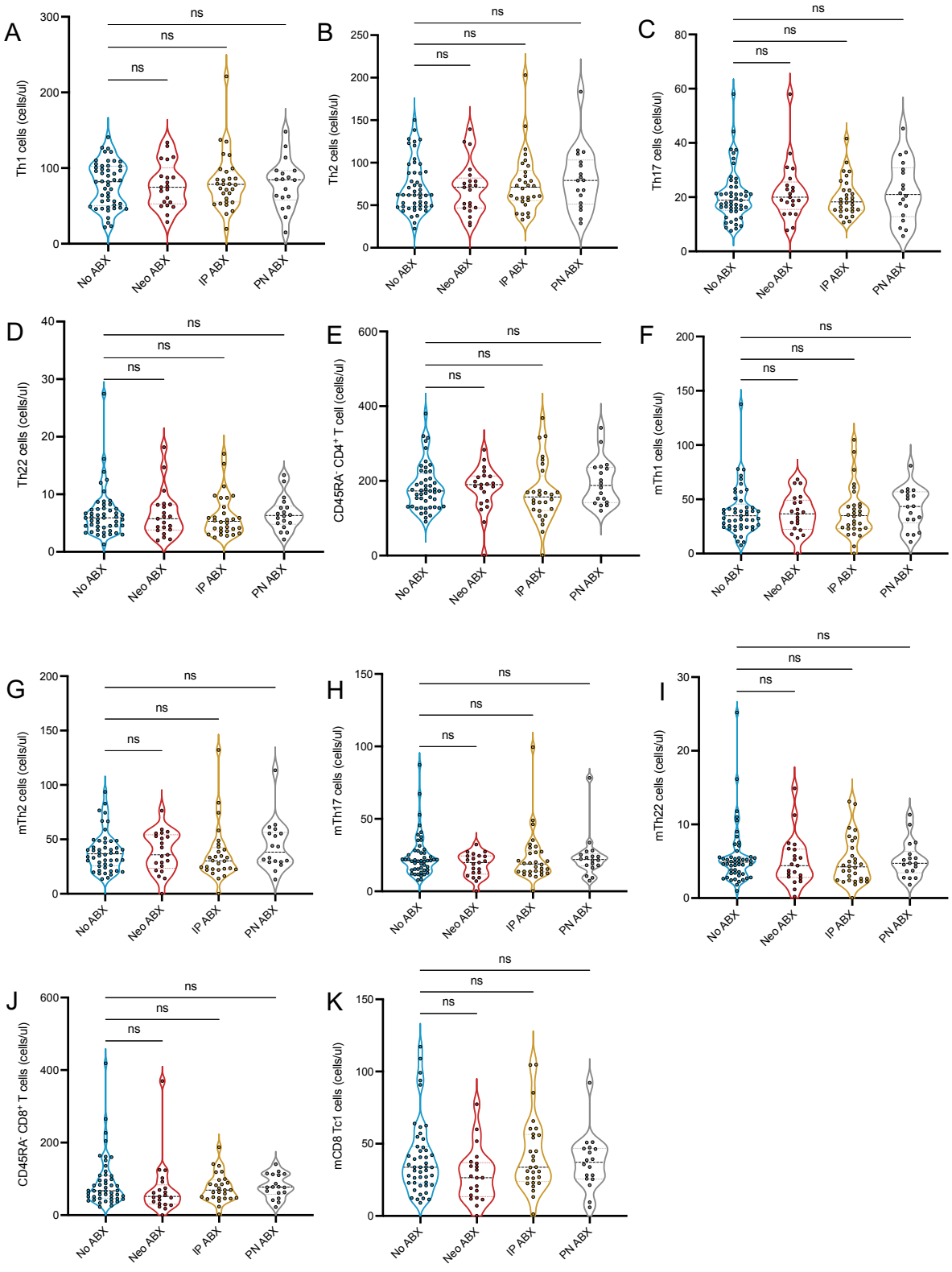

Figure 3.8| No significant differences in the circulating immune cell populations defined using the extended T cell panel when assessed by antibiotic exposure group. The absolute number of **A|** Th1 cells ($CD3^+CD4^+CCR4^+CCR3^+$), **B|** Th2 cells ($CD3^+CD4^+CCR4^+CCR6^-$), **C|** Th17 cells ($CD3^+CD4^+CCR4^+CCR6^+CCR10^-CXCR3^-$), **D|** Th22 cells ($CD3^+CD4^+CCR4^+CCR6^+CCR10^+$), **E|** $CD45RA^-$ $CD4^+$ T cells($CD3^+CD8^+CD45RA^-$), **F|** Th1 memory cells ($CD3^+CD4^+CD45RA^-CCR4^-CXCR3^+$), **G|** Th2 memory cells

($CD3^+CD4^+CCR4^+CCR6^-$), **H|** Th17 memory cells ($CD3^+CD4^+CCR4^+CCR6^+CCR10^-CXCR3^-$), **I|** Th22 memory cells ($CD3^+CD4^+CCR4^+CCR6^+CCR10^+$), **J|** $CD45RA^-$ $CD8^+$ T cells ($CD3^+CD8^+CD45RA^-$) and **K|** $CD8^+$ Tc1 memory cells ($CD3^+CD8^+CD45RA^-CCR4^-CCR10^+$). Kruskal-Wallis test was used to assess statistical significance. Dunn's multiple comparison test was used to correct for multiple comparisons within each graph. Data are represented as a Violin plot, with the thick dashed representing the median and thinner dashed lines representing the quartiles. ns = not significant.

3.2.5 Maternal intrapartum antibiotic exposure is associated with a reduced number of Tregs in the peripheral blood

Interestongly, there was a modest reduction in $CD45RA^-$ Tregs was observed in infants exposed to intrapartum antibiotics compared to unexposed infants (**Fig. 3.9A-B**). As mentioned above, there was a significant effect of sex on this population, but a reasonably even spread of sexes in each group and these differences were robust to statistical adjustment for sex (data not shown). These data suggest that maternal antibiotic exposure may impact the development of the infant's immune system in early life. In mice, maternal antibiotic exposure has been shown to impact the numbers of maternal splenic Tregs but did not affect placental Tregs (Benner et al., 2021).

To assess differences in cell frequency, $CD45RA^-$ iTregs cell subsets were also assessed as a frequency of live, total T cells, $CD4^+$ T cells and its parent iTreg population (**Fig. 3.10A-D**). There were no statistically significant differences in $CD45RA^-$ iTregs when grouped as a frequency of each parent population (**Fig. 3.10A-D**). Future studies are needed to better understand the implications of reduced $CD45RA^-$ iTregs in infants exposed to intrapartum antibiotics.

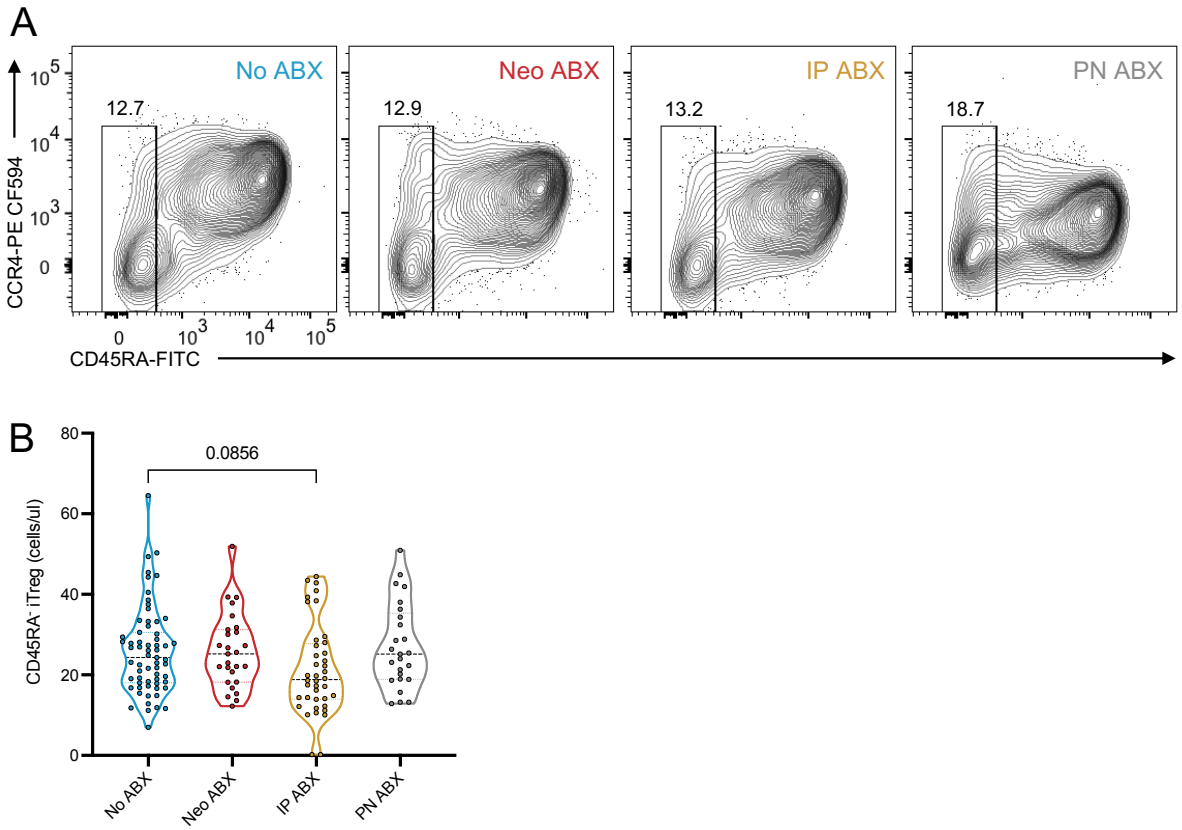

Figure 3.9| The number of CD45RA- iTregs were reduced in infants exposed to intrapartum antibiotics (IP ABX). A| Representative plots of CD45RA$^-$ Tregs ($CD3^+CD4^+CD127\text{-}CD25^+CD45RA^-$) and **B|** CD45RA$^-$ Tregs graphed by antibiotic exposure group. Kruskal-Wallis test was used to assess statistical significance. Dunn's multiple comparison test was used to correct for multiple comparisons within each graph. Data are represented as a Violin plot, with the thick dashed representing the median and thinner dashed lines representing the quartiles.

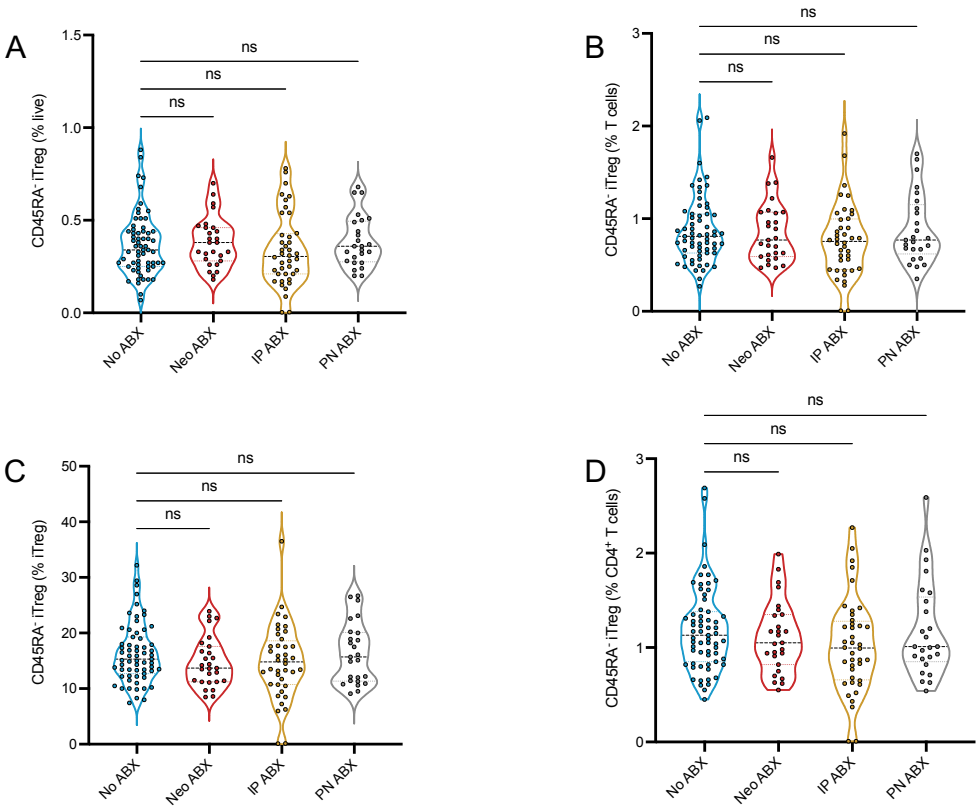

Figure 3.10| No significant differences in CD45RA$^-$ iTregs as a frequency of live and parent populations when grouped by infant ABX exposure group. CD45RA$^-$ Tregs graphed by antibiotic exposure group as a frequency of **A|** live cells, **B|** total T cells, **C|** total iTregs, and **D|** CD4$^+$ T cells. Kruskal-Wallis test was used to assess statistical significance. Dunn's multiple comparison test was used to correct for multiple comparisons within each graph. Data are represented as a Violin plot, with the thick dashed representing the median and thinner dashed lines representing the quartiles.

3.2.6 Correlations between immune cell populations and antibody responses to vaccination

To assess whether circulating immune cell populations at 7 weeks of age were correlated with subsequent antibody responses at 7 months of life, Spearman correlation analysis was performed with the month 7 serology data. The month 7 serology data was adjusted for sex, age and batch prior to correlation with linear regression analysis. The serology data was adjusted for baseline differences in antibody titres. Several statistically significant ($P < 0.05$) correlations were observed (**Fig. 3.11**). For example, the number of HLA-DR$^+$ iTreg cells in the blood at 7 weeks of age was significantly positively correlated

with IgG responses to several different polysaccharides in the PCV13 vaccine (PPS4, PPS5 and PPS18C) and with many of the antigens in the Infanrix hexa vaccine including diphtheria (DT), tetanus (TT) and pertussis toxoid (PT) and the pertussis filamentous hemagglutinin (FHA) and pertactin (PRN) proteins. $CD8^+$ Tc1m cells and their parent population, $CD45RA^-CD8^+$ T cells, were also significantly positively correlated with IgG titres against the majority of polysaccharides in the PCV13 vaccine as well as TT and to the Hib capsular polysaccharide polyriboseribitolphosphate (PRP). Several other immune cell populations were correlated with DT, including $CD8^+$ T_{EM} cells, $CD45RA^-$ iTregs, $CD4^+$ T_{EM} cells, and Th22 cells. Th22 and Th22m cells were correlated with FHA and PRN, while Th17m cells were correlated with FHA and PT. Several immune cell populations were also significantly negatively correlated with antibody titres against specific vaccine antigens (**Fig. 3.11**). For example, Th17 cells were significantly negatively associated with IgG titres against four polysaccharides in the PCV13 vaccine as well as PRP. Th2 cells and non-switched memory B cells/marginal zone B cells were negatively correlated with anti-TT IgG titres. Classical monocytes had a strong negative association with anti-FHA IgG titres. No significant correlations were detected between any immune cell populations and IgA responses to ORV.

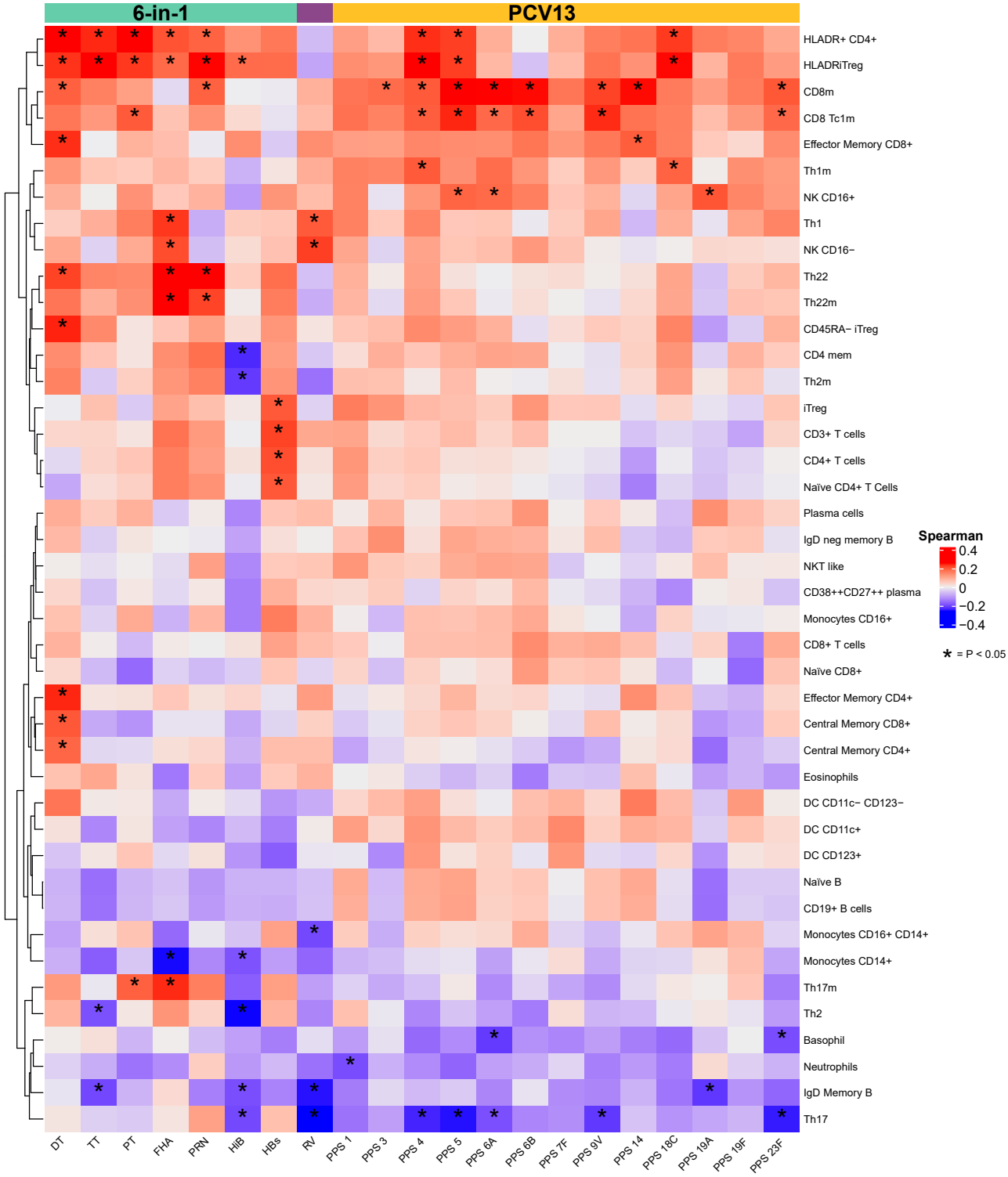

Figure 3.11| Correlations between circulating immune cell populations at week 7 of life and subsequent vaccine antibody responses at 7 months. The heatmap was generated in R Studio using ggplot2. Statistical significance was assessed via linear regression adjusting for sex, age and time at which the sample was collected during the study. *p < 0.05

3.2.7 Differences in peripheral blood immune cell populations in infants grouped by metagenomically-defined community sub-type

The effects of antibiotics on the composition of the gut microbiota are not uniform, and depending on factors such as the dose and type of antibiotic used, what species are sensitive to the specific antibiotic used, and which species colonise post-antibiotic exposure, can vary significantly between different individuals (S. Kim, Covington, & Pamer, 2017). Shotgun metagenomic sequencing and Dirichlet multinomial mixtures (DMM) modelling (carried out by Dr Feargal Ryan) revealed that infants in the AIR study could be grouped into distinct community types based on the composition of the microbiota at week 6. The 6 DMM groups were defined as; DMM-1 consisting mainly of *Klebsiella/Bacillota* (Firmicutes), DMM-2 were *B. breve* enriched, DMM-3 were *B. longum* enriched, DMM-4 were *Bacteroidota* (Bacteroidetes) enriched, DMM-5 were *E. coli* enriched and DMM-6 were *B. pseudocatenulatum* enriched (Ryan *et al.*, manuscript in preparation). The counts of immune cell populations at 7 weeks of age were compared across the 6 different groups to assess whether there were differences in peripheral blood immune cell populations based on these metagenomically-defined groups (**Appendix Fig. S2.8-2.10**). DMM-2 was chosen *a priori* as the reference group for these comparisons as this group consisted predominatly of No ABX infants (17/26) who responded well to vaccination. In addition to this, choosing a reference group prevents an excessive number of comparisons which reduces statistical power.

Infants in the *B. breve* enriched group (DMM-2) had significantly higher numbers of effector memory $CD8^+$ T cells than infants with a *B. longum* enriched microbiota (DMM-3) (**Fig. 3.12A**). Additionally, DMM-2 infants had modestly higher numbers of central

memory $CD8^+$ T cells, $CD45RA^-CD8^+$ T cells and $mCD8^+$ Tc1 cells than DMM-3 infants (**Fig. 3.12B-D)**. Interestingly, DMM-3 infants also had significantly lower responses to the PCV13 vaccine polysaccharide, PPS4, compared to DMM-2 infants (Ryan *et al.*, manuscript in preparation).

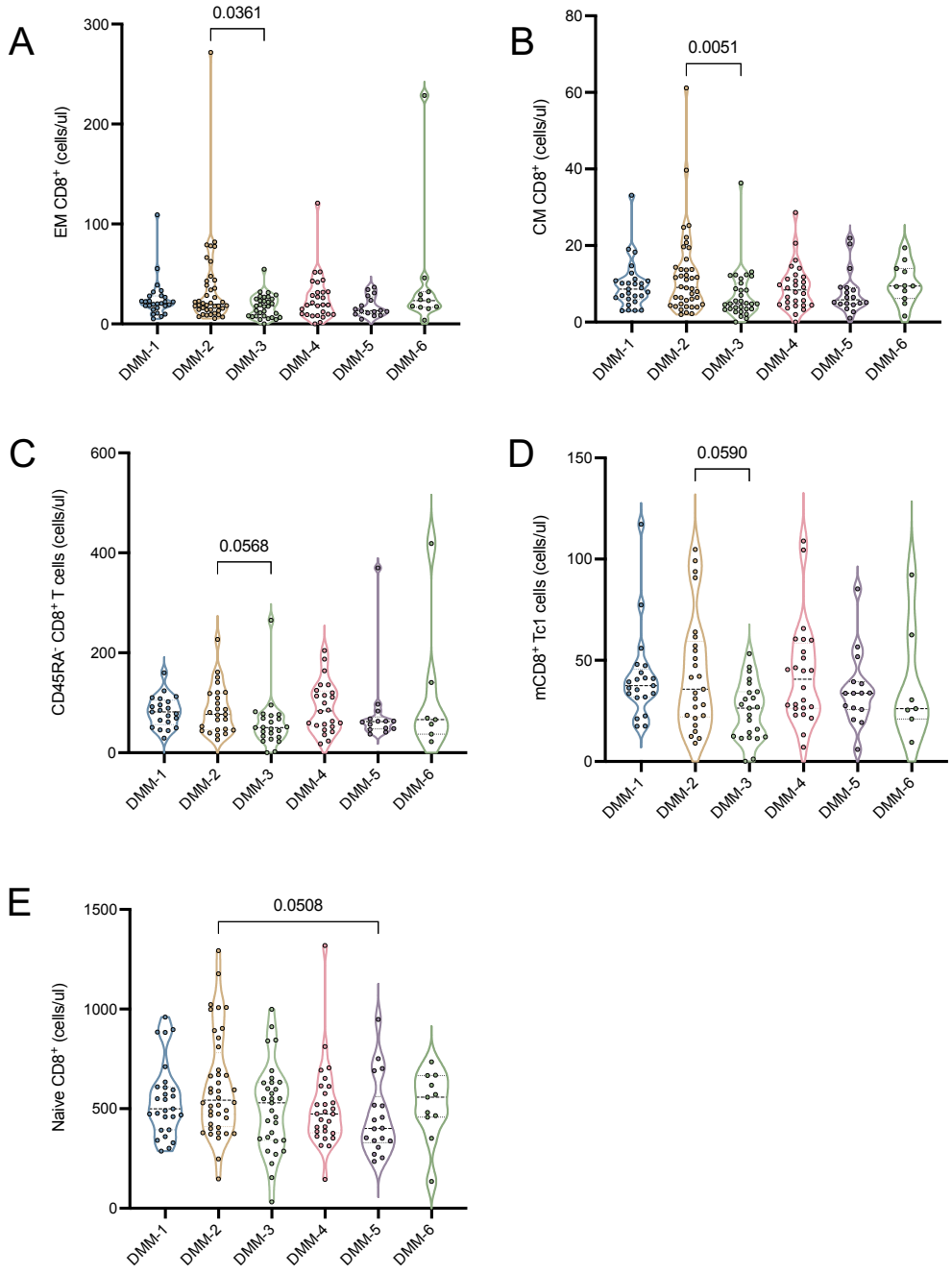

Figure 3.12| Modestly increased CD8⁺ T cell populations in infants with a B. breve enriched microbiota (DMM-2) compared to infants with a B. longum enriched microbiota (DMM-3). A| Effector memory (EM) $CD8^+$ T cells ($CD3^+CD56^-CD8^+CD45RA^-CD27^-$), **B|** Central Memory $CD8^+$ T (T_{CM}) cells ($CD3^+CD56^-CD8^+CD45RA^-CD27^+$) **C|** $CD45RA^-$ $CD8^+$ T cells ($CD3^+CD8^+CD45RA^-$) **D|** $mCD8^+$ Tc1 cells ($CD3^+CD8^+CD45RA^-CCR4^-CCR10^+$) and **E|** Naïve $CD8^+$ T-cells ($CD3^+CD56^-CD8^+CD45RA^+CD27^+$). Metagenomically defined subgroups were DMM-1 - *Klebsiella/Bacillota* enriched, DMM-2 - *B- breve* enriched, DMM-3 – *B. longum* enriched, DMM-4 - *Bacteroidota* enriched, DMM-5 - *E. coli* enriched and DMM-6 - *B. pseudocatenulatum* enriched. Kruskal-Wallis test was used to assess statistical significance. Dunn's multiple comparison test was used to correct for multiple comparisons within each graph. Data are represented as a Violin plot, with the thick dashed representing the median and thinner dashed lines representing the quartiles.

3.2.8 DMM-1 Infants have significantly higher numbers of classical monocytes and memory B cells compared to DMM-2 infants

In addition to changes observed in $CD8^+$ T cell populations, there were also higher numbers of classical monocytes and memory B cells in DMM-1 (*Klebsiella/Bacillota* enriched) infants compared to DMM-2 (*B. breve* enriched) infants (**Fig. 3.13A-B**). Previous studies have suggested that increased classical monocyte responses at birth predict subsequent allergic disease (Y. Zhang et al., 2016; Tulic et al., 2011). The observation that memory B cells were lower in infants with a *B. breve* enriched microbiota contrasts with a study in Swedish infants which reported that colonisation in early life with Bifidobacteria and *E. coli* species led to higher numbers of $CD27^+$ memory B cells in later infancy (Lundell et al., 2012). A recent study found an association between expanded circulating naïve and switched B cells, plasmablasts, and a lack of *Bifidobacteriaceae* in infants at 3 months (Henrick et al., 2021) but did not find an association between the relative abundance of *Bifidobacteriaceae* and memory B cells.

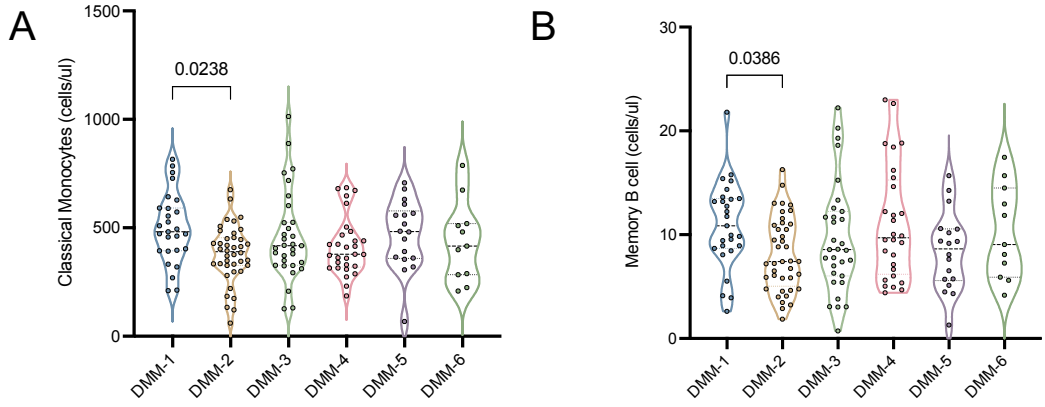

Figure 3.13| Infants with microbiomes enriched with Klebsiella and Bacillota (DMM-1) had significantly higher numbers of classical monocytes and memory B cells than B. breve (DMM-2) enriched infants. **A|** Classical Monocytes ($CD45^{+}SSC^{lo}CD3^{-}CD56^{-}CD14^{++}CD16^{-}$) and **B|** Memory B cells ($CD3^{-}CD56^{-}CD19^{+}IgD^{-}CD27^{+}$). Each DMM represents metagenomically defined subgroups: DMM 1 - *Klebsiella/Bacillota* enriched, DMM 2 - *B- breve* enriched, DMM 3 – *B. longum* enriched, DMM 4 - *Bacteroidota* enriched, DMM 5 - *E. coli* enriched and DMM 6 - *B. pseudocatenulatum* enriched. Dunn's multiple comparison test was used to correct for multiple comparisons within each graph. Data are represented as a Violin plot, with the thick dashed representing the median and thinner dashed lines representing the quartiles.

Discussion

Although antibiotics are a lifesaving clinical health intervention, their overuse is also associated with deleterious effects on immunity, particularly in infants (Shekhar & Petersen, 2020). Here, the influence of early-life antibiotic exposure on circulating immune cell populations was investigated using multi-parameter flow cytometry. Studies assessing circulating immune cell populations have been conducted in adults but to a much lesser extent in infants (Hagan et al., 2019; Nakaya et al., 2015). The AIR Study has several notable strengths, particularly utilising a multi-omic systems vaccinology approach with appropriate control for confounding factors. I individually processed infant blood for flow cytometry analysis and carried out extensive analysis of the data set based on sex, serology, antibiotic exposure status and metagenomically defined subgroups. In particular, using fresh blood samples for flow cytometry analysis is a significant strength of this study since it eliminates any potential effects due to selective subpopulation loss resulting from freeze-thaw cycles.

There are striking differences between circulating immune cell populations in infants and adults. Infants, for example, have an increased proportion of B cells and a lower proportion of activated T cells than adults, and these observations are consistent across geographical regions (Ikinciogullari et al., 2004; Borriello et al., 2022; Ding et al., 2018; van Gent et al., 2009; O'Gorman, Millard, Lowder, & Yogev, 1998). Additionally, there is a significantly higher frequency of $FoxP3^+$ Tregs in adult blood compared to infant cord blood, even though Tregs are particularly important for the maintenance of tolerance in infants during this critical window of immune system development (H. Kim et al., 2012). The normal range in B cells in infants has only recently been defined through a meta-

analysis of 28 papers (Borriello et al., 2022). As one would expect, naïve B cell populations decrease rapidly after infancy, whereas memory B cell subsets, both class-switched and non-switched, increase (Morbach, Eichhorn, Liese, & Girschick, 2010). The proportion and number of immune cell populations in the AIR Study infants were comparable to those assessed in these previously published studies (Morbach et al., 2010; Borriello et al., 2022). However, most large studies have assessed cord blood and not circulating immune cell populations in infants (van Gent et al., 2009). Significant changes in immune cell populations can be expected to occur during the critical development windows in early infancy.

Significant sex differences in the circulating immune cell populations in the AIR infants were identified, including higher numbers of $CD4^+$ T cell subsets in females compared to male infants. Other studies have found that female children and adults have higher numbers of $CD4^+$ T cells than males and a higher ratio of $CD4^+/CD8^+$ T cells (Abdullah et al., 2012; Lee et al., 1996; Lisse et al., 1997; Uppal, Verma, & Dhot, 2003). However, our study appears to be among the first to confirm that this is also the case in infants. There were also modestly higher numbers of $CD8^+$ T_{EM} cells in female infants compared to male infants in our cohort. A Chinese study analysed circulating immune cell populations in over 1000 children, including 104 infants aged 1-6 months, did not find any significant differences in $CD8^+$ T_{EM} cells in 1-6 month-old infants but instead saw significantly higher $CD4^+$ T_{EM} cells in males compared to females (Ding et al., 2018). Several previous studies have reported that males have an increased frequency of $CD8^+$ T cells from infancy to adulthood (Lee et al., 1996, Lisse et al., 1997; Uppal, Verma, & Dhot, 2003), though I did not find this to be the case in the AIR study infants. Differences in $CD8^+$ T cell populations in the AIR Study infants could be due to differences in geography (these other studies

were carried out in India, Guinea-Bissau and Asia) in addition to the socioeconomic conditions of these countries and the specific age of the AIR infants as some of these previous studies looked at a broad range of ages in their subjects. Infant males living in higher pathogen burden environments reportedly have higher numbers of basophils and monocytes compared to females up to 13 months of age (Bellamy, Hinchliffe, Crawshaw, Finn, & Bell, 2000). These differences were not observed in the AIR Study, which is perhaps unsurprising given the low burden of infectious disease in HICs such as Australia, where the AIR study was conducted. Female infants in the AIR study also had significantly higher iTregs than male infants. This is in contrast to a study in adults, which reported significantly lower numbers of $CD25^{+}$ Tregs in healthy female adults (Afshan G, Afzal N, 2012). However, a more recent study found that one of the main distinguishing sex differences in immune cell populations between cisgender men and cisgender women was significantly higher numbers and frequencies of $CD4^{+}CD25^{+}CD127^{-}$ Treg cells in cisgender women (G. A. Robinson et al., 2022). The AIR Study is the first study to make this observation in infants.

Cell populations were assessed in infants that were either not exposed to antibiotics, exposed directly to antibiotics in the neonatal period, exposed to intrapartum antibiotics, or potentially exposed to maternal antibiotics ex-partum (e.g. infants may be exposed to antibiotics through breastmilk). I observed that infants exposed to intrapartum antibiotics had a modest reduction in circulating $CD45RA^{-}$ Treg cells, an immunosuppressive antigen-experienced regulatory cell population (Silva-Neta et al., 2018; Ihara et al., 2017). This is potentially concerning, given the crucial role these cells play in maintaining peripheral tolerance and regulating T cell responses, as well as their association with the risk of allergic disease later in life (Smith et al., 2008; Strachan, 1989;

Y. Zhang et al., 2016). There is a well-established link between the microbiota and allergy in later life. For example, infants born via C-section, which disrupts the establishment of a healthy infant microbiome, have a higher risk of developing asthma (Darabi, Rahmati, Hafeziahmadi, Badfar, & Azami, 2019). Previous work has shown that enrichment of specific taxa, including *Escherichia, Ruminococcus* and *Dialister,* in the maternal microbiota is associated with higher proportions of central naïve $CD4^+$ T cells and naïve Tregs in their infant's cord blood (Gao et al., 2022). Our study did not assess the maternal microbiome. However, it is possible that maternal antibiotic exposure could have disrupted the maternal-infant microbiome exchange, contributing to the observed reduction in Tregs. Tregs are known to be influenced by changes in the microbiota, and their generation is dependent on microbiota-derived metabolites such as SCFAs (Arpaia et al., 2013). Dysbiosis in mice exposed to antibiotics *in utero* has been shown to lead to compromised Treg development and dysregulated T cell responses to infection (Xiaozhou Zhang et al., 2021). The observed reduction in Tregs in mice exposed to antibiotics *in utero* was irreversible after weaning. Interestingly, changes in Tregs can also affect the composition of the microbiota; depletion of Tregs in mice leads to an increased abundance of Firmicutes (Kehrmann et al., 2020). Breastfeeding is important for the induction of tolerogenic Tregs in newborns (H. Wood et al., 2021). However, the vast majority of infants in our study were breastfed, so this was not a confounding factor.

Grouping infants by metagenomically defined subgroups showed that *B. breve* enriched infants had higher numbers of effector memory $CD8^+$ T cells, central memory $CD8^+$ T cells, $CD45RA^-$ $CD8^+$ T cells and $mCD8^+$ Tc1 cells than infants with a microbiota enriched in *Bacteroidata.* This contrasts with recent literature in a cohort of Swedish infants which found a lack of *Bifidobacteriaceae* was associated with an expanded memory $CD8^+$ T cell

population (Henrick et al., 2021). The influence of Bifidobacterium spp. on $CD8^+$ T cell responses has been particularly appreciated in the context of cancer treatment (Sivan et al., 2015). A Bifidobacterium cocktail containing *B. breve*, *B. longum* and *B. adolescentis* was shown to enhance PD-L1 anti-tumour efficacy by activating DCs, which in turn supported the effector function of anti-tumour $CD8^+$ T cells in a mouse model of melanoma (Sivan et al., 2015). Previous studies have also shown that the upregulation of type I interferons by the plasmacytoid DCs is controlled by the microbiota, which leaves conventional DCs better equipped to prime antigen-specific T cell responses (Schaupp et al., 2020). It is therefore possible that the microbiota could also modulate the ability of DCs to enhance $CD8^+$ T cell responses after vaccination via similar mechanisms.

The study also has limitations that need to be considered. First, the AIR study only followed infants up until 15 months of life, which meant the allergy status of the enrolled infants was not assessed as this is usually characterised at 5 years of age. Assessment of the impact of antibiotics on allergies in the AIR infants could have provided valuable insights into the long-term consequences of antibiotic exposure on the immune system. Another limitation is the period in which the samples were processed; recruitment for this study was conducted over more than 2 years, a significant source of variation in the data that needed to be adjusted for in statistical analyses. Moreover, some immune cell populations of interest could not be measured with the markers in this panel, including Tfh cells. A small human study found that circulating Tfh cells derived from pre-existing memory T cells were positively associated with antibody responses to influenza vaccination (Hill et al., 2021). A heightened inflammatory gene signature in the Tfh cells of elderly participants was linked to impaired Tfh cell differentiation and weakened antibody titres (Hill et al., 2021). Assessing if Tfh cells were correlated with serology and

metagenomic data gathered in this dataset would have been of interest. Lastly, the inability to compare circulating immune cell populations at two different time points was a limiting factor. There was not sufficient blood at the week 6 timepoint for flow cytometry analysis, as a baseline blood sample for serology was required at this time point. However, if baseline blood had been assessed by flow cytometry at week 6 before the infants received their routine immunisations, changes could have been compared to those observed at week 7 post vaccination. In addition, the ability of the infants to mount an effective cellular response could have been assessed. Without the week 6 data, there is no baseline to compare the week 7 samples to, as many of the infants may still be responding to the vaccinations they received the week before. This could obscure changes due to antibiotic exposure. Changes in the cellular response from week 6 to week 7 could also have been assessed in comparison to the RNA sequencing, metagenomic, and serology data.

To summarise, the extensive flow cytometry analysis carried out as part of the AIR Study revealed multiple significant differences in immune cell populations by sex but not by antibiotic exposure. A modest reduction in $CD45RA^-$ iTregs in the intrapartum exposed infants and future work is needed to determine the importance of this cell population for the risk of allergy in later infancy and childhood.

4 A case study of two infants lacking CD16 expression on neutrophils

4.1 Introduction

The Fc gamma receptors (FcγRs) play an essential role in the immune system by recognising immunoglobulin G (IgG) coated targets (Junker, Gordon, & Qureshi, 2020). There are several classes of FcγRs, including CD16, CD32, and CD64, with various affinities for IgG (Bruhns et al., 2009). CD16, also known as FcγRIII, is a transmembrane glycoprotein and part of the Fcγ receptor (FcγR) family, found on the surface of NK cells, neutrophils, monocytes, and macrophages. CD16 consists of two Fcγ receptors, FcγRIIIa (CD16a) and FcγRIIIb (CD16b), with FcγRIIIb being one of the most abundant proteins on the surface of neutrophils (Wang & Jönsson, 2019). Although FcγRIIIa was previously believed to be exclusively expressed by NK cells and monocytes, recent evidence suggests neutrophils can also express low levels of FcγRIIIa (Golay et al., 2019; Wang & Jönsson, 2019). The functions of FcγRIIIa and FcγRIIIb include neutrophil activation, clearance of immune complexes, phagocytosis of antibody-coated pathogens, and antibody-dependent cellular cytotoxicity (ADCC) (Treffers et al., 2019; Golay et al., 2019).

FcγRIIIb is unique compared to other FcγRs as it is the only one linked to the plasma membrane by a glycosylphosphatidylinositol anchor (GPI) anchor. Its primary function in neutrophils is to eliminate spontaneously forming immune complexes, thereby dampening Fc-mediated immune responses. FcγRIIIb also participates in neutrophil activation by clustering into high-density detergent-resistant membranes, leading to

downstream signalling and Ca^{2+} mobilisation, degranulation, and cell adhesion, but not respiratory burst (Fernandes et al., 2006; Wang & Jönsson, 2019).

In this case study, we report an incidental finding of *FCGR3B* deficiency (the gene encoding FcγRIIIb/CD16b) in two infants enrolled in the Antibiotics and Immune Response (AIR) Study. This deficiency was first observed during flow cytometry analysis of peripheral blood mononuclear cells (PBMCs) collected from the infants. Due to the lack of *FCGR3B* expression, these infants initially appeared to lack neutrophils, as CD16/FcγRIII was one of the key markers used to define neutrophils in the AIR study. Subsequent analyses confirmed that the infants did have neutrophils but that these neutrophils did not express CD16/FcγRIII. RNA sequencing of whole blood samples collected from the AIR infants confirmed that *FCGR3B* was not expressed in these two infants. The implications of this finding and its potential impact on the immune function of the affected infants were further explored using functional assays conducted by clinical immunologists the Women and Children's Hospital in Adelaide, South Australia.

- Results -

As detailed in the previous chapter, extensive flow cytometry analysis was carried out on PBMCs collected from 156 infants enrolled in the AIR Study. During this analysis, the flow cytometry data for each infant was manually assessed for gating issues and irregularities. During this analysis two infants, WCH-028 and WCH-227, were identified, who appeared to lack neutrophils due to the apparent lack of the $CD16^{+}$ population (**Fig. 4.1A**). Other immune cell populations were examined but revealed no additional abnormalities (**Fig. S3.1-3.5**).

To assess why the neutrophil population was absent in these infants, the data were examined to ensure this was not due to a technical issue, such as an issue with the antibody cocktail used for staining the cells for analysis. The blood from infant WCH-228 was processed and stained on the same day as WCH-227, so this sample was used as a control (**Fig. 4.1**). WCH-228 had the expected population of neutrophils whereas WCH-227 did not (**Fig. 4.1A**). These two samples were stained with the same antibody cocktail and analysed sequentially on the same day, indicating that the apparent lack of neutrophils in these infants was unlikely due to a technical error.

Next, other gates were examined to determine whether CD16 expression was evident on different cell types (**Fig. 4.1B**). CD16 expression was observed on intermediate ($CD45^{+}SSC^{lo}CD3^{-}CD56^{-}CD14^{+}CD16^{+}$) and nonclassical monocytes ($CD45^{+}SSC^{lo}CD3^{-}CD56^{-}CD14^{-}CD16^{+}$) (**Fig. 4.1B**).

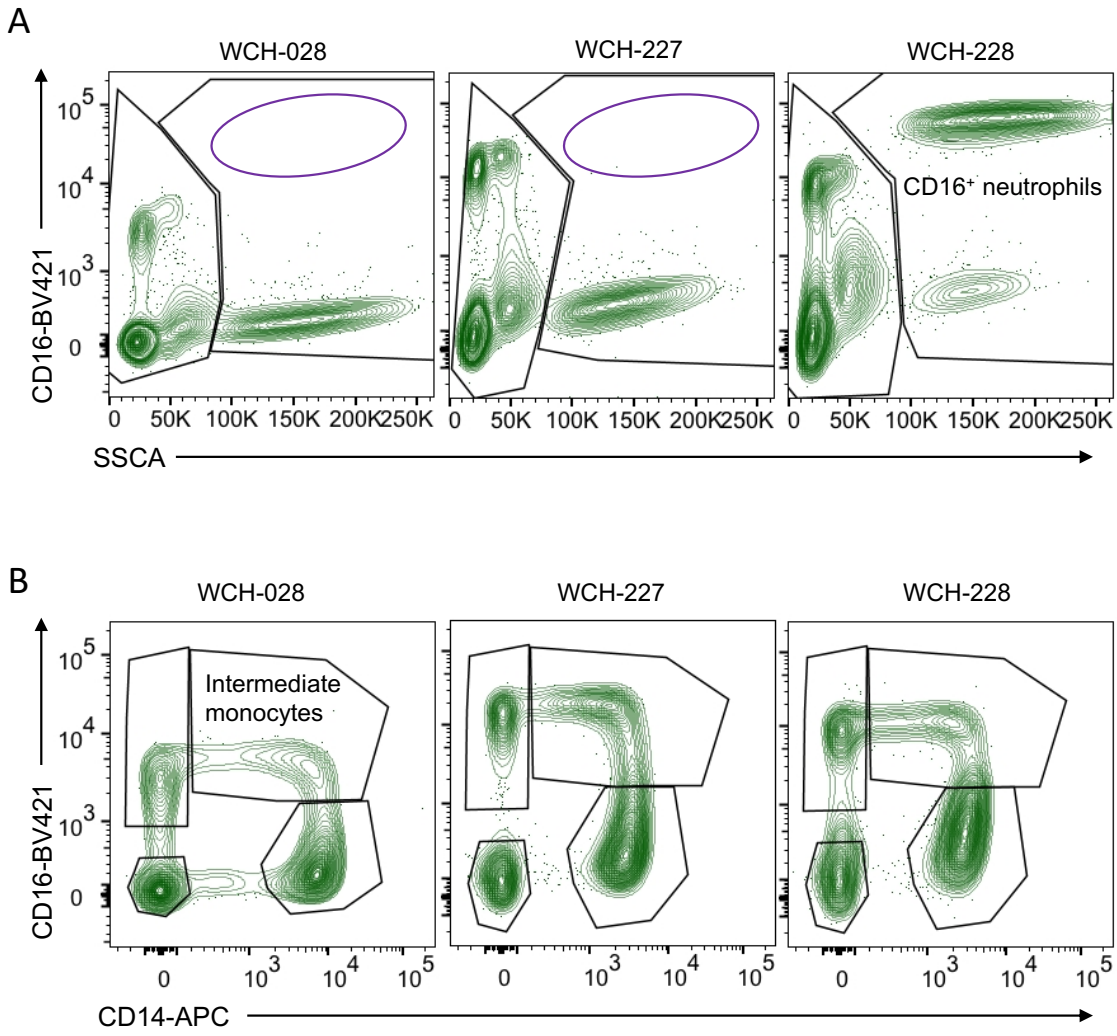

Figure 4.1| CD16^{+} neutrophils were not detected in two infants, WCH-028 and WCH-227. A| The population that would have been identifiable as CD16^{+} neutrophils (CD45^{+}SSC^{hi}) were absent in two of the AIR infants - WCH-028 and WCH-227. A representative control infant (WCH-228) that was analysed at the same time as WCH-227 is also shown. **B|** CD16 expression on Intermediate monocytes (CD45^{+}SSC^{lo}CD3^{-}CD56^{-}CD14^{+}CD16^{+}).

4.1.1 The two infants have normal proportions of CD15^{+}Siglec8^{-} neutrophils

To assess whether these infants lacked neutrophils altogether, CD15^{+}CD16^{+} neutrophil gates were compared between the two abnormal infants and the control infant, WCH-228. Gating for CD15^{+}CD16^{+} neutrophils revealed that both WCH-028 and WCH-227 had an absence of CD15^{+}CD16^{+} neutrophils. In contrast, WCH-228 had the expected population of CD15^{+}CD16^{+} neutrophils (**Fig. 4.2A**). However, there was a significantly

larger population of $CD16^{-}CD15^{+}$ cells in the WCH-028 and WCH-227 infants compared to WCH-228 (**Fig. 4.2A**). These data suggested that the expression of CD16 on neutrophils was absent in the two infants rather than a lack of neutrophils altogether.

To investigate this further, neutrophils were identified in an alternative way as $CD45^{+}SSC^{hi}CD15^{+}Siglec8^{-}$ cells. This revealed two populations – a $CD15^{+}Siglec8^{+}$ eosinophil population and a $CD15^{+}Siglec8^{-}$ neutrophil population, confirming that the two infants do not lack neutrophils (**Fig. 4.2b**). FcγRIIIa and FcγRIIIb are 96% identical at the protein level and the CD16 antibody used in our flow cytometry panel cannot distinguish between them. As mentioned previously, CD16 is made up of FcγRIIIa and FcγRIIIb. FcγRIIIb is primarily expressed on neutrophils, with only low levels of FcγRIIIa recently identified on neutrophils (Golay et al., 2019), leading us to conclude that we were detecting the cell surface expression of FcγRIIIa on other cell populations in these infants and that neutrophils from the two infants likely did not express FcγRIIIb.

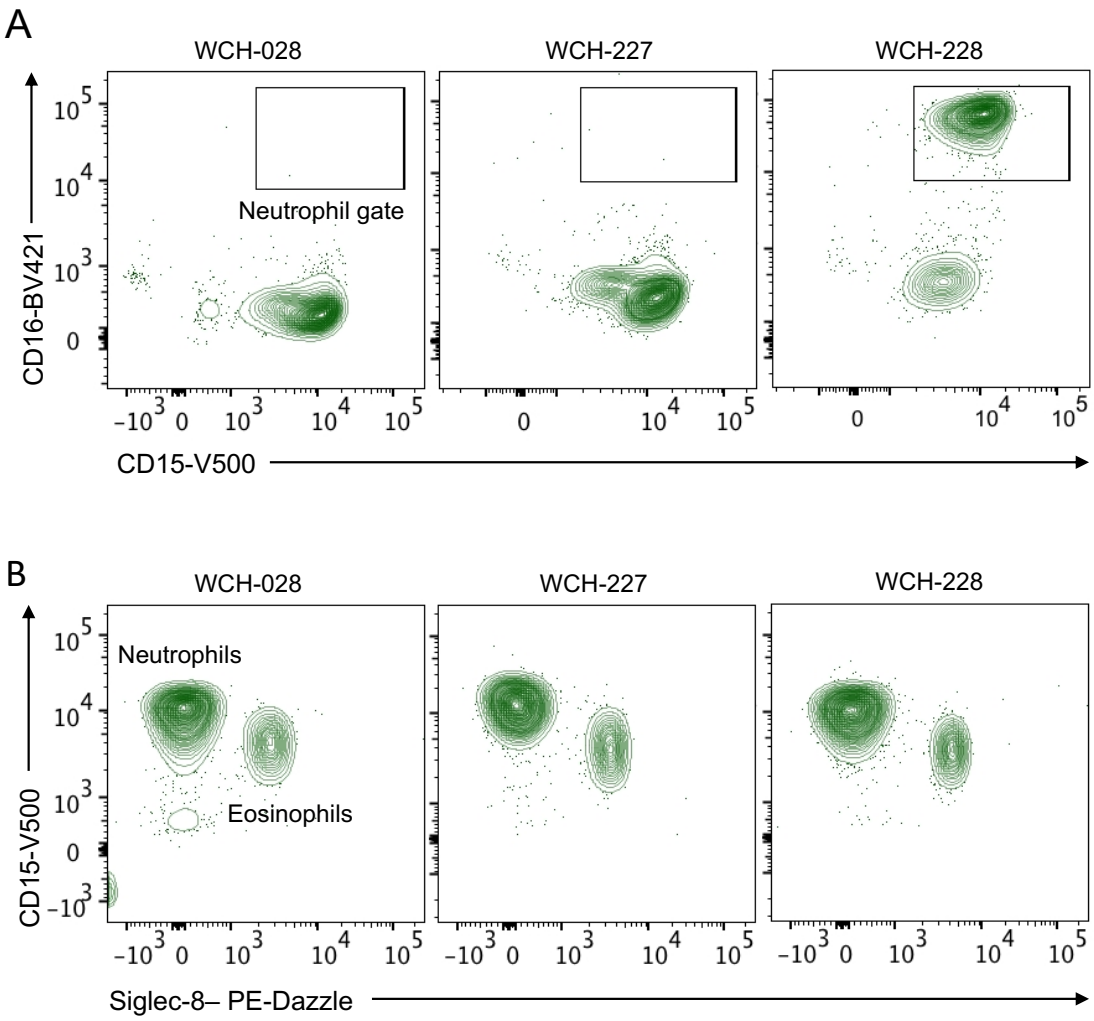

Figure 4.2| The two infants have a normal proportion of CD15^{+}Siglec8^{-} neutrophils. A| The absence of CD16^{+}CD15^{+} neutrophils (CD45^{+}SSC^{hi}) in WCH-028 and WCH-227 compared to representative control infant, WCH-228, which was analysed at the same time as WCH-227. **B|** CD15^{+}Siglec8^{+} eosinophils (CD45^{+}SSChi) and CD15^{+}Siglec8^{-} neutrophils (CD45^{+}SSChi) in WCH-028, WCH-227 and WCH-228.

4.1.2 *FCGR3A* but not *FCGR3B* is expressed in the two infants

To confirm that infants WCH-028 and WCH-227 express *FCGR3A* but not *FCGR3B*, RNA-sequencing data profiling gene expression in whole blood collected from the AIR infants at the same timepoint as the flow cytometry was performed, was examined. The RNA sequencing data confirmed that WCH-028 and WCH-227 expressed *FCGR3A* but not *FCGR3B* (**Fig. 4.3A**). Previous reports of this defect have found that the gene encoding

FcγRIIc (*FCGR2C*) was deleted in individuals with FcγRIIIb deficiency (M. De Haas, Kleijer, Van Zwieten, Roos, & Von Dem Borne, 1995). Therefore, consistent with these prior reports, the expression of *FCGR2C* was absent in these two infants (**Fig. 4.3B**), while the other AIR infants expressed both *FCGR3B* and *FCGR2C.*

Dr Feargal Ryan carried out patient – specific gene expression analysis to assess whether there was evidence for global differences in gene expression in these infants (**Table S3.1**). No obvious differences in antibody responses were observed in either infant (**Table S3.2**).

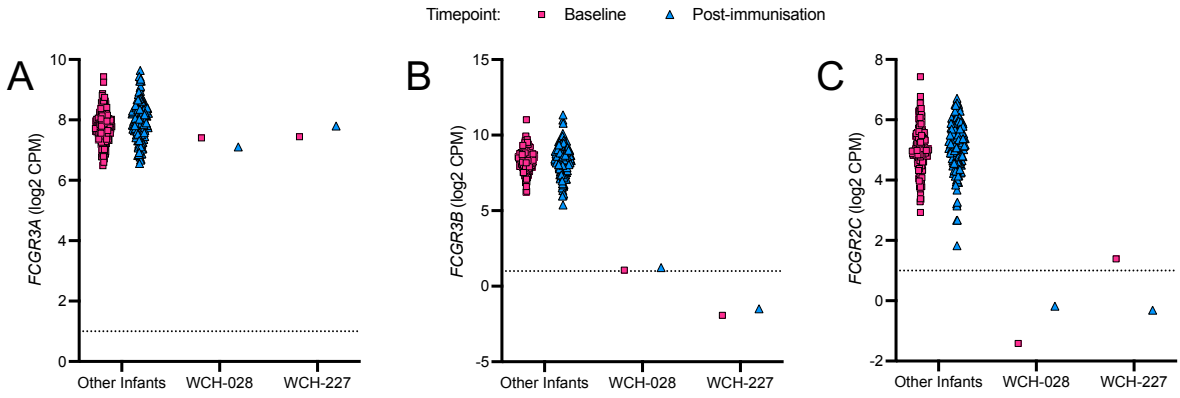

Figure 4.3| RNA sequencing data confirms that FCGR3A but not FCGR3B is expressed in the two case study infants. RNA sequencing was performed at ~6 weeks of life (baseline) and ~1-week post-immunisation. Expression of **A|** *FCGR3A* and **B|** *FCGR3B* in the AIR Study infants. **B|** The expression of FcγRIIc (CD32c) in the AIR infants. The dashed line represents point at which genes are reliably detected (< 1). Data represented as log2 Count Per Million (CPM).

4.1.3 Follow-up flow cytometry analysis of the two infants lacking FcγRIIIb expression

To further confirm the lack of expression of FcγRIIIb in the infants, WCH-028 and WCH-227, follow-up blood draws were collected one year after the AIR study completed recruitment. PBMCs were analysed on the BD FACs symphony with the same flow

cytometry panels used previously were employed to assess whether this lack of FcγRIIIb/CD16b expression was sustained. The lack of $CD16^+$ neutrophils was again observed in both infants (**Fig. 4.4**). Other functional assays were carried out by collaborators at the Women's and Children's Hospital to assess neutrophil function. These assays found no apparent defects in neutrophil function in either infant.

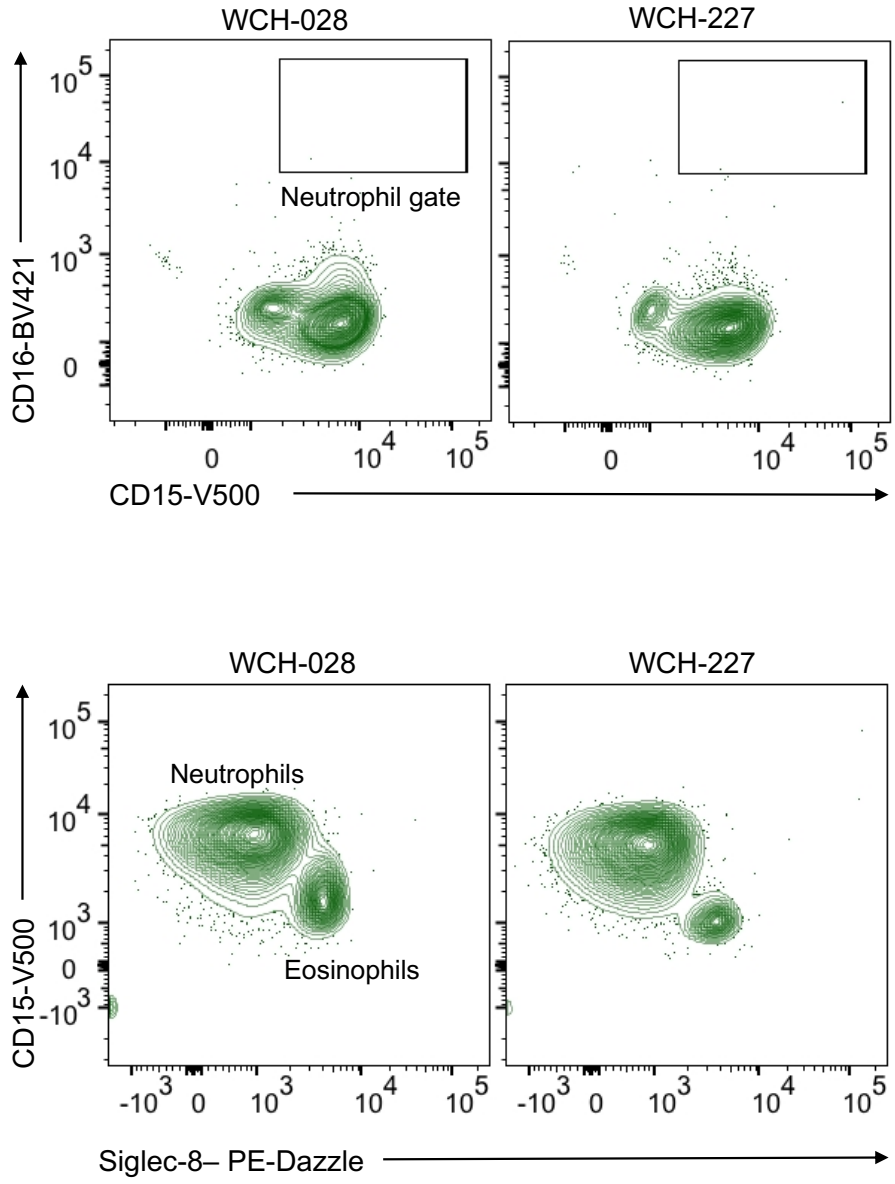

Figure 4.4| Follow-up flow cytometry analysis confirming that the $CD16^+$ neutrophil population is still absent in both case study infants. A| $CD16^+CD15^+$ neutrophils are

absent in infant WCH-028 and infant WCH-227. **B|** $CD15^{+}Siglec8^{+}$ eosinophils ($CD45^{+}SSC^{hi}$) and $CD15^{+}Siglec8^{-}$ neutrophils ($CD45^{+}SSC^{hi}$) in WCH-028 and WCH-227.

4.2 Discussion

This chapter reports a case study of two infants enrolled in the AIR study that were found to lack the expression of the gene encoding FcγRIIIb, *FCGR3B*. There is no known relationship between the infants based on the information that we have. FcγRIIIb deficiency has previously been reported as a rare deficiency at a population level, with an estimated prevalence of 0.05% (Muniz-Diaz, Madoz, Martin, & Puig, 1995;Minguela et al., 2021), so finding two unrelated infants in this cohort of 156 infants with this deficiency is quite surprising. The potential clinical significance of this lack of FcγRIIIb expression is currently poorly understood. FcγRIIIb is a GPI-anchored molecule and does not have intracellular signalling motifs but can cooperate with other Fcγ receptors to promote phagocytosis of antibody-opsonized microbes by human neutrophils. A previous case study of an individual with FcγRIIIb deficiency, which was subsequently found to be shared with other family members, did not report any overt immune deficiency (Wagner & Hänsch, 2004; Kamat & Ezekwesili, 2006). The authors speculated that redundancy in the immune system could compensate for the lack of FcγRIIIb. Other reports have suggested, however, that FcγRIIIb deficiency is linked to transient neonatal alloimmune neutropenia (Fromont et al., 1992). FCGR3B copy number variation has also been associated with an increased risk of rheumatoid arthritis, systemic autoimmunity and systemic lupus erythematosus (SLE) (Fanciulli et al., 2007; Graf et al., 2012; Minguela et al., 2021).

Another study found that FcγRIIIb is a negative regulator of neutrophil ADCC toward tumour cells and a potential target for enhancing tumour cell destruction by neutrophils (M. De Haas et al., 1995).

5 The gut microbiota is required for optimal T-dependent and T-independent B cell responses to the PCV13 vaccine.

5.1 Introduction

Growing evidence suggests an association between the composition of the gut microbiome and immune responses to vaccination. These studies include a number of observational studies in low and middle-income countries (LMICs) (Grassly et al., 2016; Harris et al., 2016, Fix et al., 2020). More recently, vaccine responses to the influenza vaccine were demonstrated to be impaired in antibiotic-exposed adults with low pre-existing immunity (Hagan et al., 2019). Previous research from our laboratory has also shown that antibody responses to several routinely administered infant vaccines are impaired in mice orally exposed to antibiotics in early life (Lynn et al., 2018), including the 13-Valent Pneumococcal Conjugate Vaccine, PCV13. The PCV13 is a mixture of outer membrane polysaccharides from 13 serotypes of *Streptococcus pneumoniae* (Jefferies, Macdonald, Faust, & Clarke, 2011). These polysaccharides are conjugated to a carrier protein (cross-reacting material 197 (CRM_{197})), to elicit a T-dependent B cell response in infants (Davies et al., 2022). Australian infants receive 4 primary doses of PCV13 as recommended under the National Immunisation Programme ("National Immunisation

Program Schedule | Australian Government Department of Health and Aged Care," 2020), and the PCV13 vaccine is administered to 72 million infants around the world every year. The efficacy of PCV13, however, remains suboptimal and variable among individuals and different populations (Davies et al., 2022; Gerard et al., 2020; Grant et al., 2016; Roca et al., 2015; Swarthout et al., 2020a, 2022; Yeh et al., 2010; L. Zhang et al., 2015). In LMICs such as Malawi, pneumococcal carriage persists in both children and adults despite PCV13 vaccine coverage of over 90% (Swarthout et al., 2020b). Similar trends have been observed in the Gambia and Kenya (Hammitt et al., 2014a; Mackenzie et al., 2022). Additionally, a large population study in Malawi children revealed waning antibody titres with all but one serotype of PCV13, falling below the correlate of protection (CoP) for PCV13 up to 52 months after vaccination (Swarthout et al., 2022).

A key source of variation that may be impacting immune responses to the PCV13 vaccine is the microbiota. Preclinical work has shown that the clonal expansion of B cells reactive to other polysaccharide antigens from the Lancefield group A carbohydrate (GAC) is microbiota-dependent (New, Dizon, Fucile, Rosenberg, Kearney, & King, 2020). The microbiota also displays exopolysaccharides which have been shown to have immune stimulatory properties when used as an adjuvant for the foot-and-mouth disease vaccine (Xiu et al., 2018). Our lab has previously shown that antibody responses to PCV13 are impaired in mice exposed to antibiotics in the first weeks of life (Lynn et al., 2018). Studies in antibiotic-treated mice, however, cannot definitively prove a causal role for the gut microbiota as one cannot rule out other immunomodulatory effects of antibiotics (Shekhar & Petersen, 2020). Germ-free (GF) mice are bred and housed in sterile isolators that prevent exposure to microorganisms if procedures are strictly adhered to. The utilisation of GF mouse models is now considered a gold-standard approach to

demonstrate a causal role for the microbiota in a phenotype of interest. Another advantage of this model is that it allows one to recolonise GF mice with specific bacterial communities of interest or even bacterial monocultures, to assess the immunomodulatory properties of individual bacterial strains of interest.

Despite growing evidence that the microbiome influences the immune response to the PCV13 vaccine, the mechanisms through which this occurs remain unclear. To assess the influence of the microbiota on PCV13 vaccine responses, extensive immune profiling in serum and secondary lymphoid organs was performed in GF and colonised mice. These assessments found significant differences in serum antibody responses between GF and colonised mice. Additionally, GF mice had a significantly lower frequency of GC B cells compared to colonised mice. These results illustrate the importance of the microbiome in the immune response to the PCV13 vaccine.

- Results -

5.1.1 Germ-free (GF) mice have impaired antibody responses to the PCV13 vaccine

The immune response to the PCV13 vaccine is impaired in mice treated with antibiotics in early life (Lynn et al., 2018). To investigate whether responses to PCV13 are also impaired in GF mice, GF mice and conventionally colonised specified pathogen-free (SPF) control mice, were vaccinated intraperitoneally at day (d)21 - 28 of life (V) with $1/10^{th}$ a human dose of PCV13, by human to animal dose conversion standards (A. B. Nair & Jacob, 2016) **(Fig. 5.1A)**. A control group of age-matched mice were immunised with PBS and maintained as mock-immunised controls. Vaccine responses were boosted 2 weeks after the initial vaccination (V+2) by re-vaccinating mice (same route and dose), which was intended to broadly mirror the 2-month window between the first and second dose of PCV13 received by Australian infants. To confirm that GF mice remained GF over the course of the experiment, regular faecal sample collection was performed and DNA was extracted from faecal samples to determine bacterial load via a 16S rRNA gene qPCR assay **(Fig. 5.1B)**. Cages were also swabbed and samples were sent to a molecular diagnostics company, ComPath (https://sahmri.org.au/compath), for further confirmation of their GF status on arrival at our GF facility **(Fig. S4.1)**.

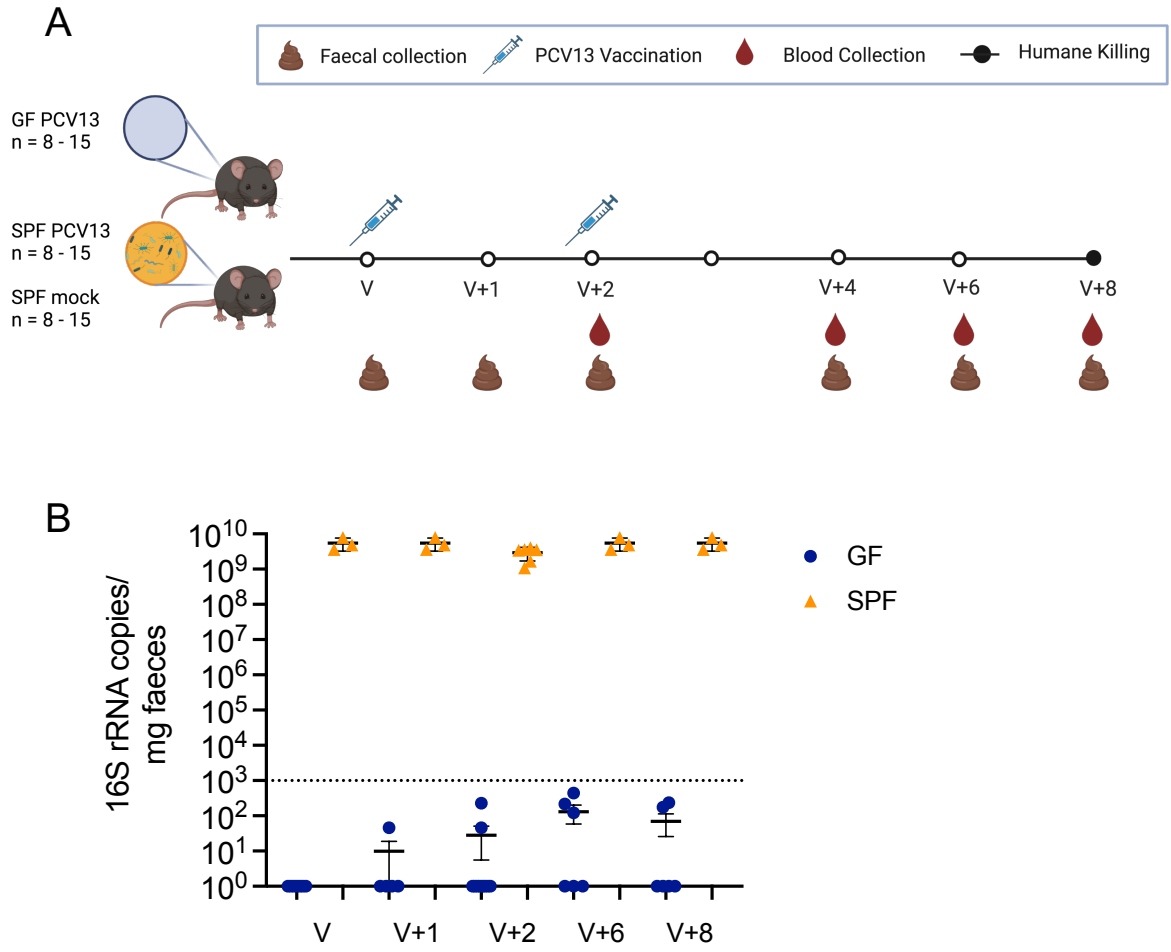

Figure 5.1| Experimental plan and GF status validation. A| Overview of the experimental design**.** GF and SPF mice were vaccinated intraperitoneally at day 28 of life (V). Vaccine responses were boosted after 2 weeks. Blood and faecal samples were collected fortnightly. **B|** 16S rRNA gene qPCR data assessing bacterial colonization at V, V+1, V+2, V+6 and V+8 weeks. The dashed line represents the limit of detection. Data are represented as mean ± SEM. Note; values from GF mice are below the limit of detection.

To assess antibody responses to vaccination in each group, serum was collected at two weeks (V+2) post-vaccination, and fortnightly subsequently until the mice were humanely culled at 8 weeks post the primary vaccination (V+8 weeks). The PCV13 vaccine conjugates polysaccharides from 13 different *Streptococcus pneumoniae* serotypes to a carrier protein, CRM_{197}. The CRM_{197} carrier protein is a non-toxic variant of diphtheria toxin that is widely used in vaccines to ensure the induction of a T cell-dependent antibody response to the conjugated polysaccharides (Uchida, Pappenheimer,

& Harper, 1972, Siegrist, 2008). Serum antibody responses against to the whole vaccine, *S. pneumoniae* polysaccharide antigens from serotypes 1 and 3 (PPS1 and PPS3) and CRM_{197} were assessed. These serotypes were chosen as PPS1 was impaired in antibiotic-exposed infants in the AIR study (see previous chapters), and PPS3 was the most prevalent serotype carried by participants in a clinical study of PCV13 vaccine efficacy in Malawi (Swarthout et al., 2020). PPS1 and PPS3 are also serotypes that cause considerable disease burden in adults despite the herd immunity provided by infant pneumococcal conjugate vaccine introduction (Örtqvist, 2001; Wuorimaa & Käyhty, 2002; Yeh et al., 2010; Davies et al., 2022). Relative to SPF mice, GF mice had significantly impaired IgG_{total} responses to the whole vaccine, PPS1 and PPS3 pre-boost at the V+2 weeks timepoint **(Fig. 5.2A-C)**. Interestingly, CRM_{197}-specific IgG_{total} responses were not significantly different between SPF and GF mice at V+2 weeks **(Fig. 5.2D)**. IgM responses pre-boost to the whole vaccine, PPS1 and PPS3 were also significantly impaired pre-boost in GF mice, with no significant differences observed in anti-CRM_{197} IgM levels **(Fig. 5.2E-H)**.

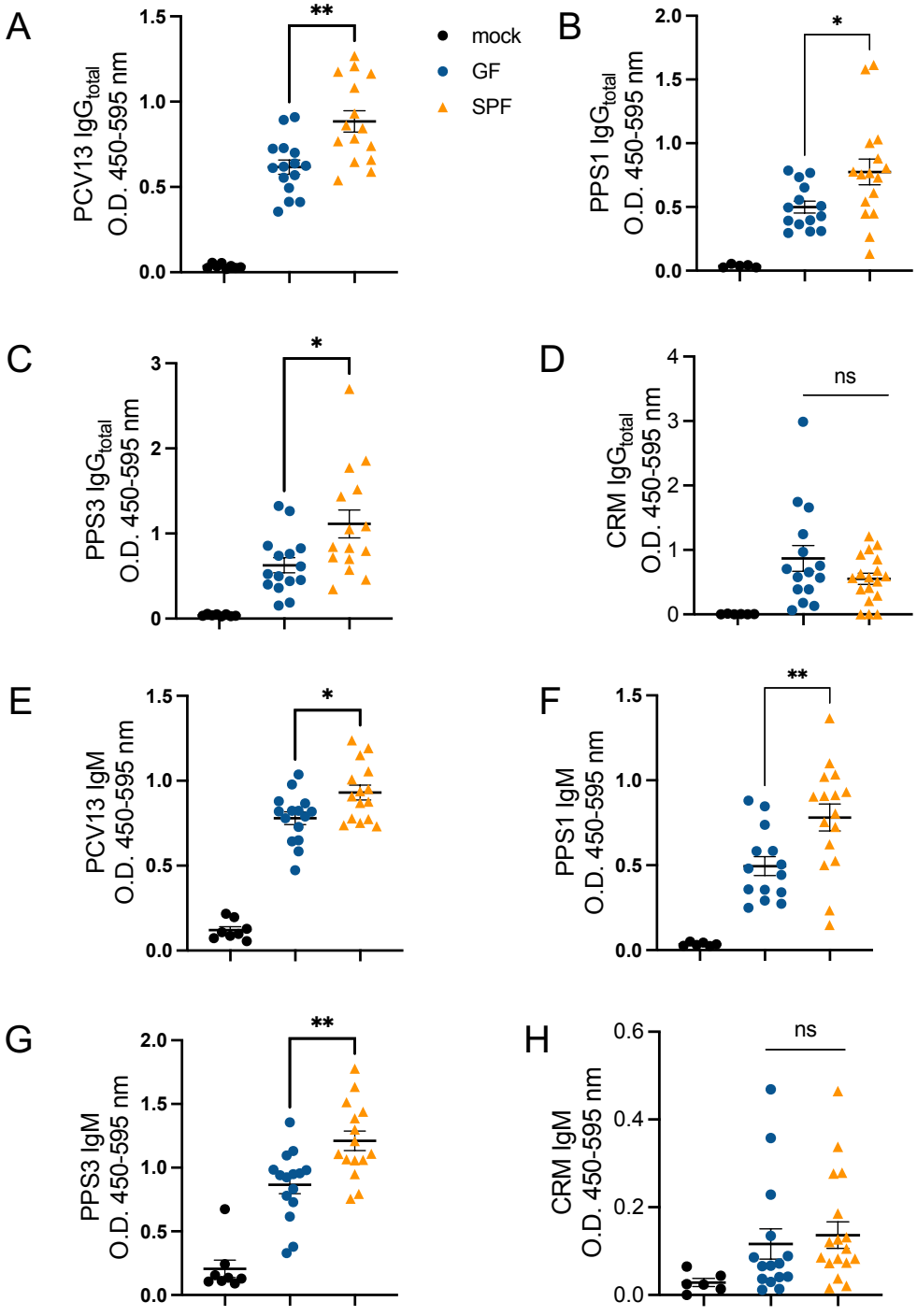

Figure 5.2| Antibody responses to the PCV13 vaccine are impaired in the serum of GF mice compared to SPF mice at V+2 weeks. IgG_{total} responses to **A|** the whole PCV13 vaccine, **B|** the polysaccharides PPS1 and **C|** PPS3 and **D|** the carrier protein CRM_{197} were assessed by ELISA in the serum of mock, GF, and SPF mice. IgM responses were also measured against **E|** the whole PCV13 vaccine, **F|** PPS1, **G|** PPS3 and **H|** CRM_{197} in mock, GF and SPF mice. Raw O.D. values are shown. Serum diluted 1/250 – 1/500. Data are represented as mean ± SEM. Mann-Whitney tests were used to assess statistical significance. *p <0.05, ** p < 0.01, ns = not significant.

IgG and IgM antibody responses to PCV13 were also assessed post-boost (i.e. second vaccine dose) at V+4, 6 and 8 weeks. GF mice had significantly impaired IgG_{total} responses to the whole vaccine, PPS1, and CRM_{197} at all time points post-boost **(Fig. 5.3A-C)**. PPS3-specific IgG_{total} responses were only significantly different at V+4 weeks and they appeared to wane later in the response in SPF mice **(Fig. 5.3D)**. The differences observed in responses to PPS1 and PPS3 are consistent with the known variation in the response to different vaccine serotypes in humans (Swarthout et al., 2022, Davies et al., 2022). GF mice also had significantly lower IgM responses to the PCV13 vaccine compared to SPF mice **(Fig. 5.3E)**. Of note, there were no significant differences in IgG_{total} (not vaccine specific) between GF and SPF mice after immunisation (**Fig. S4.2**). This suggests that the vaccine-specific response and not the overall humoral response is defective in GF mice.

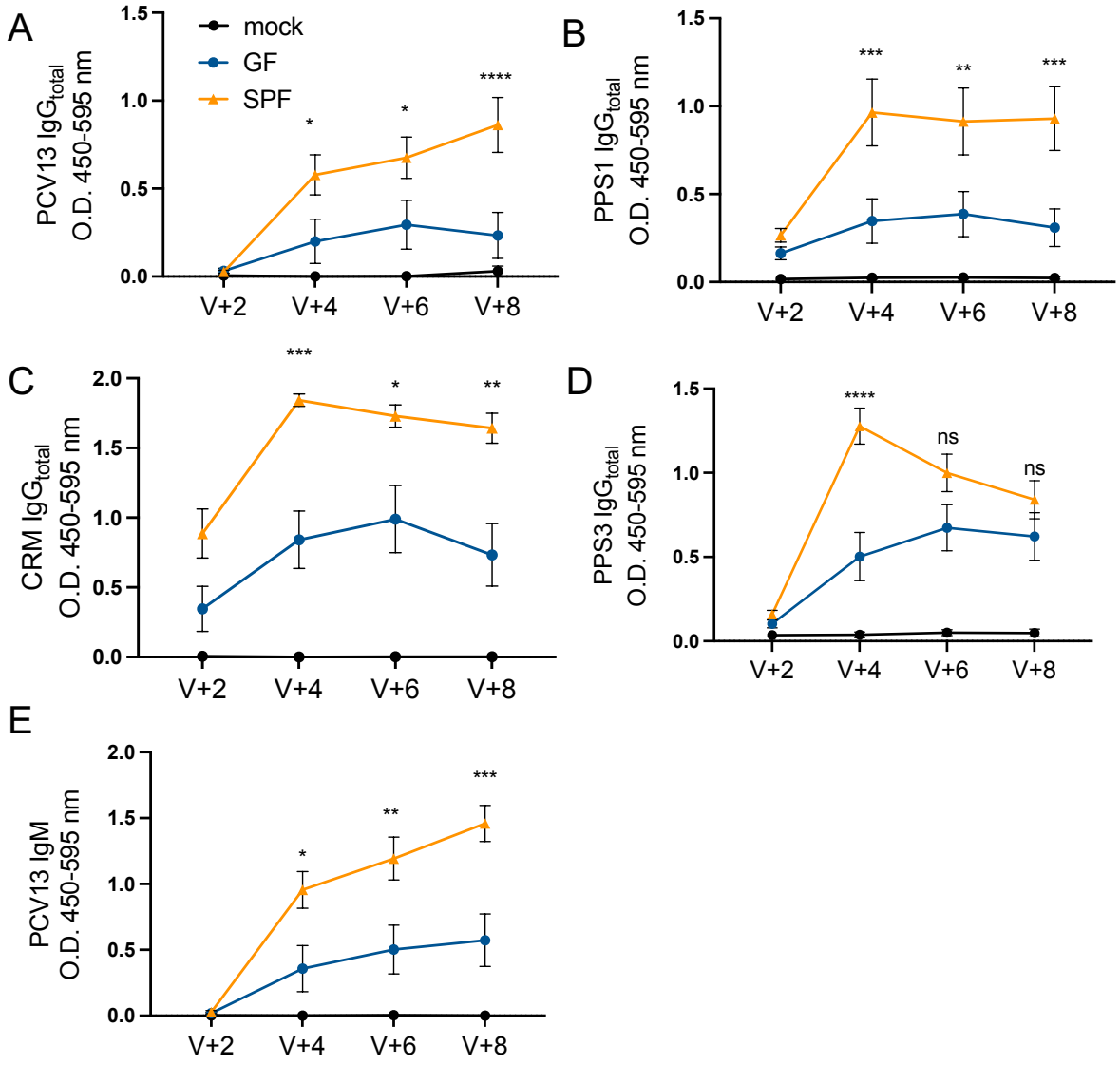

Figure 5.3| PCV13-specific antibody responses are significantly lower in GF mice compared to SPF mice after boosting. A| PCV13 **B**| PPS1 **C|** CRM_{197} and **D**| PPS3 specific IgG_{total} responses were assessed in serum by ELISA in vaccinated and mock-vaccinated GF and SPF mice at the indicated weeks post-vaccination. **E**| PCV13 specific IgM responses in the serum of GF and SPF mice. Data are represented as mean ± SEM. Raw O.D. values are shown. Serum diluted 1/2000 – 1/4000. Two-way ANOVA was used to assess statistical significance *p < 0.05, ** p < 0.01, ***p < 0.001 ****p < 0.0001.

Next, IgG subclasses were measured in the serum of SPF and GF mice after a booster dose of PCV13. Responses were measured at V+4 weeks to capture the antibody response to boosting. IgG1 is normally the most abundant IgG subclass and uniquely drives opsonophagocytic activity in PCV13-vaccinated individuals (Davies et al., 2022). GF mice had significantly lower serum IgG1 against the whole vaccine, PPS1, PPS3, and CRM_{197}

(**Fig 4A-C**)**.** GF mice also had significantly impaired IgG3 antibody responses against PCV13, PPS1, PPS3, and CRM_{197} (**Fig. 5.4D-H**). Higher baseline levels of IgG2 have predicted protection conferred by the PCV13 vaccine in immunocompromised individuals (Gerard et al., 2020; Robbins et al., 2021). GF mice also had significantly lower PCV13-specific IgG2b in their serum (**Fig. 5.4I**). This defect in the antibody response to PCV13 appears to be at least somewhat specific to this vaccine as responses to other vaccines such as the Pfizer/Biontech BNT16262 mRNA vaccine are not impaired in GF or antibiotics-treated mice (Norton et al., Gut, in revision).

IgA is an important antibody isotype against pneumococcal infection due to its production at mucosal surfaces. Interestingly, there were no differences in serum IgA titres observed between GF and SPF mice at V+4 (**Fig. 5.4J**), however, IgA is measured here in the serum and not at a mucosal surface where it primarily performs its effector functions. Overall, these results illustrate that GF mice have significantly impaired antibody responses to the PCV13 vaccine compared with SPF mice against the whole vaccine, polysaccharides within the vaccine, and the carrier protein, particularly after boosting.

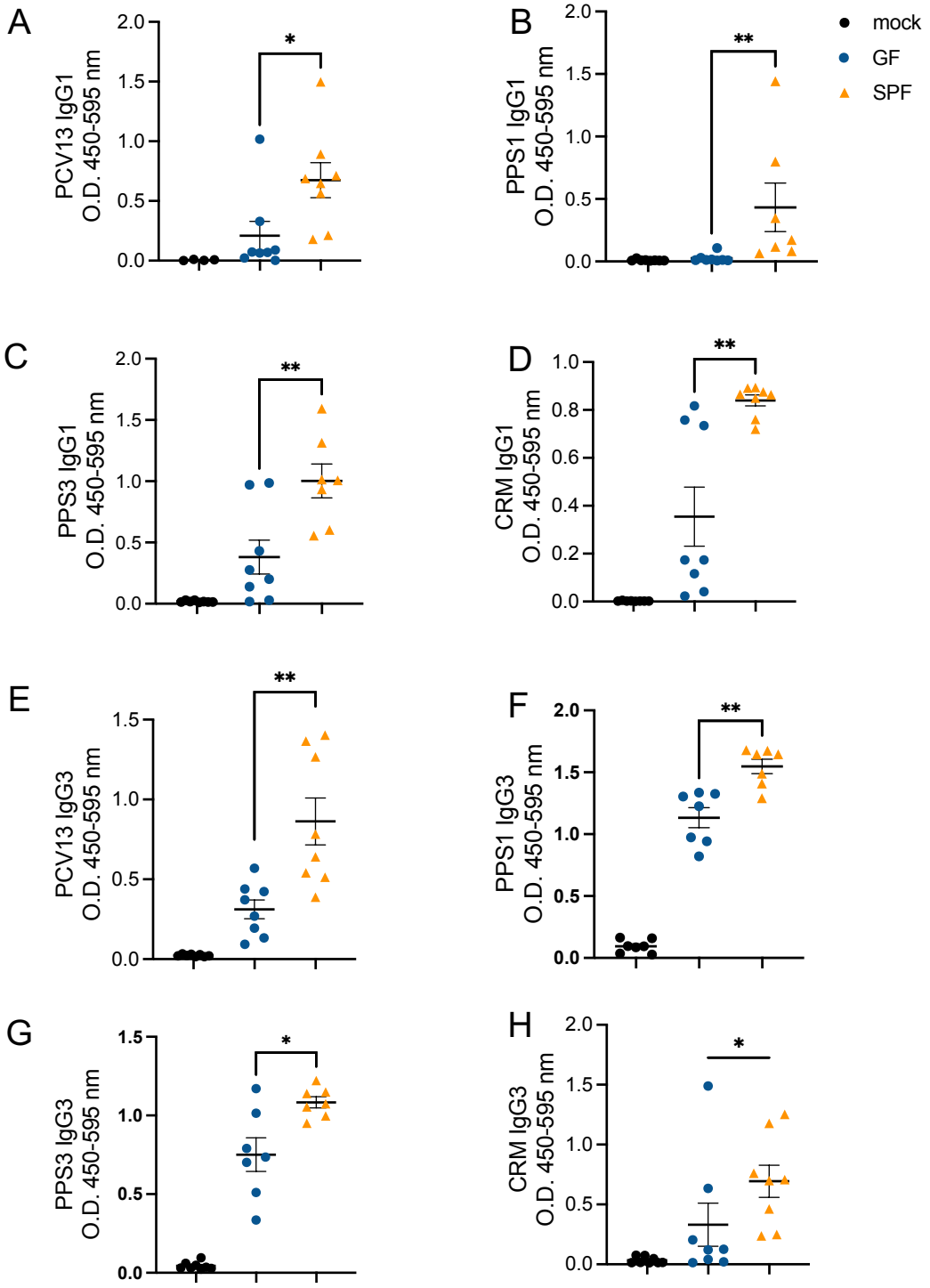
A
PCV13 IgG1
O.D. 450-595 nm
2.0
1.5
1.0
0.5
0.0
*
B
PPS1 IgG1
O.D. 450-595 nm
**
mock
GF
SPF
C
PPS3 IgG1
O.D. 450-595 nm
**
D
CRM IgG1
O.D. 450-595 nm
1.0
0.8
0.6
0.4
0.2
**
E
PCV13 IgG3
O.D. 450-595 nm
**
F
PPS1 IgG3
O.D. 450-595 nm
**
G
PPS3 IgG3
O.D. 450-595 nm
*
H
CRM IgG3
O.D. 450-595 nm
*

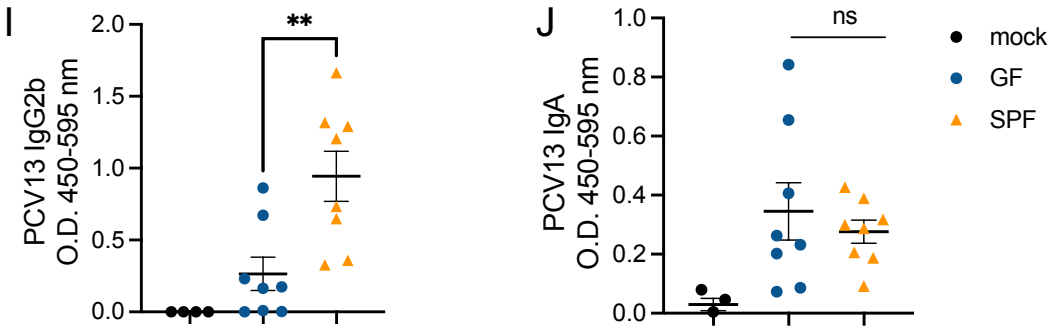

Figure 5.4| IgG1, IgG2 and IgG3 responses to PCV13 are impaired in GF compared to SPF mice. IgG1 responses to **A|** the whole PCV13 vaccine, **B|** PPS1, **C|** PPS3 and **D|** CRM_{197} were assessed by ELISA in the serum of mock, GF and SPF mice at V+4 weeks. Serum IgG3 was also measured against **E|** the whole PCV13 vaccine, **F|** PPS1, **G|** PPS3 and **H|** CRM_{197} of mock, GF and SPF mice at V+4 weeks. PCV13-specific **I|** IgG2b and **J|** IgA were also measured in the serum of mock, GF, and SPF mice at V+4 weeks. Raw O.D. values are shown. Data are represented as mean ± SEM. Mann-Whitney tests were used to assess statistical significance *p <0.05, ** p < 0.01.

5.1.2 Does colonisation of the gut microbiota restore normal responses to vaccination in GF mice?

The next step was to assess whether colonisation with an SPF microbiota could restore impaired PCV13 antibody responses in GF mice. Previously, I colonised mice with monocultures of specific bacterial strains, such as *Blautia producta, Enterobacter cloacae, Bifidobacterium longum,* that correlated with antibody responses to the PCV13 vaccine in SPF mice and AIR study infants respectively. However, colonisation with these strains at day 21 of life did not improve vaccine specific antibody responses to the PCV13 vaccine (**Fig. S4.3**). The timing of colonisation has been shown in other contexts to play a key role in shaping subsequent immune responses, and there appears to be a window of opportunity where colonising mice has the greatest influence on their immunity (Al Nabhani et al., 2019). Therefore, two methods of colonisation were employed to investigate the role of colonisation timing on PCV13 vaccine responsiveness in GF mice

(**Fig. 5.5A**). The first colonisation group consisted of mice born to former GF dams that were colonised with an SPF microbiota before pregnancy (exGF mice). The other group consisted of GF mice that directly received two fecal microbiota transfers (FMT) from an age-matched SPF microbiota by oral gavage at day (d) 21 and 24 of life. Groups of SPF and GF mice were also assessed as controls. Mice were vaccinated at d28 (V) and boosted 2 weeks later (V+2). A subset of each group was vaccinated with PBS only (mock).

To assess the success of the colonisation in the FMT group, bacterial load was assessed in each group at the time of vaccination (V). There were no significant differences in bacterial load between the SPF, exGF, or FMT groups (**Fig. 5.5B**). This qPCR also confirmed the GF status of the GF mice at the time of vaccination, while further swabs were taken at V+2 and V+4 weeks to confirm that they remained GF (**Fig. S4.4**).

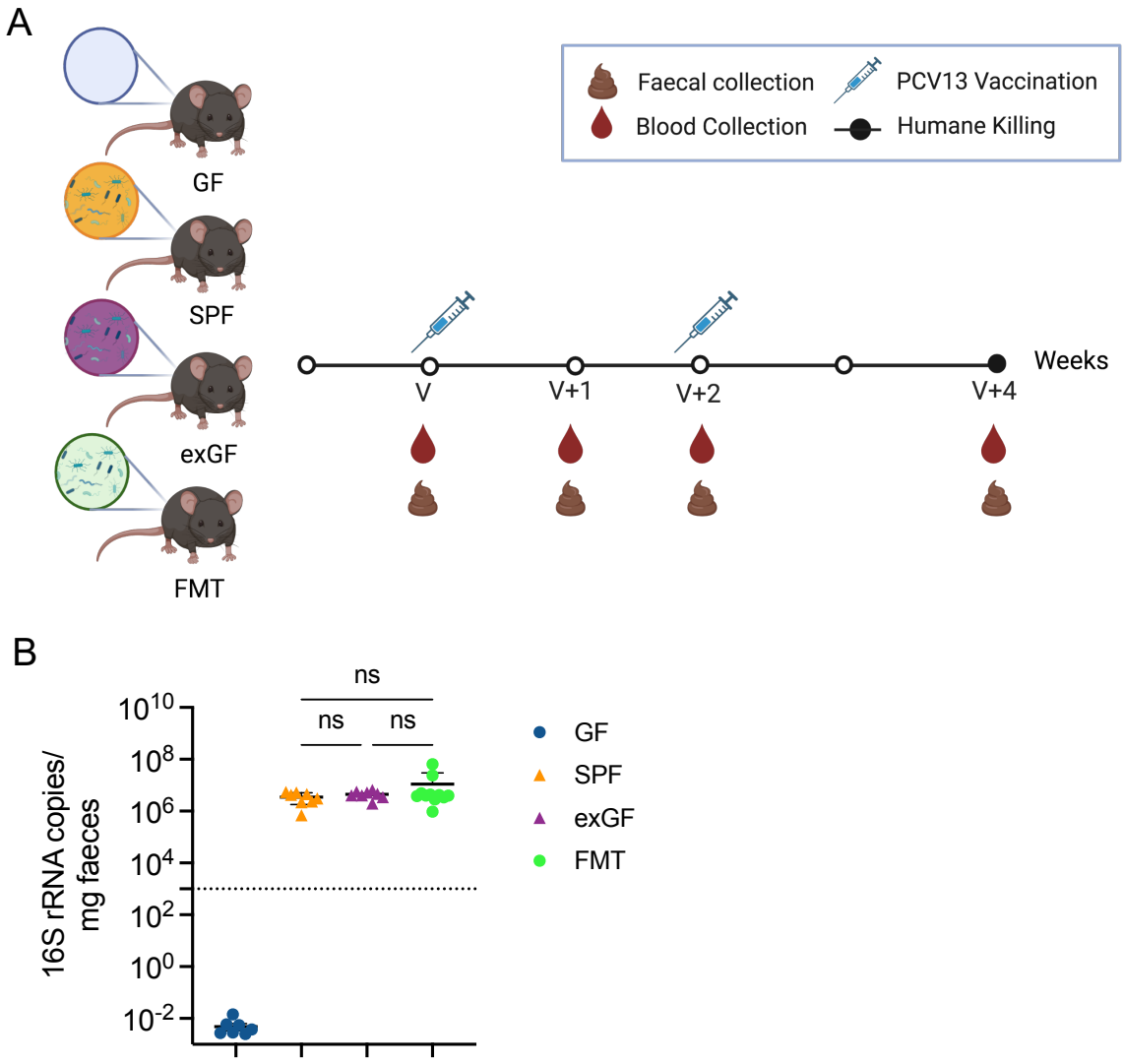

Figure 5.5| Experimental design to investigate the differences in immune responses to PCV13 between GF and colonised mice. A| Responses to the PCV13 vaccine were assessed in germ-free (GF) mice in comparison to normally colonised SPF mice, or mice born to GF dams colonised with an SPF microbiota (exGF) and mice colonised at d21 of life (FMT). Mice were vaccinated intraperitoneally with 1/10th of a human dose of PCV13 at day 28 (d28) of life and boosted 2 weeks later (V+2). Mice were humanely killed either two weeks after initial vaccination (V+2) or two weeks post boost (V+4) and spleen, bone marrow and draining lymph nodes were harvested. **B|** 16S rRNA gene qPCR data assessing bacterial load at V. Note; values from GF mice are below the limit of detection. Data are represented as mean ± SEM. One-way ANOVA was used to assess statistical significance. ns = not significant.

5.1.3 The composition of the gut microbiota is significantly different in SPF, exGF and FMT mice

To assess differences in the composition of the gut (faecal) microbiota of exGF and FMT mice in comparison to SPF mice, 16S rRNA gene sequencing was undertaken by the SA Genomics Centre on DNA extracted from faecal samples collected on the day of vaccination (V). The analysis of the 16S rRNA gene sequencing data by Dr Feargal Ryan revealed clear differences in beta diversity (community dissimilarity) between the three colonised groups (**Fig. 5.6A-B**). The most spread was found in the exGF and FMT mice, while SPF mice clustered closely together and near the exGF group (**Fig. 5.6A**), indicating that the composition of the microbiota in exGF mice is more similar to SPF mice. Unifrac analysis also revealed that the exGF and SPF mice clustered together separately from the FMT group (**Fig. 5.6B**). Next, alpha diversity was assessed (**Fig. 5.6C-D**). The first measure of alpha diversity that was assessed was Shannon diversity, which takes evenness into account. Both the exGF and FMT mice had significantly higher Shannon diversity than the SPF mice (**Fig. 5.6C**). Chao1 richness considers the diversity of rarely observed taxa. SPF mice had significantly decreased Chao1 indices at the V timepoint compared with the exGF and FMT mice, indicating significantly decreased species richness (**Fig. 5.6D**).

The relative abundance of each genus was next determined to assess differences across the different groups (**Fig. 5.6E**). Samples were broadly similar across each group, with *Lactobacillus*, *Lachnospiraceae,* and *Muribaculaceae* found in the highest relative abundance across samples (**Fig. 5.6E**). However, SPF mice had a significantly higher relative abundance of *Lactobacillus* compared with the exGF and FMT groups **(Fig. 5.6F)**. *Akkermansia* is an immunomodulatory, Gram-negative bacteria often added to probiotics

due to its benefits in reducing inflammation (Raftar et al., 2022). *Akkermansia* was found at a significantly higher relative abundance in exGF mice compared to the SPF and FMT groups **(Fig. 5.6G)**. SPF mice also had a significantly higher abundance of *Akkermansia* compared to FMT mice. *Bifidobacterium* is associated with a healthy infant gut and higher antibody responses to the PCV13 vaccine in the AIR study (**Ryan et al, Appendix 2**)*. exGF mice had a significantly higher relative abundance of *Bifidobacterium* than either SPF or FMT mice (**Fig. 5.6H**). *Alistipes* is a genus of the *Bacteroidetes* phylum of emerging interest for its associations with various diseases such as cancer, mental illness and cardiovascular disease (B. J. Parker, Wearsch, Veloo, & Rodriguez-Palacios, 2020). Both SPF and exGF mice had a significantly higher abundance of *Alistipes* than the FMT group (**Fig. 5.6I**). To further determine the similarities and differences between SPF mice vs. those colonised intergenerationally or with an FMT, the overlap in Amplicon Sequence Variants (ASVs) was examined (**Fig. 5.6J**). Surprisingly, only one ASV was found to be unique to the SPF group. In contrast, FMT mice had 37 unique ASVs, while exGF mice had just 9. The majority of overlap in ASVs found between the groups was between the SPF and exGF mice. The FMT mice shared only 1 and 3 ASVs with SPF and exGF groups, respectively, with 5 shared between both.

In conclusion, there are distinct differences between the microbiota of SPF, exGF, and FMT mice. The FMT group in particular showed clear differences compared to the SPF and exGF mice, which is evidence to suggest it may not have had sufficient time to stabilise. However, while this is the strongest explanation there are multiple explanations that are consistent this observation, such as the age at which the mice received the FMT and the differences in the conditions in which the FMT mice are housed in, which should be assessed in future experiments.

*Removed due to copyright restriction

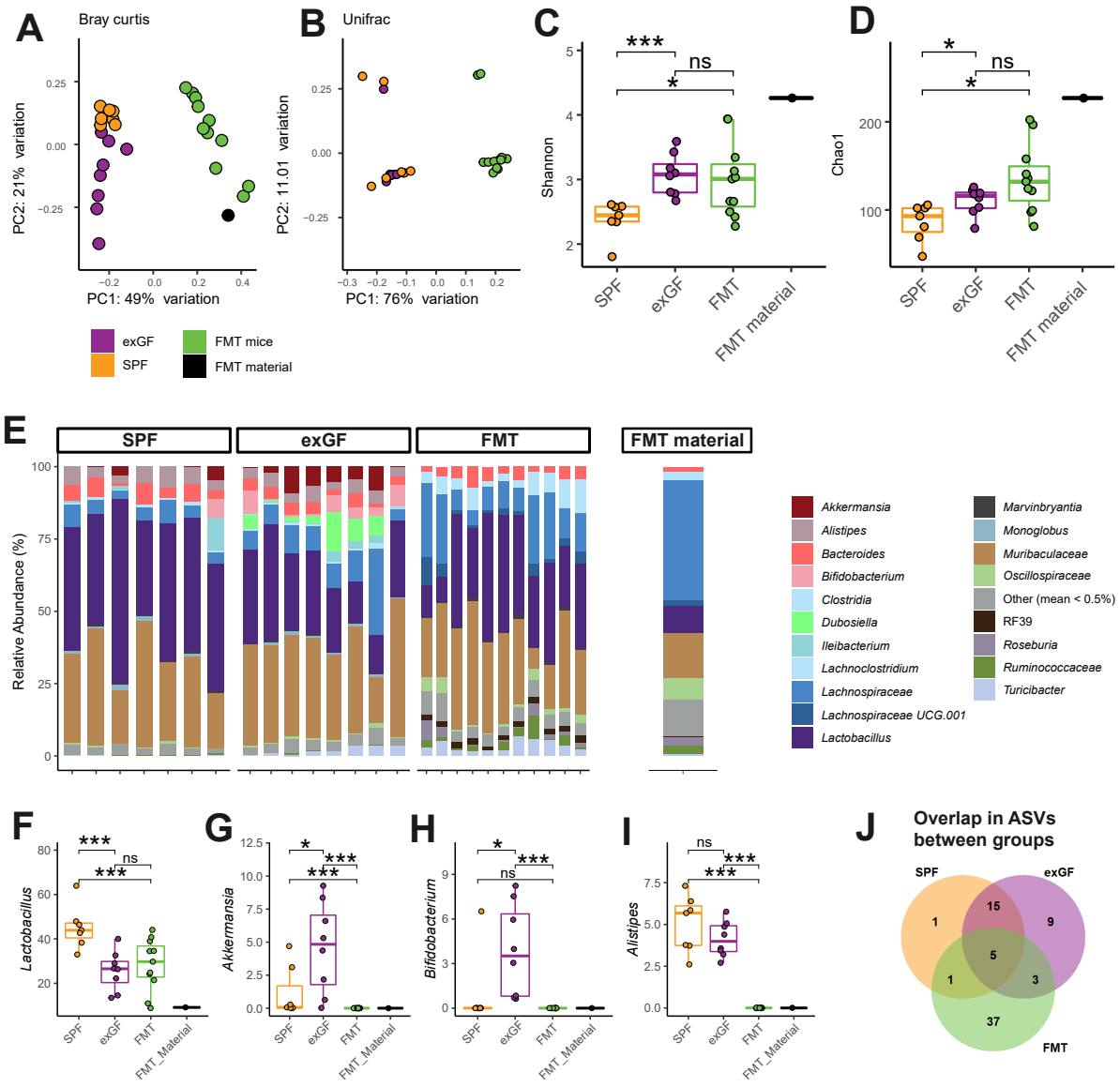

Figure 5.6| 16S rRNA gene sequencing analysis revealed differences in the composition of the gut microbiota of SPF, exGF and FMT mice. A| Principal component analysis (PCA) of Bray-Curtis dissimilarity indices and **B|** Unifrac distances calculated based on 16S rRNA gene sequencing of the fecal microbiota of SPF, exGF and FMT mice. **C|** Alpha diversity was assessed using Shannon and **D|** Chao1 indices. Data is shown as box and whisker plots. **E|** Composition of the faecal microbiota at the V timepoint. Each barplot represents the relative abundance of major taxa in samples collected from individual mice at d28 of life. **F-I|** Boxplots assessing the relative abundance of selected species at V. **J|** Piechart of ASVs shared between each group. Data are represented as mean ± SEM. Wilcox rank sum test were used to assess statistical significance *p < 0.05, ***p < 0.001, ns = not significant.

5.1.4 Colonising GF mice intergenerationally, but not at day 21 of life, partially restores primary antibody responses to PCV13.

To assess differences in antibody responses between GF, SPF, exGF and FMT mice, ELISAs were carried out to determine PCV13-specific antibody responses in serum before boosting. As previously observed (**Fig. 5.2**), GF mice had significantly lower IgG_{total} responses against the whole vaccine and PPS1 after a primary dose of PCV13, compared to SPF mice (**Fig. 5.7A-B**). Interestingly, IgG responses appeared to be at least partially restored in exGF mice, as there were no significant differences in PCV13-specific IgG_{total} responses between exGF and SPF mice (**Fig. 5.7A-D**). Furthermore, exGF mice had significantly higher IgG_{total} responses against PPS1 compared to GF mice (**Fig. 5.7B**). Responses to the whole vaccine and PPS1 were significantly impaired in FMT mice compared to SPF mice (**Fig. 5.7A-B**). A similar trend was observed for CRM_{197}- and PPS3-specific IgG_{total} responses, but these differences did not achieve statistical significance (**Fig. 5.7C-D**). These data suggest that colonisation of the gut microbiota in early life or even *in utero* is required for optimal primary antibody responses to PCV13.

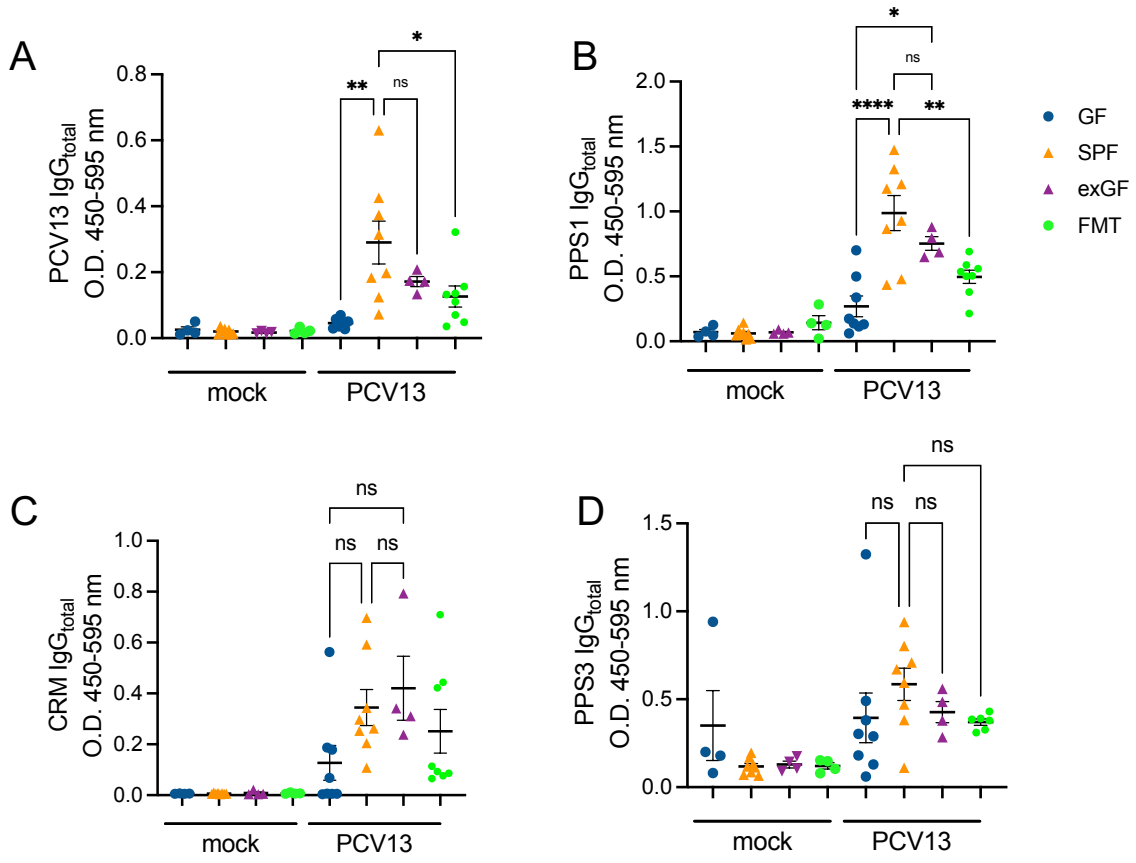

Figure 5.7| PCV13 and PPS1-specific primary IgG_{total} responses are impaired in GF and FMT mice compared to SPF mice. IgG_{total} responses to **A|** the whole PCV13 vaccine, **B|** PPS1, **C|** CRM_{197} and **D|** PPS3 in the serum of mock and PCV13-vaccinated GF, SPF, exGF and FMT mice were assessed by ELISA. Serum was collected at V+1 weeks post-vaccination. Raw O.D. values are shown. Data are represented as mean ± SEM. One-way ANOVA was used to assess statistical significance *p <0.05, ** p < 0.01 ****p < 0.0001, ns = not significant.

To evaluate the humoral immune response following a booster dose of PCV13, IgG_{total} and IgG subclass responses were assessed 2 weeks post-boost. SPF mice maintained significantly higher IgG_{total} total responses to PCV13 post-boost than GF mice (**Fig. 5.8A**). Responses were also higher in exGF and FMT mice compared to GF mice but did not reach statistical significance. As observed pre-boost, PPS1-specific IgG_{total} responses were significantly lower in GF and FMT mice post-boost compared to SPF mice, while no significant differences were observed between exGF mice and the other groups (**Fig. 5.8B**). While no significant differences in PPS3-specific IgG_{total} were observed pre-boost, SPF mice had significantly higher IgG_{total} responses compared to GF mice at V+4 weeks

(**Fig. 5.8C**). Both SPF and FMT mice had higher IgG_{total} responses against CRM_{197} than GF mice (**Fig. 5.8D**). These data indicate that the IgG_{total} response against the conjugate protein but not the polysaccharides may be restored in FMT mice post-boost.

GF mice also had significantly lower IgG1 responses to the whole vaccine, PPS3 and PPS1 post-boost compared to SPF mice (**Fig 5.8E-G**). FMT mice had significantly impaired IgG1 responses to PPS1 compared to SPF mice (**Fig. 5.8G**). There was a trend towards lower IgG1 responses against CRM_{197} in GF mice compared to SPF, exGF and FMT mice but this was not statistically significant due to outliers in the GF group (**Fig. 5.8H**).

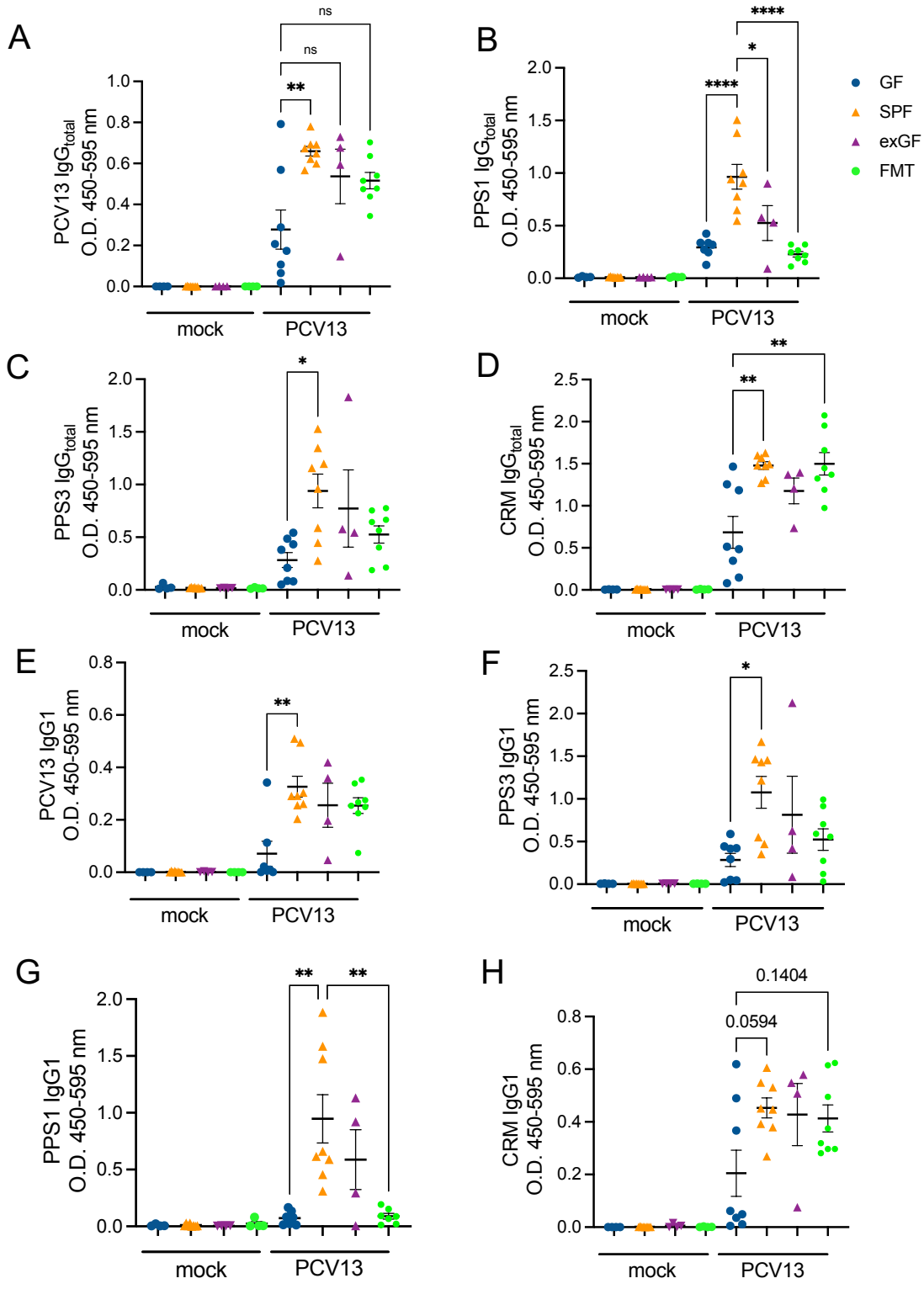

Figure 5.8| IgG$_{total}$ and IgG1 responses against PCV13, PPS1 and PPS3 are impaired in vaccinated GF mice compared to SPF mice at V+4 weeks (2 weeks post boost). IgG$_{total}$ responses to **A|** the whole PCV13 vaccine, **B|** PPS1, **C|** PPS3 and **D|** CRM$_{197}$ in the serum of mock and PCV13-vaccinated GF, SPF, exGF and FMT mice at V+4. IgG1 responses to **E|** the whole PCV13 vaccine, **F|** PPS3, **G|** PPS1 and **H|** CRM$_{197}$ in the serum of mock and PCV13 vaccinated GF, SPF, exGF and FMT mice at V+4. Raw O.D. values are shown. Data are

represented as mean ± SEM. One-way ANOVA was used to assess statistical significance *p <0.05, ** p < 0.01 ***p < 0.001, ns = not significant.

Next, IgG3 responses were assessed in both mock and vaccinated GF, SPF, exGF and FMT mice (**Fig. 5.9**). GF, exGF and FMT mice all had significantly lower IgG3 responses to whole vaccine and PPS1 compared to SPF mice (**Fig. 5.9A-B**). In addition to this, GF and FMT mice had significantly lower IgG3 responses to PPS3 than SPF mice, although this was not the case for the exGF group (**Fig. 5.9C**). IgG3 responses to PPS3 in the FMT group were significantly lower than in the exGF mice (**Fig. 5.9C**). IgG3 responses to CRM_{197} were also impaired in GF mice compared to SPF mice (**Fig. 5.9D**). Responses to IgG2b were also assessed against the whole vaccine, but not polysaccharides or the conjugate protein due to time constraints (**Fig. 5.9E**). There were no significant differences between any of the groups (**Fig. 5.9E**).

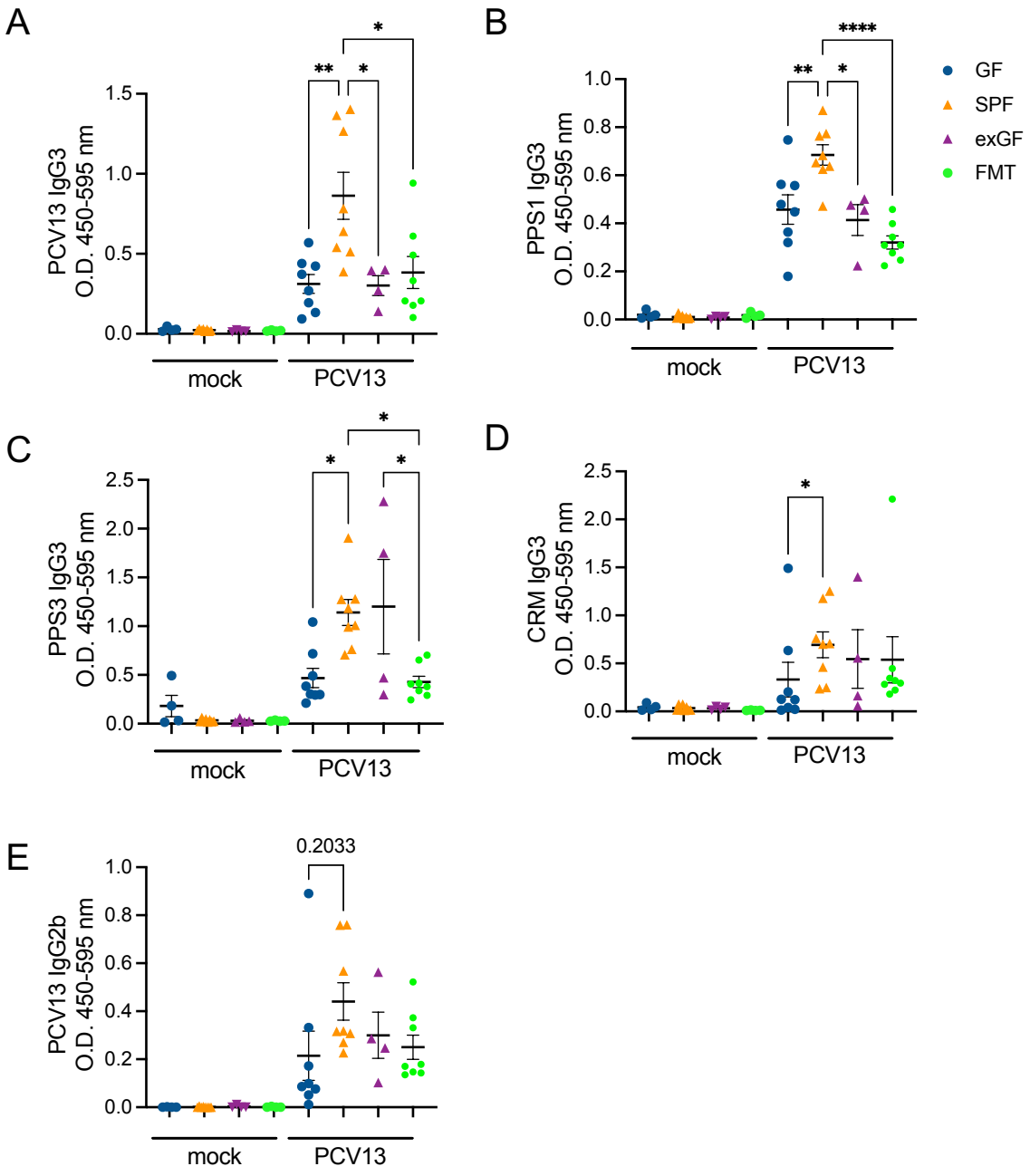

Figure 5.9| IgG3 responses against PCV13 and PPS1 are impaired in vaccinated GF and exGF mice compared to SPF mice at V+4. IgG3 responses to **A|** the whole PCV13 vaccine, **B|** PPS1, **C|** PPS3 and **D|** CRM_{197} in the serum of mock and PCV13 vaccinated GF, SPF, exGF and FMT mice at V+4. **E|** IgG2b responses to the whole PCV13 vaccine in the serum of mock and PCV13 vaccinated GF, SPF, exGF and FMT mice at V+4. Raw O.D. values are shown. Data are represented as mean ± SEM. One-way ANOVA was used to assess statistical significance *p <0.05, ** p < 0.01 ***p < 0.001.

Finally, IgM responses were assessed in all groups. PCV13-vaccinated SPF mice had significantly higher serum IgM responses to PPS1 than GF, SPF and FMT (**Fig. 5.10A**). In

contrast, only the GF group had significantly lower IgM responses to PPS3 (**Fig. 5.10B**). SPF mice had significantly higher PCV13 specific IgM responses than GF and FMT mice (**Fig. 5.10C**), while SPF mice had higher CRM_{197} specific IgM responses than the FMT group (**Fig. 5.10D**).

Overall, there are numerous differences in antibody responses between SPF, exGF and FMT mice, with the FMT groups often presenting as an intermediate phenotype. These findings suggest that the timing of colonisation is important in determining how well the immune system of GF mice can recover from an absence of interactions with and signals from the microbiota.

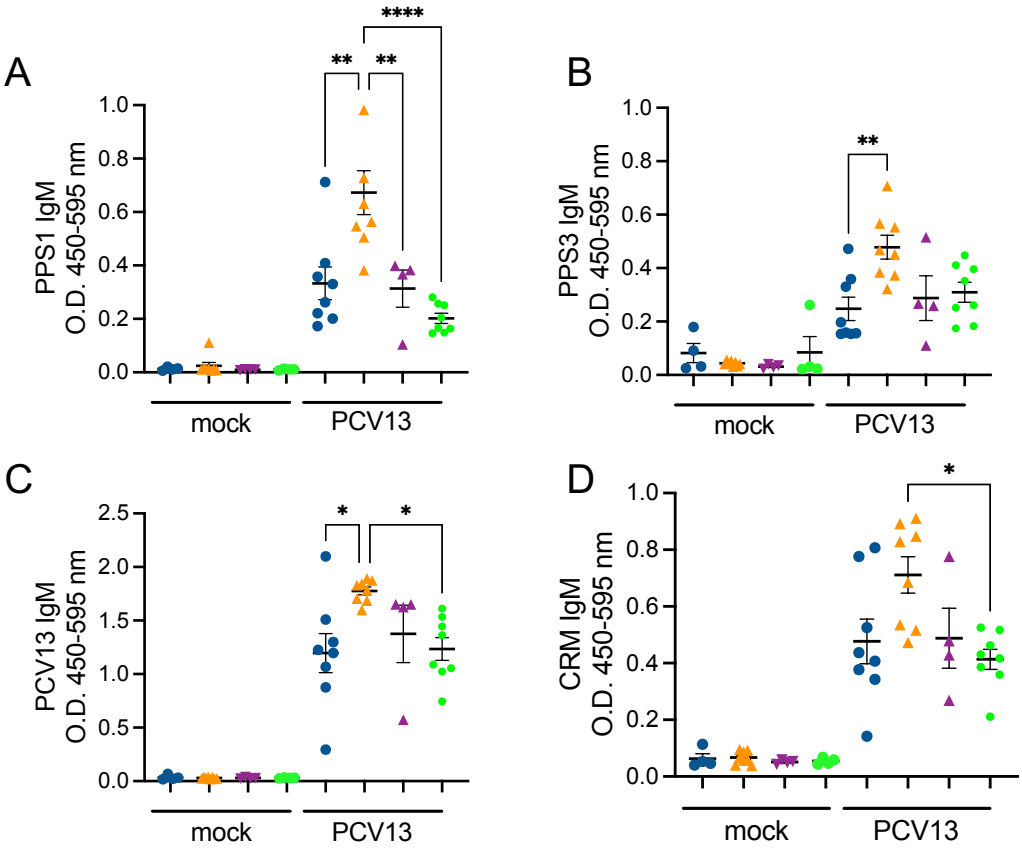

Figure 5.10| PPS1, PPS3 and PCV13-specific IgM responses are impaired in GF mice compared to SPF mice at V+4. IgM responses to **A|** PPS1, **B|** PPS3, **C|** PCV13 and **D|** CRM_{197} in mock and PCV13 vaccinated GF, SPF, exGF and FMT mice at V+4. Raw O.D. values are shown. Data are represented as mean ± SEM. One-way ANOVA was used to assess statistical significance. ** $p < 0.01$ ****$p < 0.0001$.

5.1.5 GF and FMT mice have reduced proportions of antibody-secreting cells in their spleens compared to exGF mice

Measuring the numbers of antibody-secreting cells (ASCs) in primary and secondary lymphoid organs provides insight into antibody production at a cellular level. The bone marrow is generally thought of as a niche for the long-term maintenance of long-lived plasma cells. To assess differences in ASCs between the groups, GF, SPF, exGF and FMT mice were humanely culled two weeks post-boost (V+4). Spleens and bone marrow were harvested from immunised mice and mock-immunised controls. There was a significant induction of IgG^+ ASCs in the spleens of SPF and exGF mice compared to mock controls but not in the GF or FMT groups when measured by ELISpot (**Fig. 5.11A**). PCV13 immunised SPF mice had significantly higher numbers of IgG^+ ASCs in the bone marrow compared to mock SPF mice, but this was not the case for GF, exGF or FMT mice (**Fig. 5.11B**), although exGF mice were not significantly different compared to SPF mice. These data demonstrate robust antibody responses in SPF and exGF mice, but not GF and FMT mice.

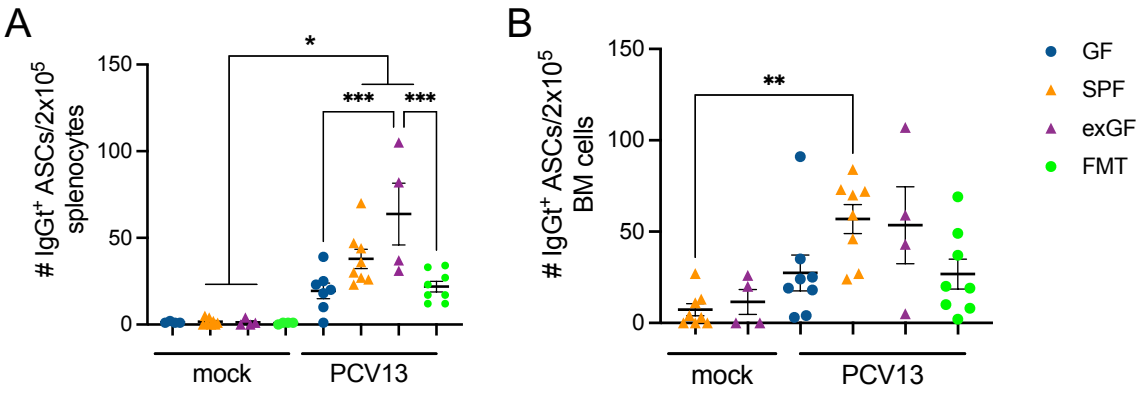

Figure 5.11| There is a lower number of IgG$^+$ ASCs in the spleens of GF and FMT mice compared to SPF and exGF mice at V+4. PCV13-specific IgG$^+$ ASCs were assessed in the **A|** spleen and **B|** bone marrow cells using an ELISpot assay. Cells were added to PCV13-coated ELISpot plates at a concentration of 2x10^5 cells/well in complete media and cultured at 37°C for 72h. Cells were not harvested from the bone marrow of GF and FMT mocks due to time constraints. Data are represented as mean ± SEM. One-way ANOVA was used to assess statistical significance. *p <0.05, ** p < 0.01 ***p < 0.001.

5.1.6 Significant differences in major B cell populations between PCV13 vaccinated GF and colonised mice

The impairment of serum antibody responses and reduction of ASCs following the immunisation of GF mice indicate that GF mice have a deficiency in their B cell responses to the PCV13 vaccine. B cell responses to vaccination include several different stages including differentiation and class-switching, the formation of germinal centres (GCs), the production of short and long lived PCs and the generation of memory B cells. To assess the different stages of the B cell response in GF versus colonised mice, mock and vaccinated GF, SPF, exGF and FMT mice from this experiment were humanely culled two weeks post-boost (V+4) and their spleens and draining (mediastinal) lymph nodes were collected and processed into single cell suspensions for flow cytometry analysis using the gating strategy outlined **in Figure 5.12**. This time point was chosen to capture changes in adaptive B cell populations after the height of the cellular response (Lederer et al., 2020). The B cell flow cytometry panel was designed to define total B cells (B220$^+$ CD19$^+$),

antigen-experienced IgD^- B cells ($B220^+$ $CD19^+IgD^-$), IgM^+IgD^- B cells ($B220^+CD19^+IgM^+IgD^-$), IgD^+IgM^- B cells ($CD19^+BB20^+IgD^+IgM^-$), GC B cells ($B220^+$ $CD19^+$ IgD^- $GL7^+$ Fas^+), antigen-specific CRM_{197}^+ GC B cells ($B220^+$ $CD19^+$ IgD^- $GL7^+$ Fas^+ CRM^+), memory B cells ($B220^+CD19^+IgD^-CD138^-GL7^-CD27^+CD38^+$), IgM^+ memory B cells ($B220^+CD19^+IgD^-CD138^-GL7^-CD27^+CD38^+IgM^+$) and plasma cells (PCs) ($B220^+IgD^-Sca\text{-}1^+CD138^+$) (**Fig. 5.12**). These flow cytometry panels were selected based on the recent publication by Lederer et al. analysing the GC response to a novel SARS-CoV-2 vaccine (Lederer et al., 2020). Additionally, the Stem cell antigen-1 (Sca-1) marker was incorporated to improve PC identification (Wilmore, Jones, & Allman, 2017).

To assess differences in antigen-specific GC B cells, the CRM_{197} carrier protein was conjugated to biotin (Fina Biosolutions, USA).

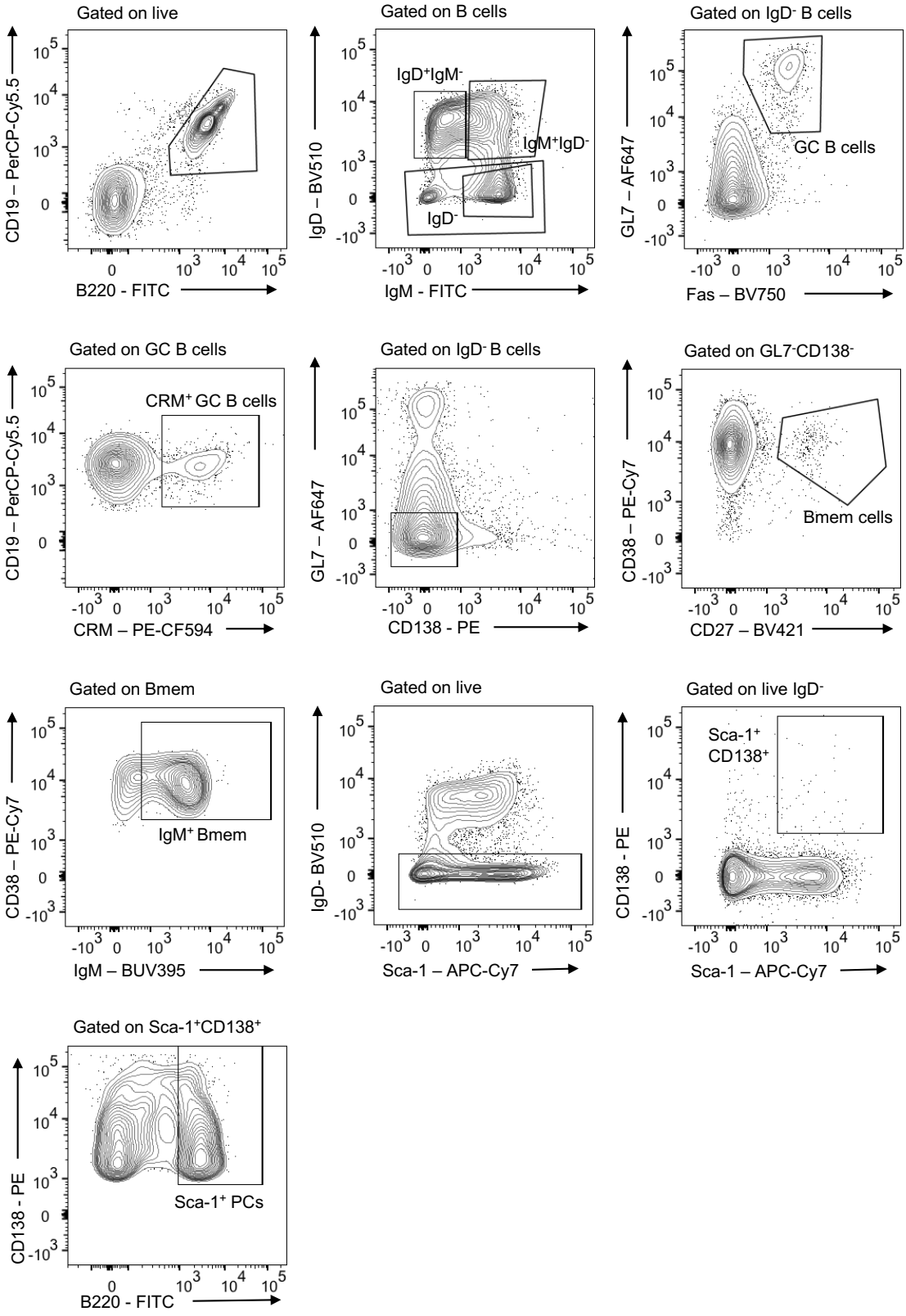

Figure 5.12| B cell gating strategy. Cells were pre-gated on FSC x SSC for lymphocytes, followed by singlet discrimination and live cell gating. B cells were gated on the $CD19^{+}B220^{+}$ population. B cells were split into various populations based on their expression of IgM and IgD, including IgD^{-}, $IgD^{+}IgM^{-}$ and $IgM^{+}IgD^{-}$ B cell populations. The IgD^{-} population was gated

on to define $GL7^+$ Fas^+ GC B cells. This population was further gated on a biotinylated CRM_{197} probe to define antigen-specific CRM_{197}^+ GC B cells. The IgD^- population was gated on to exclude the plasma cell and GC B cell markers GL7 and CD138. This $GL7^-CD138^-$ population was used to define $CD38^+CD27^+$ memory B cells. This was further gated on IgM expression to define IgM^+ memory B cells. An IgD^- population was gated from total live cells. This population was used to identify a $Sca\text{-}1^+CD138^+$ subset, which was further gated on the $B220^+$ population to define $Sca\text{-}1^+$ plasma cells.

When plotted as fold-change, there were no differences in the proportion of splenic $B220^+CD19^+$ B cells between any of the groups (**Fig. 5.13A**). In contrast, there was a significant increase of $B220^+CD19^+$ B cells in the exGF mice in the dLN following immunisation (V+4) compared to GF, SPF and FMT mice (**Fig. 5.13B**).

Unlike other immunoglobulins, IgD is expressed almost exclusively at the cell surface and is not secreted (White, Shen, Word, Tucker, & Blattner, 1985). IgD expression is downregulated after contact with cognate $CD4^+$ T cell help or foreign antigen exposure, which means this IgD^- population is the parent population of many antigen-experienced cell types including GC B cells, memory B cells and PCs (Lederer et al., 2020, Wilmore, Jones, & Allman, 2017). As expected, there was a significant increase in splenic IgD^- B cells as a proportion of total B cells in vaccinated SPF mice compared to mock SPF mice (**Fig. 5.13C**). In contrast, there were no significant differences in the proportion of splenic IgD^- B cells between immunised GF, exGF or FMT mice, relative to mock immunised mice. These data suggest impaired class-switching or a reduction in proliferation in splenic B cells in these groups of mice. In contrast to splenic IgD^- B cells, there was a significantly higher frequency of IgD^- B cells in the dLN of SPF, exGF, and FMT but not GF mice after vaccination (**Fig. 5.13D**). Since there is a particularly strong impairment of serum antibody responses in GF mice compared to the other groups, these data may explain why

responses to vaccination are partially and often fully restored in exGF and FMT mice but not GF mice.

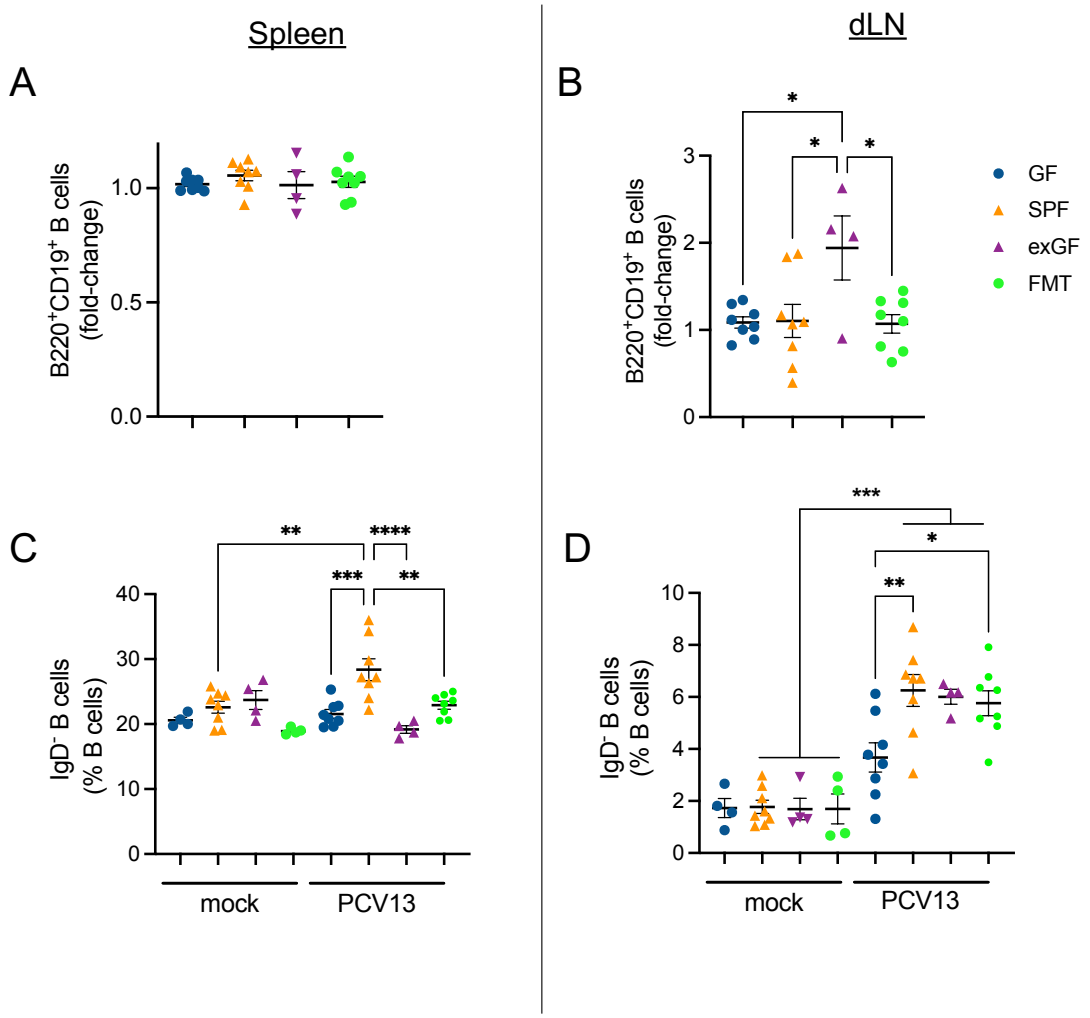

Figure 5.13| GF mice have a lower frequency of antigen-experienced B cells compared to SPF mice. $B220^{+}CD19^{+}$ B cells plotted as fold-change relative to mock in **A|** the spleens and **B|** mediastinal lymph nodes of GF, SPF, exGF and FMT mice at V+4 weeks. $B220^{+}CD19^{+}IgD^{-}$ B cells as a frequency of total $B220^{+}CD19^{+}$ B cells in **C|** the spleens and **D|** mediastinal lymph nodes of GF, SPF, exGF and FMT mice at V+4 weeks. Data are represented as mean ± SEM. One-way ANOVA was used to assess statistical significance. *p <0.05, ** p < 0.01 ***p < 0.001, ****p < 0.0001.

5.1.7 The proportion of Germinal Centre B cells is not significantly lower in GF mice following primary immunisation with PCV13

Optimal T-dependent responses to vaccination are driven by the formation of GCs in secondary lymphoid organs such as the spleen and draining lymph nodes. Activated B cells undergo affinity maturation and somatic hypermutation in GCs, eventually

differentiating into antibody-secreting long-lived PCs and memory B cells (N. S. De Silva & Klein, 2015; M. Silva et al., 2017; Stebegg et al., 2018; Waide et al., 2020). Earlier in this chapter, it was demonstrated that GF mice had significantly impaired antibody responses to vaccination compared to SPF mice before boosting at V+2 (**Fig. 5.2**). To assess whether GC formation was impaired in PCV13 immunised GF mice, the proportion of total (i.e. not vaccine antigen-specific) GC B cells (defined as $CD19^+B220^+IgD^-GL7^+Fas^+$ B cells (Lederer et al., 2020)) was assessed in the spleen and dLN of GF, SPF, exGF and FMT mice at 2 weeks after the first dose of PCV13.

The frequency of total GC B cells and antigen-specific CRM_{197} GC B cells were assessed via flow cytometry using the CRM_{197} probe at V+2 (**Fig. 5.14**). Interestingly, while there was a significant increase in total and CRM_{197}^+ GC B cells in PCV13 vaccinated GF and SPF compared to the mock group, there were no statistically significant differences observed in the proportion of GC B cells or CRM_{197}^+ GC B cells in the spleens of vaccinated GF and SPF mice at V+2 (**Fig. 5.14A-C**). Therefore, it seems likely that there may be other differences early in the B cell response to vaccination that lead to the impaired antibody response observed in GF mice pre-boost. It is also possible that there were significant differences in GC responses at V+1 weeks that were resolved by V+2.

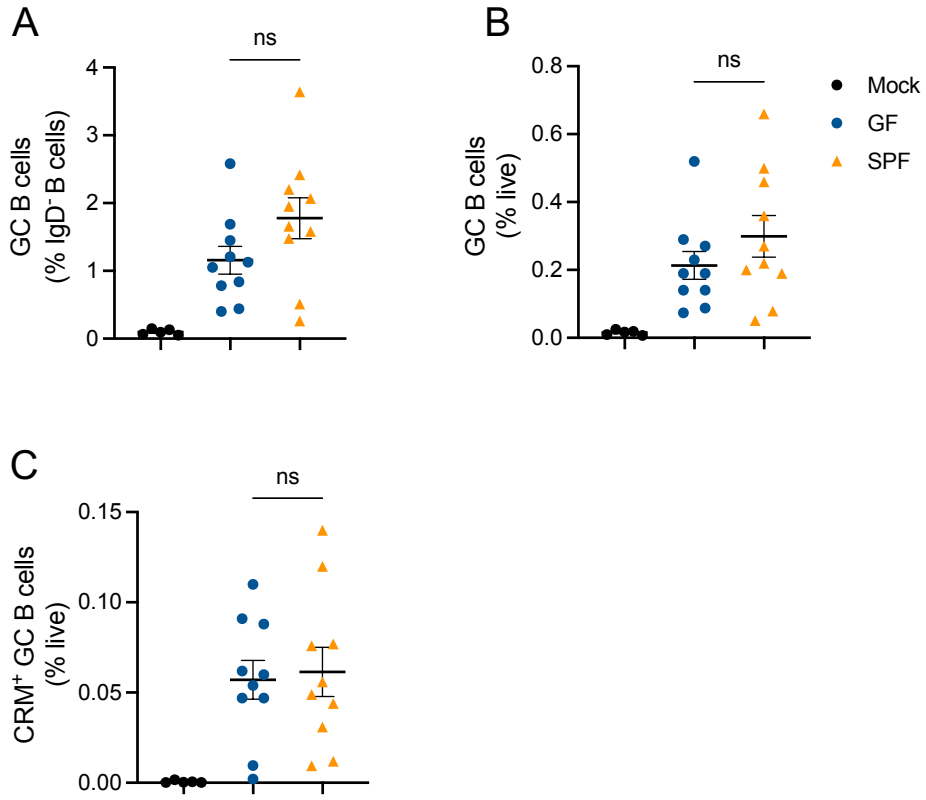

Figure 5.14| No significant difference in the proportion of total or CRM_{197}-specific GC B cells in PCV13-vaccinated GF vs SPF mice at V+2. $GL7^+Fas^+$ GC B cells the spleens of GF, SPF and mock mice at V+2 weeks as a frequency of **A|** their parent IgD^- population and **B|** total live cells. Cells were pre-gated on live $CD19^+B220^+IgD^-$ populations. **C|** CRM_{197}^+ GC B cells were also assessed in the spleens of GF, SPF and mock mice as a frequency of total live cells. These cells were pre-gated on GC B cells as detailed. Data are represented as mean ± SEM. Mann-Whitney tests were used to assess statistical significance.

As there were no differences at V+2, differences in GC responses were assessed in an independent experiment between GF and colonised (exGF, FMT and SPF) mice post-boost at V+4 weeks (i.e. 2 weeks after boosting with a second dose of PCV13) (**Fig. 5.15A**). There was a significant induction of total GC B cells after the second dose of PCV13 in both the spleen and dLN of SPF, exGF and FMT mice compared to mock immunised mice (**Fig. 5.15A-C**). In contrast, there was no significant induction of total GC B cells in either tissue in vaccinated GF mice (**Fig. 5.15B-C**). Interestingly, FMT mice had a significantly

reduced proportion of total GC B cells compared to SPF mice in the spleen but not dLN (**Fig. 5.15B-C**).

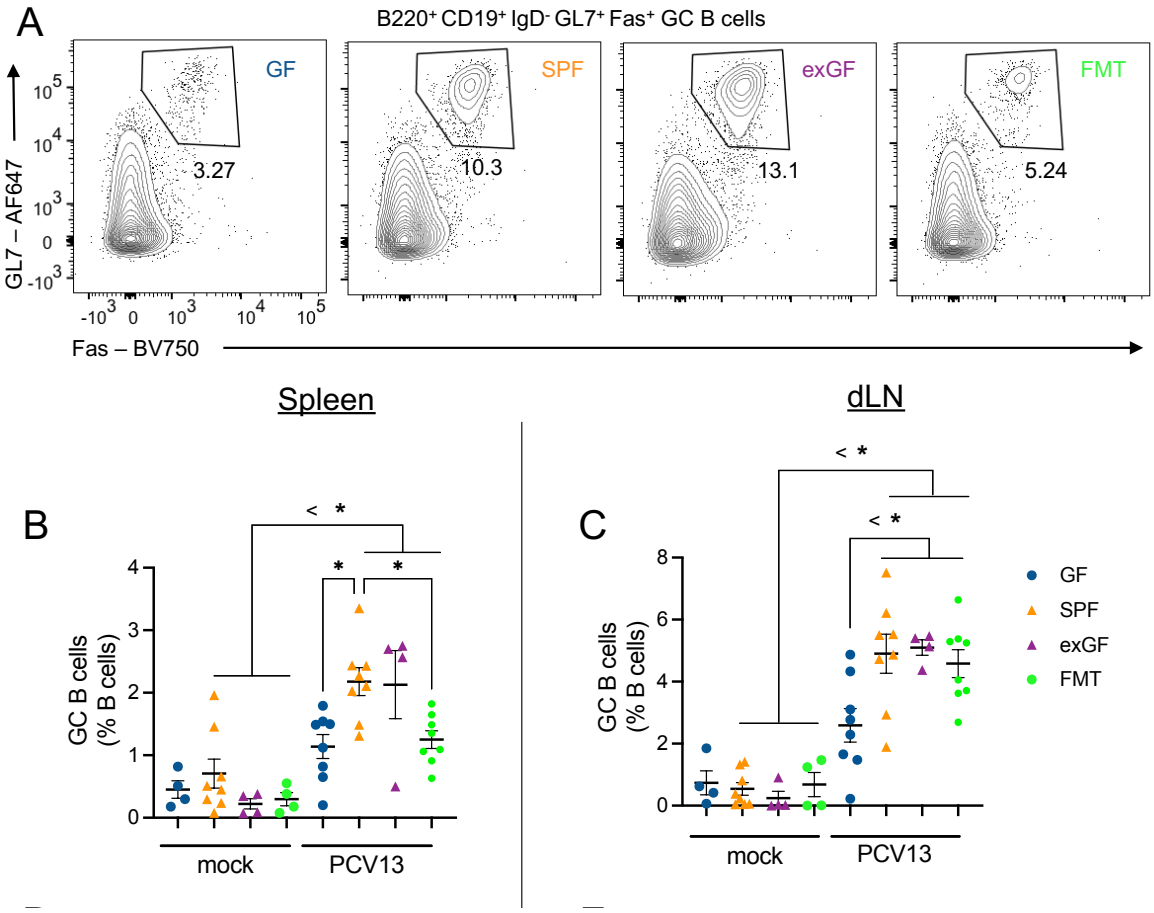

Figure 5.15| GF mice had a significantly lower frequency of total GC B cells in the spleen and dLN compared to SPF, exGF and FMT mice. A| Representative flow cytometry of GC B cells ($GL7^+Fas^+$) in the spleen of vaccinated GF, SPF, exGF and FMT mice. Cells were pre-gated on live $CD19^+B220^+IgD^-$ cells. **B-C|** Frequency of GC B cells in the spleen and mediastinal lymph node as a proportion of B cells. Data are represented as mean ± SEM. One-way ANOVA was used to assess statistical significance. *p <0.05, <* = each group comparison is at least p<0.05.

Next, I assessed whether antigen-specific (i.e. CRM_{197}^+) GC B cells induced by immunisation with PCV13 were also impaired in GF mice. CRM-specific B cells were first assessed as a proportion of total B cells (**Fig. 5.16A-C**). The CRM_{197} probe demonstrated specificity for CRM_{197}^+ GC B cells as minimal to no binding of the probe was observed in the mock vaccinated groups (**Fig. S4.5**). There was a significant induction of CRM-specific

GC B cells in the spleens of vaccinated GF, SPF and exGF mice compared to mock immunised controls when assessed as a frequency of B cells (**Fig. 5.16B**). There were no significant differences in CRM_{197}-specific GC B cells between any of the vaccinated groups in the spleen, although there was a trend towards lower responses in the FMT group compared to the SPF group (**Fig. 5.16B**). GF mice had significantly lower proportions of antigen-specific GC B cells in the dLN compared to FMT mice (**Fig. 5.16C**), though interestingly, not exGF or SPF mice.

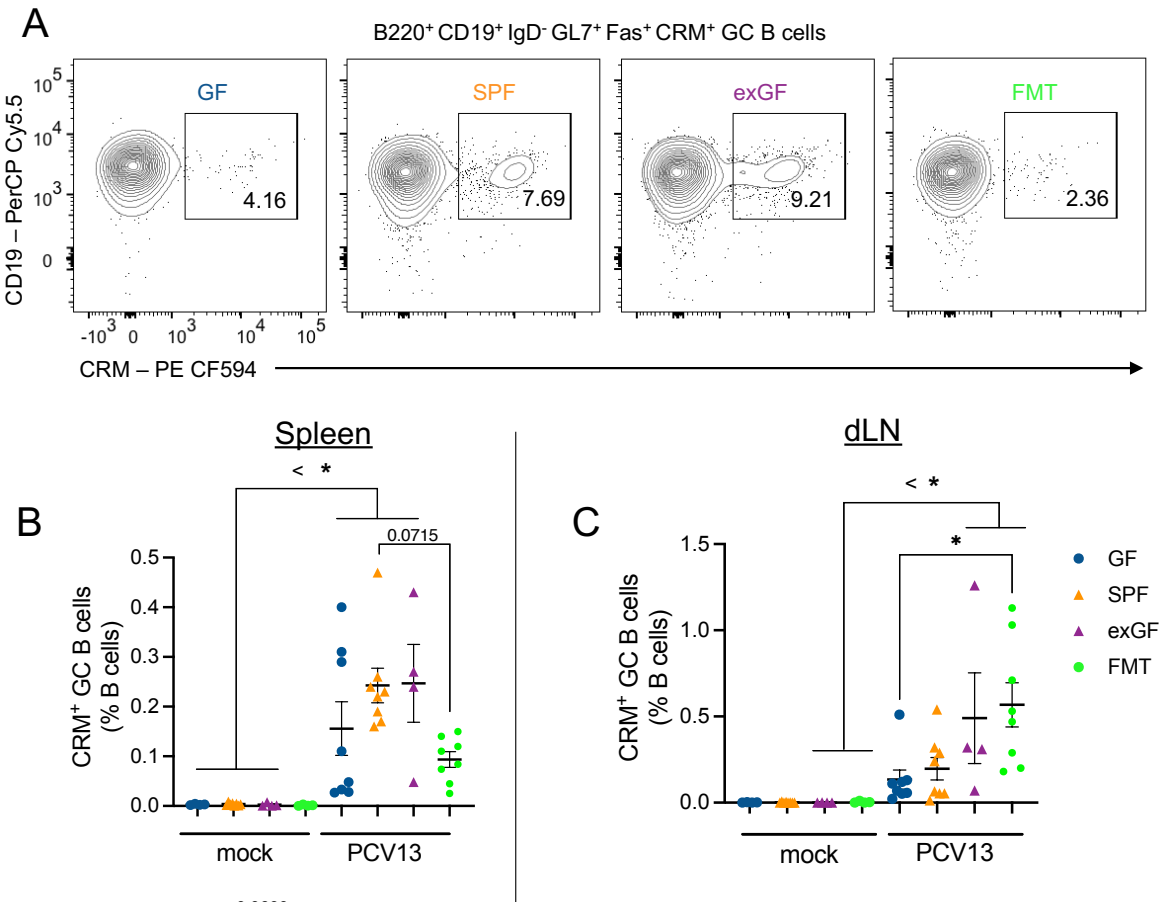

Figure 5.16| Significantly higher frequency of CRM_{197}^+ GC B cells in vaccinated FMT mice in the draining lymph node but not spleen. A| Representative flow cytometry analysis of CRM_{197}^+ GC B cells ($CRM_{197}^+GL7^+Fas^+$) in the spleen of vaccinated GF, SPF, exGF and FMT mice. Cells were pre-gated on live $CD19^+B220^+IgD^-GL7^+Fas^+$ populations. **B-C|** Frequency of CRM_{197}^+ GC B cells in the **B|** spleen and **C|** draining mediastinal lymph node of vaccinated GF, SPF, exGF and FMT mice as a proportion of B cells. Data are represented as mean ± SEM. One-way ANOVA was used to assess statistical significance *p <0.05, ***p <0.001.

Interestingly, CRM_{197}-specific GC B cells were not significantly different in GF mice compared to SPF mice. This may be due to some unexpected outliers in the GF mouse data in this experiment. In a subsequent independent experiment, GF mice had a significantly reducted frequency of CRM_{197}-specific GC B cells in the spleen compared to both SPF and exGF mice, when plotted as a frequency of both class-switched IgD^- B cells and total B cells (**Fig. 5.17A-B**).

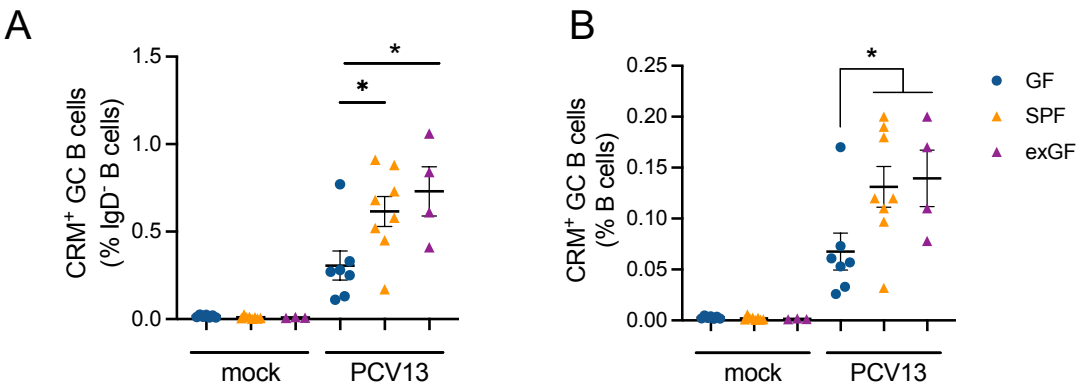

Figure 5.17| There was a significantly higher frequency of CRM_{197}^+ GC B cells in the spleens of SPF and exGF mice compared to GF mice at V+4. CRM_{197}^+ GC B cells ($CRM_{197}^+GL7^+Fas^+$) in the spleens of vaccinated GF, SPF and exGF mice at V+4 as a frequency of **A|** IgD^- B cells and **B|** total $CD19^+B220^+$ B cells. Cells were pre-gated on live $CD19^+B220^+IgD^-GL7^+Fas^+$ populations. Data are represented as mean ± SEM. One-way ANOVA was used to assess statistical significance. *p <0.05.

5.1.8 GF mice have significantly lower proportions of Tfh cells following PCV13 immunisation

GC formation is largely dependent on T cell help, specifically from T-follicular helper (Tfh) cells (Stebegg et al., 2018). Therefore, it is plausible that lower numbers of Tfh cells could explain the observed reduction in GC B cells. To investigate this hypothesis further, several T cell subsets, including Tfh cells, were assessed in GF, SPF, exGF, and FMT mice at V+4 weeks (**Fig. 5.18**). This T cell panel was used to define $CD3^+$ T cells ($CD3^+CD19^-$), $CD4^+$ T cells ($CD3^+CD19^-CD4^+$), activated $CD4^+$ T cells ($CD3^+CD19^-CD4^+CD44^{hi}CD62l^-$),

central memory CD4⁺ T cells (CD3⁺CD19⁻CD4⁺CD44^{hi}CD62l⁺), naïve T cells (CD3⁺CD19⁻CD4⁺CD44⁻CD62l⁺) (**Fig. S4.6**) and Tfh cells (CD3⁺CD19⁻CD4⁺CD44^{hi}CD62l⁻ CXCR5⁺Bcl-6⁺ or CXCR5⁺PD-1⁺ or CXCR5⁺Bcl6⁺ICOS⁺) (Lederer et al., 2020).

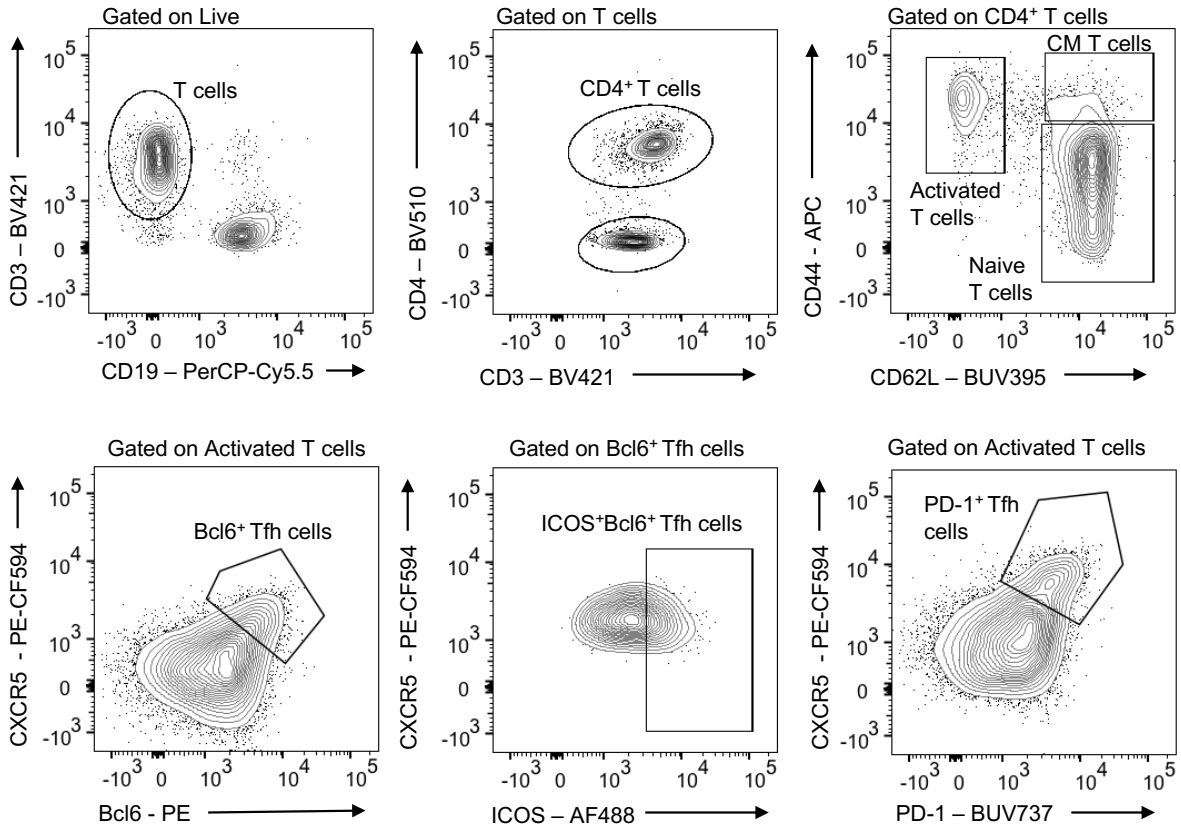

Figure 5.18| Tfh cell gating strategy. Cells were pre-gated on FSC x SSC for lymphocytes, followed by singlet discrimination and live cell gating. Total CD3⁺ T cells were gated on the CD3⁺CD19⁻ population. These were further gated by their CD4 expression to define CD4⁺ T cells. CD4⁺ T cells were gated on based on their CD44 and CD62L expression to identify activated CD4⁺ T cells (CD3⁺CD19⁻CD4⁺CD44^{hi}CD62L⁻), central memory CD4⁺ T cells (CD3⁺CD19⁻CD4⁺CD44^{hi}CD62L⁺), and naïve T cells (CD3⁺CD19⁻CD4⁺CD44⁻CD62L⁺). Tfh cells (CD3⁺CD19⁻CD4⁺CD44^{hi}CD62L⁻ CXCR5⁺Bcl-6⁺ or CXCR5⁺PD-1⁺ or CXCR5⁺Bcl6⁺ICOS⁺) were pre-gated on activated T cells.

Tfh cells are integral for B cell maturation, including class switching, clonal expansion and the production of short-lived PCs (Shi et al., 2018). First, CD3⁺CD19⁻CD4⁺CD44^{hi}B22D62L⁻ CXCR5⁺PD-1⁺ Tfh cells, which are GC homing T cell subset, were assessed by flow cytometry in the spleens and dLNs of GF, SPF, exGF and FMT mice. There were no

significant differences in the Tfh subsets assessed in the spleen (**Fig. S4.7**). In contrast, there was a significant reduction in the frequency of Tfh cells, expressed as a proportion of activated T cells, or as a proportion of total $CD4^+$ T cells, in the draining mediastinal lymph nodes of PCV13-vaccinated GF mice compared to SPF and exGF mice (**Fig. 5.19A-C**). There were significantly fewer Tfh cells in the lymph node of PCV13 vaccinated FMT mice than exGF mice when assessed as both a frequency of activated T cells and of $CD4^+$ T cells (**Fig. 5.19B-C**).

Bcl6 is a lineage marker used to define Tfh cells (**Fig. 5.19D**) and is necessary for Tfh function (Choi et al., 2020). Interestingly, a significant induction of $Bcl6^+$ Tfh cells was only observed in the vaccinated exGF group when comparing vaccinated mice to mocks (**Fig. 5.19E**). When comparing across vaccinated groups, there was a significant increase in the frequency of SPF and exGF $Bcl6^+$ Tfh cells in SPF and exGF mice compared to the GF and FMT mice (**Fig. 5.19E**).

Together with the reduction of GC B cells seen in the spleen and lymph node, the impaired Tfh response in GF mice indicates a defective GC response to the PCV13 vaccine in GF mice, likely explaining why serum antibody responses post-boost to the vaccine are impaired.

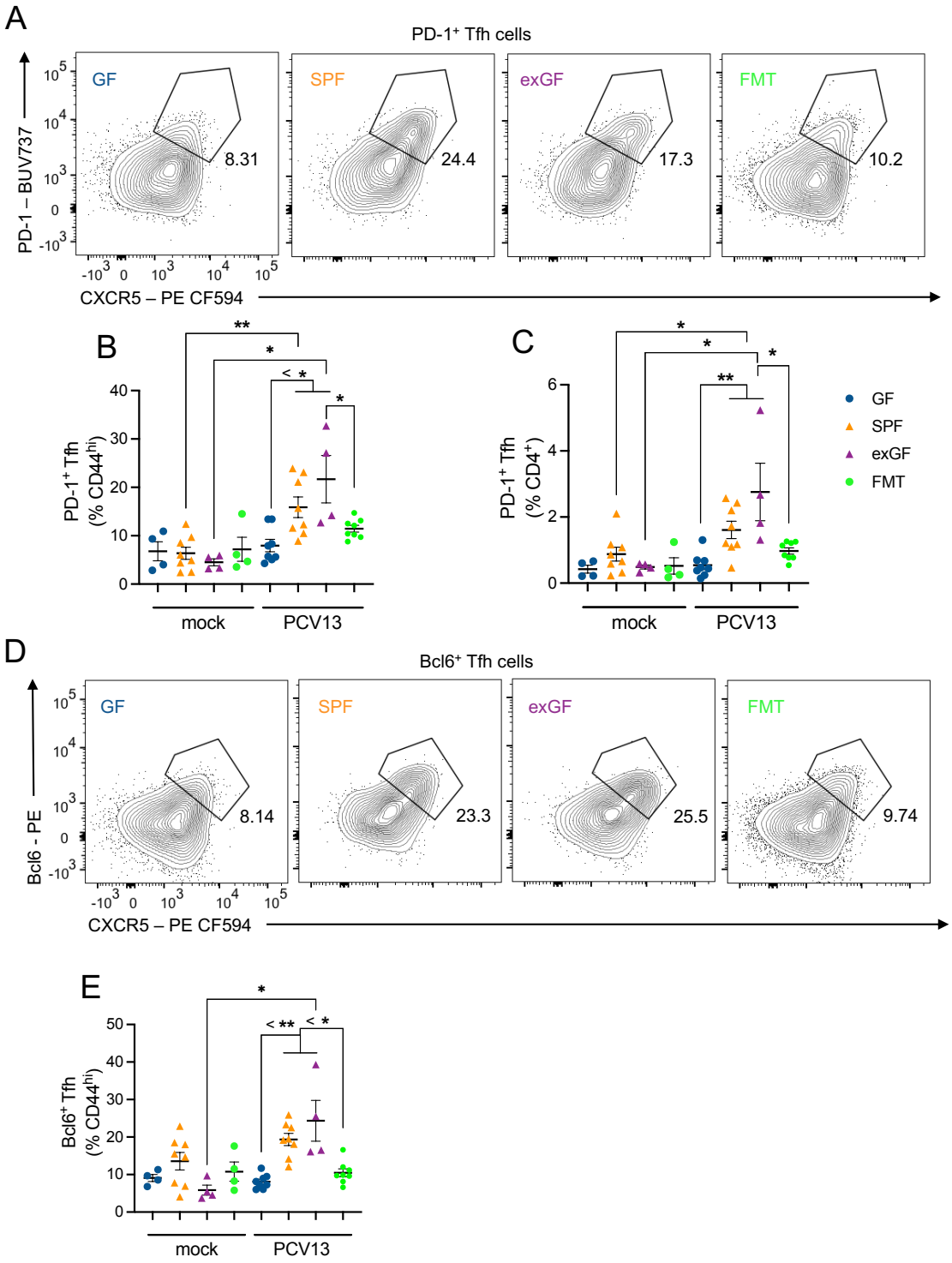

Figure 5.19| GF and FMT mice have significantly lower frequencies of Tfh cells than SPF and exGF mice. A| Representative analysis of PD-1$^+$ Tfh cells (CXCR5$^+$PD-1$^+$) in the mediastinal lymph nodes of vaccinated GF, SPF, exGF and FMT mice. Cells were pre-gated on live CD3$^+$CD19$^-$CD4$^+$CD44^{hi}CD62L$^-$ populations. **B-C|** Frequency of PD-1$^+$ Tfh cells in the mediastinal lymph node as a **B|** proportion of CD44^{hi} T cells and **C|** CD4$^+$ T cells. **D|** Representative analysis of Bcl6$^+$ Tfh cells (CXCR5$^+$PD-1$^+$) in the mediastinal lymph nodes of vaccinated GF, SPF, exGF and FMT mice. Cells were pre-gated on live CD3$^+$CD4$^+$CD44^{hi}B220$^-$CD62L$^-$ populations. **E|** Frequency of Bcl6$^+$ Tfh cells in the mediastinal lymph node as a proportion of CD44^{hi} T cells. Data are represented as mean ± SEM. One-way ANOVA was used to assess statistical significance. *p <0.05, **p <0.0

5.1.9 GF mice have a significantly lower frequency of plasma cells and memory B cells compared to SPF and FMT mice in the spleen

Antibody-producing PCs proliferate in the spleen and lymph node before entering the circulation soon after vaccination. This population generally increases significantly after boosting. Most PCs leave the spleen and enter circulation, meaning only a small proportion are expected to be resident in the spleen and mediastinal lymph nodes of these mice. To assess this small population, both Sca-1 and CD138 were used as markers to define PCs, as well as B220 (**Fig. 5.20A-B**) (Wilmore et al., 2017). There was a significantly higher induction of PCs in the spleens of SPF and FMT groups (and a similar trend in exGF mice) compared to GF mice (**Fig. 5.20A**). In contrast, exGF mice had a significantly higher induction of PCs than GF and FMT groups in the mediastinal lymph node (**Fig. 5.20B**). A limitation of this analysis is that antigen-specific PCs could not be assessed in these mice.

The GC reaction in secondary lymphoid organs results in the production of long-lived memory B cells which are primed for a swift response to subsequent antigen exposure (N. S. De Silva & Klein, 2015). Memory B cells expressing IgM were assessed in the spleen and draining lymph node (**Fig. 5.20C-D**). The proportion of $B220^{+}CD19^{+}IgD^{-}CD138^{-}GL7^{-}CD27^{+}CD38^{+}IgM^{+}$ memory B cells in the spleen was significantly higher in mock immunised SPF and exGF mice compared to mock GF mice (**Fig. 5.20C**). A similar trend was seen after vaccination, as PCV13-immunised SPF, exGF and FMT had a significantly higher proportion of IgM^{+} B memory cells than GF mice (**Fig. 5.20C**).

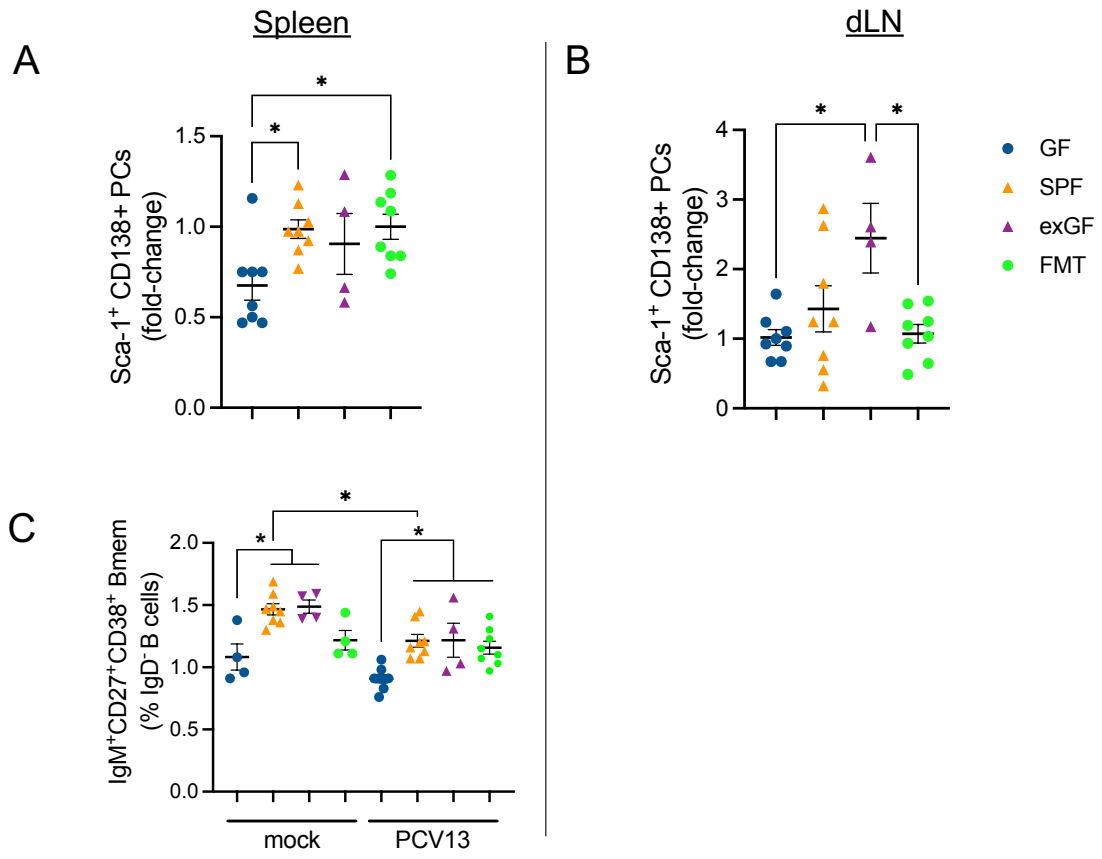

Figure 5.20| Significantly lower frequencies of plasma cells in the spleens and lymph nodes of GF mice. A-B| Frequency of $B220^{+}IgD^{-}Sca\text{-}1^{+}CD138^{+}$ plasma cells (PCs) in the spleens and mediastinal lymph nodes of mock and vaccinated GF, SPF, exGF and FMT mice as a frequency of IgD^{-} B cells. **C|** Frequency of $B220^{+}CD19^{+}IgD^{-}CD138^{-}GL7^{-}CD27^{+}CD38^{+}IgM^{+}$ memory B cells in the spleens of mock and vaccinated GF, SPF, exGF and FMT mice as a frequency of IgD^{-} B cells. Data are represented as mean ± SEM. One-way ANOVA was used to assess statistical significance *p <0.05, ***p <0.001.

5.1.10 GF mice have lower proportions of memory B cells in their bone marrow than SPF mice

Changes to B cell populations including memory B cells and PCs also occur in the bone marrow after immunisation (Lederer et al., 2020). To assess these changes, cells from the bone marrow of GF, FMT, exGF and SPF mice were assessed via flow cytometry to enumerate the proportion of their memory B cells and plasma cell populations. Interestingly, the proportion of $CD19^{+}B220^{+}$ B cells significantly increased in the bone marrow of vaccinated GF and SPF mice at V+4 weeks (**Fig. 5.21A**). GF mice had

significantly reduced proportions of $B220^{+}CD19^{+}IgD^{-}CD138^{-}GL7^{-}CD27^{+}CD38^{+}IgM^{+}$ memory B cells in their bone marrow compared to SPF mice as a frequency of both total B cells and live cells (**Fig. 5.21B-C**). In addition, only SPF mice had a significant induction of IgM^{+} B memory cells after PCV13-vaccination (**Fig. 5.21C**). The lower proportion of memory B cells observed in the bone marrow of GF mice could explain why GF mice have impaired antibody responses even post-boost.

The frequency of $CD19^{+}B220^{+}IgD^{-}Sca\text{-}1^{+}CD138^{+}$ PCs was also assessed in the bone marrow of mock and PCV13 immunised mice at 2 weeks following the 2^{nd} dose. Surprisingly, FMT mice had a significantly higher proportion of PCs in the bone marrow compared to either SPF or exGF mice, both as a proportion of IgD^{-} and as a proportion of live cells (**Fig. 5.21D-E**). FMT mice also a significantly higher frequency of PCs as a frequency of live cells compared to GF mice after vaccination (**Fig. 5.21E**). In addition, FMT mice were the only group to be significantly induced after PCV13-vaccination (**Fig. 5.21D-E**).

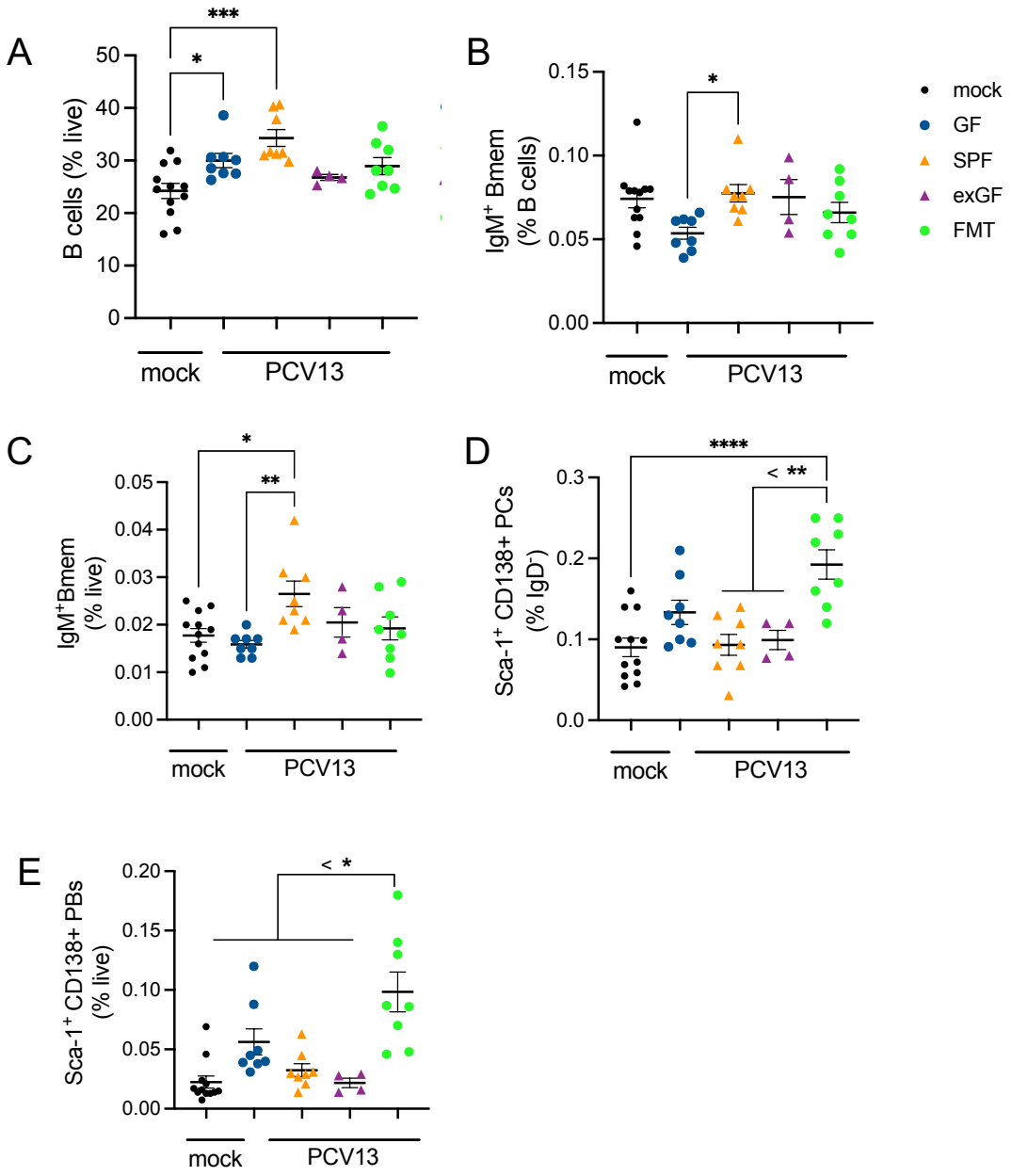

Figure 5.21| Significantly lower frequencies of IgM$^+$ memory B cells in the bone marrow of GF mice compared to SPF mice and significantly higher frequencies of plasma cells in the bone marrow of FMT mice compared to SPF and exGF mice. A| Frequency of CD19$^+$B220$^+$ B cells in the bone marrow of mock mice and vaccinated GF, SPF, exGF and FMT mice as a frequency of live cells. **B-C|** Frequency of B220$^+$CD19$^+$IgD$^-$CD138$^-$GL7$^-$ CD27$^+$CD38$^+$IgM$^+$ memory B cells in the bone marrow of mock mice and vaccinated GF, SPF, exGF and FMT mice as a frequency of B cells and live cells. **D-E|** Frequency of B220$^+$IgD$^-$ Sca-1$^+$CD138$^+$ plasma cells (PCs) in the bone marrow of mock mice and vaccinated GF, SPF, exGF and FMT mice as a frequency of B cells and live cells. Data are represented as mean ± SEM. One-way ANOVA was used to assess statistical significance. *p <0.05, ***p <0.001.

5.1.11 Innate-like B-1 cells in the peritoneum of GF mice and SPF mice post-vaccination

As discussed earlier in this chapter, antibody responses to the PCV13 vaccine (a conjugated polysaccharide vaccine) were impaired 2 weeks after the primary dose of PCV13 in germ-free (GF) compared to SPF mice (**Fig. 5.2**). Interestingly, however, there were no significant differences in the frequency of germinal centre B cells in PCV13-vaccinated GF compared to SPF mice pre-boost **(Fig. 5.14)**. These data suggest that, pre-boost, T-dependent humoral immune responses to the PCV13 vaccine are not impaired in GF mice. Given these data, I hypothesised that a defect in innate-like B cell responses could explain the significantly lower PCV13-specific antibody titres observed in GF mice pre-boost. Consistent with this hypothesis, recent studies have shown that innate-like B-1 cell responses to other polysaccharides are dependent on the microbiota via a MyD88-dependent pathway (New, Dizon, Fucile, Rosenberg, Kearney, & King, 2020). To assess differences in B-1 cells in GF and SPF mice, mice were vaccinated as d21 of life (V) and humanely killed before the day they would usually receive their second dose of PCV13 at V+2 weeks. To assess differences in the frequency of B-1 cells, flow cytometry analysis was carried out on cells from the peritoneal cavity, where B-1 cell populations are particularly prevalent (Ha et al., 2006). The frequency of B-1 cells in the peritoneal cavity of SPF mice was significantly higher compared to GF mice after vaccination as a frequency of total B cells (**Fig. 5.22A-B**). However, immunisation is associated with a significant reduction of B-1 cells, leaving the relevance of a higher proportion of B-1 cells in SPF mice unclear (**Fig. 5.22A-B**).

Total B-1 cells can be further divided into B-1a and B-1b cells based on their expression of CD5 (New, Dizon, Fucile, Rosenberg, Kearney, & King, 2020). There was a significantly higher frequency of both $CD5^+$ B-1a cells and $CD5^-$ B-1b cells in SPF mice compared to GF mice (**Fig. 5.22C-E**). There was a significant reduction in B-1 but not B-1b cells after immunisation in SPF mice (**Fig. 5.22C-E**).

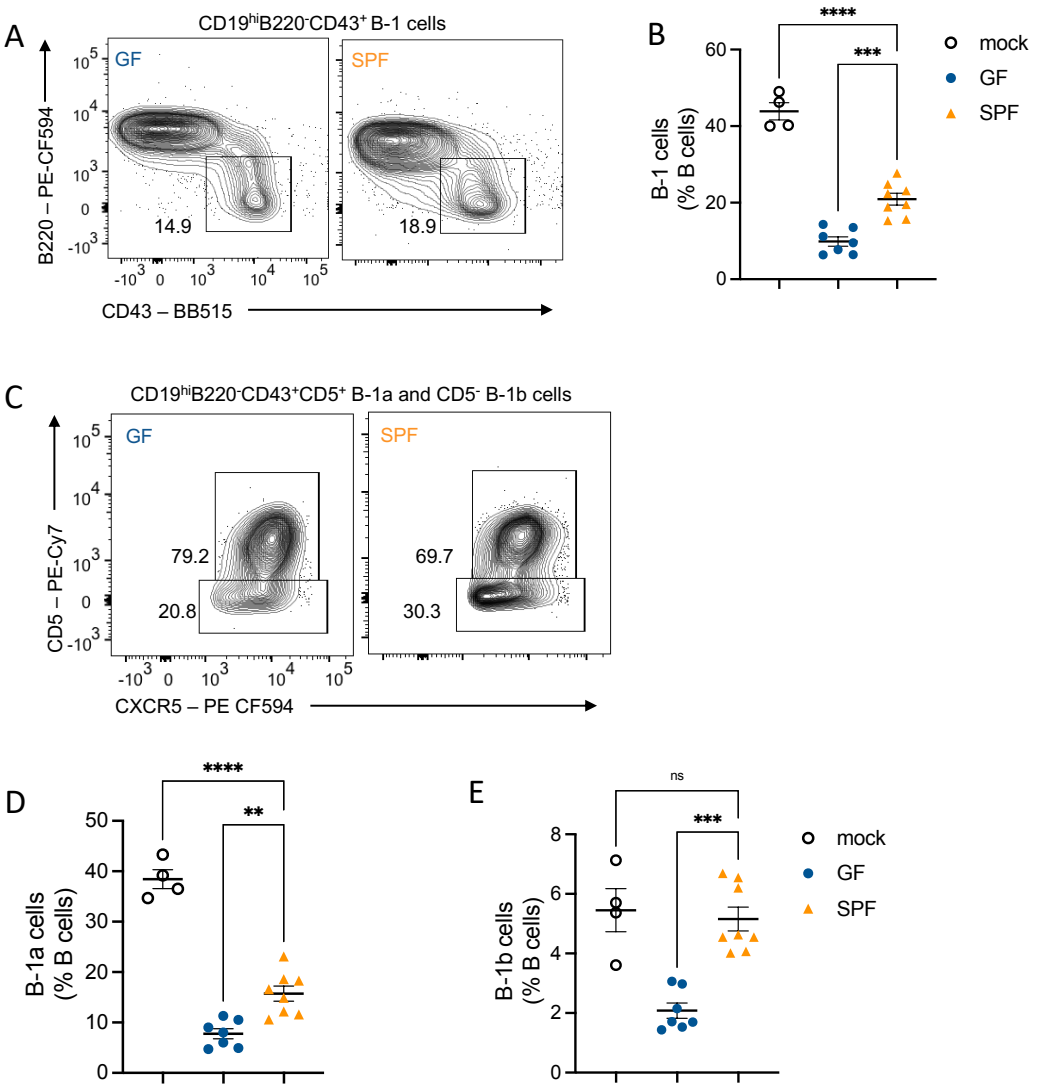

Figure 5.22| Vaccinated GF mice had a significantly lower proportion of B-1 cells in the peritoneum than SPF mice. A| Representative analysis of B-1 cells ($B220^{-}CD43^{+)}$ in the peritoneum of vaccinated GF and SPF mice 2 weeks post-immunisation with PCV13. Cells were pre-gated on live $CD19^{hi}$ populations. **B|** $CD19^{hi}B220^{-}CD43^{+}$ B-1 cells as a frequency of B cells ($CD19^{hi}$). **C|** Representative analysis of B-1a ($CD5^{+}$) and B-1b ($CD5^{-}$) cells in the peritoneum of vaccinated GF and SPF mice. Cells were pre-gated on B-1 cells ($CD19^{hi}B220^{-}CD43^{+}$). **D|** $CD19^{hi}B220^{-}CD43^{+}CD5^{+}$ B-1a cells and **E|** $CD19^{hi}B220^{-}CD43^{+}CD5^{-}$ B-1b cells as a frequency of $CD19^{+}$ B cells in mock, GF and SPF mice 2-weeks post-immunisation with PCV13. Data are represented as mean ± SEM. Mann-Whitney test was used to assess statistical significance. **p < 0.01, ***p < 0.001, ns = not significant.

5.2 Discussion

The microbiota has a crucial role in the development of the immune system in early life, but little is known about the consequences microbiota disruption could have on infant immunisation (D. J. Lynn, Benson, Lynn, & Pulendran, 2021; Robertson, Manges, Finlay, & Prendergast, 2019). Research previously undertaken by our lab found a significant impairment in antibody responses to live and adjuvanted infant vaccines in mice in exposed to antibiotics early life (Lynn et al., 2018). However, further work is needed to determine whether this effect was partially mediated by the effects of antibiotics on the microbiota. To investigate this further, I expanded on this existing knowledge by extensively assessing responses to the PCV13 vaccine in GF mice and compared responses to PCV13-vaccinated conventional SPF mice and mice recolonised at different timepoints.

Humoral and cellular responses to PCV13 vaccination

The production of several IgG subclasses is essential to optimal humoral immunity in mice (Collins, 2016). IgG_{total} responses were significantly impaired in GF and FMT mice against the whole PCV13 vaccine and PPS1 compared to SPF mice. Therefore, extensive characterisation of different IgG subclasses was subsequently carried out to assess if this reduction in IgG_{total} was due to a specific defect in class switching. In GF mice, IgG subclass responses to PCV13 were significantly impaired against the whole vaccine, the polysaccharides PPS1 and PPS3, and the conjugate protein CRM_{197}, compared to SPF mice. IgG3 is particularly important in T-independent antigen responses due to its primary role in complement fixation and the recruitment of inflammatory cells. IgG3 also relies heavily on co-expression with other murine antibody isotypes, such as IgG1, as it

cannot bind Fc gamma receptors (FcγR)(Neuberger & Rajewsky, 1981). Interestingly, GF, exGF, and FMT mice had significantly impaired IgG3 responses to the whole PCV13 vaccine, PPS1 and PPS3, compared to SPF mice. Even though other subclasses were not impaired in exGF and FMT mice compared to SPF mice, the lack of IgG3 could have consequences for the overall protection provided by other subclasses, which function in harmony with each other providing 'layered protection' (Collins, 2016). Therefore, lower IgG3 could result in a loss of control during early infection, increased pathogen replication, and rampant inflammation and death. This hypothesis could be assessed using preclinical pneumococcal infection models to assess early and late infection in GF and colonised mice after PCV13 immunisation.

Surprisingly, SPF mice had a persistent IgM response, increasing up to 8 weeks post-vaccination. Although not usually observed for other vaccines, the relatively high IgM response in SPF mice is consistent with prior studies (Nakao et al., 2022). Compared with PPSV23 and a novel highly immunogenic polysaccharide *Escherichia coli* vaccine platform, CPS14^{+}MVs, PCV13 elicited a Th2 skewed IgG1 response with a relatively strong IgM response a year on from vaccination (Nakao et al., 2022).

While there was no significant reduction in the frequency of GC B cells prior to boosting, there was a significant loss of the GC response in GF mice after boosting relative to SPF mice. Concomitant with this reduction in GC B cells was a significant reduction in the number of PCV13-specific ASCs in the spleen and bone marrow of GF mice. The reduction in GC B cells could explain why GF mice have impaired serum antibody responses, as one of the main outputs of the GC reaction is class-switched, affinity-matured ASCs (N. S. De Silva & Klein, 2015; Stebegg et al., 2018). Interestingly, antigen-specific responses to the

conjugate protein were lower in the draining lymph node and spleens of GF mice compared with colonised mice but did not reach statistical significance. The lack of impaired antigen-specific responses in GF mice was surprising, given the dramatic reduction in the antibody response in GF mice. Results from an independent experiment showed that consistent with antibody response data, CRM_{197}^{+} GC B cells were significantly impaired in GF mice compared to SPF and exGF mice after immunisation at the same timepoint. It is possible that CRM_{197}^{+} GC B cells do not reflect polysaccharide-specific B cells, which were unable to be assessed in our study due to the lack of a specific polysaccharides-targetted probe. Further future investigation into polysaccharide antigen-specific GC B cells would provide useful further insight.

Consistent with impaired GC responses, GF and FMT mice also had significantly impaired Tfh cell responses in their draining mediastinal lymph nodes compared to exGF and SPF mice. Colonisation at day 28 was not sufficient to restore this response. A recent study found that the timing of colonisation had a significant influence on several immune cell populations (Archer et al., 2023). While Tfh cells were not assessed in this study, total $CD4^{+}$ T cells were significantly impaired in mice colonised at 4 weeks of life compared to mice colonised from birth (Archer et al., 2023). The gut microbiota has been previously shown to indirectly influence Tfh cell function in distal sites. In a mouse model of autoimmune arthritis, segmented filamentous bacteria were shown to influence systemic immunity through the induction of Tfh cells. Segmented filamentous bacteria were capable of driving the differentiation of Tfh cells, which led to their eventual egress from Peyer's Patches to lymphoid tissues to induce GC responses and autoantibody production (Teng et al., 2016). Another study found that Tfh cells primed by the microbiota in Peyer's Patches were essential to GC formation in the spleen after *Plasmodium yoelii infection*

(Waide et al., 2020). Future work could assess whether Tfh cells from distal sites influence GC formation in the spleen and draining lymph nodes after PCV13 vaccination.

One seemingly contradictory observation arising from this work was the increase in the frequency of PCs in FMT mice, relative to SPF and exGF mice, as determined by flow cytometry, despite the poorer PCV13-specific antibody responses observed in FMT mice. The higher proportion of bone marrow PCs in the FMT mice compared to SPF and exGF mice could have resulted from an earlier response to the introduction of the microbiota to these previously GF mice. This hypothesis is partially supported by the observation that FMT mice had fewer PCV13-specific ASCs in the spleen and bone marrow relative to exGF and SPF, as measured by ELISpot assay. Unlike our flow cytometry analysis, ELISpot quantified antigen-specific cells. These data suggest that the increased frequency of PCs in FMT mice may be in response to non-vaccine antigens, likely derived from the microbiota.

Innate-like B cell responses to PCV13 vaccination

The frequency of GC B cells was not significantly lower in GF mice before boosting, despite impaired PCV13-specific antibody responses in GF mice at this timepoint. The initial response to T-independent antigens, such as polysaccharides, is primarily mediated by innate-like B-1 cells and marginal zone B cells (New, Dizon, Fucile, Rosenberg, Kearney, & King, 2020). In addition, the frequency of B-1 cells in the early response to PCV13 in GF versus SPF was of particular interest as a recent study showed that polysaccharide-specific clonality of B-1 cells was pre-programmed by the microbiota (New, Dizon, Fucile, Rosenberg, Kearney, & King, 2020). Indeed, GF mice had a significantly lower frequency of innate-like B-1 cells compared to SPF mice after one dose of PCV13. The two subsets

of B-1 cells, divided by their expression of CD5, each have important roles in the early immune response to *S. pneumoniae*. B-1a cells are a source of natural antibodies, while B-1b cells have been previously shown to be important regulators of the anti-polysaccharide response to *S. pneumoniae* (K. M. Haas, Poe, Steeber, & Tedder, 2005). Therefore, the finding that GF mice had a significantly lower frequency of B-1, B-1a and B-1b cells compared to SPF mice could contribute to lower protection provided by the PCV13 vaccine in GF mice.

The frequency of B-1 cells decreased in SPF mice two weeks after PCV13 vaccination. B-1 cells may migrate from the peritoneum after immunisation to the omentum, a visceral adipose tissue that contributes to peritoneal immunity (Meza-Perez & Randall, 2017). B-1a cells predominately migrate out of the peritoneal cavity after LPS stimulation compared to B-1b cells, accompanied by upregulation of CXCR4 and sensitivity towards CXCL12 and CXCL10 (Moon, Lee, Shin, & Kim, 2012). Additionally, studies have found that the intraperitoneal administration of LPS drives the translocation of B-1 cells mediated by TLR signalling to the milky spots of the omentum (Ha et al., 2006; Maruya et al., 2011; Okabe & Medzhitov, 2014), where they undergo differentiation into IgM- and IgA-secreting cells, and some of which may potentially colonise the intestine (Fagarasan, Kawamoto, Kanagawa, & Suzuki, 2010; Suzuki, Maruya, Kawamoto, & Fagarasan, 2010). Although we see a reduction of B-1 cells in SPF mice after PCV13-vaccination, it is unclear if this is also the case in GF mice because of the lack of a GF mock group in this experiment and further work is needed to assess this.

The impact of timing of colonisation on PCV13-specific immune responses:

There were significant differences in alpha and beta gut microbial diversity between SPF, exGF and FMT mice when assessed by 16S rRNA gene sequencing at the time of vaccination. As both exGF and FMT mice were colonised with an SPF microbiota, I expected the groups to be more similar. The FMT group, in particular, showed clear differences compared to the SPF and exGF mice. It is possible that distinct differences in the microbiota between the groups altered immune responses to vaccination. For example, the presence or absence of a single organism can dramatically alter the immune state. The genus *Dubosiell*a was exclusively detected in exGF mice, while immunomodulatory *Alistepes* were only present in SPF mice (B. J. Parker et al., 2020). While the relative abundance of taxa in a gnotobiotic zebrafish model did not predict neutrophil responsiveness, one species alone (*Shewanella*) was capable of the highest immune suppression of any other species in the community (Rolig, Parthasarathy, Burns, Bohannan, & Guillemin, 2015). It is also well-established that the intestinal eukaryote, Blastocytis, protects against Inflammatory Bowel Disease (IBD) and colitis (Billy et al., 2021).

The source of the FMT material administered to the FMT group and exGF dams was day 21 SPF mouse caecal material processed sterilely and anaerobically. Therefore, the 16S rRNA sequencing results are not intuitive at first glance, as it would not be possible for the FMT mice, in particular, to be colonised with anything but taxa found in the SPF caeca as they are housed in isolators (**Fig. 5.6**). Unique ASVs were observed in the FMT group compared to SPF mice, even though their FMT was prepared from material collected from other SPF mice, though collection was several months earlier. These data suggest that the composition of the SPF microbiome in the SAHMRI facility could have drifted over time

(see evidence of this in the next chapter). It is possible that the unique ASVs found in FMT mice may be present in the SPF group but were below the threshold of detection. There are reported differences in the composition of microbiota found in the caecum and feces, which could be a contributing factor (Tanca et al., 2017). In addition, rarer species may be in higher relative abundance in the FMT group as the microbiomes of these mice have yet to stabilise, and rarer taxa may briefly have a niche to fill before being outcompeted by other taxa over time. Cage effects may also drive microbiota composition changes, in addition to the fact that SPF mice were housed at a different facility to exGF and FMT mice.

Surprisingly, colonisation of GF mice with an FMT of material collected from age-matched FMT mice at day 21 of life did not wholly restore impaired PCV13-specific responses observed in GF mice. However, intergenerational colonisation of exGF mice with an SPF microbiota restored the majority of subclass responses to PCV13 in exGF mice. These data suggest that the timing of colonisation is essential for the optimal function of the immune system in response to vaccination.

Utilising two different colonisation times in these experiments highlighted the importance of the microbiome for immune system development. Surprisingly, colonisation of GF mice with an FMT of material collected from age-matched FMT mice at day 21 of life did not wholly restore impaired PCV13-specific responses observed in GF mice. However, intergenerational colonisation of exGF mice with an SPF microbiota restored the majority of subclass responses to PCV13 in exGF mice. In addition, the immune responses of exGF mice were more similar to those of SPF mice compared to FMT mice. These data suggest that the timing of colonisation is essential for restoring

responses to the PCV13 vaccine. This 'window of opportunity' for the immunogenic effects of microbial colonisation in early life has been reported by other groups (Al Nabhani & Eberl, 2020, Lynn et al., 2018). In addition, this window of opportunity is restricted to early life, with previous work by Lynn et al demonstrating that mice exposed to antibiotics as adults do not have impaired PCV13-specific antibody responses, in contrast to mice exposed in early life (Lynn et al., 2018). Intergenerational colonisation of exGF mice generated an enhanced response to PCV13 vaccination compared to the FMT group, though responses were not fully restored by 2 weeks post-boost. However, restoration of responses to PCV13 vaccination in the exGF group may have been more apparent if there were more than n = 4 in this colonisation group. Interestingly, IgG_{total} responses to PCV13 appeared to be 'rescued' in FMT mice after boost, with FMT apparently rescuing the T-dependent response in these mice post-boosting, however, FMT mice had impaired IgM responses against the whole vaccine, PPS1, and CRM_{197}.

There were limitations to these experiments that need to be considered for future work. First, while PCs were assessed, antigen-specific PCs were not assessed in these experiments. Therefore, while the frequency in PCs were not different between SPF and GF mice, it is possible there were functional differences that were not detected. Similarly, antigen-specific memory B cells were not measured to assess vaccine-specific memory. Assessing clonal expansion of the B cell repertoire using B-cell receptor (BCR) sequencing to lineage-trace B cell clones in GF vs SPF mice should be considered in future experiments. Another limitation of this study was the small size of the exGF group (n=3-4). The small group size and spread in the exGF group may result in some statistical comparisons being underpowered. Finally, while 16S rRNA gene sequencing data can assess the relative abundance of different genera and differences in diversity, it is difficult

to establish what specific taxa did not transfer via FMT and whether a nonbacterial component did not transfer (e.g. fungi etc.).

In conclusion, this study highlights the essential role microbiota colonisation has in driving optimal PCV13 vaccine responses in early life. Microbiota-deficient mice have impaired humoral responses to PCV13 stemming from poor GC formation or persistence and a reduction in ASC formation. These defects in the humoral response may be underpinned by a failure of GF mice to efficiently generate a Tfh response to vaccination, ultimately compromising the quality and longevity of vaccine-specific immune responses. Finding ways to manipulate this microbial environment to enhance infant vaccine responses could be a cheap and effective solution to enhance the efficacy of existing vaccines.

6 Determining the role of pattern recognition receptors in mediating the influence of the microbiota on responses to the PCV13 vaccine in early life

6.1 Introduction

Adjuvants are immune-stimulatory agents added to many different vaccines to enhance, accelerate or prolong antigen-specific immune responses. These include aluminium salt (alum), emulsions and liposome-based stimulants, several of which stimulate innate immunity via pattern recognition receptors (PRRs) (Ong, Lian, Kawasaki, & Kawai, 2021). Members of the microbiota display molecular structures called microbial-associated molecular patterns (MAMPs), which are also recognised by PRRs. They include a range of molecules, such as lipopolysaccharide (LPS), flagellin and peptidoglycan (Sommer & Bäckhed, 2013). These MAMPs are recognised by PRRs such as Toll-like receptors (TLRs) and nucleotide-binding oligomerisation domain-like receptors, or NOD-like receptors (NLRs). Therefore, it is plausible that MAMPs encoded by the gut microbiota could act as natural adjuvants by signalling through these PRRs.

There is evidence to suggest that the microbiota can act as a natural vaccine adjuvant. Oh *et al*. found that antibiotic-treated, germ-free (GF) or *Tlr5*$^{-/-}$ mice (a PRR which recognises flagellin) have impaired antibody responses to the non-adjuvanted seasonal influenza vaccine (Oh et al., 2014). However, subsequent experiments by Lynn *et al*. could not

replicate these findings when responses to a similar influenza vaccine or the PCV13 vaccine were compared in *Tlr5*$^{-/-}$ and littermate wildtype (WT) mice (Lynn et al., 2018). More recently, microbiota dependent innate-like B-1 cell responses to group A streptococcus (GAS) were shown to be mediated through a MyD88-dependent pathway, a key adaptor protein downstream of most TLRs (New, Dizon, Fucile, Rosenberg, Kearney, & King, 2020). B-1 cells produce antibodies in a T-independent manner and play a particularly important role in responses to polysaccharides (K. M. Haas et al., 2005). Bacterial LPS detected through TLR4 has been previously shown to enhance the immune response to vaccination (Georg & Sander, 2019; Kasturi et al., 2011), however, it has not yet been demonstrated whether TLR4-mediated detection of LPS produced by the gut microbiota can influence immune response to vaccination. Taken together, these data suggest that, as yet, undefined PRRs could mediate the influence of the microbiota on vaccine responses in early life. To investigate the potential role of PRRs in mediating responses to vaccination, humoral immune responses to the PCV13 vaccine were assessed in mice deficient in MyD88, TLR4 and TLR2.

6.1.1 Assessing responses to the PCV13 vaccine in *Myd88*$^{-/-}$ mice following early life antibiotics exposure

MyD88 acts as a critical adaptor protein that relays signals downstream of multiple TLRs (Deguine & Barton, 2014). To investigate whether the microbiota mediates its influence on PCV13 vaccine responses via a MyD88-dependent pathway, antibody responses to the PCV13 vaccine were assessed in wildtype (wt) and *Myd88*$^{-/-}$ mice with or without antibiotic treatment to weaning (ABX) (**Fig. 6.1**). Antibiotics administered in early life significantly reduces bacterial load in the gut of infant mice and induces a state of dysbiosis at weaning, once antibiotic exposure has ceased. Microbial products produced by the microbiota, such as LPS, peptidoglycan and lipoteichoic acid, can translocate across the gut to influence the host's immune response (Ignacio, Morales, Câmara, & Almeida, 2016). These molecules are sensed by innate immune receptors such as TLRs, and MyD88 acts as an adaptor downstream of many of these pathways, relaying signals regulating the immune response. Therefore, this experiment investigated whether mice deficient in MyD88 have impaired responses following maternal antibiotics exposure.

This experiment utilised the same early-life antibiotic treatment schedule published previously (Lynn et al., 2018). Briefly, mice heterozygous for *Myd88* were mated. Pregnant dams were either left untreated or treated with antibiotics (ampicillin and neomycin) in their drinking water until pups were 21 days old. Upon weaning, *Myd88*$^{-/-}$ and wt mice were cohoused within their respective treatment groups. Mice were vaccinated with PCV13 one week after the cessation of antibiotics and boosted two weeks later. A control group of 5 wt mice were mock vaccinated with PBS. Faecal and blood

samples were collected throughout the experiment to assess the impact of antibiotics exposure on the composition of the fecal microbiota and to assess PCV13-specific antibody responses in the serum (**Fig. 6.1**).

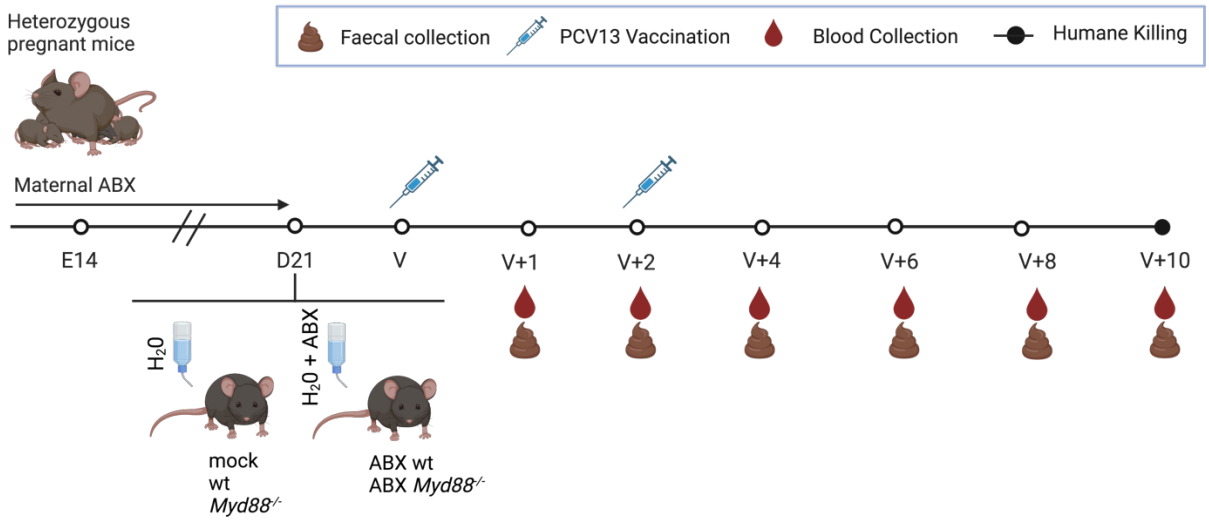

Figure 6.1| Experimental design. To assess the role of MyD88 in the response to the pneumococcal conjugate vaccine, PCV13, mice heterozygous for *Myd88* were bred. One group of pregnant dams were treated with antibiotics in their drinking water from embryonic day 14 (E14). Pups were genotyped and, upon weaning at day 21 of life (D21), were split into cages cohousing wt and *Myd88*$^{-/-}$ mice within their treatment groups (mock n = 5; wt, *Myd88*$^{-/-}$, ABX wt, ABX *Myd88*$^{-/-}$ n = 10/group). Mice were vaccinated intraperitoneally with either PBS (mock) or with 1/10th of a human dose of PCV13 in PBS at day 28 of life (V) and boosted 2 weeks later (V+2). Mice were humanely culled at V+10 weeks.

6.1.2 No significant differences in PCV13-specific antibody responses in *Myd88*$^{-/-}$ mice after one vaccine dose.

To assess differences in the antibody response after one dose of the vaccine, serum IgG and IgM responses against the whole vaccine and two polysaccharides in the PCV13 vaccine (PPS1 and PPS3) were assessed by ELISA two weeks after the first dose of PCV13 was administered (V+2) (**Fig. 6.2**). There was a trend towards lower PCV13, PPS1, and PPS3-specific IgG_{total} and IgM responses in *Myd88*$^{-/-}$ mice compared to wt mice, but the differences did not reach statistical significance (**Fig. 6.2A-E**). Furthermore, ABX

treatment of wt and *Myd88*$^{-/-}$ mice had no significant impact on PCV13-specific IgG and IgM responses (**Fig. 6.2A-E**).

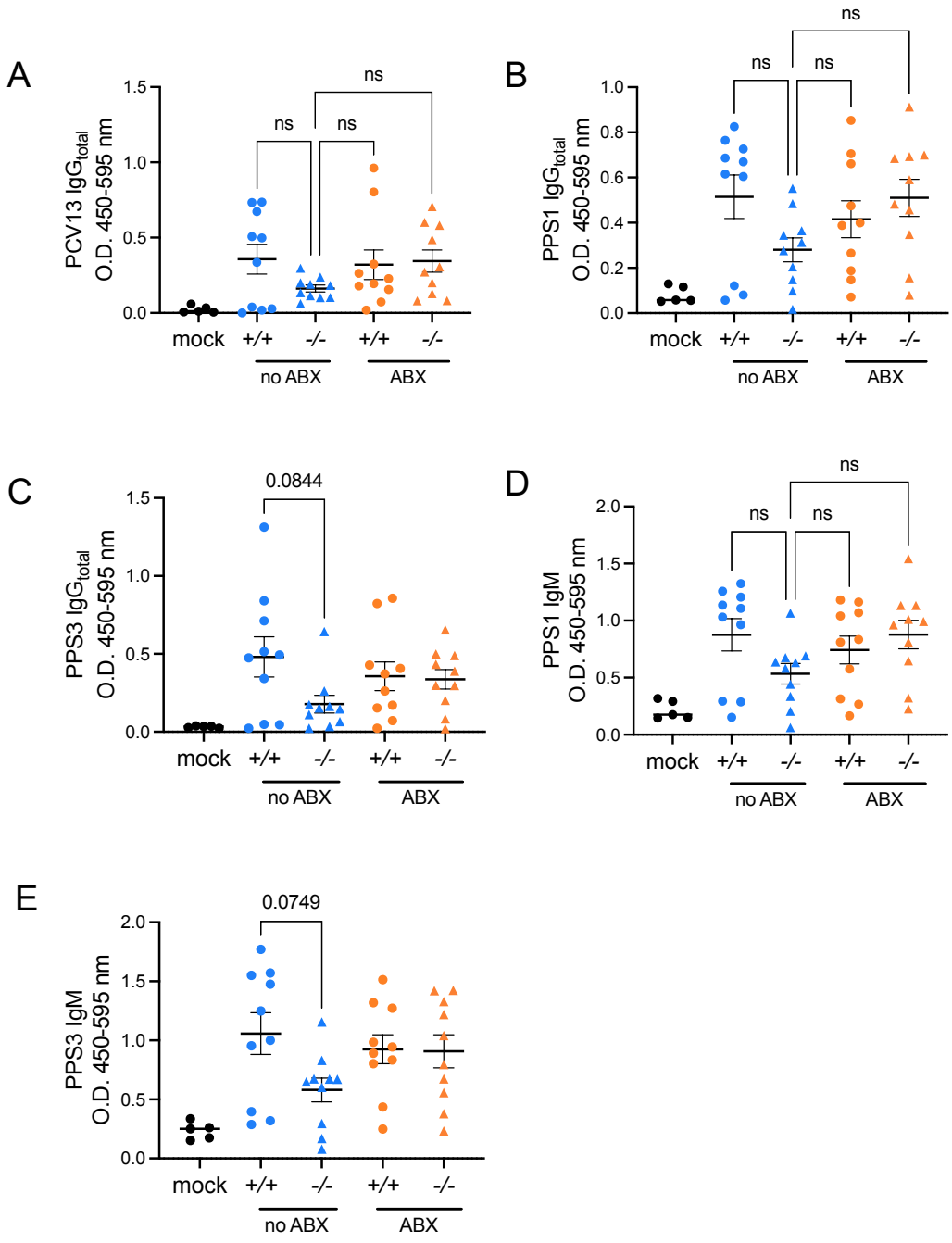

Figure 6.2| Antibody responses were not significantly different in *Myd88*$^{-/-}$ mice after one dose of PCV13. IgG$_{total}$ responses to **A|** the whole PCV13 vaccine, **B|** the polysaccharides PPS1 and **C|** PPS3 were assessed by ELISA in the serum of mock, wt (+/+) and *Myd88*$^{-/-}$ (-/-) mice with (ABX) and without (No ABX) antibiotic treatment. IgM responses against **D|** PPS1 and **E|** PPS3. Raw O.D. values are shown. Data are represented as mean ± SEM. A One-way ANOVA was used to assess statistical significance. ns = not significant.

6.1.3 PCV13-specific antibody responses were significantly impaired in *Myd88*$^{-/-}$ mice after two vaccine doses

To induce a robust and durable antibody response, booster doses of PCV13 are administered to human infants at 2-month intervals in Australia and elsewhere. To model this preclinically, PCV13-specific IgG and IgM responses were assessed at 2, 4, 6 and 8 weeks following the second vaccine dose (V+4 to V+10 weeks). PCV13-specific IgG_{total}, IgG1, IgG2b, IgG3 and IgM responses were significantly impaired in *Myd88*$^{-/-}$ mice compared to wt mice (**Fig. 6.3A-F**).

IgG_{total} responses to PPS1 and PPS3 were also assessed in all groups after boosting (**Fig. 6.4**). There were no significant differences in anti-PPS1 or PPS3 IgG_{total} titres between any of the groups at V+4 weeks. However, there was a modest, but not statistically significant, impairment in *Myd88*$^{-/-}$ mice compared to wt mice (**Fig. 6.4A-B**). Anti-PPS1 IgG_{total} was significantly lower in *Myd88*$^{-/-}$ mice at V+6 weeks and V+10 weeks, with a similar trend for anti-PPS3 responses (**Fig. 6.4C-F**). Interestingly, antibiotic treatment had no impact on anti-PPS1 or PPS3 IgG_{total} responses **(Fig. 6.4A-F)**.

Surprisingly, antibiotic treatment of *Myd88*$^{-/-}$ mice led to significantly higher PCV13-specific IgG_{total}, IgG1 and IgM (but not IgG2b and IgG3) responses compared to untreated *Myd88*$^{-/-}$ mice **(Fig. 6.3A-B, F)**. These data suggest an interaction between *Myd88* deficiency and the gut microbiota, which plays an important role in influencing PCV13-specific IgG response post-vaccination, perhaps driving a bias towards Th1 subclasses. These interactions are investigated further below using 16S rRNA gene sequencing.

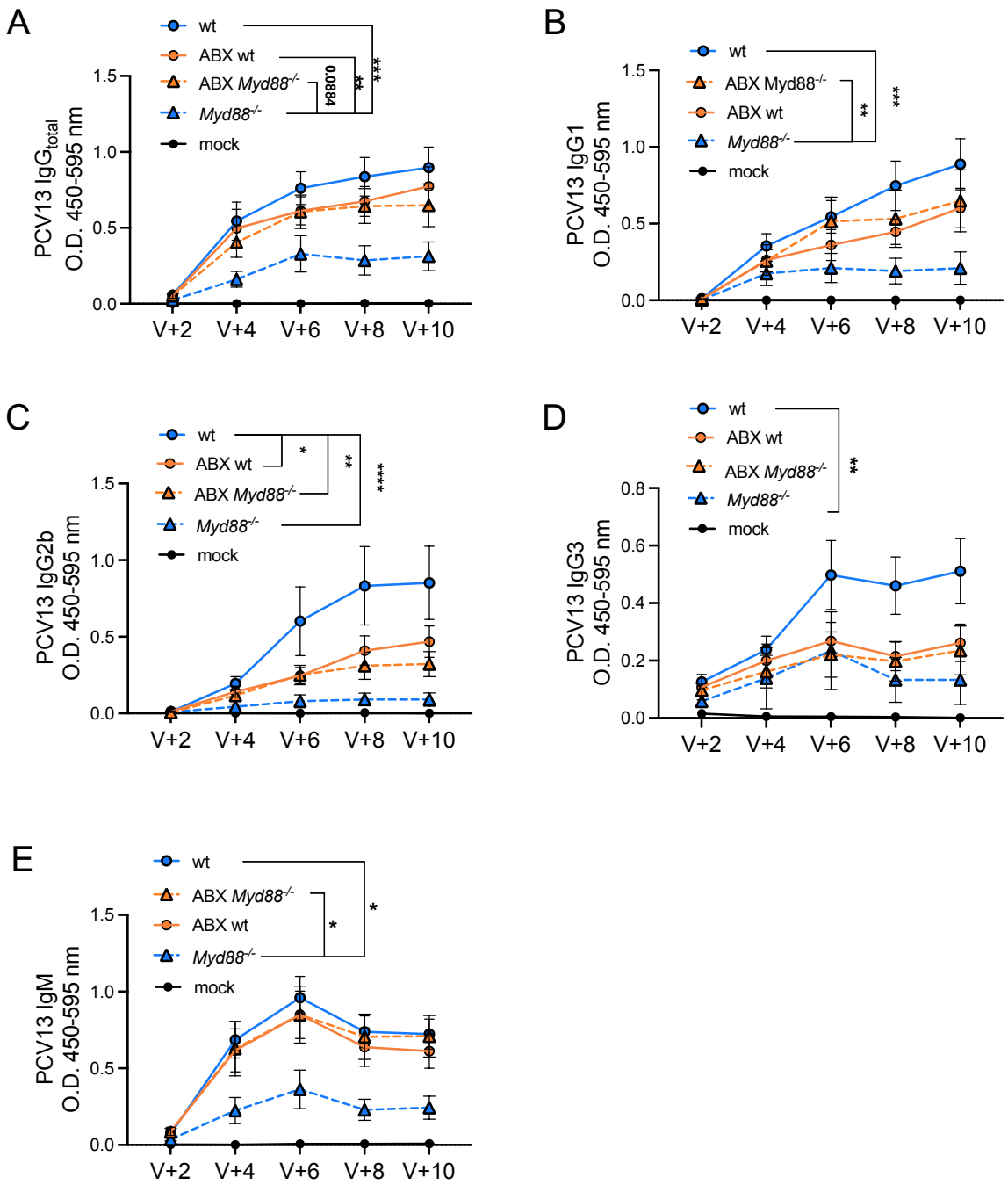

Figure 6.3| PCV13-specific antibody responses were significantly lower in *Myd88*$^{-/-}$ mice. PCV13-specific **A**| IgG_{Total}, **B**| IgG1, **C|** IgG2b, and **D**| IgG3 were assessed in the serum of mock, wt (+/+) and *Myd88*$^{-/-}$ (-/-) mice with (ABX) and without antibiotic treatment at the indicated weeks post-vaccination. **E**| PCV13-specific IgM responses in serum. Raw O.D. values are shown. Data are represented as mean ± SEM. Two-way ANOVA was used to assess statistical significance. Representative statistics at V+10 weeks are shown. *p < 0.05, ** p < 0.01, ***p < 0.001, ****p < 0.0001.

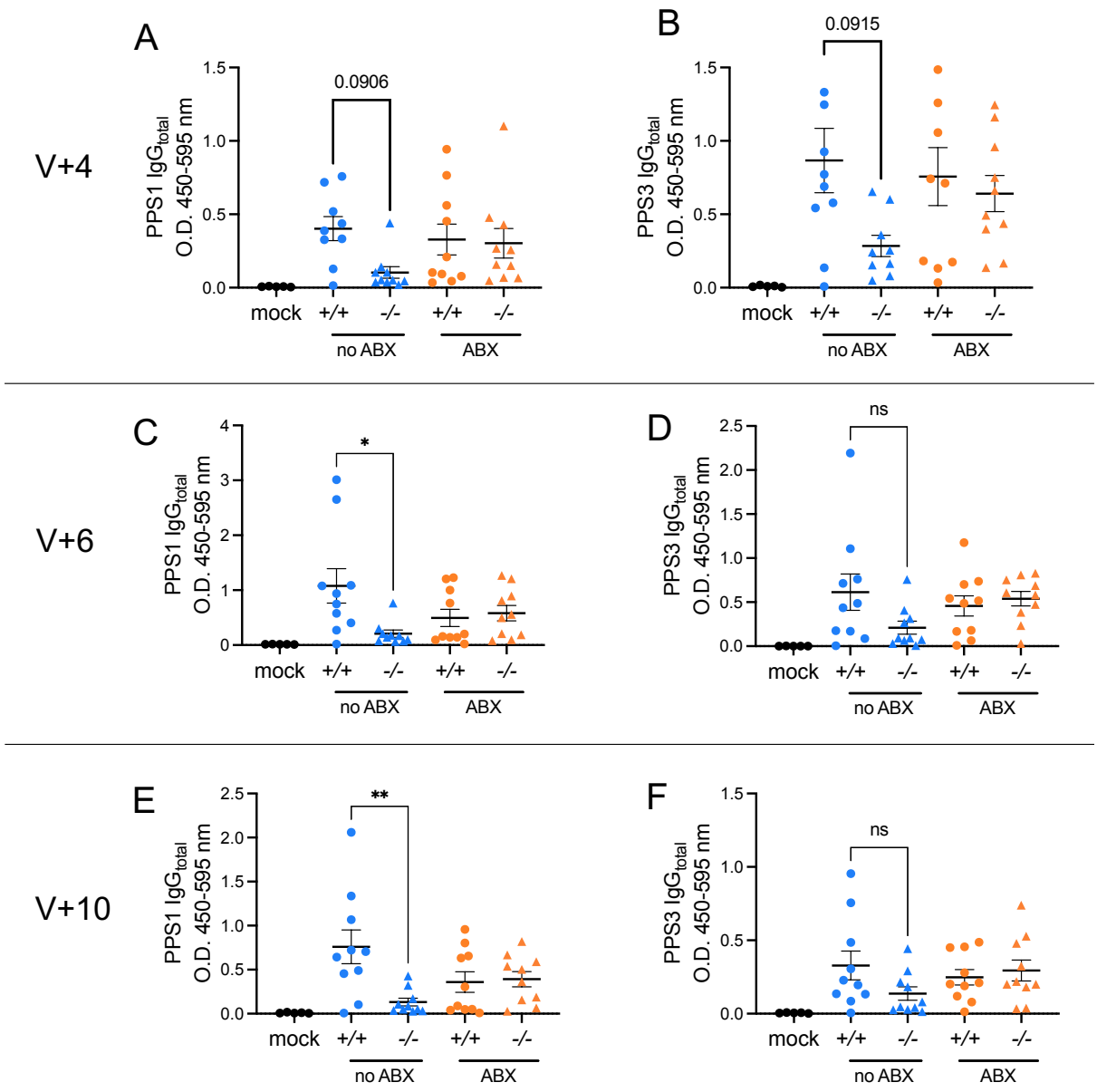

Figure 6.4| Anti-PPS1 IgGtotal responses were significantly impaired in *Myd88*$^{-/-}$ mice. IgG_{total} responses to **A|** PPS1 and **B|** PPS3 in the serum of mock, wt and *Myd88*$^{-/-}$ ABX treated and untreated mice at V+4 weeks. IgG_{total} responses to **C|** PPS1 and **D|** PPS3 in the serum of mock, wt and *Myd88*$^{-/-}$ ABX treated and untreated mice at V+6 weeks. IgG_{total} responses to **E|** PPS1 and **F|** PPS3 in the serum of mock, wt and *Myd88*$^{-/-}$ ABX treated and untreated mice at V+10 weeks. Raw O.D. values are shown. A one-way ANOVA was used to assess statistical significance. Data are represented as mean ± SEM. *p < 0.05, ** p < 0.01, ns = not significant.

6.1.4 There were no significant differences in innate-like B-1 cells in the peritoneum of *Myd88*$^{-/-}$ mice

As mentioned previously, New *et al*. found that the influence of the microbiota on polysaccharide-specific B-1 cell responses is mediated through a MyD88-dependent pathway (New, Dizon, Fucile, Rosenberg, Kearney, & King, 2020). To investigate whether *Myd88*$^{-/-}$ mice have impaired B1 cell responses to the PCV13 vaccine, I assessed the frequency of B-1 cells in mock and PCV13-vaccinated wt and *Myd88*$^{-/-}$ mice two weeks post-vaccination with PCV13. There were no significant differences in the proportion of B-1 cells in the peritoneum of *Myd88*$^{-/-}$ mice compared to wt mice (**Fig. 6.5**). However, there was a significant reduction the frequency of B-1 cells in *Myd88*$^{-/-}$ mice after vaccination. In addition, there was a significant reduction of B-1a cells in both wt and *Myd88*$^{-/-}$ mice two weeks post-vaccination. These data suggest that vaccination induces B-1 cell egress from the peritoneum. However, MyD88 signalling is not required for B-1 cell retention and/or migration from the peritoneum during vaccination.

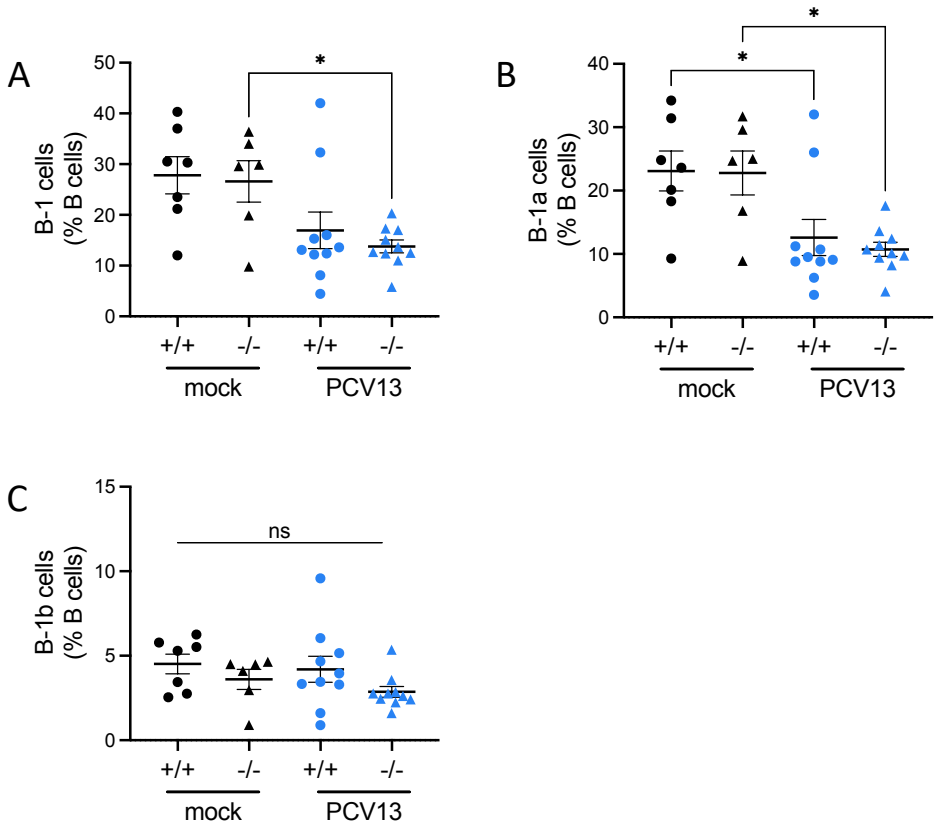

Figure 6.5| *Myd88*$^{-/-}$ mice do not have a lower frequency of B-1 cells compared to wildtype (wt) mice. The frequency of **A|** B-1 cells, **B|** B-1a cells and **C|** B-1b cells in mock and PCV13-vaccinated wt (+/+) and *Myd88*$^{-/-}$ (-/-) SPF mice two weeks post-immunisation with PCV13. Data are represented as mean ± SEM. A one-way ANOVA was used to assess statistical significance. *p < 0.05, ns = not significant.

6.1.5 *Myd88*$^{-/-}$ mice have impaired germinal centre formation

The germinal centre (GC) reaction leads to the formation of short- and long-lived plasma cells that produce the antibodies needed for vaccine-induced protection against infectious disease. To assess whether a defect in the GC response was responsible for poorer antibody responses observed in *Myd88*$^{-/-}$ mice, mock, wt and *Myd88*$^{-/-}$ mice were vaccinated/mock vaccinated as described previously and humanely culled 2 weeks after the first dose of PCV13 (V+2). The frequency of GC B cells and CRM_{197}-specific GC B cells in the spleens of PCV13 vaccinated *Myd88*$^{-/-}$ mice was significantly lower in comparison to wt mice at V+2 weeks (**Fig. 6.6A-B**). In addition, there was no significant induction of GC B cells in PCV13-vaccinated *Myd88*$^{-/-}$ mice compared to mock vaccinated mice (**Fig.**

6.6A-B), indicating a failure of GC formation at this timepoint in *Myd88*$^{-/-}$ mice. This defect in GC responses is interesting as there were no significant differences in antibody responses between *Myd88*$^{-/-}$ and wt mice at this timepoint, although there was a trend towards lower responses in *Myd88*$^{-/-}$ mice (**Fig. 6.2)**. Additionally, there was a moderately lower frequency of plasma cells in the spleens of PCV13-vaccinated *Myd88*$^{-/-}$ mice compared to vaccinated wt mice at V+2 weeks (**Fig. 6.6C**). Surprisingly, the frequency of plasma cells in PCV13-vaccinated *Myd88*$^{-/-}$ mice was significantly lower than in mock-vaccinated *Myd88*$^{-/-}$ mice. A defect in GC formation leading to an overall reduction in PCs in *Myd88*$^{-/-}$ mice provides a plausible explanation for the lower antibody titres observed in *Myd88*$^{-/-}$ mice.

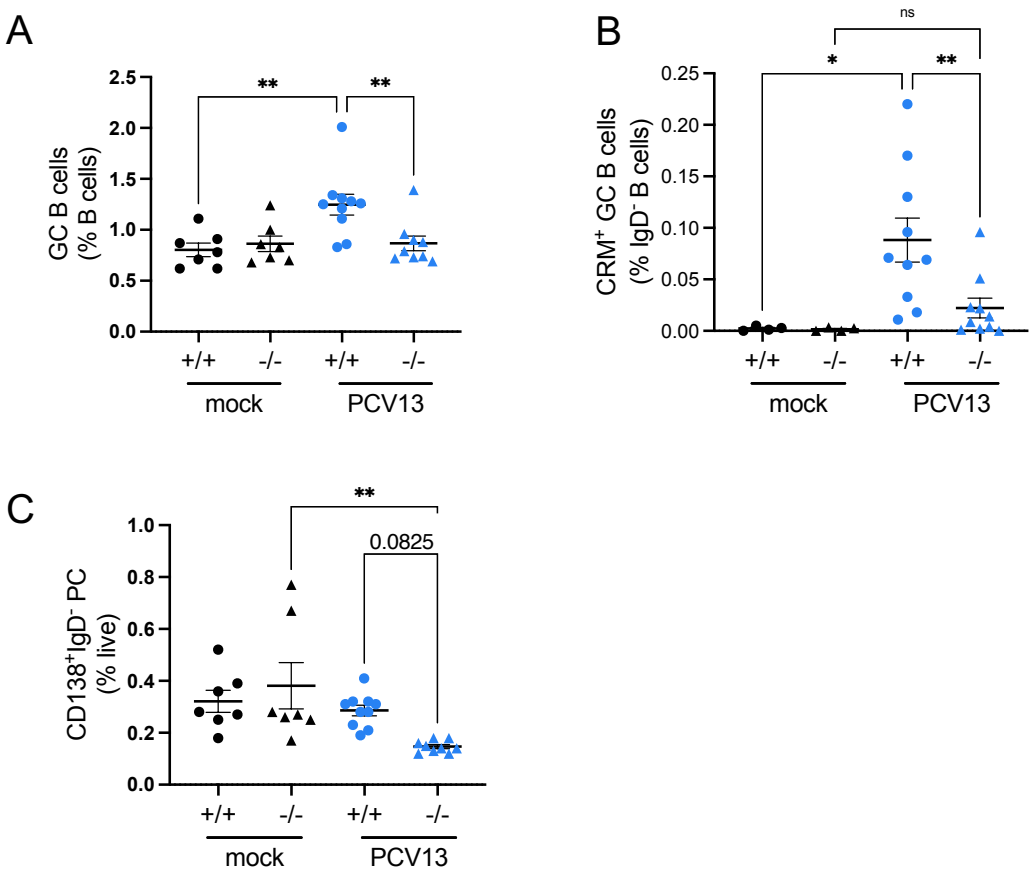

Figure 6.6| The proportion of GC B cells in the spleens of *Myd88*$^{-/-}$ (-/-) mice is significantly lower than wildtype (+/+) mice 2 weeks after PCV13 vaccination. A| $CD19^+IgD^-Fas^+GL7^+$ GC B cells as a frequency of $CD19^+$ B cells, **B|** $CD19^+IgD^-Fas^+GL7^+CRM_{197}^+$ GC B cells as a frequency of IgD^- B cells and **C|** $CD138^+IgD^-$ plasma cells (PCs) as a frequency of live cells in wt and *Myd88*$^{-/-}$ mice 2 weeks post-immunisation with PCV13. Data are represented as mean ± SEM. A one-way ANOVA was used to assess statistical significance. *p < 0.05, ** p < 0.01.

6.1.6 PCV13-specific $CD8^+$ T cell cytokine recall responses are impaired in *Myd88*$^{-/-}$ and antibiotic-treated mice

$CD8^+$ T cells contribute to the immunity provided by many licenced vaccines by producing cytokines, such as IFNγ (C.-A. Siegrist, 2008). To assess differences in $CD8^+$ T cell cytokine recall responses in *Myd88*$^{-/-}$ mice compared to wt mice (with and without antibiotic treatment), splenocytes collected from mice at V+10 weeks were stimulated *in vitro* for 72 hours with whole PCV13 vaccine. The frequency of $IFN\gamma^+$ $CD8^+$ T cells was then

assessed by flow cytometry. There was a significant reduction in the frequency of IFNγ producing cytotoxic CD8⁺ T cells in both *Myd88*$^{-/-}$ mice and antibiotic-treated wt mice compared to control SPF mice (**Fig. 6.7**). These data indicate that both the gut microbiota and MyD88 signalling play a critical role in PCV13-specific T cell responses in mice.

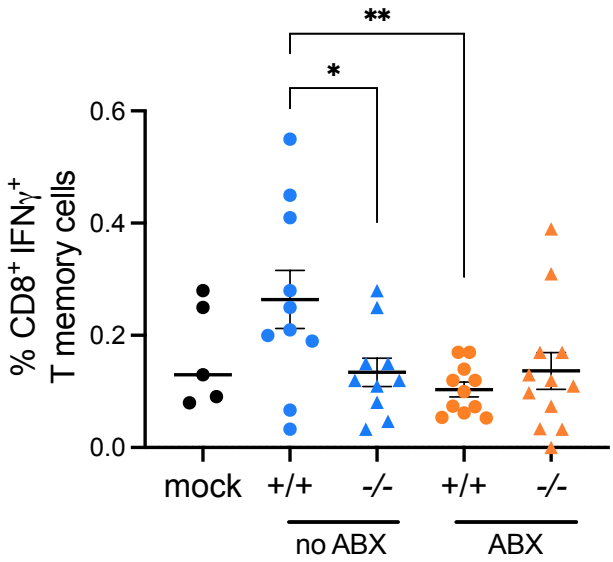

Figure 6.7| *Myd88*$^{-/-}$ (-/-) and antibiotic-treated (ABX) mice have significantly impaired CD8+ T cell cytokine recall responses compared to untreated (no ABX) wt (+/+) mice. Splenocytes (2.5x10^6 cells) were collected at V+10 weeks and stimulated *in vitro* for 72h with 1ug/ml of whole PCV13 vaccine diluted in RPMI media. Flow cytometry analysis was used to assess total IFNγ$^+$CD8$^+$ T cells as a frequency of CD8$^+$ T cells. Data are represented as mean ± SEM. One-way ANOVA was used to assess statistical significance. *p < 0.05, ** p < 0.01.

6.1.7 16S rRNA gene sequencing to assess the composition of the microbiota in *Myd88*$^{-/-}$ mice with and without antibiotic treatment

As discussed above, antibiotic treatment of *Myd88*$^{-/-}$ mice appeared to rescue the impaired PCV13-specific IgG responses (particularly IgG1 responses) observed in untreated *Myd88*$^{-/-}$ mice. These data suggested an interaction between genotype and the microbiota. One possibility we considered was that the composition of the microbiota was significantly different in *Myd88*$^{-/-}$ compared to wt mice and that it was these differences that were responsible for the impaired IgG responses to the PCV13 vaccine observed in *Myd88*$^{-/-}$ mice. To assess this, 16S rRNA gene sequencing was carried out on

faecal sample collected from wt and *Myd88*$^{-/-}$ mice, with and without antibiotic treatment. Samples were collected from mice at the time of first vaccination (V, at ~28 days of life).

The composition of the faecal microbiota in untreated wt and *Myd88*$^{-/-}$ mice was very similar **(Fig. 6.8A, D)** and the Shannan diversity and Chao1 richness indices were not significantly different **(Fig. 6B-C)**. These data suggest that differences in the composition of the microbiota do not explain the impaired PCV13-specific antibody responses observed in *Myd88*$^{-/-}$ mice, however, it is important to note that the faecal samples were collected at day 28 of life (1 week after weaning) and that wt and *Myd88*$^{-/-}$ mice were co-housed, so that we cannot rule out differences in the composition of the microbiota in early life between the genotypes.

As expected, there were clear differences in the composition of the microbiota between untreated and antibiotic-treated mice, regardless of genotype (**Fig. 6.8A, D**). For example, untreated mice had an increased relative abundance of *Muribaculaceae* and *Lactobacilli* while ABX mice had an increased relative abundance of *Turicibacter* and *Romboutsia*, and in some ABX mice blooms of *Blautia* were evident. As expected, Shannan diversity and Chao1 richness indices were significantly lower in ABX compared to untreated mice **(Fig. 6.8B-C)**. There were no statistically significant correlations ($P > 0.1$) identified between the relative abundance of any taxon in the microbiota and the antibody response data (data not shown). In conclusion, while there were clear differences in the composition and diversity of ABX and untreated mice, there were no obvious differences that could explain the observed differences in antibody responses between *Myd88*$^{-/-}$ and ABX *Myd88*$^{-/-}$ mice.

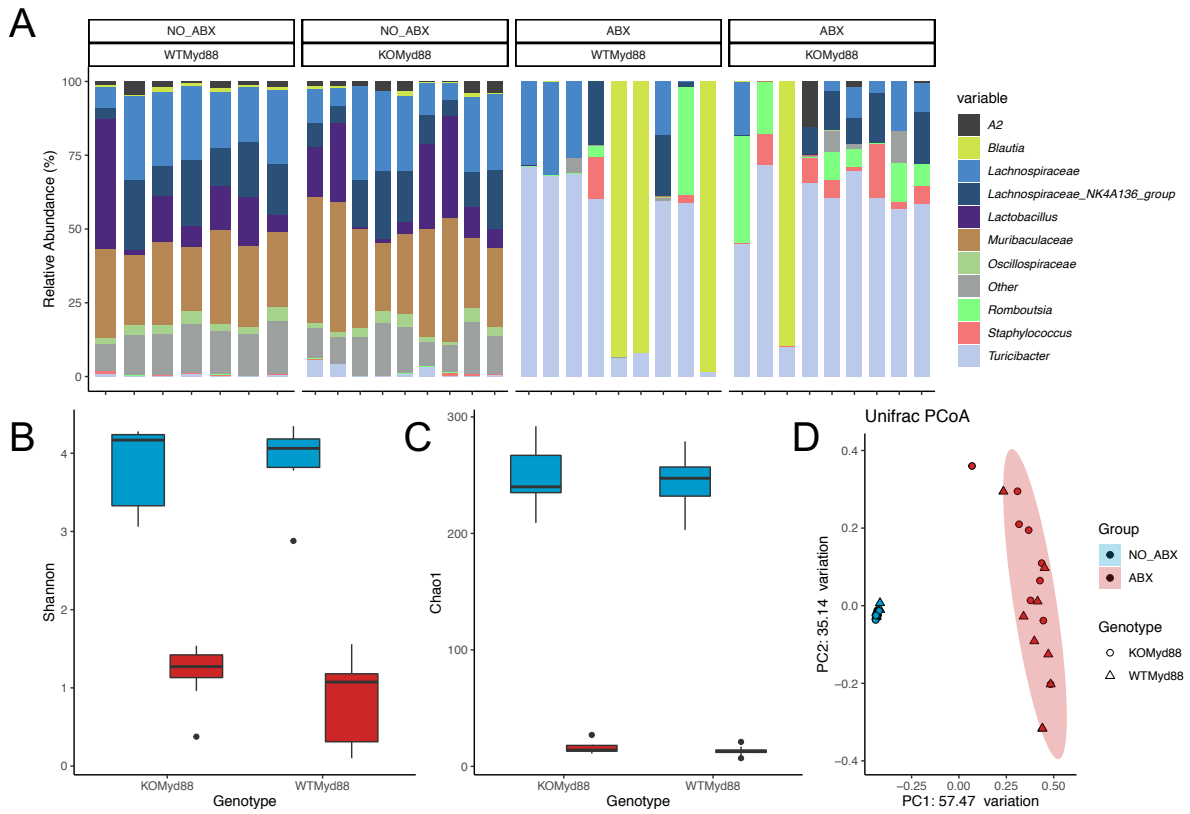

Figure 6.8| 16S rRNA gene sequencing analysis reveals differences in the gut microbiota composition of untreated and ABX groups. A| Composition of the faecal microbiota at the V timepoint calculated based on 16S rRNA gene sequencing of the fecal microbiota of untreated (NO_ABX) wt and *Myd88*$^{-/-}$ mice and ABX wt and *Myd88*$^{-/-}$ mice. Each barplot represents the relative abundance of major taxa in samples collected from individual mice at d28 of life. **B|** Beta diversity was assessed using Shannon and **C|** Chao1 indices. **D|** Principal component analysis (PCA) of Unifrac distances. The 16S rRNA gene sequencing was carried out by the SA Genomics Centre on DNA extracted from faecal samples and analysis of the 16S rRNA gene sequencing data and figure generation by Dr Feargal Ryan.

6.1.8 No impairment in primary antibody responses to the PCV13 vaccine in *Tlr4*$^{-/-}$ mice

MyD88 deficiency significantly impacted PCV13-specific antibody responses. As mentioned previously, the recognition of LPS produced by the microbiota by TLR4 has the potential to act as a natural adjuvant for vaccine responses via both MyD88-dependent and independent pathways. Therefore, using the same experimental design as

in the *Myd88*$^{-/-}$ experiment (**Fig. 6.1**), antibody responses to the PCV13 vaccine were assessed in wt and *Tlr4*$^{-/-}$ mice with or without ABX exposure in early life.

To assess antibody responses to the PCV13 vaccine after one dose of PCV13, IgG_{total} was measured against the whole PCV13 vaccine, PPS1 and PPS3 was assessed in serum collected at V+2 weeks (**Fig. 6.9**). There was a significant impairment in the antibody responses to the PCV13 vaccine in wt ABX mice compared to untreated wt mice (**Fig. 6.9A**). The wt ABX group also had significantly impaired IgG_{total} responses to PPS1 compared to untreated *Tlr4*$^{-/-}$ mice and a modest but not statistically significant impairment compared to the untreated wt mice (**Fig. 6.9A**). There were no significant differences in PPS3-specific IgG responses in any groups (**Fig. 6.9C**).

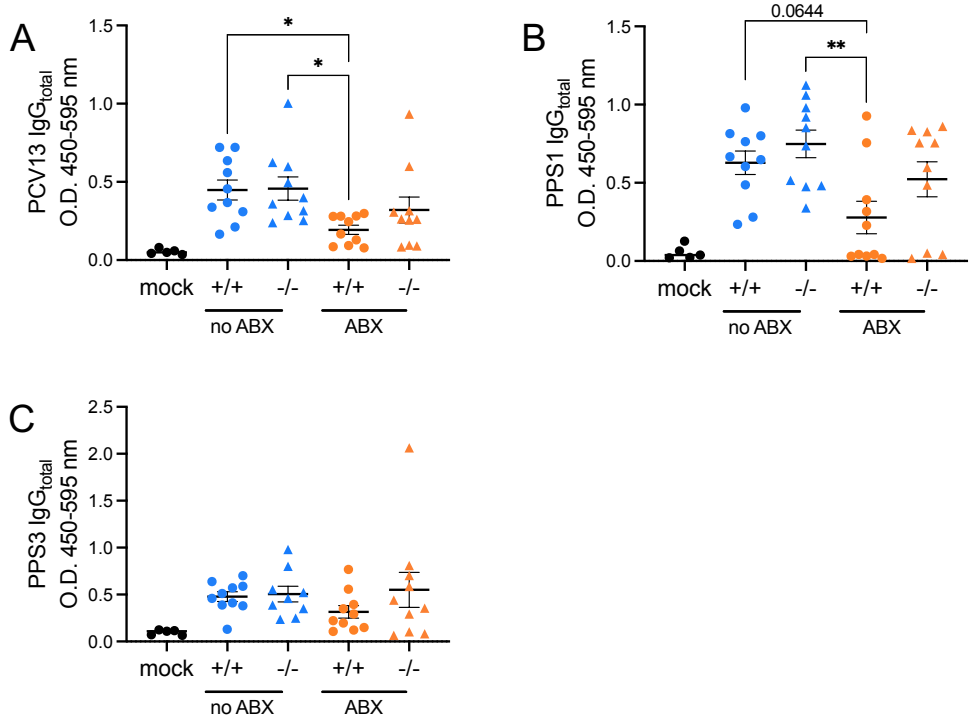

Figure 6.9| Antibody responses were not significantly different between wildtype (+/+) and *Tlr4*$^{-/-}$ (-/-) mice after one dose of PCV13. IgG_{total} responses to **A|** the whole PCV13 vaccine, **B|** the polysaccharides PPS1 and **C|** PPS3 were assessed by ELISA in the serum of mock, wt and *Tlr4*$^{-/-}$ untreated (no ABX) and antibiotic-treated (ABX) mice. Raw O.D. values are shown. Data are represented as mean ± SEM. One-way ANOVA was used to assess statistical significance. *p < 0.05. ns = not significant.

6.1.9 No significant defect in the antibody responses to the PCV13 vaccine in *Tlr4*$^{-/-}$ mice after boosting.

To assess the antibody response to vaccination in *Tlr4*$^{-/-}$ mice after boosting, PCV13 whole-vaccine and polysaccharide-specific antibody responses were assessed in serum collected from all 5 groups post-boost throughout the experiment. There was a significant impairment in the PCV13-specific IgG_{total} response in ABX wt mice compared to untreated wt mice (**Fig. 6.10A**), as previously reported (Lynn et al., 2018). There was no significant reduction in anti-PPS1 IgG_{total} responses in ABX mice (**Fig. 6.10B**). However, there was a significant impairment in anti-PPS3 IgG_{total} responses at V+4 (**Fig. 6.10C**). In contrast to *Myd88*$^{-/-}$ mice, PCV13-, PPS1- and PPS3-specific IgG_{total} responses were not impaired in

Tlr4$^{-/-}$ mice (**Fig. 6.10A-C**). There were also no significant differences in anti-PCV13, -PPS1 or -PPS3 IgM responses (**Fig. S5.1**). These data indicate that while ABX in early life significantly impairs IgG_{total} responses to the PCV13 vaccine, TLR4 signalling is not required.

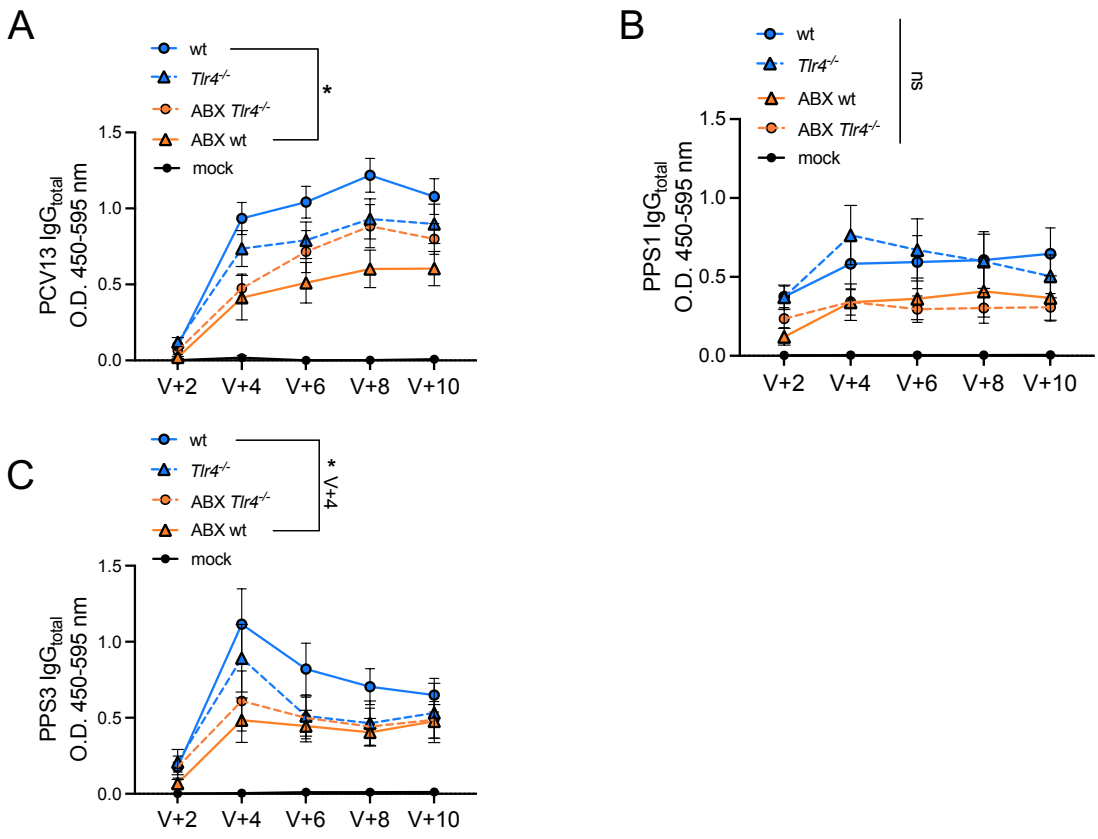

Figure 6.10| Antibody responses to the PCV13 vaccine were not significantly different between wildtype (+/+) and *Tlr4*$^{-/-}$ (-/-) mice after boosting. IgG_{total} responses to **A|** the whole PCV13 vaccine, **B|** the polysaccharides PPS1 and **C|** PPS3 were assessed by ELISA in the serum of mock, wt and *Tlr4*$^{-/-}$ untreated (no ABX) and antibiotic-treated (ABX) mice. Raw O.D. values are shown. Data are represented as mean ± SEM. One-way ANOVA was used to assess statistical significance. *$p < 0.05$. ns = not significant.

6.1.10 *Tlr2*$^{-/-}$ mice have impaired antibody responses to the PCV13 vaccine before boosting

While TLR4 deficiency did not significantly impact IgG responses to the PCV13 vaccine, there are however, many other TLRs that signal via MyD88 and recognise mediate the natural adjuvant capabilities of the microbiota. Toll-like receptor 2 (TLR2), for example, recognises bacterial cell-wall components such as peptidoglycan, lipoteichoic acid and lipoprotein from Gram-positive bacteria; lipoarabinomannan from mycobacteria; and zymosan from yeast and signals via a MyD88-dependent pathway (Rakoff-Nahoum, Paglino, Eslami-Varzaneh, Edberg, & Medzhitov, 2004; McDermott et al., 2014). To assess if signalling via a TLR2-dependent pathway was required for optimal antibody responses to PCV13, the same experimental design as outlined above for *Myd88*$^{-/-}$ and *Tlr4*$^{-/-}$ mice was employed (**Fig. 6.1**). Interestingly, PCV13-specific IgG_{total} responses were significantly lower in *Tlr2*$^{-/-}$ mice, compared to wt mice, two weeks after the first dose of PCV13 was administered (**Fig. 6.11A**). Reduced IgG_{total} responses in *Tlr2*$^{-/-}$ mice were, however, no longer observed following the booster dose (**Fig. 6.11B-D**). These data suggest that TLR2 signalling is partially required for primary antibody responses to PCV13 but not for the memory response. Interestingly, there were no significant differences in PCV13-specific IgG_{total} responses between antibiotic-treated and untreated mice in this experiment (**Fig. 6.11A-D**).

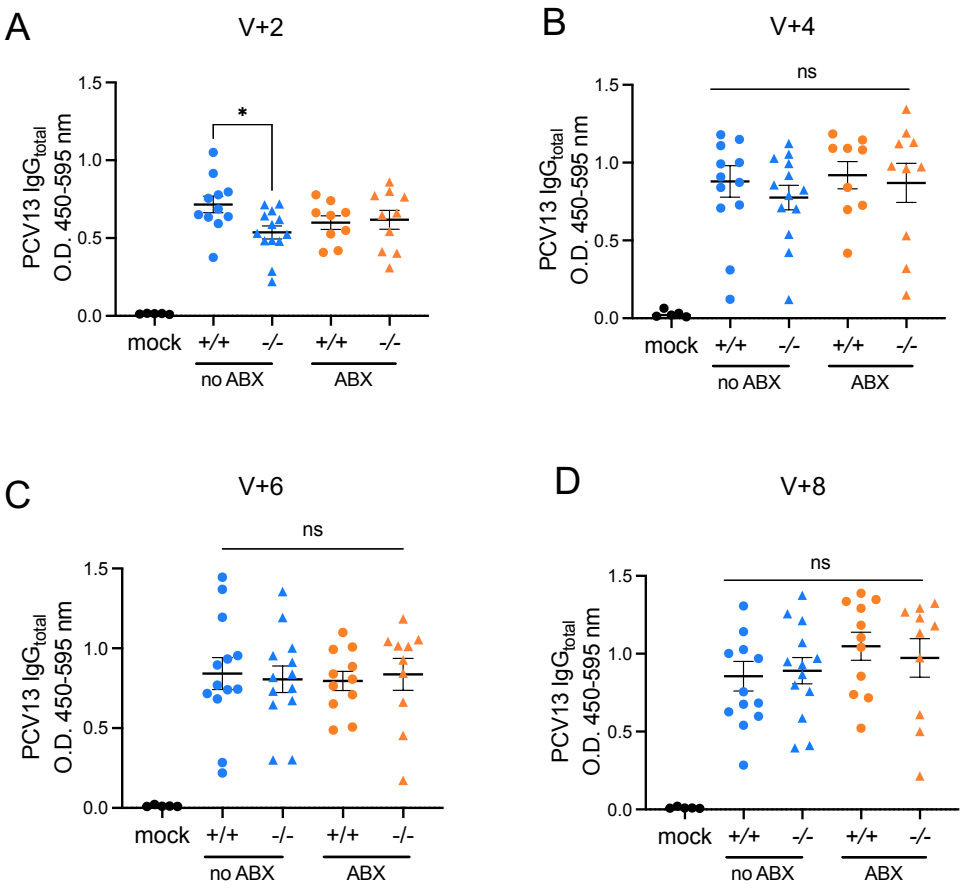

Figure 6.11| Antibody responses to the PCV13 vaccine were significantly lower in *Tlr2*$^{-/-}$ mice two weeks after the first dose of PCV13 but not after boosting. IgG_{total} responses to the whole PCV13 vaccine were assessed by ELISA in the serum collected from mock, wt and *Tlr2*$^{-/-}$ mice, with and without antibiotic treatment at **A|** V+2 **B|** V+4, **C|** V+6 and **D|** V+8 weeks. Raw O.D. values are shown. Data are represented as mean ± SEM. One-way ANOVA was used to assess statistical significance. *p < 0.05.

6.1.11 The composition of the microbiota varies across different experiments but not by genotype

Microbiome drift over time has the potential to influence established experimental phenotypes. This may have occurred in the SAHMRI mouse facility between these gene knockout experiments, potentially accounting for differences in the lack of impairment in ABX mice in the *Myd88*$^{-/-}$ and *Tlr2*$^{-/-}$ experiments. To assess differences in the microbiome composition across these experiments, 16S rRNA gene sequencing was carried out on DNA extracted from faecal samples from individual mice from the untreated groups across the three experiments (**Fig. 6.12**). As these experiments were conducted within a few months of each other, the sequencing results were anticipated to reveal that the composition of the microbiota was broadly similar in wt mice in different experiments. Instead, we observed significant differences in the composition of the microbiota of wt mice in each of the three experiments (**Fig. 6.12A**). Within each experiment, however, the composition of the microbiota in wt and *Myd88*$^{-/-}$, *Tlr2*$^{-/-}$ or *Tlr4*$^{-/-}$ mice was very similar. There were no significant differences in Shannon diversity or Choa1 richness between wt and knockout mice in any of the 3 experiments (**Fig. 6.12B-C**). Cohousing of knockout mice in each of these experiments appears to have been sufficient to prevent any changes to the composition as the microbiota driven by deficiency in any of the genes investigated (S. J. Robertson, Lemire, Croitoru, Girardin, & Correspondence, 2019).

Consistent with these data, samples from each experiment clustered separately regardless of genotype, illustrating similarities between groups within experiments, but differences across experiments (**Fig. 6.12D**). Differences in the composition of the microbiota in control SPF mice in different experiments may explain why antibiotic treatment sometimes leads to impaired responses to vaccination but other times does not.

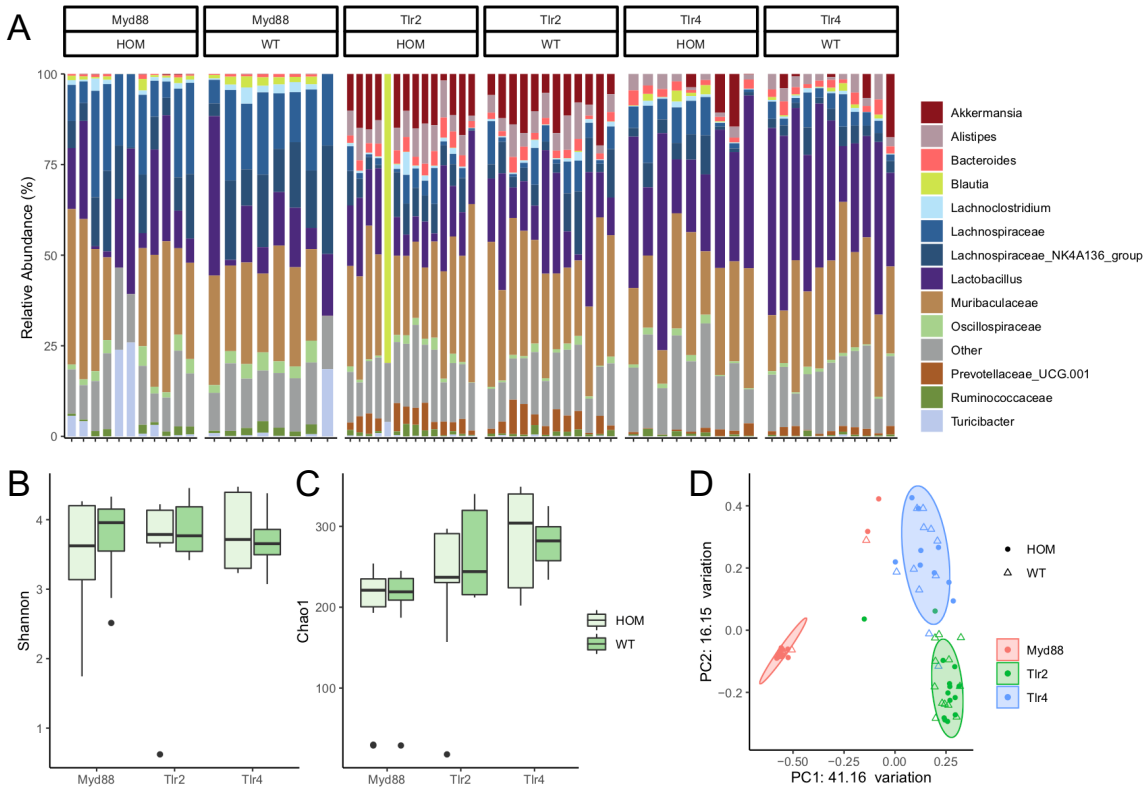

Figure 6.12| 16S rRNA gene sequencing analysis reveals differences in the composition of the fecal microbiota across different experiments. A| Composition of the faecal microbiota across 3 experiments in wildtype (WT) and genetically deficient mice (HOM). Each barplot represents the relative abundance of major taxa in faecal samples collected from individual mice on day 28 of life. **B|** Beta diversity was assessed using Shannon and **C|** Chao1 indices. **D|** Alpha diversity was assessed using principal component analysis (PCA) of Unifrac distances.

6.1.12 Significant differences in gene expression in the spleen hours post-PCV13 immunisation

Our data indicate that the gut microbiota plays a critical role in both T-dependent and T-independent responses to the PCV13 vaccine. These data suggest that the gut microbiota could also regulate the initial innate immune response following immunisation with the PCV13 vaccine. To assess this, mice were humanely culled at 0, 6, 12 and 24h post-vaccination with PCV13 and the spleens and draining lymph nodes were collected in a manner that preserved RNA integrity (**Fig. 6.13A**). Next, RT-qPCR was employed to assess the expression of selected genes that encode key cytokines and chemokines that

have been previously shown to be induced following intraperitoneal challenge with heat-killed *Streptococcus pneumoniae* (*S. pneumoniae*) capsular type 14 were assessed (Khan, Chen, Wu, Paton, & Snapper, 2005) (**Fig 6.13B-E**). SPF mice had significantly higher expression of *Ifng* compared to GF mice at 6 and 24h post-vaccination (**Fig. 6.13B**). Surprisingly, GF mice had significantly higher expression of *Il6* and *Il12a* compared to SPF mice at baseline (0h) and 6h and 12h post-vaccination (**Fig. 6.13C-D**). Expression of the chemokine CCL3 was also assessed, and SPF mice had higher expression of this chemokine at both 6h and 24h post-vaccination (**Fig. 6.13E**).

In summary, GF mice have significantly different baseline and PCV13-induced cytokine production compared to SPF mice. These differences in the cytokine and chemokine response to PCV13 have the potential to influence systemic immunity and potentially humoral responses to vaccination. Future work using cells preserved from this experiment will assess these differences more thoroughly using single cell RNA sequencing.

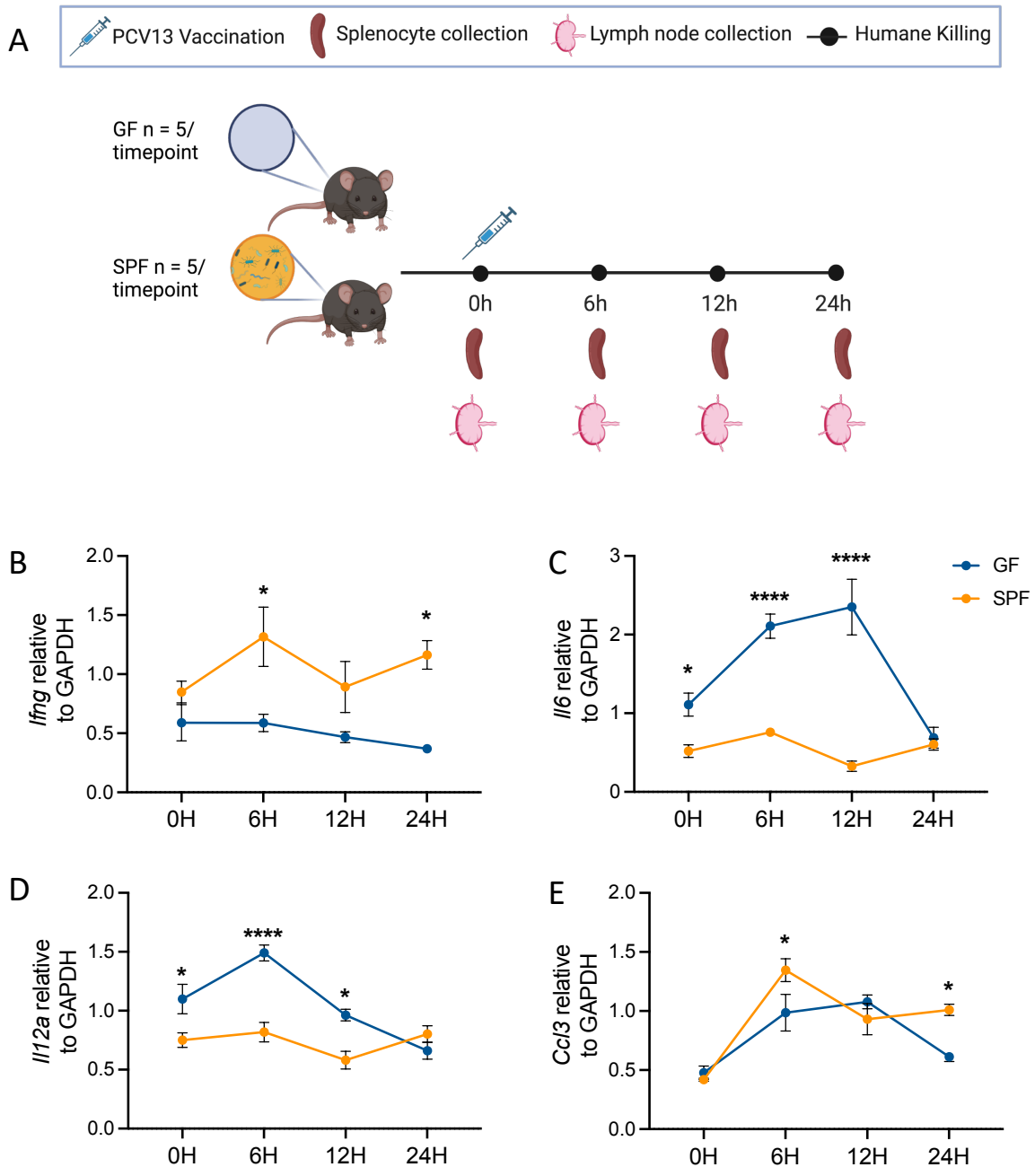

Figure 6.13| Significant differences in the expression of *Ifng*, *Il6*, *Il12a* and *Ccl3* hours after PCV13 vaccination in germ-free (GF) compared to conventional SPF mice. A| Experimental timeline. Age-matched GF and SPF mice were vaccinated with PCV13 at day 21 of life and humanely killed at 0, 6, 12 and 24 hours post-immunisation. Single-cell suspensions of splenocytes and mediastinal lymph nodes were frozen in preservation media for subsequent analysis. The expression of **B|** *Ifng*, **C|** *Il6*, **D|** *Il12a* and **E|** *Ccl3* was assessed relative to the housekeeping gene GAPDH by RT-qPCR. Data are represented as the mean ± SEM. *p < 0.05, ****p < 0.0001.

6.2 Discussion

The influence of the microbiota on the immune response to vaccination has become increasingly apparent over the last decade. However, the mechanisms through which the microbiome modulates these immune responses remain incompletely understood (D. J. Lynn et al., 2021). Here, the potential for the microbiota to act as a natural adjuvant by signalling via TLRs was assessed.

Post boosting, MyD88, but not TLR4 and TLR2, was necessary for antibody responses to the PCV13 vaccine. The impaired IgG response in *Myd88*$^{-/-}$ mice was likely due to a lower frequency of GC B cells in the spleens of *Myd88*$^{-/-}$ mice compared to wt mice. Surprisingly, antibiotics treatment in early life resulted in an apparent 'recovery' of impaired IgG_{total}, IgG1, IgG3 and IgM responses in observed in *Myd88*$^{-/-}$ mice. Finally, the kinetics of the *Ifng*, *Il6*, *Il12a* and *Ccl3* response in the spleen after PCV13 vaccination revealed significant differences in the expression of these cytokines and the chemokine, CCL3, between GF and SPF mice.

Myd88$^{-/-}$ mice had impaired antibody responses to PCV13 post-boost, illustrating a critical role for MyD88-dependent signalling in mediating the immune response to the PCV13 vaccine. Previous studies have shown that MyD88 is required for optimal cytokine, chemokine and antibody responses to heat-killed *S. pneumoniae* type 14, and *Myd88*$^{-/-}$ mice are more likely to succumb to live *S. pneumoniae* type 14 challenge than wildtype mice (Khan et al., 2005). Interestingly, antibody responses to the PCV13 vaccine were not significantly different in antibiotic-treated *Myd88*$^{-/-}$ mice compared to the untreated wt and ABX groups, suggesting that recolonisation of the microbiota following

antibiotic exposure might be able to restore impaired vaccine responses through a MyD88-independent pathway. If this hypothesis is true, it likely depends on which taxa recolonise following antibiotic exposure. Intraepithelial lymphocytes protect gut barrier integrity via the production of the inflammatory cytokine IL-6 in a MyD88-dependent manner (Kuhn et al., 2018). The combination of antibiotics-induced dysbiosis and MyD88 deficiency may lead to increased gut leakiness and adjuvanting signals from the microbiota through a MyD88-independent pathway.

The finding that antibiotics treated *Myd88*$^{-/-}$ mice had a significantly higher IgG1 response in comparison to *Myd88*$^{-/-}$ in the absence of antibiotic exposure after boost was surprising. The IgG1 antibody compartment has the highest number of mutations and is therefore likely to have the highest antigen-binding affinity of any antibody subclass (Collins, 2016). However, IgG1 has the potential to block complement activation by other subclasses, and this has a role in preventing uncontrolled IgG-mediated inflammation (Lilienthal et al., 2018). It is unclear whether this potential imbalance of IgG1 could leave the host more susceptible to pneumococcal infection after PCV13 vaccination. Future work should assess the functional implications of antibody subclass imbalance using infectious challenge models.

IgG2b is considered to be produced as part of the T-independent response (Deenick, Hasbold, & Hodgkin, 1999; Collins, 2016). Antibiotic treated and *Myd88*$^{-/-}$ mice had impaired IgG2b responses against the whole PCV13 vaccine compared to wt mice. The dependence of IgG2b responses to PCV13 on a MyD88-dependent pathway further illustrates the potential importance of MyD88 and the microbiota in the T -independent response.

The frequency of GC B cells, but not innate-like B-1 cells, was impaired in *Myd88*$^{-/-}$ mice after vaccination. As seen in the previous chapter, there was an egress of B-1 cells out of the peritoneum after vaccination in both wt and *Myd88*$^{-/-}$ mice. B-1 cells translocate to the milky spots of the omentum via TLR signalling after the intraperitoneal administration of LPS (Ha et al., 2006; Maruya et al., 2011; Okabe & Medzhitov, 2014). I cannot not rule out that there may be differences in B-1 cell frequencies in other organs.

Myd88$^{-/-}$ mice had a modest but not significant impairment of splenic PCs. However, the impaired IgG response in *Myd88*$^{-/-}$ mice was likely due to a lower frequency of GC B cells in the spleens of *Myd88*$^{-/-}$ mice compared to wt mice. Prior studies identified a role for the MyD88 pathway in PC accumulation in the bone marrow (Guay, Andreyeva, Garcea, Welsh, & Szomolanyi-Tsuda, 2007; Kang et al., 2011; Neves et al., 2010). A study assessing responses to *Salmonella typhimurium* infection found that *Myd88*$^{-/-}$ mice had a significantly lower proportion of CD138^{+} PCs and a delay in the generation of PCs compared to wt mice after infection (Neves et al., 2010). However, *Myd88*$^{-/-}$ mice had no differences in the frequency of splenic GC B cells after infection compared to wt mice (Neves et al., 2010). Two other studies showed that *Myd88*$^{-/-}$ mice had defective ASC responses in the bone marrow of influenza-immunised and polyomavirus-infected mice, but GC B cells frequencies were not impaired in *Myd88*$^{-/-}$ mice in either experimental model (Kang et al., 2011; Guay, Andreyeva, Garcea, Welsh, & Szomolanyi-Tsuda, 2007). Therefore, the defect in GC B cell responses in PCV13 vaccinated *Myd88*$^{-/-}$ mice contrasts with these previous studies, illustrating that the MyD88 pathway may be particularly important for immune responses to PCV13 vaccine antigens compared to live viral and bacterial infections. The literature presented also contrasts with the finding that *Myd88*$^{-}$

$^{-/-}$ mice had a modest but not statistically significant reduction in the frequency of PCs compared to wt mice.

There was a significant reduction in the frequency of IFNγ producing cytotoxic $CD8^+$ T cells in both *Myd88*$^{-/-}$ mice and antibiotic-treated wt mice compared to untreated wt mice (**Fig. 6.6**). This is in contrast to previously published data, which demonstrated exacerbated IFNγ responses after antibiotic treatment in early-life to PCV13 (Lynn et al., 2018). However, Lynn et al. measured total IFNγ, not T cell-specific IFNγ; therefore, differences in other cell types' production of IFNγ may account for these differences.

The antibody response to the PCV13 vaccine is independent of TLR4. TLR4 signals through both MyD88-dependent and independent (TRIF) pathways. Therefore, a defect in MyD88, but not TLR4, suggests that a different receptor upstream or MyD88 is required for optimal antibody responses to the PCV13 vaccine. In an infection model of *S. pneumoniae*, *Tlr4*$^{-/-}$ mice were more susceptible to infection than wt mice (Sánchez-Tarjuelo et al., 2020). The severity of *S. pneumoniae* was even greater in *Tlr4*$^{-/-}$ mice than in *Myd88*$^{-/-}$ mice, as there were higher bacterial colony-forming units (CFU) in the lungs of *Tlr4*$^{-/-}$ mice. This was attributed to changes in the pro-inflammatory cytokine profile, weaker myeloid cell lung infiltration and lack of Th1 induction (Sánchez-Tarjuelo et al., 2020). The importance of TLR4 in responding to *S. pneumoniae* infection means assessing functional differences after PCV13 vaccination may also be of interest.

The importance of the TLR2 pathway for immunity to pneumococcus has been previously reported by Khan *et al*., who showed that *Tlr2*$^{-/-}$ mice exhibited impaired antibody responses to several proteins and polysaccharides in response to *S. pneumoniae*

administered intraperitoneally (Khan et al., 2005; Sen, Khan, Chen, & Snapper, 2005). However, the data from this chapter showed that while IgG_{total} responses to primary vaccination were impaired in *Tlr2*$^{-/-}$ mice, there were no significant differences in IgG_{total} antibody responses to the whole vaccine after boosting. This experiment provides evidence further that the TLR2 pathway is important for the initial humoral immune response to PCV13 vaccination.

The final experiment in this chapter sought to define differences in the early innate immune response to PCV13 vaccination, as it appears that the microbiota influences both T-dependent and independent responses to PCV13 vaccination. Splenic cytokines were assessed by RT qPCR at baseline (0h) and 6h, and 12h post-vaccination. Interestingly, GF mice had a dysregulated cytokine response to vaccination and were defective in their induction of *Ifng* and *Ccl3* but had heightened *Il6* and *Il12a* expression. IL-12, IFN-γ, and CCL3 have each been separately associated with the promotion of type 1 adaptive immunity, while IL-6 has been found to facilitate type 2 immunity (Luther & Cyster, 2001; Murphy & Reiner, 2002; Velazquez-Salinas, Verdugo-Rodriguez, Rodriguez, & Borca, 2019). In addition, IL-6 and IL-12 are strictly myeloid-derived, whereas IFN-γ is produced by T cells but also by NK cells, invariant T cells and ILC1s post-immunisation (Ignacio et al., 2016), potentially illustrating a dysregulated innate response and dampened adaptive response in GF mice to PCV13 vaccination. Surprisingly, GF mice had higher baseline levels of *Il6* compared to SPF mice. Previous studies have reported that IL-6 levels measured by ELISA in the spleens of GF mice and those colonised by pathobionts were not significantly different after culturing with PMA and ionomycin, however, this would stimulate T cell and not innate responses (Sato, Yokoji, Yamada, Nakajima, & Yamazaki, 2018).

GF mice may exhibit exacerbated and uncontrolled systemic innate responses to PCV13 antigens due to a lack of exposure to microbiota-derived antigens. These cytokine and chemokine were also measured during the early-life window where mice have exacerbated responses to the microbiota (Al Nabhani et al., 2019). SPF mice undergo a 'weaning reaction' marked by exacerbated baseline cytokine responses induced by the microbiota, which does not occur in GF mice and leads to dysregulated RORγt^{+} Treg responses later in life (Al Nabhani et al., 2019). Splenocytes and draining lymph node cells have been cryopreserved from my experiment in order to carry out single-cell sequencing for a more extensive transcriptional analysis of the defects in the early response to PCV13 vaccination.

Some important limitations of this work need to be addressed in future studies. For example, MyD88 was knocked out systemically, so which immune cell populations mediate these effects remains to be determined. I presented evidence from previous studies suggesting that MyD88 in B cells or intestinal intraepithelial lymphocytes could drive this impairment in humoral responses to the PCV13 vaccine. Future work should assess cell-type specific knockouts of MyD88 using Myd88$^{fl/fl}$, CD23-Cre or IL-6-Cre mice to restrict myd88 deficiency to populations of interest. Another limitation of this study is that polysaccharides are already known to stimulate the TLR2 pathway. Therefore, these experiments cannot specifically assess whether these signals come from the microbiota, vaccine, or adjuvant. Future experiments are needed in genetically deficient GF mice, e.g. *Myd88*$^{-/-}$ GF mice, to further elucidate the role of these receptors in mediating natural adjuvanting signals from the microbiota. Assessing specific bacterial species in a gnotobiotic mouse model could also help to identify specific bacteria that support optimal

antibody responses. Finally, due to time constraints, gene expression analysis was limited to a select number of proinflammatory cytokines and chemokines, leaving it unclear whether a defect in GF mice is critical for promoting type 1 or 2 immunity. Future work will involve single-cell RNA sequencing analysis to more comprehensively characterise differences in gene expression and cellular composition of the draining lymph node in GF compared to SPF mice in the hours post-immunisation.

7 Discussion

The COVID-19 pandemic has brought global attention to the importance of effective vaccines. However, vaccine responses remain suboptimal in vulnerable populations, including infants and older adults. Vaccine immunogenicity is also higher in high-income countries (HICs) and low- and middle-income countries (LMICs) where vaccines are most needed (Patel et al., 2013; Clark et al., 2019; Hallander et al., 2002; Lalor et al., 2009). In parallel, there is growing evidence of a relationship between the microbiome and vaccine responsiveness. A recent study assessing human adults with low pre-existing immunity to influenza found impaired antibody responses to the flu vaccine after antibiotics exposure, suggesting that the microbiota may substantially influence primary rather than memory responses to vaccination (Hagan et al., 2019). Preclinical experiments in mice by Lynn et al. also demonstrated that antibiotic-induced microbial dysbiosis in early life led to significantly impaired antibody responses to both live and adjuvanted vaccines (Lynn et al., 2018). However, prior to this thesis whether antibiotic exposure could influence vaccine responses in human infants had not yet been investigated. The mechanisms through which the microbiome influenced vaccine responses also remain unclear. Several mechanisms have been proposed. Immunomodulatory molecules produced by the microbiota, such as liposaccharide and flagellin, may modulate immune responses to vaccination by acting as natural adjuvants, via recognition by pattern recognition receptors (PRRs) such as Toll-like receptors (TLRs) expressed by antigen-presenting cells. Previous studies have shown that sensing of the microbiota through TLR5 was necessary for optimal antibody responses to the trivalent influenza vaccine in mice (Oh et al., 2014), but whether this is the case for other vaccines and TLRs had yet to be explored. Furthermore, the influence of the microbiota on innate-like B-1 cell responses

to the immunodominant cell-wall polysaccharide of Group A streptococcus (GAS) was shown previously to be dependent on signalling through a MyD88 dependent pathway, a key adaptor protein for several TLRs. However, whether this had implications for polysaccharide vaccines such as PCV13 remained to be explored.

In this dissertation, I present several preclinical and clinical studies that have furthered our understanding of the impact of the microbiome on immune responses to vaccination in early life. The dependency of optimal humoral and cellular responses to PCV13 on the microbiota was elucidated. In addition, I found a contextual dependency on MyD88 for effective antibody responses to the PCV13 vaccine. Elucidating the complex relationship between the microbiome and vaccine responsiveness has opened new possibilities for the exploration of microbiota-targeted interventions to improve vaccine responsiveness in infants. In addition, this work examined flow cytometry data as part of a large clinical study, the Antibiotics and Immune Response Study, an extensive systems vaccinology study that found impaired responses to infant vaccines in infants directly exposed to antibiotics in the neonatal period.

Preclinical studies

Though a number of observational clinical cohort studies have found an association between vaccine responses and the microbiome (Huda et al., 2019, 2014;V. Harris et al., 2018; V. C. Harris et al., 2016;Parker et al., 2018; Fix et al., 2020;Zhao et al., 2020;Praharaj et al., 2019), very little mechanistic work has been carried out to prove a causative role. Preclinical studies in mouse models are an effective and relatively cheap system to probe whether associations found in observational clinical studies are likely causally related. To control for the complexity and interdependency of multiple variables associated with

the immune response, it was necessary to use a GF mouse model. GF mice have advantages over antibiotics treatment models. GF mice are a completely sterile system, free of all microorganisms, viruses and fungi, allowing exclusive colonisation with a particular monoculture or specific microbiota (Kennedy, King, & Baldridge, 2018). However, there are also some drawbacks. GF mice are expensive, requiring expensive isolators in a separate facility to conventionally colonised SPF mice, new genotypes must be derived GF, and not all experiments are feasible in a GF environment. GF mice also have specific immune developmental defects, such as dysregulated natural killer T cell tolerance, lack of mucosal invariant T cell imprinting to promote tissue repair and elevated IgE resulting in exaggerated allergic reactions (Cahenzli, Köller, Wyss, Geuking, & McCoy, 2013; Constantinides et al., 2019; Hansen et al., 2012; Olszak et al., 2012; Archer et al., 2023). Despite these drawbacks, GF mice are considered a gold-standard approach to demonstrate a casual relationship between the microbiota and a phenotype of interest.

Prior to this dissertation, it was known that mice treated with antibiotics in early life had impaired responses to infant vaccines such as PCV13 (Lynn et al., 2018). This body of work has recapitulated these findings in a GF mouse model, demonstrating that the effects of antibiotics were likely due to their impact on the microbiota and not off-target effects of the antibiotics (Shekhar & Petersen, 2020). Furthermore, extensive flow cytometry analysis of the spleen, draining lymph nodes, peritoneum and bone marrow of GF and colonised mice demonstrated that impaired antibody responses in GF mice coincide with defects in germinal centre (GC) formation, potentially stemming from differences in the early cytokine and innate-like B-1 cell responses. Bacterial polysaccharides, such as those found in the PCV13 vaccine, are generally expected to elicit T-independent responses. However, GF mice appear to have impaired T-dependent and

independent responses to the PCV13 vaccine. Polysaccharides in the PCV13 vaccine are conjugated to the carrier protein CRM_{197}, which could be why it appears to induce both T-dependent and independent antibody responses in immunised mice.

Most studies to date assessing the impact of the microbiota on GC responses have assessed GC formation in Peyer's Patches in the gastrointestinal tract. For example, aged mice have been shown to have defective GC reactions in their gut Peyer's Patches (Stebegg et al., 2019). However, cohousing aged mice with younger adult mice and administering an FMT from adult mice can restore defective GC response in aged mice (Stebegg et al., 2019). More recent work found that the composition of the gut microbiota could influence splenic GC formation in response to *Plasmodium yoelii.* In this study, Tfh cells were shown to be primed by the microbiota in the Peyer's Patches before they migrated to the spleen. GF mice colonised with the microbiota from *Plasmodium yoelii*-resistant mice were resistant to infection with *Plasmodium yoelii*, demonstrating that GC formation was microbiota dependent (Waide et al., 2020). In addition, resistant mice had a wider range of parasite-specific antibodies and higher BCR repertoire diversity.

GCs are usually formed via T-dependent responses that result in robust and long lasting immunity against infection and disease (N. S. De Silva & Klein, 2015). Recently, fate-mapping of B cells found that T-independent GCs can also lead to the generation of long-lived plasma cells and memory B cells (Liu et al., 2022). In addition, infant B cells have an intrinsic inability to form GCs. However, T-dependent derived memory cells and PCs persist longer (Akkaya, Kwak, & Pierce, 2019; Liu et al., 2022). The persistence of PCs appears to be pre-programmed, and extending the duration of the GC reaction favourably selects for long-lived plasma cells (M. J. Robinson et al., 2022). Therefore, utilising

gnotobiotic mice to discover microbiota-targeted interventions with the ability to prolong the GC response would be particularly helpful in boosting infant vaccine responses.

The timing of gut microbial colonisation is a key factor influencing immune responses in later life (Al Nabhani et al., 2019). FMT mice in my experiments which received the FMT at day 21 of life, did not have restored antibody responses to vaccination compared to SPF mice, but intergenerationally colonised exGF mice largely did. Further work is needed to determine when colonisation needs to occur post birth for optimal antibody responses after PCV13 vaccination. Another group recently showed that the timing of colonising GF mice with a conventional microbiota had a significant effect on splenic immune cell populations in adulthood (Archer et al., 2023). GF mice colonised with a normal microbiota at birth had normal cell frequencies in the spleen in adulthood. In contrast, those not colonised until 4 weeks of life had significantly higher dendritic cells (DCs), macrophages, B cells and Tregs compared to conventional mice but lower $CD8^+$ T cells (Archer et al., 2023). Therefore, it is perhaps not surprisingly that antibody responses were not restored in the FMT group in my experiments (which were colonised at day 21 of life), as defects in key immune cell populations in GF mice were likely not reversible with an FMT alone at this timepoint. However, mice colonised with an SPF microbiota before birth (exGF) was sufficient to largely restore IgG tites to levels comparable to conventional mice.

I also showed that mice deficient in MyD88 had severely impaired immune responses to PCV13 vaccination. Therefore, MyD88-dependent TLR signalling may be involved in the immune response to the PCV13 vaccine. Interestingly, though IgG and IgM responses to

vaccination were severely impaired in *Myd88*$^{-/-}$ mice, MyD88/IRAK4 deficient humans have impaired IgM but not IgG responses against T-independent pneumococcal antigens (Maglione et al., 2014). It is possible that this is the case as, unlike mice, humans have fully formed secondary lymphoid tissues. TLR2 was necessary for the initial response to PCV13 in mice, but not after boosting, which contrasts with previous work illustrating the role of TLR2 signalling in pneumococcal polysaccharide immune responses (Sen et al., 2005). However, MyD88 but not TLR2 was necessary for protection against *Streptococcus pneumoniae* (*S. pneumoniae)* (Khan et al., 2005). TLR knockout experiments could also be impacted by redundancy in different TLR pathways (Chauhan, Shukla, Chattopadhyay, & Saha, 2017). I also observed that the significant impairment of antibody responses in GF and *Myd88*$^{-/-}$ mice were accompanied by significantly lower frequencies of GC B cells. My data suggests that the mechanism by which *Myd88*$^{-/-}$ mice and GF mice have impaired immune responses to the PCV13 vaccine could be similar. Surprisingly, antibiotics induced dysbiosis from early life antibiotics exposure restored impaired antibody responses in *Myd88*$^{-/-}$ mice. Further work is needed in a genetically deficient GF model to assess whether GF *Myd88*$^{-/-}$ mice have impaired responses to PCV13, in contrast to the 'rescued' response in antibiotics exposed mice.

The infiltration of IFNγ-dependent Sca-1 monocytes into lymphoid organs during secondary infection was previously reported to cause GC collapse (Biram et al., 2022). A similar mechanism may mediate impaired antibody and GC B cell frequencies in *Myd88*$^{-/-}$ mice and could explain why antibiotics treatment 'rescued' the impaired antibody observed in *Myd88*$^{-/-}$ mice. One possibility is that *Myd88*$^{-/-}$ mice have increased inflammation due to dysbiosis and decreased gut barrier integrity. Antibiotics exposure

may have reduced this colonisation and may have restored gut barrier integrity, reducing inflammation and the induction of Sca-1^{+} monocytes, restoring GC B cell responses. However, 16S rRNA gene sequencing data showed no evidence of pathogenic gut microbiota colonisation after early life antibiotics exposure in *Myd88*$^{-/-}$ mice. Still, future work should assess Sca-1^{+} monocyte infiltration in the spleen and lymph nodes of antibiotic treated and FMT mice.

Microbiota drift in animal facilities can change experimental phenotypes over time. 16S rRNA gene sequencing revealed differences in the composition over time between different experiments. Differences in the microbiota between the control SPF mice in Tlr2, Tlr4 and MyD88 experiments may partly explain why responses to PCV13 were impaired in antibiotics treated mice in some experiments but were not impaired in others. The species that recolonised these mice is also vastly different from taxa recolonised antibiotics exposed mice in previous work by Lynn et al. (Lynn et al., 2021). A confounding factor in this analysis could be differences in the amount of time that the samples from each experiment were stored. Although all V timepoint samples were extracted around the same time, each of the experiments took place 2-5 months apart, which does not rule out the possibility that this may have had an effect on the composition of the microbiome in the faecal samples when assessed by 16S sequencing.

B-1 cells are frontline players in the early humoral responses, alongside marginal zone (MZ) B cells, to T-independent antigens (K. M. Haas et al., 2005; Martin, Oliver, & Kearney, 2001). T-independent antigens are identified by their high molecular weight, repetitive epitopes, and slow degradation within the body. T-independent antigens, such as bacterial capsular polysaccharides, can induce quick antibody responses by cross-linking

multivalent BCR without the need for assistance from T cells restricted by major histocompatibility complex class II (Mond, Lees, & Snapper, 1995). The polysaccharide specific clonality of B-1 cells have been previously shown to be pre-programmed by the microbiota, directing their response in a MyD88 dependent manner (New, Dizon, Fucile, Rosenberg, Kearney, & King, 2020). However, while there were significantly higher B-1, B-1a and B-1b cells in SPF mice compared to GF mice after vaccination, there was a reduction in these populations in the peritoneum is cell subset after vaccination. This reduction of the frequency of B-1 cells after immunisation was also observed in wt and *Myd88*$^{-/-}$ mice. One study found a higher accumulation of B-1 cells in the peritoneum of GF mice compared to conventionally colonised SPF mice under homeostasis (Ha et al., 2006). The authors suspected steady-state signals from the microbiota led to the constant migration of B-1 cells out of the peritoneum mediated by TLR sensing of the microbiota, but that an absence of these signals in GF mice led to their accumulation in the peritoneum (Ha et al., 2006). Further work needs to examine the importance of B-1 cells programmed by the microbiota in the response to infant polysaccharide vaccines.

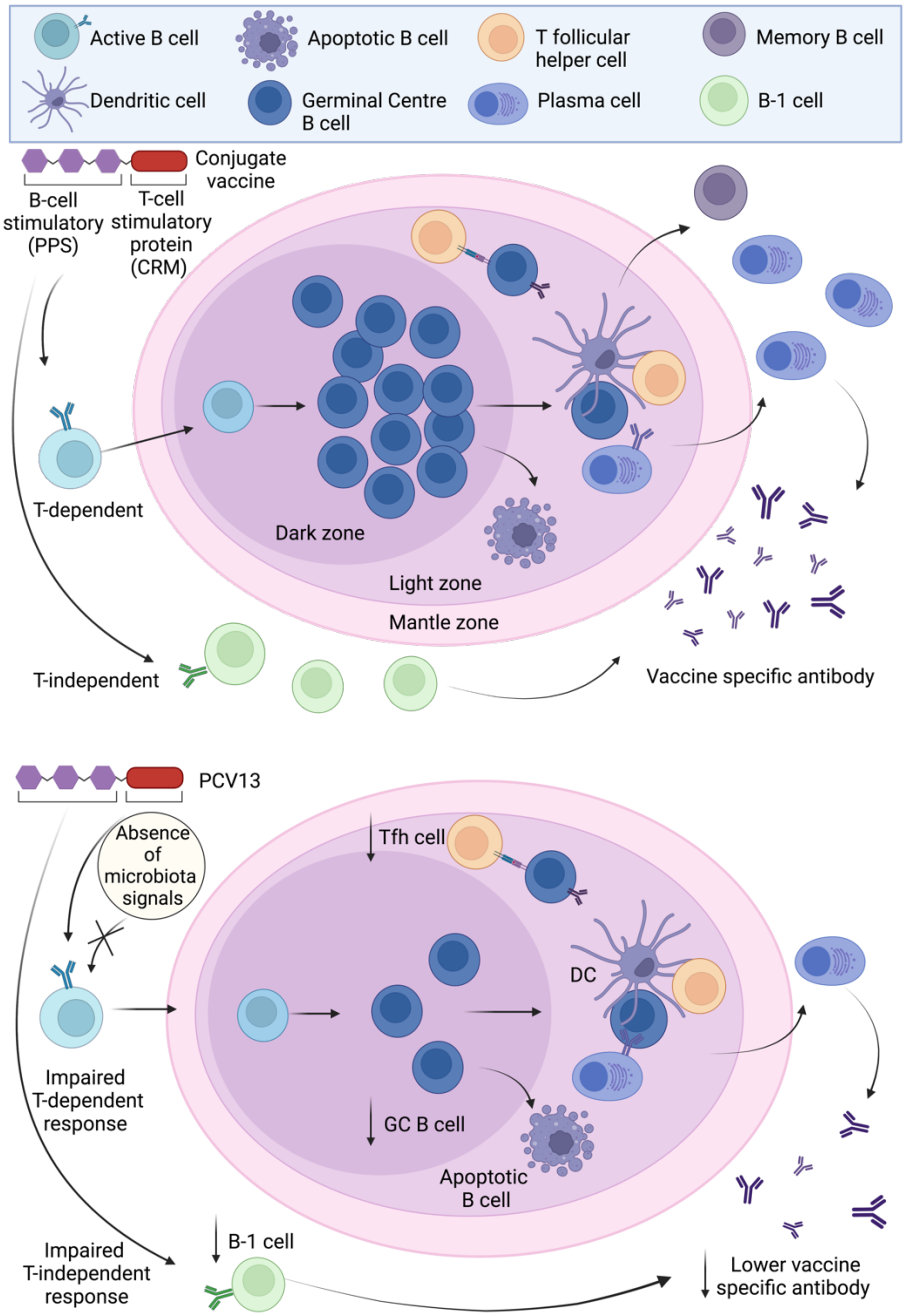

Figure 7.1| PCV13 elicits both T-dependent and independent antibody responses. The PCV13 vaccine consists of the carrier protein CRM_{197} conjugated to polysaccharides against 13 serotypes of *Streptococcus pneumoniae*. This vaccine generated a T-dependent response in which antigen-presenting cells presented vaccine antigens to T cells (such as Tfh cells) in the lymph nodes and spleen, contributing to the formation of GCs where B cells undergo affinity maturation, somatic hypermutation, class switching, and differentiation into plasma cells that produce high-affinity antibodies. PCV13 also generated a T-independent response, activating innate-like B cells (such as B-1 cells) that produce antibodies without T cell help. Both T-dependent and independent responses to the PCV13 vaccine were impaired in GF mice.

Other models used to assess the impact of the microbiota

As discussed, while GF mice are useful preclinical model to assess the impact of the microbiota on immune responses, they have drawbacks, including impaired T regulatory function (Östman, Rask, Wold, Hultkrantz, & Telemo, 2006). In addition, GF mice can only partially replicate the intricate interactions within the microbiota-competent environment of conventional mice. Consequently, future studies should consider other, more physiologically relevant models. One way to more accurately assess vaccine responses is by utilising mice with a 'wild' microbiome. The seminal paper in this field found that laboratory SPF mice cohoused with pet shop mice exhibited a more 'mature' immune system than standard SPF mice (Beura et al., 2016). Rosshart et al. subsequently created a 'chimeric meta-organism' model, where they colonised laboratory mice with a 'natural microbiota' made up of the microbiota of closely related wild mice (Rosshart et al., 2017). This model had the benefit of maintaining the genetic background of the laboratory mouse but adding the natural diversity of a wild microbiota. These chimeric mice were protected against a lethal influenza viral infection. This group also created a 'wildling' model that better phenocopied human immune responses (Rosshart et al., 2019). Interestingly, a more recent paper found that SPF mice cohoused with pet-store mice had poorer vaccine immunogenicity to the influenza vaccine than SPF mice (Fiege et al., 2021). Therefore, a wild mouse model for vaccine responses could be used in the future as a more accurate way to recapitulate human responses to vaccination.

Despite their drawbacks, GF mice can also be used as a blank canvas to ensure reproducibility in the assessment of the effects of specific microbial strains and communities on the immune response to vaccination. For example, using defined bacterial communities in mouse models can ensure reproducibility across experiments

and control for phenotype changes due to microbiome drift over time (Bolsega et al., 2019; Brugiroux et al., 2016; Eberl et al., 2020; Rolhion et al., 2019). Alternatively, humanised GF mice can be colonised with a human microbiota for improved translation to human studies. Finally, one group used gnotobiotic mice to 'screen' for probiotic strains that could improve vaccine responsiveness (Geva-Zatorsky et al., 2017). This same model could be used to screen probiotic strains that could be administered to antibiotic-exposed human infants in order to improve subsequent responses to immunisation.

The AIR Study

This dissertation involved extensive flow cytometry and subsequent analysis undertaken as part of the AIR Study, a keystone systems vaccinology study, in preparation for publication. The AIR Study enrolled more than 255 full-term, healthy, and vaginally delivered infants. Infants required 5 visits for whole blood and faecal sample collection to assess the composition of the microbiota using shotgun metagenomics, vaccine antibody responses, whole blood transcriptomics (RNAseq) and multi-parameter immunophenotyping by flow cytometry analysis. Neonates directly exposed to antibiotics had impaired antibody responses to their routine immunisations, most notably to the PCV13 vaccine at 7 months. Previous systems vaccinology studies have primarily been limited to adults. Remarkably little work has been carried out profiling circulating immune cell populations in human infants after vaccination. Investigating the effects of antibiotics exposure on circulating immune cell populations could explain impaired responses to vaccination observed in this study. The vast majority of the infant's immune cell populations were unchanged between antibiotic exposure groups, though a modest decrease in circulating $CD45RA^-$ iTregs was observed in infants exposed to

intrapartum antibiotics. Flow cytometry analysis also highlighted sex differences in immune cell populations during this critical developmental window.

Previous studies have attempted to elucidate the effects of antibiotics induced dysbiosis on immune responses to vaccination in early life, but in far less depth. A study in Indian infants assessing the effect of azithromycin exposure did not find a significant impact of these antibiotics on responses to OPV (Grassly et al., 2016a). Antibiotics were administered 11 days before vaccination to improve impaired responses resulting from environmental enteropathy and pathogenic intestinal bacteria, and a reduction in both was observed. This did not impact OPV responses (Grassly et al., 2016a). This cohort drastically differs from the AIR Study infants as there is little pathogen burden in Australia and consequently do not suffer from environmental enteropathy. In another study, antibiotic exposure in children under 2 was negatively associated with antibody responses to DTaP and PCV, though no analysis of the microbiota or other samples was carried out in this study, and children were not age-matched (Chapman et al., 2022). An impressive study assessing thousands of records on Taiwan's National Health Insurance Research Database found an association between early-life antibiotic exposure and varicella occurrence pre- and post-varicella vaccine introduction (T. L. Lin et al., 2022). This study took advantage of existing healthcare data, which did not include data on the microbiota composition. A conflicting study found that antibiotics exposure from day 7 of life was associated with an increase in seropositivity to ORV at 7 months in infants from Peru, Brazil and South Africa (St Jean et al., 2022). However, the authors concluded that a theoretical removal of inappropriate antibiotics courses would have little effect on population seropositivity in these populations. Finally, a retrospective study of over 1000 infants from the United States assessed the impact of antibiotic exposure in the 14 days

before receiving ORV (E. J. Anderson et al., 2020). Infants exposed to antibiotics had no significant differences in RV-specific IgA compared to infants who did not receive antibiotics. However, this study vastly differed from the antibiotics exposure period assessed in the AIR Study, and data recording potential antibiotic exposure outside the period of 14 days before the vaccination was not assessed. These studies highlight the importance of our comprehensive systems vaccinology approach.

Human infants have much poorer responses to vaccination than adults, particularly in response to T-independent antigens (C. A. Siegrist & Aspinall, 2009). Therefore, circumventing the immature infant immune response and manufacturing effective vaccines is particularly important to protect vulnerable populations. However, manipulating the microbiota to give infants the best chance at effectively responding to existing vaccines is also necessary until this is achieved. Antibiotic exposure in AIR Study infants was associated with reduced bifidobacterial colonisation, which correlated with vaccine responses. An increased relative abundance of *Bifidobacterium* spp. has previously been found to be associated with increased SCFA production (Fukuda et al., 2011). SCFAs, such as acetate and butyrate, have immunomodulatory properties that can support B cell metabolism, plasma cell differentiation and class switching, resulting in higher overall antibody production (M. Kim et al., 2016). In addition, *Bifidobacterium* spp. can metabolise Human Milk Oligosaccharides (HMOs) found in breast milk into SCFAs, supporting B cell differentiation and antibody responses (M. Kim et al., 2016). Therefore, administering a bifidobacterial-based probiotic after antibiotic exposure could be considered for future RCTs to improve vaccine responses in antibiotic exposed infants.

Limitations

These studies have potential limitations that must be considered. For example, while the frequency and number of circulating populations were assessed via multiparameter flow cytometry analysis in the AIR study, functional differences were not. This means that although infants have similar numbers of the vast majority of the immune cell populations assessed, I cannot rule out functional changes to these populations.

Although PCV13 is usually administered to humans intramuscularly, previous experiments by our lab demonstrated that intramuscular vaccination with PCV13 was very poorly immunogenic in mice. Therefore, the route of vaccination needs to be considered in the experiments presented in this dissertation as all mouse experiments used the intraperitoneal route of immunisation. One possibility for the improved for the improved immunogenicity to the PCV13 vaccine when vaccinated intraperitoneally is that mice may have a particular dependence on peritoneal innate-like B-1 cell responses to the PCV13 vaccine. My work has predominantly focused on the gut microbiota, however, site-specific microbial communities also influence immunity at the immunisation site. Intradermal vaccines can be influenced by the skin microbiota (Erin Chen, Fischbach, & Belkaid, 2018). NOD2 sensing of the microbiota was necessary for responses to intranasal immunisation with a model antigen (D. J. Kim et al., 2016). The intranasal microbiota is also associated with IgA response to live attenuated influenza vaccine (Salk et al., 2016). The predictive power of experiments in SPF mice to predict human responses must also be considered. The results observed in mouse models are often not recapitulated in humans. Challenges have been felt in many research areas, such as the assessment of cancer immunotherapies and disease modelling (Beura et al., 2016; Jameson & Masopust, 2018). However, fundamental differences in mouse and human

immunology, such as its activation status, create challenges for vaccine studies (Jameson & Masopust, 2018).

Future directions

Moving forward, several questions now need to be addressed. First, future work needs to uncover the specific strains of bacteria in the microbiota necessary for optimal early-life antibody responses to vaccination (Di Luccia et al., 2020). Previous cohort studies have been limited in this regard as they have used 16S rRNA sequencing, which lacks species-specific and strain-specific resolution, rather than shotgun metagenomics.

Direct antibiotic exposure impaired antibody responses to infant vaccines, leaving infants potentially vulnerable to infectious disease. Multivariate logistic regression at 7 months detected a significant decrease in the proportion of the AIR Study infants achieving seroprotection for PCV13 in both the neonates directly exposed to antibiotics (PPS14 & PPS19A) and infants exposed to post natal antibiotics (PPS9V & PPS19A). This left a significant proportion of infants below the desired protective threshold, though correlates of protection for PCV13 are highly serotype specific (Andrews et al., 2014). How big a problem waning protection could be on a population scale in a HIC such as Australia with a low infectious disease burden needs to be clarified. The next step for this work is to investigate potential ways to prevent dysbiosis in antibiotics exposed infants or manufacture vaccines that can overcome antibiotic-induced impairment of antibody responses. A more straightforward intervention could involve the recommendation of an additional booster vaccine dose for antibiotic exposed infants. However, a health economic assessment of the value of such intervention in populations with low risk of infection would be necessary. In addition, in some cases boosting with polysaccharide

vaccines actually leads to a reduction in antibody titres (Brynjolfsson et al., 2012; González-Fernández, Faro, & Fernández, 2008).

Assessing whether lower antibody titres correlate with a higher risk of infectious disease and allergy is also necessary. Previous studies have shown that GF mice have heightened OVA-induced allergic airway inflammation, illustrating the importance of the microbiota in the maintenance of immune tolerance (Herbst et al., 2011). Furthermore, mice exposed to azithromycin as pups had increased susceptibility to house dust mite allergen later in life, driven by IgE and IL-13 produced by $CD4^+$ T cells (Borbet et al., 2022). Vaccines can also have a 'reciprocal' impact on the microbiome. For example, while lowering the proportion of serotype-specific pneumococci in the nasopharynx, pneumococcal immunisation is also associated with increased anaerobes and streptococci (Biesbroek et al., 2014). In addition, increased *Streptococcus* has also been reported on the nasopharyngeal microbiome of infants after PCV10 immunisation (Salgado et al., 2020). This reciprocal impact on the microbiome combined with the consequences of antibiotics induced dysbiosis could have profound consequences for risk of disease.

The overuse and overreliance on antibiotics must also be considered, as up to 50% of Australian infants are exposed to antibiotics (H. Anderson et al., 2017). This is higher than in other developed countries, such as the US, where intravenous antibiotic administration is around 14% for term and late-preterm neonates and over 90% for extremely preterm neonates (Flannery et al., 2018). This is largely due to precautions against neonatal sepsis, though most are antibiotics administered are precautionary as there are still few tools for effective diagnosis of neonatal sepsis (Stocker et al., 2023). Antimicrobial resistance is also a growing threat to global public health (Shekhar & Petersen, 2020). We

hope that the AIR Study can influence policy around the overuse of antibiotics in both mother and infant, particularly as antibiotics have a disproportional effect on infants compared to adults while their microbiota is unstable and their immune system is developing. Interestingly, there was no evidence that intrapartum antibiotic exposure with no direct infant exposure impacted vaccine responses of infants in the AIR Study (Ryan et al.**,** in preparation). Therefore, prescribing antibiotics for group B streptococcus carriage could continue as it is only direct antibiotic exposure in the neonatal period that was of concern for infant antibody responses. However, the impact of antibiotics is not restricted to effects on the infant but could have consequences later in life. A previous study by our lab showed that early-life antibiotics exposure resulted in divergent microbiota composed of two distinct community types in each cage, one of which impacted longevity, immunity and insulin resistance (Lynn et al., 2021). Due to the unintended risks of early life antibiotic exposure, better antibiotic stewardship practices are required, including a combination of regulatory changes to packet sizes and repeat prescriptions, pubic campaigns, education and academic input, as well as strategies in the clinic for delaying prescriptions and support tools for clinical decisions and patient information sheets (Glasziou, Dartnell, Biezen, Morgan, & Manski-Nankervis, 2022).

Engineered bifidobacterial probiotics could be a promising option for negating the negative effects of antibiotics in early life due to associations between bifidobacterial and B cell antibody responses (M. Kim et al., 2016). The *Bifidobacterium bifidum* and *Lactobacillus acidophilus* containing licensed probiotic, Infloran, showed promising results in preclinical models and improved humoral responses to infant vaccines in GF mice (Ryan et al., in preparation). Engineered live bacteria therapeutics are also in the pipeline and being tested for use after antibiotic-induced dysbiosis (Cubillos-Ruiz et al.,

2022). This engineered *Lactococcus lactis* can degrade residual antibiotics commensal disruptors, β-lactams, without disrupting commensal species needed for resistance against invasive pathogens such as *Clostridioides difficile* (Cubillos-Ruiz et al., 2022). However, RCTs to date that have assessed the effect of probiotic interventions on vaccine responses have been carried out in small and healthy populations, and have had mixed results (Zimmermann & Curtis, 2018; D. J. Lynn, Benson, Lynn, & Pulendran, 2021). An RCT in vaccinated, antibiotic exposed infants, is needed to determine the specific effects of probiotics on the dysbiotic microbiota and, consequently, the immune system. The type of dysbiosis induced by antibiotics may also be important. For example, whether the antibiotics are narrow or broad spectrum may also need to be considered, in addition to geographical location, as the microbiota varies significantly between regions, particularly between HICs and LMICs.

There are numerous possibilities for future preclinical work utilising mouse models to assess other mechanisms through which the microbiome influences the immune response to infant vaccines. Antibody avidity and neutralisation capacity in GF, *myd88*$^{-/-}$ and antibiotics exposed mice requires further examination. BCR repertoire sequencing after early life in these vaccine-impaired groups would allow an even more in-depth analysis of differences in the antigen-specific antibody repertoire (Waide et al., 2020; New et al., 2020). The impact of antibiotic exposure on vaccine-mediated protection in a pneumococcal infection challenge model should also be assessed. Finally, another question is whether epigenetic imprinting or innate training by the microbiota on the immune system in early life is necessary for vaccine responses (Negi, Das, Pahari, Nadeem, & Agrewala, 2019; Woo & Alenghat, 2022). This could be assessed using an

assay for transposase-accessible chromatin with sequencing (ATAC-Seq) (Grandi, Modi, Kampman, & Corces, 2022).

There are polysaccharides for 13 pneumococcal serotypes contained within the PCV13 vaccine. However, only responses to the conjugate protein, CRM_{197}, were assessed to measured antigen-specific GC B cells as no antibodies specific to the polysaccharides within the PCV13 vaccine are available. Future work should include the assessment of polysaccharide-specific GC B cells. In addition, while these experiments have focused on the PCV13 vaccine, experiments assessing a model antigen such as ovalbumin (OVA) could give further mechanistic insight into the specific bacteria influencing T-dependent immune responses. This would allow extensive analysis opportunities to assess T cells specific for OVA. Immunomodulatory species could then be evaluated against other infant and adult vaccines.

While this dissertation has focused on the impact of the microbiota in early life, there are implications for other cohorts with poor vaccine immunogenicity, such as obese and older individuals (Siegrist & Aspinall, 2009; Painter, Ovsyannikova, & Poland, 2015; Zimmermann & Curtis, 2019). Unique issues surround these individuals, such as the progressive increase of a proinflammatory immune environment in old age (inflammaging) and immunosenescence (Ademokun et al., 2011; Ciabattini et al., 2018; Sen, Chen, & Snapper, 2006; Nakaya et al., 2015). For example, individuals with higher BMIs had a more significant decline in influenza-specific antibody titres a year after influenza vaccination than healthy-weight individuals and decreased $CD8^+$ T cell and IFNγ production (Sheridan et al., 2012). Therefore, the efficacy of probiotics and other microbiota-targeted therapies should also be assessed in these vulnerable groups.

Bibliography

Abdullah, M., Chai, P. S., Chong, M. Y., Tohit, E. R. M., Ramasamy, R., Pei, C. P., & Vidyadaran, S. (2012). Gender effect on in vitro lymphocyte subset levels of healthy individuals. *Cellular Immunology*, *272*(2), 214–219. https://doi.org/10.1016/j.cellimm.2011.10.009

Ademokun, A., Wu, Y. C., Martin, V., Mitra, R., Sack, U., Baxendale, H., … Dunn-Walters, D. K. (2011). Vaccination-induced changes in human B-cell repertoire and pneumococcal IgM and IgA antibody at different ages. *Aging Cell*, *10*(6), 922–930. https://doi.org/10.1111/j.1474-9726.2011.00732.x

Afshan G, Afzal N, Q. S. (2012). CD4+CD25(hi) regulatory T cells in healthy males and females mediate gender difference in the prevalence of autoimmune diseases. *Clin Lab*, *58*.

Agnandji, S. T., Lell, B., Fernandes, J. F., Abossolo, B. P., Kabwende, A. L., Adegnika, A. A., … Schellenberg, D. (2014). Efficacy and Safety of the RTS,S/AS01 Malaria Vaccine during 18 Months after Vaccination: A Phase 3 Randomized, Controlled Trial in Children and Young Infants at 11 African Sites. *PLOS Medicine*, *11*(7), e1001685. https://doi.org/10.1371/JOURNAL.PMED.1001685

Akatsu, H., Arakawa, K., Yamamoto, T., Kanematsu, T., Matsukawa, N., Ohara, H., & Maruyama, M. (2013, October 1). Lactobacillus in jelly enhances the effect of influenza vaccination in elderly individuals. *Journal of the American Geriatrics Society*. John Wiley & Sons, Ltd. https://doi.org/10.1111/jgs.12474

Akkaya, M., Kwak, K., & Pierce, S. K. (2019). B cell memory: building two walls of protection against pathogens. *Nature Reviews Immunology 2019 20:4*, *20*(4), 229–238. https://doi.org/10.1038/s41577-019-0244-2

Al Nabhani, Z., Dulauroy, S., Marques, R., Cousu, C., Al Bounny, S., Déjardin, F., … Eberl, G. (2019). A Weaning Reaction to Microbiota Is Required for Resistance to Immunopathologies in the Adult. *Immunity*, *50*(5), 1276–1288.e5. https://doi.org/10.1016/j.immuni.2019.02.014

Al Nabhani, Z., & Eberl, G. (2020). Imprinting of the immune system by the microbiota early in life. *Mucosal Immunology*, *13*(2), 183–189. https://doi.org/10.1038/s41385-020-0257-y

Alfaleh, K., & Anabrees, J. (2014). Probiotics for prevention of necrotizing enterocolitis in preterm infants. *Evidence-Based Child Health*, *9*(3), 584–671. https://doi.org/10.1002/EBCH.1976

Amenyogbe, N., Levy, O., & Kollmann, T. R. (2015). Systems vaccinology: A promise for the young and the poor. *Philosophical Transactions of the Royal Society B: Biological Sciences*, *370*(1671). https://doi.org/10.1098/rstb.2014.0340

Anderson, E. J., Lopman, B., Yi, J., Libster, R., Buddy Creech, C., El-Khorazaty, J., … Edwards, K. (2020). Effect of Concomitant Antibiotic and Vaccine Administration on Serologic Responses to Rotavirus Vaccine. *Journal of the Pediatric Infectious Diseases Society*, *9*(4), 479–482. https://doi.org/10.1093/JPIDS/PIZ044

Anderson, H., Vuillermin, P., Jachno, K., Allen, K. J., Tang, M. L., Collier, F., … Burgner, D. (2017). Prevalence and determinants of antibiotic exposure in infants: A population-derived Australian birth cohort study. *Journal of Paediatrics and Child Health*, *53*(10), 942–949. https://doi.org/10.1111/jpc.13616

Anderson, R. M., & May, R. M. (1985). Vaccination and herd immunity to infectious

diseases. *Nature*, *318*(6044), 323–329. https://doi.org/10.1038/318323a0
Andrews, N. J., Waight, P. A., Burbidge, P., Pearce, E., Roalfe, L., Zancolli, M., … Goldblatt, D. (2014). Serotype-specific effectiveness and correlates of protection for the 13-valent pneumococcal conjugate vaccine: A postlicensure indirect cohort study. *The Lancet Infectious Diseases*, *14*(9), 839–846. https://doi.org/10.1016/S1473-3099(14)70822-9
Archer, D., Perez-Muñoz, M. E., Tollenaar, S., Veniamin, S., Cheng, C. C., Richard, C., … Walter, J. (2023). The importance of the timing of microbial signals for perinatal immune system development. *Microbiome Research Reports*, *2*(2), 11. https://doi.org/10.20517/MRR.2023.03
Arpaia, N., Campbell, C., Fan, X., Dikiy, S., Van Der Veeken, J., Deroos, P., … Rudensky, A. Y. (2013). Metabolites produced by commensal bacteria promote peripheral regulatory T-cell generation. *Nature*, *504*(7480), 451–455. https://doi.org/10.1038/nature12726
Arrieta, M. C., Arévalo, A., Stiemsma, L., Dimitriu, P., Chico, M. E., Loor, S., … Finlay, B. (2018). Associations between infant fungal and bacterial dysbiosis and childhood atopic wheeze in a nonindustrialized setting. *Journal of Allergy and Clinical Immunology*, *142*(2), 424–434.e10. https://doi.org/10.1016/J.JACI.2017.08.041
Ashhurst, T. M., Marsh-Wakefield, F., Putri, G. H., Spiteri, A. G., Shinko, D., Read, M. N., … King, N. J. C. (2022). Integration, exploration, and analysis of high-dimensional single-cell cytometry data using Spectre. *Cytometry. Part A : The Journal of the International Society for Analytical Cytology*, *101*(3), 237–253. https://doi.org/10.1002/CYTO.A.24350
Assaf-Casals, A., & Dbaibo, G. (2016). Meningococcal quadrivalent tetanus toxoid conjugate vaccine (MenACWY-TT, Nimenrix™): A review of its immunogenicity, safety, co-administration, and antibody persistence. *Human Vaccines & Immunotherapeutics*, *12*(7), 1825. https://doi.org/10.1080/21645515.2016.1143157
Awate, S., Babiuk, L. A., & Mutwiri, G. (2013). Mechanisms of action of adjuvants. *Frontiers in Immunology*. https://doi.org/10.3389/fimmu.2013.00114
Baden, L. R., Karita, E., Mutua, G., Bekker, L. G., Gray, G., Page-Shipp, L., … Welsh, S. (2016). Assessment of the safety and immunogenicity of 2 novel vaccine platforms for HIV-1 prevention: A randomized trial. *Annals of Internal Medicine*, *164*(5), 313–322. https://doi.org/10.7326/M15-0880/SUPPL_FILE/M15-0880_SUPPLEMENT.PDF
Barbier, A. J., Jiang, A. Y., Zhang, P., Wooster, R., & Anderson, D. G. (2022, May 9). The clinical progress of mRNA vaccines and immunotherapies. *Nature Biotechnology*. Nature Publishing Group. https://doi.org/10.1038/s41587-022-01294-2
Bellamy, G. J., Hinchliffe, R. F., Crawshaw, K. C., Finn, A., & Bell, F. (2000). Total and differential leucocyte counts in infants at 2, 5 and 13 months of age. *Clinical & Laboratory Haematology*, *22*(2), 81–87. https://doi.org/10.1046/j.1365-2257.2000.00288.x
Benner, M., Lopez-Rincon, A., Thijssen, S., Garssen, J., Ferwerda, G., Joosten, I., … Hogenkamp, A. (2021). Antibiotic Intervention Affects Maternal Immunity During Gestation in Mice. *Frontiers in Immunology*, *12*, 3347. https://doi.org/10.3389/FIMMU.2021.685742/BIBTEX
Beura, L. K., Hamilton, S. E., Bi, K., Schenkel, J. M., Odumade, O. A., Casey, K. A., … Masopust, D. (2016). Normalizing the environment recapitulates adult human immune traits in laboratory mice. *Nature 2016 532:7600*, *532*(7600), 512–516.

https://doi.org/10.1038/nature17655
Bhattacharjee, A., Burr, A. H. P., Overacre-Delgoffe, A. E., Tometich, J. T., Yang, D., Huckestein, B. R., … Hand, T. W. (2021). Environmental enteric dysfunction induces regulatory T cells that inhibit local CD4+ T cell responses and impair oral vaccine efficacy. *Immunity*, *54*(8), 1745–1757.e7. https://doi.org/10.1016/j.immuni.2021.07.005
Biesbroek, G., Wang, X., Keijser, B. J. F., Eijkemans, R. M. J., Trzciński, K., Rots, N. Y., … Bogaert, D. (2014). Seven-valent pneumococcal conjugate vaccine and nasopharyngeal microbiota in healthy children. *Emerging Infectious Diseases*, *20*(2), 201–210. https://doi.org/10.3201/EID2002.131220
Billy, V., Lhotská, Z., Jirků, M., Kadlecová, O., Frgelecová, L., Parfrey, L. W., & Pomajbíková, K. J. (2021). Blastocystis Colonization Alters the Gut Microbiome and, in Some Cases, Promotes Faster Recovery From Induced Colitis. *Frontiers in Microbiology*, *12*, 646. https://doi.org/10.3389/FMICB.2021.641483/BIBTEX
Biram, A., Liu, J., Hezroni, H., Davidzohn, N., Schmiedel, D., Khatib-Massalha, E., … Shulman, Z. (2022). Bacterial infection disrupts established germinal center reactions through monocyte recruitment and impaired metabolic adaptation. *Immunity*, *55*(3), 442–458.e8. https://doi.org/10.1016/J.IMMUNI.2022.01.013
Bittinger, K., Zhao, C., Li, Y., Ford, E., Friedman, E. S., Ni, J., … Wu, G. D. (2020). Bacterial colonization reprograms the neonatal gut metabolome. *Nature Microbiology 2020 5:6*, *5*(6), 838–847. https://doi.org/10.1038/s41564-020-0694-0
Boge, T., Rémigy, M., Vaudaine, S., Tanguy, J., Bourdet-Sicard, R., & van der Werf, S. (2009a). A probiotic fermented dairy drink improves antibody response to influenza vaccination in the elderly in two randomised controlled trials. *Vaccine*, *27*(41), 5677–5684. https://doi.org/10.1016/J.VACCINE.2009.06.094
Boge, T., Rémigy, M., Vaudaine, S., Tanguy, J., Bourdet-Sicard, R., & van der Werf, S. (2009b). A probiotic fermented dairy drink improves antibody response to influenza vaccination in the elderly in two randomised controlled trials. *Vaccine*, *27*(41), 5677–5684. https://doi.org/10.1016/j.vaccine.2009.06.094
Bolsega, S., Basic, M., Smoczek, A., Buettner, M., Eberl, C., Ahrens, D., … Bleich, A. (2019). Composition of the Intestinal Microbiota Determines the Outcome of Virus-Triggered Colitis in Mice. *Frontiers in Immunology*, *10*(July), 1708. https://doi.org/10.3389/fimmu.2019.01708
Bolyen, E., Rideout, J. R., Dillon, M. R., Bokulich, N. A., Abnet, C. C., Al-Ghalith, G. A., … Caporaso, J. G. (2019). Reproducible, interactive, scalable and extensible microbiome data science using QIIME 2. *Nature Biotechnology*, *37*(8), 852–857. https://doi.org/10.1038/S41587-019-0209-9
Borbet, T. C., Pawline, M. B., Zhang, X., Wipperman, M. F., Reuter, S., Maher, T., … Blaser, M. J. (2022). Influence of the early-life gut microbiota on the immune responses to an inhaled allergen. *Mucosal Immunology*, *15*(5), 1000–1011. https://doi.org/10.1038/S41385-022-00544-5
Borriello, F., Pasquarelli, N., Law, L., Rand, K., Raposo, C., Wei, W., … Derfuss, T. (2022). Normal B-cell ranges in infants: A systematic review and meta-analysis. *Journal of Allergy and Clinical Immunology*, *150*(5), 1216–1224. https://doi.org/10.1016/j.jaci.2022.06.006
Bosch, M., Méndez, M., Pérez, M., Farran, A., Fuentes, M. C., & Cuñé, J. (2012). Lactobacillus plantarum CECT7315 y CECT7316 estimula la producción de inmunoglobulinas tras la vacunación contra la influenza en ancianos. *Nutricion Hospitalaria*, *27*(2), 504–509. https://doi.org/10.3305/nh.2012.27.2.5519

Brugiroux, S., Beutler, M., Pfann, C., Garzetti, D., Ruscheweyh, H. J., Ring, D., … Stecher, B. (2016). Genome-guided design of a defined mouse microbiota that confers colonization resistance against Salmonella enterica serovar Typhimurium. *Nature Microbiology*, *2*(2), 1–12. https://doi.org/10.1038/nmicrobiol.2016.215

Bruhns, P., Iannascoli, B., England, P., Mancardi, D. A., Fernandez, N., Jorieux, S., & Daëron, M. (2009). Specificity and affinity of human Fcgamma receptors and their polymorphic variants for human IgG subclasses. *Blood*, *113*(16), 3716–3725. https://doi.org/10.1182/BLOOD-2008-09-179754

Brynjolfsson, S. F., Henneken, M., Bjarnarson, S. P., Mori, E., Del Giudice, G., & Jonsdottir, I. (2012). Hyporesponsiveness Following Booster Immunization With Bacterial Polysaccharides Is Caused by Apoptosis of Memory B Cells. *The Journal of Infectious Diseases*, *205*(3), 422–430. https://doi.org/10.1093/INFDIS/JIR750

Bunout, D., Barrera, G., Hirsch, S., Gattas, V., De La Maza, M. P., Haschke, F., … Muñoz, C. (2004a). Effects of a nutritional supplement on the immune response and cytokine production in free-living Chilean elderly. *Journal of Parenteral and Enteral Nutrition*, *28*(5), 348–354. https://doi.org/10.1177/0148607104028005348

Bunout, D., Barrera, G., Hirsch, S., Gattas, V., De La Maza, M. P., Haschke, F., … Muñoz, C. (2004b). Effects of a nutritional supplement on the immune response and cytokine production in free-living Chilean elderly. *Journal of Parenteral and Enteral Nutrition*, *28*(5), 348–354. https://doi.org/10.1177/0148607104028005348

Cahenzli, J., Köller, Y., Wyss, M., Geuking, M. B., & McCoy, K. D. (2013). Intestinal microbial diversity during early-life colonization shapes long-term IgE levels. *Cell Host & Microbe*, *14*(5), 559–570. https://doi.org/10.1016/J.CHOM.2013.10.004

Cait, A., Mooney, A., Poyntz, H., Shortt, N., Jones, A., Gestin, A., … Gasser, O. (2021). Potential Association Between Dietary Fibre and Humoral Response to the Seasonal Influenza Vaccine. *Frontiers in Immunology*, *12*. https://doi.org/10.3389/FIMMU.2021.765528

Callahan, B. J., McMurdie, P. J., Rosen, M. J., Han, A. W., Johnson, A. J. A., & Holmes, S. P. (2016). DADA2: High-resolution sample inference from Illumina amplicon data. *Nature Methods 2016 13:7*, *13*(7), 581–583. https://doi.org/10.1038/nmeth.3869

Chapman, T. J., Pham, M., Bajorski, P., & Pichichero, M. E. (2022). Antibiotic Use and Vaccine Antibody Levels. *Pediatrics*, *149*(5). https://doi.org/10.1542/peds.2021-052061

Chauhan, P., Shukla, D., Chattopadhyay, D., & Saha, B. (2017). Redundant and regulatory roles for Toll-like receptors in Leishmania infection. *Clinical and Experimental Immunology*, *190*(2), 167. https://doi.org/10.1111/CEI.13014

Cheung, K. S., Lam, L. K., Zhang, R., Ooi, P. H., Tan, J. T., To, W. P., … Leung, W. K. (2022). Association between Recent Usage of Antibiotics and Immunogenicity within Six Months after COVID-19 Vaccination. *Vaccines*, *10*(7), 1–11. https://doi.org/10.3390/vaccines10071122

Choe, Y. J., Blatt, D. B., Lee, H. J., & Choi, E. H. (2020). Associations between geographic region and immune response variations to pneumococcal conjugate vaccines in clinical trials: A systematic review and meta-analysis. *International Journal of Infectious Diseases*, *92*, 261–268. https://doi.org/10.1016/j.ijid.2019.12.021

Choi, J., Diao, H., Faliti, C. E., Truong, J., Rossi, M., Bélanger, S., … Crotty, S. (2020). Bcl-6 is the nexus transcription factor of T follicular helper cells via repressor-of-repressor circuits. *Nature Immunology 2020 21:7*, *21*(7), 777–789. https://doi.org/10.1038/s41590-020-0706-5

Church, J. A., Rukobo, S., Govha, M., Lee, B., Carmolli, M. P., Chasekwa, B., … Prendergast,

A. J. (2019). The Impact of Improved Water, Sanitation, and Hygiene on Oral Rotavirus Vaccine Immunogenicity in Zimbabwean Infants: Substudy of a Cluster-randomized Trial. *Clinical Infectious Diseases: An Official Publication of the Infectious Diseases Society of America*, *69*(12), 2074. https://doi.org/10.1093/CID/CIZ140

Ciabattini, A., Nardini, C., Santoro, F., Garagnani, P., Franceschi, C., & Medaglini, D. (2018). Vaccination in the elderly: The challenge of immune changes with aging. *Seminars in Immunology*, *40*, 83–94. https://doi.org/10.1016/J.SMIM.2018.10.010

Ciabattini, A., Olivieri, R., Lazzeri, E., & Medaglini, D. (2019). Role of the microbiota in the modulation of vaccine immune responses. *Frontiers in Microbiology*. Frontiers Media S.A. https://doi.org/10.3389/fmicb.2019.01305

Clark, A., van Zandvoort, K., Flasche, S., Sanderson, C., Bines, J., Tate, J., … Jit, M. (2019). Efficacy of live oral rotavirus vaccines by duration of follow-up: a meta-regression of randomised controlled trials. *The Lancet Infectious Diseases*, *19*(7), 717–727. https://doi.org/10.1016/S1473-3099(19)30126-4

Collier, F. M., Tang, M. L. K., Martino, D., Saffery, R., Carlin, J., Jachno, K., … Ponsonby, A.-L. (2015). The ontogeny of naïve and regulatory CD4+ T-cell subsets during the first postnatal year: a cohort study. *Clinical & Translational Immunology*, *4*(3), e34. https://doi.org/10.1038/CTI.2015.2

Collins, A. M. (2016, November 1). IgG subclass co-expression brings harmony to the quartet model of murine IgG function. *Immunology and Cell Biology*. Nature Publishing Group. https://doi.org/10.1038/icb.2016.65

Constantinides, M. G., Link, V. M., Tamoutounour, S., Wong, A. C., Perez-Chaparro, P. J., Han, S. J., … Belkaid, Y. (2019a). MAIT cells are imprinted by the microbiota in early life and promote tissue repair. *Science*, *366*(6464). https://doi.org/10.1126/science.aax6624

Constantinides, M. G., Link, V. M., Tamoutounour, S., Wong, A. C., Perez-Chaparro, P. J., Han, S. J., … Belkaid, Y. (2019b). MAIT cells are imprinted by the microbiota in early life and promote tissue repair. *Science*, *366*(6464). https://doi.org/10.1126/SCIENCE.AAX6624/SUPPL_FILE/AAX6624-CONSTANTINIDES-SM.PDF

Cubillos-Ruiz, A., Alcantar, M. A., Donghia, N. M., Cárdenas, P., Avila-Pacheco, J., & Collins, J. J. (2022). An engineered live biotherapeutic for the prevention of antibiotic-induced dysbiosis. *Nature Biomedical Engineering*, *6*(7), 910–921. https://doi.org/10.1038/s41551-022-00871-9

Cully, M. (2019). Microbiome therapeutics go small molecule. *Nature Reviews. Drug Discovery*, *18*(8), 569–572. https://doi.org/10.1038/D41573-019-00122-8

Darabi, B., Rahmati, S., Hafeziahmadi, M. R., Badfar, G., & Azami, M. (2019). The association between caesarean section and childhood asthma: an updated systematic review and meta-analysis. *Allergy, Asthma, and Clinical Immunology : Official Journal of the Canadian Society of Allergy and Clinical Immunology*, *15*(1), 62. https://doi.org/10.1186/S13223-019-0367-9

Davies, L. R. L., Cizmeci, D., Guo, W., Luedemann, C., Alexander-Parrish, R., Grant, L., … Alter, G. (2022). Polysaccharide and conjugate vaccines to Streptococcus pneumoniae generate distinct humoral responses. *Science Translational Medicine*, *14*(656), eabm4065. https://doi.org/10.1126/SCITRANSLMED.ABM4065/SUPPL_FILE/SCITRANSLMED.ABM4065_MDAR_REPRODUCIBILITY_CHECKLIST.PDF

Dbaibo, G., Amanullah, A., Claeys, C., Izu, A., Jain, V. K., Kosalaraksa, P., … Innis, B. L.

(2020). Quadrivalent Influenza Vaccine Prevents Illness and Reduces Healthcare Utilization Across Diverse Geographic Regions During Five Influenza Seasons: A Randomized Clinical Trial. *The Pediatric Infectious Disease Journal*, *39*(1), e1–e10. https://doi.org/10.1097/INF.0000000000002504

De Haas, M., Kleijer, M., Van Zwieten, R., Roos, D., & Von Dem Borne, A. E. G. K. (1995). Neutrophil FcγRIIIb deficiency, nature, and clinical consequences: A study of 21 individuals from 14 families. *Blood*, *86*(6), 2403–2413. https://doi.org/10.1182/blood.v86.6.2403.bloodjournal8662403

de Koff, E. M., van Baarle, D., van Houten, M. A., Reyman, M., Berbers, G. A. M., van den Ham, F., … Fuentes, S. (2022). Mode of delivery modulates the intestinal microbiota and impacts the response to vaccination. *Nature Communications*, *13*(1), 6638. https://doi.org/10.1038/s41467-022-34155-2

De Silva, N. S., & Klein, U. (2015). Dynamics of B cells in germinal centres. *Nature Reviews Immunology*, *15*(3), 137–148. https://doi.org/10.1038/nri3804

Deenick, E. K., Hasbold, J., & Hodgkin, P. D. (1999). Switching to IgG3, IgG2b, and IgA Is Division Linked and Independent, Revealing a Stochastic Framework for Describing Differentiation. *The Journal of Immunology*, *163*(9), 4707–4714. https://doi.org/10.4049/jimmunol.163.9.4707

Deguine, J., & Barton, G. M. (2014). MyD88: A central player in innate immune signaling. *F1000Prime Reports*, *6*. https://doi.org/10.12703/P6-97

DeSantis, T. Z., Hugenholtz, P., Larsen, N., Rojas, M., Brodie, E. L., Keller, K., … Andersen, G. L. (2006). Greengenes, a chimera-checked 16S rRNA gene database and workbench compatible with ARB. *Applied and Environmental Microbiology*, *72*(7), 5069–5072. https://doi.org/10.1128/AEM.03006-05/ASSET/4D1C009B-60E8-48F2-ADAD-D79A7453DABA/ASSETS/GRAPHIC/ZAM0070668890002.JPEG

Dhiman, N., Ovsyannikova, I. G., Vierkant, R. A., Ryan, J. E., Shane Pankratz, V., Jacobson, R. M., & Poland, G. A. (2008). Associations between SNPs in toll-like receptors and related intracellular signaling molecules and immune responses to measles vaccine: Preliminary results. *Vaccine*, *26*(14), 1731–1736. https://doi.org/10.1016/j.vaccine.2008.01.017

Di Luccia, B., Ahern, P. P., Griffin, N. W., Cheng, J., Guruge, J. L., Byrne, A. E., … Gordon, J. I. (2020). Combined Prebiotic and Microbial Intervention Improves Oral Cholera Vaccination Responses in a Mouse Model of Childhood Undernutrition. *Cell Host and Microbe*, *27*(6), 899–908.e5. https://doi.org/10.1016/j.chom.2020.04.008

di Sant'Agnese, P. A. (1950). Simultaneous immunization of newborn infants against diphtheria, tetanus, and pertussis; production of antibodies and duration of antibody levels in an eastern metropolitan area. *American Journal of Public Health*, *40*(6), 674–680. https://doi.org/10.2105/AJPH.40.6.674

Didierlaurent, A. M., Morel, S., Lockman, L., Giannini, S. L., Bisteau, M., Carlsen, H., … Garçon, N. (2009). AS04, an Aluminum Salt- and TLR4 Agonist-Based Adjuvant System, Induces a Transient Localized Innate Immune Response Leading to Enhanced Adaptive Immunity. *The Journal of Immunology*, *183*(10), 6186–6197. https://doi.org/10.4049/jimmunol.0901474

Ding, Y., Zhou, L., Xia, Y., Wang, W., Wang, Y., Li, L., … Zhao, X. (2018). Reference values for peripheral blood lymphocyte subsets of healthy children in China. *Journal of Allergy and Clinical Immunology*, *142*(3), 970–973.e8. https://doi.org/10.1016/j.jaci.2018.04.022

Dominguez-Bello, M. G., Godoy-Vitorino, F., Knight, R., & Blaser, M. J. (2019). Role of the microbiome in human development. *Gut*, *68*(6), 1108–1114.

https://doi.org/10.1136/gutjnl-2018-317503
Donaldson, G. P., Lee, S. M., & Mazmanian, S. K. (2015). Gut biogeography of the bacterial microbiota. *Nature Reviews Microbiology*. https://doi.org/10.1038/nrmicro3552
Douglas, G. M., Maffei, V. J., Zaneveld, J. R., Yurgel, S. N., Brown, J. R., Taylor, C. M., … Langille, M. G. I. (2020). PICRUSt2 for prediction of metagenome functions. *Nature Biotechnology 2020 38:6*, *38*(6), 685–688. https://doi.org/10.1038/s41587-020-0548-6
Dunais, B., Bruno, P., Touboul, P., Degand, N., Sakarovitch, C., Fontas, E., … Pradier, C. (2015). Impact of the 13-valent pneumococcal conjugate vaccine on nasopharyngeal carriage of Streptococcus pneumoniae among children attending group daycare in Southeastern France. *Pediatric Infectious Disease Journal*, *34*(3), 286–288. https://doi.org/10.1097/INF.0000000000000559
Eberl, C., Ring, D., Münch, P. C., Beutler, M., Basic, M., Slack, E. C., … Stecher, B. (2020). Reproducible Colonization of Germ-Free Mice With the Oligo-Mouse-Microbiota in Different Animal Facilities. *Frontiers in Microbiology*, *10*(January), 1–15. https://doi.org/10.3389/fmicb.2019.02999
Einstein, M. H., Takacs, P., Chatterjee, A., Sperling, R. S., Chakhtoura, N., Blatter, M. M., … Dubin, G. (2014). Comparison of long-term immunogenicity and safety of human papillomavirus (HPV)-16/18 AS04-adjuvanted vaccine and HPV-6/11/16/18 vaccine in healthy women aged 18-45 years: End-of-study analysis of a Phase III randomized trial. *Human Vaccines and Immunotherapeutics*, *10*(12), 3435–3445. https://doi.org/10.4161/hv.36121
Erin Chen, Y., Fischbach, M. A., & Belkaid, Y. (2018). Skin microbiota–host interactions. *Nature 2018 553:7689*, *553*(7689), 427–436. https://doi.org/10.1038/nature25177
Fagarasan, S., Kawamoto, S., Kanagawa, O., & Suzuki, K. (2010). Adaptive immune regulation in the gut: T cell-dependent and T cell-independent IgA synthesis. *Annual Review of Immunology*, *28*, 243–273. https://doi.org/10.1146/ANNUREV-IMMUNOL-030409-101314
Fanciulli, M., Norsworthy, P. J., Petretto, E., Dong, R., Harper, L., Kamesh, L., … Aitman, T. J. (2007). FCGR3B copy number variation is associated with susceptibility to systemic, but not organ-specific, autoimmunity. *Nature Genetics 2007 39:6*, *39*(6), 721–723. https://doi.org/10.1038/ng2046
Fernandes, M. J. G., Rollet-Labelle, E., Paré, G., Marois, S., Tremblay, M. L., Teillaud, J. L., & Naccache, P. H. (2006). CD16b associates with high-density, detergent-resistant membranes in human neutrophils. *Biochemical Journal*, *393*(1), 351–359. https://doi.org/10.1042/BJ20050129
Fiege, J. K., Block, K. E., Pierson, M. J., Nanda, H., Shepherd, F. K., Mickelson, C. K., … Langlois, R. A. (2021). Mice with diverse microbial exposure histories as a model for preclinical vaccine testing. *Cell Host and Microbe*, *29*(12), 1815–1827.e6. https://doi.org/10.1016/j.chom.2021.10.001
Fix, J., Chandrashekhar, K., Perez, J., Bucardo, F., Hudgens, M. G., Yuan, L., … Becker-Dreps, S. (2020). Association between gut microbiome composition and rotavirus vaccine response among Nicaraguan infants. *American Journal of Tropical Medicine and Hygiene*, *102*(1), 213–219. https://doi.org/10.4269/ajtmh.19-0355
Flannery, D. D., Ross, R. K., Mukhopadhyay, S., Tribble, A. C., Puopolo, K. M., & Gerber, J. S. (2018). Temporal Trends and Center Variation in Early Antibiotic Use Among Premature Infants. *JAMA Network Open*, *1*(1), e180164–e180164. https://doi.org/10.1001/JAMANETWORKOPEN.2018.0164

Fluckiger, A., Daillère, R., Sassi, M., Sixt, B. S., Liu, P., Loos, F., … Zitvogel, L. (2020). Cross-reactivity between tumor MHC class I–restricted antigens and an enterococcal bacteriophage. *Science*, *369*(6506), 936–942. https://doi.org/10.1126/SCIENCE.AAX0701/SUPPL_FILE/AAX0701_FLUCKIGER_SM.PDF

Fourati, S., Cristescu, R., Loboda, A., Talla, A., Filali, A., Railkar, R., … Sékaly, R. P. (2016). Pre-vaccination inflammation and B-cell signalling predict age-related hyporesponse to hepatitis B vaccination. *Nature Communications*, *7*, 1–12. https://doi.org/10.1038/ncomms10369

Fra-Bido, S., Walker, S. A., Innocentin, S., & Linterman, M. A. (2021). Optimized immunofluorescence staining protocol for imaging germinal centers in secondary lymphoid tissues of vaccinated mice. *STAR Protocols*, *2*(3). https://doi.org/10.1016/J.XPRO.2021.100499

Fromont, P., Bettaieb, A., Skouri, H., Floch, C., Poulet, E., Duedari, N., & Bierling, P. (1992). Frequency of the polymorphonuclear neutrophil Fc gamma receptor III deficiency in the French population and its involvement in the development of neonatal alloimmune neutropenia. *Blood*, *79*(8), 2131–2134. https://doi.org/10.1182/blood.v79.8.2131.2131

Fukuda, S., Toh, H., Hase, K., Oshima, K., Nakanishi, Y., Yoshimura, K., … Ohno, H. (2011). Bifidobacteria can protect from enteropathogenic infection through production of acetate. *Nature*, *469*(7331), 543–549. https://doi.org/10.1038/NATURE09646

Gao, Y., O'Hely, M., Quinn, T. P., Ponsonby, A. L., Harrison, L. C., Frøkiær, H., … Vuillermin, P. (2022). Maternal gut microbiota during pregnancy and the composition of immune cells in infancy. *Frontiers in Immunology*, *13*(September), 1–11. https://doi.org/10.3389/fimmu.2022.986340

Garrett, W. S. (2019). Immune recognition of microbial metabolites. *Nature Reviews Immunology 2019 20:2*, *20*(2), 91–92. https://doi.org/10.1038/s41577-019-0252-2

Georg, P., & Sander, L. E. (2019). Innate sensors that regulate vaccine responses. *Current Opinion in Immunology*, *59*, 31–41. https://doi.org/10.1016/J.COI.2019.02.006

Gerard, A. L., Goulenok, T., Bahuaud, M., Francois, C., Aucouturier, P., Moins-Teisserenc, H., … Sacre, K. (2020). Serum IgG2 levels predict long-term protection following pneumococcal vaccination in systemic lupus erythematosus (SLE). *Vaccine*, *38*(44), 6859–6863. https://doi.org/10.1016/j.vaccine.2020.08.065

Geva-Zatorsky, N., Sefik, E., Kua, L., Pasman, L., Tan, T. G., Ortiz-Lopez, A., … Kasper, D. L. (2017). Mining the Human Gut Microbiota for Immunomodulatory Organisms. *Cell*, *168*(5), 928–943.e11. https://doi.org/10.1016/j.cell.2017.01.022

Gilmartin, A. A., & Petri, W. A. (2015). Exploring the role of environmental enteropathy in malnutrition, infant development and oral vaccine response. *Philosophical Transactions of the Royal Society B: Biological Sciences*, *370*(1671). https://doi.org/10.1098/RSTB.2014.0143

Glasziou, P., Dartnell, J., Biezen, R., Morgan, M., & Manski-Nankervis, J. A. (2022). Antibiotic stewardship: A review of successful, evidence-based primary care strategies. *Australian Journal of General Practice*, *51*(1–2), 15–20. https://doi.org/10.31128/AJGP-07-21-6088

Golay, J., Valgardsdottir, R., Musaraj, G., Giupponi, D., Spinelli, O., & Introna, M. (2019). Human neutrophils express low levels of FcγRIIIA, which plays a role in PMN activation. *Blood*, *133*(13), 1395–1405. https://doi.org/10.1182/BLOOD-2018-07-864538

González-Fernández, Á., Faro, J., & Fernández, C. (2008). Immune responses to polysaccharides: Lessons from humans and mice. *Vaccine*, *26*(3), 292–300. https://doi.org/10.1016/J.VACCINE.2007.11.042

Graf, S. W., Lester, S., Nossent, J. C., Hill, C. L., Proudman, S. M., Lee, A., & Rischmueller, M. (2012). Low copy number of the FCGR3B gene and rheumatoid arthritis: A case-control study and meta-analysis. *Arthritis Research and Therapy*, *14*(1), 1–7. https://doi.org/10.1186/AR3731/FIGURES/2

Graham, F. (2023). Daily briefing: mRNA vaccine for RSV shows promise. *Nature*. https://doi.org/10.1038/D41586-023-00126-W

Grandi, F. C., Modi, H., Kampman, L., & Corces, M. R. (2022). Chromatin accessibility profiling by ATAC-seq. *Nature Protocols 2022 17:6*, *17*(6), 1518–1552. https://doi.org/10.1038/S41596-022-00692-9

Grant, L. R., Hammitt, L. L., O'Brien, S. E., Jacobs, M. R., Donaldson, C., Weatherholtz, R. C., … O'Brien, K. L. (2016). Impact of the 13-valent pneumococcal conjugate vaccine on pneumococcal carriage among American Indians. *Pediatric Infectious Disease Journal*, *35*(8), 907–914. https://doi.org/10.1097/INF.0000000000001207

Grassly, N. C., Kang, G., & Kampmann, B. (2015). Biological challenges to effective vaccines in the developing world. *Philosophical Transactions of the Royal Society B: Biological Sciences*, *370*(1671). https://doi.org/10.1098/rstb.2014.0138

Grassly, N. C., Praharaj, I., Babji, S., Kaliappan, S. P., Giri, S., Venugopal, S., … Kang, G. (2016a). The effect of azithromycin on the immunogenicity of oral poliovirus vaccine: a double-blind randomised placebo-controlled trial in seronegative Indian infants. *The Lancet Infectious Diseases*, *16*(8), 905–914. https://doi.org/10.1016/S1473-3099(16)30023-8

Grassly, N. C., Praharaj, I., Babji, S., Kaliappan, S. P., Giri, S., Venugopal, S., … Kang, G. (2016b). The effect of azithromycin on the immunogenicity of oral poliovirus vaccine: a double-blind randomised placebo-controlled trial in seronegative Indian infants. *The Lancet Infectious Diseases*, *16*(8), 905–914. https://doi.org/10.1016/S1473-3099(16)30023-8

Gronlund, M. M., Arvilommi, H., Kero, P., Lehtonen, O. P., & Isolauri, E. (2000). Importance of intestinal colonisation in the maturation of humoral immunity in early infancy: A prospective follow up study of healthy infants aged 0-6 months. *Archives of Disease in Childhood: Fetal and Neonatal Edition*, *83*(3). https://doi.org/10.1136/fn.83.3.f186

Guay, H. M., Andreyeva, T. A., Garcea, R. L., Welsh, R. M., & Szomolanyi-Tsuda, E. (2007). MyD88 is required for the formation of long-term humoral immunity to virus infection. *Journal of Immunology (Baltimore, Md. : 1950)*, *178*(8), 5124–5131. https://doi.org/10.4049/JIMMUNOL.178.8.5124

Guerrant, R. L., Oriá, R. B., Moore, S. R., Oriá, M. O. B., & Lima, A. A. A. M. (2008, September). Malnutrition as an enteric infectious disease with long-term effects on child development. *Nutrition Reviews*. https://doi.org/10.1111/j.1753-4887.2008.00082.x

Guilliams Hervé Luche, M., Ardouin, L., Grégoire, C., Christelle Langlet, B., Tamoutounour, S., & Henri, S. (2012). Role during Intramuscular Immunization Dendritic Cells and Reveals Their Distinct Monocyte-Derived and Conventional CD64 Expression Distinguishes. *J Immunol*, *188*, 1751–1760. https://doi.org/10.4049/jimmunol.1102744

Ha, S. A., Tsuji, M., Suzuki, K., Meek, B., Yasuda, N., Kaisho, T., & Fagarasan, S. (2006). Regulation of B1 cell migration by signals through Toll-like receptors. *The Journal*

of Experimental Medicine, *203*(11), 2541. https://doi.org/10.1084/JEM.20061041
Haas, K. M., Poe, J. C., Steeber, D. A., & Tedder, T. F. (2005). B-1a and B-1b cells exhibit distinct developmental requirements and have unique functional roles in innate and adaptive immunity to S. pneumoniae. *Immunity*, *23*(1), 7–18. https://doi.org/10.1016/j.immuni.2005.04.011
Hagan, T., Cortese, M., Rouphael, N., Boudreau, C., Linde, C., Maddur, M. S., … Pulendran, B. (2019). Antibiotics-Driven Gut Microbiome Perturbation Alters Immunity to Vaccines in Humans. *Cell*, *178*(6), 1313–1328.e13. https://doi.org/10.1016/j.cell.2019.08.010
Hajj Hussein, I., Chams, N., Chams, S., El Sayegh, S., Badran, R., Raad, M., … Jurjus, A. (2015). Vaccines Through Centuries: Major Cornerstones of Global Health. *Frontiers in Public Health*, *3*. https://doi.org/10.3389/fpubh.2015.00269
Hallander, H. O., Paniagua, M., Espinoza, F., Askelöf, P., Corrales, E., Ringman, M., & Storsaeter, J. (2002). Calibrated serological techniques demonstrate significant different serum response rates to an oral killed cholera vaccine between Swedish and Nicaraguan children. *Vaccine*, *21*(1–2), 138–145. https://doi.org/10.1016/S0264-410X(02)00348-1
Halsey, N., & Galazka, A. (1985). The efficacy of DPT and oral poliomyelitis immunization schedules initiated from birth to 12 weeks of age. *Bulletin of the World Health Organization*.
Hammitt, L. L., Akech, D. O., Morpeth, S. C., Karani, A., Kihuha, N., Nyongesa, S., … Scott, J. A. G. (2014a). Population effect of 10-valent pneumococcal conjugate vaccine on nasopharyngeal carriage of Streptococcus pneumoniae and non-typeable Haemophilus influenzae in Kilifi, Kenya: findings from cross-sectional carriage studies. *The Lancet Global Health*, *2*(7), e397–e405. https://doi.org/10.1016/S2214-109X(14)70224-4
Hammitt, L. L., Akech, D. O., Morpeth, S. C., Karani, A., Kihuha, N., Nyongesa, S., … Scott, J. A. G. (2014b). Population effect of 10-valent pneumococcal conjugate vaccine on nasopharyngeal carriage of Streptococcus pneumoniae and non-typeable Haemophilus influenzae in Kilifi, Kenya: Findings from cross-sectional carriage studies. *The Lancet Global Health*, *2*(7), e397–e405. https://doi.org/10.1016/S2214-109X(14)70224-4
Han, M., Huang, Y., Gui, H., Xiao, Y., He, M., Liu, J., … Huang, S. (2022). Dynamic changes in host immune system and gut microbiota are associated with the production of SARS-CoV-2 antibodies. *Gut*, gutjnl-2022-327561. https://doi.org/10.1136/gutjnl-2022-327561
Hansen, C. H. F., Nielsen, D. S., Kverka, M., Zakostelska, Z., Klimesova, K., Hudcovic, T., … Hansen, A. K. (2012). Patterns of early gut colonization shape future immune responses of the host. *PloS One*, *7*(3). https://doi.org/10.1371/JOURNAL.PONE.0034043
Harris, V., Ali, A., Fuentes, S., Korpela, K., Kazi, M., Tate, J., … de Vos, W. M. (2018). Rotavirus vaccine response correlates with the infant gut microbiota composition in Pakistan. *Gut Microbes*, *9*(2), 93–101. https://doi.org/10.1080/19490976.2017.1376162
Harris, V. C. (2018). The Significance of the Intestinal Microbiome for Vaccinology: From Correlations to Therapeutic Applications. *Drugs*, *78*(11), 1063–1072. https://doi.org/10.1007/s40265-018-0941-3
Harris, V. C., Armah, G., Fuentes, S., Korpela, K. E., Parashar, U., Victor, J. C., … de Vos, W. M. (2016). The infant gut microbiome correlates significantly with rotavirus

vaccine response in rural Ghana. *The Journal of Infectious Diseases*.
Harris, V. C., Armah, G., Fuentes, S., Korpela, K. E., Parashar, U., Victor, J. C., … de Vos, W. M. (2017). Significant Correlation Between the Infant Gut Microbiome and Rotavirus Vaccine Response in Rural Ghana. *The Journal of Infectious Diseases*, *215*(1), 34–41. https://doi.org/10.1093/infdis/jiw518
Harris, V. C., Haak, B. W., Handley, S. A., Jiang, B., Velasquez, D. E., Hykes, B. L., … Wiersinga, W. J. (2018). Effect of Antibiotic-Mediated Microbiome Modulation on Rotavirus Vaccine Immunogenicity: A Human, Randomized-Control Proof-of-Concept Trial. *Cell Host and Microbe*, *24*(2), 197–207.e4. https://doi.org/10.1016/j.chom.2018.07.005
Healey, G. R., Golding, L., Schick, A., Majdoubi, A., Lavoie, P. M., & Vallance, B. A. (2023). Gut microbiome and dietary fibre intake strongly associate with IgG function and maturation following SARS-CoV-2 mRNA vaccination. *Gut*, gutjnl-2022-328556. https://doi.org/10.1136/GUTJNL-2022-328556
Hegazy, A. N., West, N. R., Stubbington, M. J. T., Wendt, E., Suijker, K. I. M., Datsi, A., … Powrie, F. (2017). Circulating and Tissue-Resident CD4+ T Cells With Reactivity to Intestinal Microbiota Are Abundant in Healthy Individuals and Function Is Altered During Inflammation. *Gastroenterology*, *153*(5), 1320–1337.e16. https://doi.org/10.1053/j.gastro.2017.07.047
Heinsbroek, E., Tafatatha, T., Phiri, A., Swarthout, T. D., Alaerts, M., Crampin, A. C., … French, N. (2018). Pneumococcal carriage in households in Karonga District, Malawi, before and after introduction of 13-valent pneumococcal conjugate vaccination. *Vaccine*, *36*(48), 7369–7376. https://doi.org/10.1016/j.vaccine.2018.10.021
Henrick, B. M., Chew, S., Casaburi, G., Brown, H. K., Frese, S. A., Zhou, Y., … Smilowitz, J. T. (2019). Colonization by B. infantis EVC001 modulates enteric inflammation in exclusively breastfed infants. *Pediatric Research*, *86*(6), 749–757. https://doi.org/10.1038/S41390-019-0533-2
Henrick, B. M., Rodriguez, L., Lakshmikanth, T., Pou, C., Henckel, E., Arzoomand, A., … Brodin, P. (2021). Bifidobacteria-mediated immune system imprinting early in life. *Cell*, *184*(15), 3884–3898.e11. https://doi.org/10.1016/j.cell.2021.05.030
Herbst, T., Sichelstiel, A., Schär, C., Yadava, K., Bürki, K., Cahenzli, J., … Harris, N. L. (2011). Dysregulation of allergic airway inflammation in the absence of microbial colonization. *American Journal of Respiratory and Critical Care Medicine*, *184*(2), 198–205. https://doi.org/10.1164/RCCM.201010-1574OC
Hill, D. L., Whyte, C. E., Innocentin, S., Le Lee, J., Dooley, J., Wang, J., … Linterman, M. A. (2021). Impaired HA-specific T follicular helper cell and antibody responses to influenza vaccination are linked to inflammation in humans. *ELife*, *10*, 1–30. https://doi.org/10.7554/eLife.70554
Hirota, M., Tamai, M., Yukawa, S., Taira, N., Matthews, M. M., Toma, T., … Ishikawa, H. (2022). Human immune and gut microbial parameters associated with inter-individual variations in COVID-19 mRNA vaccine-induced immunity. *BioRxiv*, 2022.08.08.503075. Retrieved from https://www.biorxiv.org/content/10.1101/2022.08.08.503075v1%0Ahttps://www.biorxiv.org/content/10.1101/2022.08.08.503075v1.abstract
Huda, M. N., Ahmad, S. M., Alam, M. J., Khanam, A., Kalanetra, K. M., Taft, D. H., … Stephensen, C. B. (2019). Bifidobacterium abundance in early infancy and vaccine response at 2 years of age. *Pediatrics*, *143*(2). https://doi.org/10.1542/peds.2018-1489

Huda, M. N., Lewis, Z., Kalanetra, K. M., Rashid, M., Ahmad, S. M., Raqib, R., … Stephensen, C. B. (2014). Stool microbiota and vaccine responses of infants. *Pediatrics*, *134*(2). https://doi.org/10.1542/peds.2013-3937

Humphrey, J. H., Mbuya, M. N. N., Ntozini, R., Moulton, L. H., Stoltzfus, R. J., Tavengwa, N. V., … Makoni, T. (2019). Independent and combined effects of improved water, sanitation, and hygiene, and improved complementary feeding, on child stunting and anaemia in rural Zimbabwe: a cluster-randomised trial. *The Lancet Global Health*, *7*(1), e132–e147. https://doi.org/10.1016/S2214-109X(18)30374-7

Hunter, N., Nadkarni, M. A., Jacques, N. A., Martin, F. E., Jacques, N. A., & Hunter, N. (2015). Determination of bacterial load by real-time PCR using a broad-range (universal) probe and primers set. *Microbiology*, *148*(1), 257–266. https://doi.org/10.1099/00221287-148-1-257

Ignacio, A., Morales, C. I., Câmara, N. O. S., & Almeida, R. R. (2016). Innate Sensing of the Gut Microbiota: Modulation of Inflammatory and Autoimmune Diseases. *Frontiers in Immunology*, *7*(FEB), 1. https://doi.org/10.3389/FIMMU.2016.00054

Ihara, F., Sakurai, D., Horinaka, A., Makita, Y., Fujikawa, A., Sakurai, T., … Okamoto, Y. (2017). CD45RA−Foxp3high regulatory T cells have a negative impact on the clinical outcome of head and neck squamous cell carcinoma. *Cancer Immunology, Immunotherapy*, *66*(10), 1275–1285. https://doi.org/10.1007/s00262-017-2021-z

Ikincioğullari, A., Kendirli, T., Doğu, F., Eğin, Y., & Reisli, I. (2004). Peripheral blood lymphocyte subsets in healthy Turkish children. *Turkish Journal of Pediatrics*, *46*(2), 125–130.

Isolauri, E., Joensuu, J., Suomalainen, H., Luomala, M., & Vesikari, T. (1995). Improved immunogenicity of oral D x RRV reassortant rotavirus vaccine by Lactobacillus casei GG. *Vaccine*, *13*(3), 310–312. https://doi.org/10.1016/0264-410X(95)93319-5

Jameson, S. C., & Masopust, D. (2018). What Is the Predictive Value of Animal Models for Vaccine Efficacy in Humans? *Cold Spring Harbor Perspectives in Biology*, *10*(4), a029132. https://doi.org/10.1101/CSHPERSPECT.A029132

Jefferies, J. M., Macdonald, E., Faust, S. N., & Clarke, S. C. (2011). Human Vaccines 13-valent pneumococcal conjugate vaccine (PCV13). *Landes Bioscience 1012 Human Vaccines*, *7*(10), 10. https://doi.org/10.4161/hv.7.10.16794

Julla, J. B., Ballaire, R., Ejlalmanesh, T., Gautier, J. F., Venteclef, N., & Alzaid, F. (2019). Isolation and analysis of human monocytes and adipose tissue macrophages. In *Methods in Molecular Biology* (Vol. 1951, pp. 33–48). Humana Press Inc. https://doi.org/10.1007/978-1-4939-9130-3_3

Junker, F., Gordon, J., & Qureshi, O. (2020). Fc Gamma Receptors and Their Role in Antigen Uptake, Presentation, and T Cell Activation. *Frontiers in Immunology*, *11*, 1393. https://doi.org/10.3389/FIMMU.2020.01393

Kamat, A. V., & Ezekwesili, R. (2006). Chance Detection of CD16 Deficiency on Polymorphonuclear Neutrophils in Iron Deficiency Anemia. *Blood*, *108*(11), 3839. https://doi.org/10.1182/BLOOD.V108.11.3839.3839

Kandasamy, S., Chattha, K. S., Vlasova, A. N., Rajashekara, G., & Saif, L. J. (2015). Lactobacilli and Bifidobacteria enhance mucosal B cell responses and differentially modulate systemic antibody responses to an oral human rotavirus vaccine in a neonatal gnotobiotic pig disease model. *Gut Microbes*, *5*(5), 639–651. https://doi.org/10.4161/19490976.2014.969972

Kang, S.-M., Yoo, D.-G., Kim, M.-C., Song, J.-M., Park, M.-K., O, E., … Compans, R. W. (2011). MyD88 Plays an Essential Role in Inducing B Cells Capable of Differentiating into

Antibody-Secreting Cells after Vaccination. *Journal of Virology*, *85*(21), 11391. https://doi.org/10.1128/JVI.00080-11
Kasturi, S. P., Skountzou, I., Albrecht, R. A., Koutsonanos, D., Hua, T., Nakaya, H. I., … Pulendran, B. (2011a). Programming the magnitude and persistence of antibody responses with innate immunity. *Nature*, *470*(7335), 543–550. https://doi.org/10.1038/nature09737
Kasturi, S. P., Skountzou, I., Albrecht, R. A., Koutsonanos, D., Hua, T., Nakaya, H. I., … Pulendran, B. (2011b). Programming the magnitude and persistence of antibody responses with innate immunity. *Nature*, *470*(7335), 543–550. https://doi.org/10.1038/NATURE09737
Kehrmann, J., Effenberg, L., Wilk, C., Schoemer, D., Ngo Thi Phuong, N., Adamczyk, A., … Buer, J. (2020). Depletion of Foxp3+ regulatory T cells is accompanied by an increase in the relative abundance of Firmicutes in the murine gut microbiome. *Immunology*, *159*(3), 344–353. https://doi.org/10.1111/imm.13158
Kennedy, E. A., King, K. Y., & Baldridge, M. T. (2018). Mouse microbiota models: Comparing germ-free mice and antibiotics treatment as tools for modifying gut bacteria. *Frontiers in Physiology*, *9*(OCT), 1534. https://doi.org/10.3389/FPHYS.2018.01534/BIBTEX
Khan, A. Q., Chen, Q., Wu, Z. Q., Paton, J. C., & Snapper, C. M. (2005). Both innate immunity and type 1 humoral immunity to Streptococcus pneumoniae are mediated by MyD88 but differ in their relative levels of dependence on toll-like receptor 2. *Infection and Immunity*, *73*(1), 298–307. https://doi.org/10.1128/IAI.73.1.298-307.2005
Kim, D.-J. D. J., Seo, S.-U. U., Inohara, N., Núñez, G., Rosenstiel, P., Kim, D.-J. D. J., … Núñez, G. (2016). Nod2-mediated recognition of the microbiota is critical for mucosal adjuvant activity of cholera toxin. *Nature Medicine*, *22*(5), 524–530. https://doi.org/10.1038/nm.4075
Kim, H., Moon, H. W., Hur, M., Park, C. M., Yun, Y. M., Hwang, H. S., … Sohn, I. S. (2012). Distribution of CD4+CD25highFoxP3+ regulatory T-cells in umbilical cord blood. *Journal of Maternal-Fetal and Neonatal Medicine*, *25*(10), 2058–2061. https://doi.org/10.3109/14767058.2012.666591
Kim, M., Qie, Y., Park, J., & Kim, C. H. (2016). Gut Microbial Metabolites Fuel Host Antibody Responses. *Cell Host and Microbe*, *20*(2), 202–214. https://doi.org/10.1016/j.chom.2016.07.001
Kim, S., Covington, A., & Pamer, E. G. (2017, September 1). The intestinal microbiota: Antibiotics, colonization resistance, and enteric pathogens. *Immunological Reviews*. Blackwell Publishing Ltd. https://doi.org/10.1111/imr.12563
Klein, S. L., & Flanagan, K. L. (2016, October 1). Sex differences in immune responses. *Nature Reviews Immunology*. Nature Publishing Group. https://doi.org/10.1038/nri.2016.90
Korpela, K., & de Vos, W. M. (2018). Early life colonization of the human gut: microbes matter everywhere. *Current Opinion in Microbiology*, *44*, 70–78. https://doi.org/10.1016/j.mib.2018.06.003
Kotler, E., Halpern, Z., Sharon, I., Federici, S., Cohen, Y., Dori-Bachash, M., … Ben-Zeev Brik, R. (2018). Post-Antibiotic Gut Mucosal Microbiome Reconstitution Is Impaired by Probiotics and Improved by Autologous FMT. *Cell*, *174*(6), 1406–1423.e16. https://doi.org/10.1016/j.cell.2018.08.047
Koyama, M., Mukhopadhyay, P., Schuster, I. S., Henden, A. S., Hülsdünker, J., Varelias, A., … Hill, G. R. (2019). MHC Class II Antigen Presentation by the Intestinal Epithelium

Initiates Graft-versus-Host Disease and Is Influenced by the Microbiota. *Immunity*, *51*(5), 885–898.e7. https://doi.org/10.1016/j.immuni.2019.08.011
Kuhn, K. A., Schulz, H. M., Regner, E. H., Severs, E. L., Hendrickson, J. D., Mehta, G., … Colgan, S. P. (2018). Bacteroidales recruit IL-6-producing intraepithelial lymphocytes in the colon to promote barrier integrity. *Mucosal Immunology*, *11*(2), 357–368. https://doi.org/10.1038/mi.2017.55
Kukkonen, K., Nieminen, T., Poussa, T., Savilahti, E., & Kuitunen, M. (2006). Effect of probiotics on vaccine antibody responses in infancy - A randomized placebo-controlled double-blind trial. *Pediatric Allergy and Immunology*, *17*(6), 416–421. https://doi.org/10.1111/j.1399-3038.2006.00420.x
Kuppala, V. S., Meinzen-Derr, J., Morrow, A. L., & Schibler, K. R. (2011). Prolonged initial empirical antibiotic treatment is associated with adverse outcomes in premature infants. *Journal of Pediatrics*, *159*(5), 720–725. https://doi.org/10.1016/j.jpeds.2011.05.033
Lai, G. C., Tan, T. G., & Pavelka, N. (2018). The mammalian mycobiome: A complex system in a dynamic relationship with the host. *Wiley Interdisciplinary Reviews: Systems Biology and Medicine*. https://doi.org/10.1002/wsbm.1438
Lalor, M. K., Ben-Smith, A., Gorak-Stolinska, P., Weir, R. E., Floyd, S., Blitz, R., … Dockrell, H. M. (2009). Population Differences in Immune Responses to Bacille Calmette-Guérin Vaccination in Infancy. *The Journal of Infectious Diseases*, *199*(6), 795–800. https://doi.org/10.1086/597069
Lazarus, R. P., John, J., Shanmugasundaram, E., Rajan, A. K., Thiagarajan, S., Giri, S., … Kang, G. (2018). The effect of probiotics and zinc supplementation on the immune response to oral rotavirus vaccine: A randomized, factorial design, placebo-controlled study among Indian infants. *Vaccine*, *36*(2), 273–279. https://doi.org/10.1016/j.vaccine.2017.07.116
Lederer, K., Castaño, D., Gómez Atria, D., Oguin, T. H., Wang, S., Manzoni, T. B., … Locci, M. (2020). SARS-CoV-2 mRNA Vaccines Foster Potent Antigen-Specific Germinal Center Responses Associated with Neutralizing Antibody Generation. *Immunity*, *53*(6), 1281–1295.e5. https://doi.org/10.1016/j.immuni.2020.11.009
Lee, B.-W., Yap, H.-K., Chew, F.-T., Quah, T.-C., Prabhakaran, K., Chan, G. S. H., … Seah, C.-C. (1996). Age- and sex-related changes in lymphocyte subpopulations of healthy Asian subjects: From birth to adulthood. *Cytometry*, *26*(1), 8–15. https://doi.org/10.1002/(SICI)1097-0320(19960315)26:1<8::AID-CYTO2>3.0.CO;2-E
Lee, J. Le, & Linterman, M. A. (2022). Mechanisms underpinning poor antibody responses to vaccines in ageing. *Immunology Letters*, *241*, 1. https://doi.org/10.1016/J.IMLET.2021.11.001
Legoux, F., Bellet, D., Daviaud, C., El Morr, Y., Darbois, A., Niort, K., … Lantz, O. (2019). Microbial metabolites control the thymic development of mucosal-associated invariant T cells. *Science*, *366*(6464), 494–499. https://doi.org/10.1126/science.aaw2719
Levine, M. M., Kotloff, K. L., Barry, E. M., Pasetti, M. F., & Sztein, M. B. (2007). Clinical trials of Shigella vaccines: two steps forward and one step back on a long, hard road. *Nature Reviews Microbiology 2007 5:7*, *5*(7), 540–553. https://doi.org/10.1038/nrmicro1662
Levitz, S. M., & Golenbock, D. T. (2012, March 16). Beyond empiricism: Informing vaccine development through innate immunity research. *Cell*. https://doi.org/10.1016/j.cell.2012.02.012

Li, H., Limenitakis, J. P., Greiff, V., Yilmaz, B., Schären, O., Urbaniak, C., … Macpherson, A. J. (2020). Mucosal or systemic microbiota exposures shape the B cell repertoire. *Nature*, *584*(7820), 274–278. https://doi.org/10.1038/s41586-020-2564-6

Lilienthal, G. M., Rahmöller, J., Petry, J., Bartsch, Y. C., Leliavski, A., & Ehlers, M. (2018). Potential of murine IgG1 and Human IgG4 to inhibit the classical complement and Fcγ receptor activation pathways. *Frontiers in Immunology*, *9*(MAY), 1. https://doi.org/10.3389/FIMMU.2018.00958/FULL

Lin, A., Bik, E. M., Costello, E. K., Dethlefsen, L., Haque, R., Relman, D. A., & Singh, U. (2013). Distinct Distal Gut Microbiome Diversity and Composition in Healthy Children from Bangladesh and the United States. *PLoS ONE*, *8*(1). https://doi.org/10.1371/journal.pone.0053838

Lin, T. L., Fan, Y. H., Chang, Y. L., Ho, H. J., Liang, L. L., Chen, Y. J., & Wu, C. Y. (2022). Early-Life Antibiotic Exposure Associated With Varicella Occurrence and Breakthrough Infections: Evidence From Nationwide Pre-Vaccination and Post-Vaccination Cohorts. *Frontiers in Immunology*, *13*. https://doi.org/10.3389/FIMMU.2022.848835

Lisse, I. M., Aaby, P., Whittle, H., Jensen, H., Engelmann, M., & Christensen, L. B. (1997). T-lymphocyte subsets in West African children: Impact of age, sex, and season. *Journal of Pediatrics*, *130*(1), 77–85. https://doi.org/10.1016/S0022-3476(97)70313-5

Liu, X., Zhao, Y., & Qi, H. (2022). T-independent antigen induces humoral memory through germinal centers. *Journal of Experimental Medicine*, *219*(3). https://doi.org/10.1084/jem.20210527

Lu, L. Y., Chu, J. J., Lu, P. J., Sung, P. K., Hsu, C. M., & Tseng, J. C. (2008). Expression of intracellular transforming growth factor-betal in CD4 +CD25+ cells in patients with systemic lupus erythematosus. *Journal of Microbiology, Immunology and Infection*, *41*(2), 165–173. Retrieved from https://europepmc.org/article/med/18473105

Lundell, A.-C., Björnsson, V., Ljung, A., Ceder, M., Johansen, S., Lindhagen, G., … Rudin, A. (2012). Infant B Cell Memory Differentiation and Early Gut Bacterial Colonization. *The Journal of Immunology*, *188*(9), 4315–4322. https://doi.org/10.4049/jimmunol.1103223

Luther, S. A., & Cyster, J. G. (2001). Chemokines as regulators of T cell differentiation. *Nature Immunology*, *2*(2), 102–107. https://doi.org/10.1038/84205

Lynch, S. V., & Pedersen, O. (2016). The Human Intestinal Microbiome in Health and Disease. *New England Journal of Medicine*, *375*(24), 2369–2379. https://doi.org/10.1056/NEJMRA1600266/SUPPL_FILE/NEJMRA1600266_DISCLOSURES.PDF

Lynn, D. J., Benson, S. C., Lynn, M. A., & Pulendran, B. (2021). Modulation of immune responses to vaccination by the microbiota: implications and potential mechanisms. *Nature Reviews Immunology 2021*, 1–14. https://doi.org/10.1038/s41577-021-00554-7

Lynn, D. J., & Pulendran, B. (2017). The potential of the microbiota to influence vaccine responses. *Journal of Leukocyte Biology*, jlb.5MR0617-216R. https://doi.org/10.1189/jlb.5mr0617-216r

Lynn, M. A., Eden, G., Ryan, F. J., Bensalem, J., Wang, X., Blake, S. J., … Lynn, D. J. (2021). The composition of the gut microbiota following early-life antibiotic exposure affects host health and longevity in later life. *Cell Reports*, *36*(8), 109564. https://doi.org/10.1016/j.celrep.2021.109564

Lynn, M. A., Tumes, D. J., Choo, J. M., Sribnaia, A., Blake, S. J., Leong, L. E. X., … Lynn, D. J.

(2018). Early-Life Antibiotic-Driven Dysbiosis Leads to Dysregulated Vaccine Immune Responses in Mice. *Cell Host and Microbe*, *23*(5), 653–660.e5. https://doi.org/10.1016/j.chom.2018.04.009

Mackenzie, G. A., Osei, I., Salaudeen, R., Hossain, I., Young, B., Secka, O., … Greenwood, B. (2022). A cluster-randomised, non-inferiority trial of the impact of a two-dose compared to three-dose schedule of pneumococcal conjugate vaccination in rural Gambia: the PVS trial. *Trials*, *23*(1). https://doi.org/10.1186/s13063-021-05964-5

Madhi, S. A., Cunliffe, N. A., Steele, D., Witte, D., Kirsten, M., Louw, C., … Neuzil, K. M. (2010). Effect of Human Rotavirus Vaccine on Severe Diarrhea in African Infants. *New England Journal of Medicine*, *362*(4), 289–298. https://doi.org/10.1056/NEJMoa0904797

Martin, F., Oliver, A. M., & Kearney, J. F. (2001). Marginal zone and B1 B cells unite in the early response against T-independent blood-borne particulate antigens. *Immunity*, *14*(5), 617–629. https://doi.org/10.1016/S1074-7613(01)00129-7

Maruya, M., Suzuki, K., Fujimoto, H., Miyajima, M., Kanagawa, O., Wakayama, T., & Fagarasan, S. (2011). Vitamin A-dependent transcriptional activation of the nuclear factor of activated T cells c1 (NFATc1) is critical for the development and survival of B1 cells. *Proceedings of the National Academy of Sciences of the United States of America*, *108*(2), 722–727. https://doi.org/10.1073/PNAS.1014697108/-/DCSUPPLEMENTAL

Maruyama, M., Abe, R., Shimono, T., Iwabuchi, N., Abe, F., & Xiao, J. Z. (2015). The effects of non-viable Lactobacillus on immune function in the elderly: a randomised, double-blind, placebo-controlled study. *Http://Dx.Doi.Org/10.3109/09637486.2015.1126564*, *67*(1), 67–73. https://doi.org/10.3109/09637486.2015.1126564

Maruyama, M., Abe, R., Shimono, T., Iwabuchi, N., Abe, F., & Xiao, J. Z. (2016). The effects of non-viable Lactobacillus on immune function in the elderly: A randomised, double-blind, placebo-controlled study. *International Journal of Food Sciences and Nutrition*, *67*(1), 67–73. https://doi.org/10.3109/09637486.2015.1126564

Matsuda, F., Chowdhury, M. I., Saha, A., Asahara, T., Nomoto, K., Tarique, A. A., … Qadri, F. (2011). Evaluation of a probiotics, Bifidobacterium breve BBG-01, for enhancement of immunogenicity of an oral inactivated cholera vaccine and safety: A randomized, double-blind, placebo-controlled trial in Bangladeshi children under 5 years of age. *Vaccine*, *29*(10), 1855–1858. https://doi.org/10.1016/j.vaccine.2010.12.133

McDermott, A. J., Huffnagle, G. B., Anderson, R. M., May, R. M., Mcdermott, A. J., & Huffnagle, G. B. (2014). The microbiome and regulation of mucosal immunity. *Immunology*, *142*(1), 24–31. https://doi.org/10.1111/imm.12231

McMurdie, P. J., & Holmes, S. (2013). phyloseq: An R Package for Reproducible Interactive Analysis and Graphics of Microbiome Census Data. *PLOS ONE*, *8*(4), e61217. https://doi.org/10.1371/JOURNAL.PONE.0061217

McQuade, E. T. R., Platts-Mills, J. A., Gratz, J., Zhang, J., Moulton, L. H., Mutasa, K., … Houpt, E. R. (2020). Impact of Water Quality, Sanitation, Handwashing, and Nutritional Interventions on Enteric Infections in Rural Zimbabwe: The Sanitation Hygiene Infant Nutrition Efficacy (SHINE) Trial. *The Journal of Infectious Diseases*, *221*(8), 1379–1386. https://doi.org/10.1093/INFDIS/JIZ179

Mendonça, S. A., Lorincz, R., Boucher, P., & Curiel, D. T. (2021). Adenoviral vector vaccine platforms in the SARS-CoV-2 pandemic. *Npj Vaccines 2021 6:1*, *6*(1), 1–14. https://doi.org/10.1038/s41541-021-00356-x

Mesin, L., Ersching, J., & Victora, G. D. (2016). Germinal Center B Cell Dynamics.

Immunity, *45*(3), 471–482. https://doi.org/10.1016/J.IMMUNI.2016.09.001
Meza-Perez, S., & Randall, T. D. (2017). Immunological Functions of the Omentum. *Trends in Immunology*, *38*(7), 526–536. https://doi.org/10.1016/J.IT.2017.03.002
Michael, H., Paim, F. C., Miyazaki, A., Langel, S. N., Fischer, D. D., Chepngeno, J., … Vlasova, A. N. (2021). Escherichia coli Nissle 1917 administered as a dextranomar microsphere biofilm enhances immune responses against human rotavirus in a neonatal malnourished pig model colonized with human infant fecal microbiota. *PLOS ONE*, *16*(2), e0246193. https://doi.org/10.1371/JOURNAL.PONE.0246193
Miller, J. E., Wu, C., Pedersen, L. H., De Klerk, N., Olsen, J., & Burgner, D. P. (2018). Maternal antibiotic exposure during pregnancy and hospitalization with infection in offspring: A population-based cohort study. *International Journal of Epidemiology*, *47*(2), 561–571. https://doi.org/10.1093/ije/dyx272
Minguela, A., Salido, E. J., Soto-Ramírez, M. F., Olga, M. A., Leal, J. D., García-Garay, M. C., … Campillo, J. A. (2021). Low-affinity immunoglobulin gamma Fc region receptor III-B (FcγRIIIB, CD16B) deficiency in patients with blood and immune system disorders. *British Journal of Haematology*, *195*(5), 743–747. https://doi.org/10.1111/BJH.17828
Mohr, E., & Siegrist, C. A. (2016, August 1). Vaccination in early life: Standing up to the challenges. *Current Opinion in Immunology*. Elsevier Ltd. https://doi.org/10.1016/j.coi.2016.04.004
Mond, J. J., Lees, A., & Snapper, C. M. (1995). T cell-independent antigens type 2. *Annual Review of Immunology*, *13*, 655–692. https://doi.org/10.1146/ANNUREV.IY.13.040195.003255
Moon, H., Lee, J. G., Shin, S. H., & Kim, T. J. (2012). LPS-Induced Migration of Peritoneal B-1 Cells is Associated with Upregulation of CXCR4 and Increased Migratory Sensitivity to CXCL12. *Journal of Korean Medical Science*, *27*(1), 27. https://doi.org/10.3346/JKMS.2012.27.1.27
Moore, C. E., Hennig, B. J., Perrett, K. P., Hoe, J. C., Lee, S. J., Fletcher, H., … Pollarda, A. J. (2012). Single nucleotide polymorphisms in the toll-like receptor 3 and CD44 genes are associated with persistence of vaccine-induced immunity to the serogroup C meningococcal conjugate vaccine. *Clinical and Vaccine Immunology*, *19*(3), 295–303. https://doi.org/10.1128/CVI.05379-11
Morbach, H., Eichhorn, E. M., Liese, J. G., & Girschick, H. J. (2010). Reference values for B cell subpopulations from infancy to adulthood. *Clinical and Experimental Immunology*, *162*(2), 271. https://doi.org/10.1111/J.1365-2249.2010.04206.X
Moroishi, Y., Gui, J., Nadeau, K. C., Morrison, H. G., Madan, J., & Karagas, M. R. (2022). A prospective study of the infant gut microbiome in relation to vaccine response. *Pediatric Research*, (May), 1–7. https://doi.org/10.1038/s41390-022-02154-0
Mu, Q., Kirby, J., Reilly, C. M., & Luo, X. M. (2017). Leaky gut as a danger signal for autoimmune diseases. *Frontiers in Immunology*, *8*(MAY), 598. https://doi.org/10.3389/FIMMU.2017.00598/BIBTEX
Mullié, C., Yazourh, A., Thibault, H., Odou, M. F., Singer, E., Kalach, N., … Romond, M. B. (2004). Increased poliovirus-specific intestinal antibody response coincides with promotion of Bifidobacterium longum-infantis and Bifidobacterium breve in infants: A randomized, double-blind, placebo-controlled trial. *Pediatric Research*, *56*(5), 791–795. https://doi.org/10.1203/01.PDR.0000141955.47550.A0
Muniz-Diaz, E., Madoz, P., Martin, O. D. L. C., & Puig, L. (1995). The Polymorphonuclear Neutrophil FcγRlllb Deficiency Is More Frequent Than Hitherto Assumed. *Blood*, *86*(10), 3999.

https://doi.org/10.1182/BLOOD.V86.10.3999.BLOODJOURNAL86103999
Murphy, K. M., & Reiner, S. L. (2002). The lineage decisions of helper T cells. *Nature Reviews. Immunology*, *2*(12), 933–944. https://doi.org/10.1038/NRI954
Muyanja, E., Ssemaganda, A., Ngauv, P., Cubas, R., Perrin, H., Srinivasan, D., … Trautmann, L. (2014). Immune activation alters cellular and humoral responses to yellow fever 17D vaccine. *The Journal of Clinical Investigation*, *124*(7), 3147–3158. https://doi.org/10.1172/JCI75429
Nadeem, S., Maurya, S. K., Das, D. K., Khan, N., & Agrewala, J. N. (2020). Gut Dysbiosis Thwarts the Efficacy of Vaccine Against Mycobacterium tuberculosis. *Frontiers in Immunology*, *11*(May), 1–12. https://doi.org/10.3389/fimmu.2020.00726
Nair, A. B., & Jacob, S. (2016). A simple practice guide for dose conversion between animals and human. *Journal of Basic and Clinical Pharmacy*, *7*(2), 27. https://doi.org/10.4103/0976-0105.177703
Nair, N., Gans, H., Lew-Yasukawa, L., Long-Wagar, A. C. C., Arvin, A., & Griffin, D. E. E. (2007). Age-Dependent Differences in IgG Isotype and Avidity Induced by Measles Vaccine Received during the First Year of Life. *The Journal of Infectious Diseases*, *196*(9), 1339–1345. https://doi.org/10.1086/522519
Nakao, R., Kobayashi, H., Iwabuchi, Y., Kawahara, K., Hirayama, S., Ramstedt, M., … Ohnishi, M. (2022). A highly immunogenic vaccine platform against encapsulated pathogens using chimeric probiotic Escherichia coli membrane vesicles. *Npj Vaccines 2022 7:1*, *7*(1), 1–17. https://doi.org/10.1038/s41541-022-00572-z
Nakaya, H. I., Hagan, T., Duraisingham, S. S., Lee, E. K., Kwissa, M., Rouphael, N., … Pulendran, B. (2015). Systems Analysis of Immunity to Influenza Vaccination across Multiple Years and in Diverse Populations Reveals Shared Molecular Signatures. *Immunity*, *43*(6), 1186–1198. https://doi.org/10.1016/j.immuni.2015.11.012
Nakaya, H. I., Wrammert, J., Lee, E. K., Racioppi, L., Marie-Kunze, S., Haining, W. N., … Pulendran, B. (2011). Systems biology of vaccination for seasonal influenza in humans. *Nature Immunology 2011 12:8*, *12*(8), 786–795. https://doi.org/10.1038/ni.2067
National Immunisation Program Schedule | Australian Government Department of Health and Aged Care. (n.d.). Retrieved January 20, 2023, from https://www.health.gov.au/topics/immunisation/when-to-get-vaccinated/national-immunisation-program-schedule?language=und
Negi, S., Das, D. K., Pahari, S., Nadeem, S., & Agrewala, J. N. (2019). Potential role of gut microbiota in induction and regulation of innate immune memory. *Frontiers in Immunology*, *10*(OCT), 2441. https://doi.org/10.3389/FIMMU.2019.02441/BIBTEX
Neuberger, M. S., & Rajewsky, K. (1981). Activation of mouse complement by monoclonal mouse antibodies. *European Journal of Immunology*, *11*(12), 1012–1016. https://doi.org/10.1002/EJI.1830111212
Neuman, H., Forsythe, P., Uzan, A., Avni, O., & Koren, O. Antibiotics in early life: dysbiosis and the damage done, 42 § (2018). https://doi.org/10.1093/femsre/fuy018
Neves, P., Lampropoulou, V., Calderon-Gomez, E., Roch, T., Stervbo, U., Shen, P., … Fillatreau, S. (2010). Signaling via the MyD88 adaptor protein in B cells suppresses protective immunity during Salmonella typhimurium infection. *Immunity*, *33*(5), 777–790. https://doi.org/10.1016/J.IMMUNI.2010.10.016
New, J. S., Dizon, B. L. P., Fucile, C. F., Rosenberg, A. F., Kearney, J. F., & King, R. G. (2020). Neonatal Exposure to Commensal-Bacteria-Derived Antigens Directs

Polysaccharide-Specific B-1 B Cell Repertoire Development. *Immunity*, *53*(1), 172–186.e6. https://doi.org/10.1016/j.immuni.2020.06.006
New, J. S., Dizon, B. L. P., Fucile, C. F., Rosenberg, A. F., Kearney, J. F., King, R. G., … Kearney, J. F. (2020). Article Neonatal Exposure to Commensal-Bacteria-Derived Antigens Directs Polysaccharide-Specific B-1 B Cell Repertoire Development Article Neonatal Exposure to Commensal-Bacteria-Derived Antigens Directs Polysaccharide-Specific B-1 B Cell Repertoire Devel. *Immunity*, *53*(1), 1–15. https://doi.org/10.1016/j.immuni.2020.06.006
Ng, S. C., Peng, Y., Zhang, L., Mok, C. K., Zhao, S., Li, A., … Tun, H. M. (2022a). Gut microbiota composition is associated with SARS-CoV-2 vaccine immunogenicity and adverse events. *Gut*, *71*(6), 1106–1116. https://doi.org/10.1136/gutjnl-2021-326563
Ng, S. C., Peng, Y., Zhang, L., Mok, C. K., Zhao, S., Li, A., … Tun, H. M. (2022b). Gut microbiota composition is associated with SARS-CoV-2 vaccine immunogenicity and adverse events. *Gut*, (January), gutjnl-2021-326563. https://doi.org/10.1136/gutjnl-2021-326563
Nzenze, S. A., Shiri, T., Nunes, M. C., Klugman, K. P., Kahn, K., Twine, R., … Madhi, S. A. (2013). Temporal changes in pneumococcal colonization in a rural african community with high HIV prevalence following routine infant pneumococcal immunization. *Pediatric Infectious Disease Journal*, *32*(11), 1270–1278. https://doi.org/10.1097/01.inf.0000435805.25366.64
O'Gorman, M. R. G., Millard, D. D., Lowder, J. N., & Yogev, R. (1998). Lymphocyte subpopulations in healthy 1-3-day-old infants. *Communications in Clinical Cytometry*, *34*(5), 235–241. https://doi.org/10.1002/(SICI)1097-0320(19981015)34:5<235::AID-CYTO5>3.0.CO;2-0
Oh, J. Z., Ravindran, R., Chassaing, B., Carvalho, F. A., Maddur, M. S., Bower, M., … Pulendran, B. (2014). TLR5-mediated sensing of gut microbiota is necessary for antibody responses to seasonal influenza vaccination. *Immunity*, *41*(3), 478–492. https://doi.org/10.1016/j.immuni.2014.08.009
Ojima, M. N., Gotoh, A., Takada, H., Odamaki, T., Xiao, J.-Z., Katoh, T., & Katayama, T. (2020). Bifidobacterium bifidum Suppresses Gut Inflammation Caused by Repeated Antibiotic Disturbance Without Recovering Gut Microbiome Diversity in Mice. *Frontiers in Microbiology*, *11*, 1349. https://doi.org/10.3389/fmicb.2020.01349
Okabe, Y., & Medzhitov, R. (2014). Tissue-specific signals control reversible program of localization and functional polarization of macrophages. *Cell*, *157*(4), 832–844. https://doi.org/10.1016/j.cell.2014.04.016
Olin, A., Henckel, E., Chen, Y., Lakshmikanth, T., Pou, C., Mikes, J., … Brodin, P. (2018). Stereotypic Immune System Development in Newborn Children. *Cell*, *174*(5), 1277–1292.e14. https://doi.org/10.1016/j.cell.2018.06.045
Olszak, T., An, D., Zeissig, S., Vera, M. P., Richter, J., Franke, A., … Blumberg, R. S. (2012). Microbial exposure during early life has persistent effects on natural killer T cell function. *Science (New York, N.Y.)*, *336*(6080), 489–493. https://doi.org/10.1126/SCIENCE.1219328
Ong, G. H., Lian, B. S. X., Kawasaki, T., & Kawai, T. (2021, October 6). Exploration of Pattern Recognition Receptor Agonists as Candidate Adjuvants. *Frontiers in Cellular and Infection Microbiology*. Frontiers Media S.A. https://doi.org/10.3389/fcimb.2021.745016
Örtqvist, Å. (2001). Pneumococcal vaccination: current and future issues. *European Respiratory Journal*, *18*(1), 184–195.

https://doi.org/10.1183/09031936.01.00084401
Östman, S., Rask, C., Wold, A. E., Hultkrantz, S., & Telemo, E. (2006). Impaired regulatory T cell function in germ-free mice. *European Journal of Immunology*, *36*(9), 2336–2346. https://doi.org/10.1002/eji.200535244
Ovsyannikova, I. G., Dhiman, N., Haralambieva, I. H., Vierkant, R. A., O'Byrne, M. M., Jacobson, R. M., & Poland, G. A. (2010). Rubella vaccine-induced cellular immunity: Evidence of associations with polymorphisms in the Toll-like, vitamin A and D receptors, and innate immune response genes. *Human Genetics*, *127*(2), 207–221. https://doi.org/10.1007/s00439-009-0763-1
Painter, S. D., Ovsyannikova, I. G., & Poland, G. A. (2015). The weight of obesity on the human immune response to vaccination. *Vaccine*, *33*(36), 4422–4429. https://doi.org/10.1016/J.VACCINE.2015.06.101
Palucka, K., Banchereau, J., & Mellman, I. (2010, October 29). Designing vaccines based on biology of human dendritic cell subsets. *Immunity*. Elsevier. https://doi.org/10.1016/j.immuni.2010.10.007
Parker, B. J., Wearsch, P. A., Veloo, A. C. M., & Rodriguez-Palacios, A. (2020). The Genus Alistipes: Gut Bacteria With Emerging Implications to Inflammation, Cancer, and Mental Health. *Frontiers in Immunology*, *11*, 906. https://doi.org/10.3389/FIMMU.2020.00906/BIBTEX
Parker, E. P. K., Bronowski, C., Sindhu, K. N. C., Babji, S., Benny, B., Carmona-Vicente, N., … Iturriza-Gómara, M. (2021). Impact of maternal antibodies and microbiota development on the immunogenicity of oral rotavirus vaccine in African, Indian, and European infants. *Nature Communications*, *12*(1). https://doi.org/10.1038/s41467-021-27074-1
Parker, E. P. K., Praharaj, I., Zekavati, A., Lazarus, R. P., Giri, S., Operario, D. J., … Grassly, N. C. (2018). Influence of the intestinal microbiota on the immunogenicity of oral rotavirus vaccine given to infants in south India. *Vaccine*, *36*(2), 264–272. https://doi.org/10.1016/j.vaccine.2017.11.031
Pasin, C., Balelli, I., Van Effelterre, T., Bockstal, V., Solforosi, L., Prague, M., … Thiébaut, R. (2019). Dynamics of the Humoral Immune Response to a Prime-Boost Ebola Vaccine: Quantification and Sources of Variation. *Journal of Virology*, *93*(18), 579–598. https://doi.org/10.1128/JVI.00579-19/ASSET/4F992DD0-BF8E-4BF6-8002-AE65B4FF89E4/ASSETS/GRAPHIC/JVI.00579-19-F0011.JPEG
Patel, M., Glass, R. I., Jiang, B., Santosham, M., Lopman, B., & Parashar, U. (2013). A Systematic Review of Anti-Rotavirus Serum IgA Antibody Titer as a Potential Correlate of Rotavirus Vaccine Efficacy. *The Journal of Infectious Diseases*, *208*(2), 284–294. https://doi.org/10.1093/INFDIS/JIT166
Patriarca, P. A., Wright, P. F., & John, T. J. (1991). Factors Affecting the Immunogenicity of Oral Poliovirus Vaccine in Developing Countries: Review. *Reviews of Infectious Diseases*, *13*(5), 926–939. https://doi.org/10.1093/CLINIDS/13.5.926
Perez-Muñoz, M. E., Arrieta, M. C., Ramer-Tait, A. E., & Walter, J. (2017). A critical assessment of the "sterile womb" and "in utero colonization" hypotheses: Implications for research on the pioneer infant microbiome. *Microbiome*. BioMed Central Ltd. https://doi.org/10.1186/s40168-017-0268-4
Polack, F. P., Thomas, S. J., Kitchin, N., Absalon, J., Gurtman, A., Lockhart, S., … Gruber, W. C. (2020). Safety and Efficacy of the BNT162b2 mRNA Covid-19 Vaccine. *New England Journal of Medicine*, *383*(27), 2603–2615. https://doi.org/10.1056/NEJMOA2034577/SUPPL_FILE/NEJMOA2034577_PROTOCOL.PDF

Praharaj, I., Parker, E. P. K., Giri, S., Allen, D. J., Silas, S., Revathi, R., … Kang, G. (2019). Influence of Nonpolio Enteroviruses and the Bacterial Gut Microbiota on Oral Poliovirus Vaccine Response: A Study from South India. *The Journal of Infectious Diseases*, *219*(8), 1178–1186. https://doi.org/10.1093/INFDIS/JIY568

Prendergast, A. J., & Kelly, P. (2016, June 1). Interactions between intestinal pathogens, enteropathy and malnutrition in developing countries. *Current Opinion in Infectious Diseases*. Lippincott Williams and Wilkins. https://doi.org/10.1097/QCO.0000000000000261

Price, M. N., Dehal, P. S., & Arkin, A. P. (2010). FastTree 2 – Approximately Maximum-Likelihood Trees for Large Alignments. *PLOS ONE*, *5*(3), e9490. https://doi.org/10.1371/JOURNAL.PONE.0009490

Pro, S. C., Lindestam Arlehamn, C. S., Dhanda, S. K., Carpenter, C., Lindvall, M., Faruqi, A. A., … Sette, A. (2018). Microbiota epitope similarity either dampens or enhances the immunogenicity of disease-associated antigenic epitopes. *PLoS ONE*, *13*(5), e0196551. https://doi.org/10.1371/journal.pone.0196551

Pulendran, B., Kumar, P., Cutler, C. W., Mohamadzadeh, M., Van Dyke, T., & Banchereau, J. (2001). Lipopolysaccharides from Distinct Pathogens Induce Different Classes of Immune Responses In Vivo. *The Journal of Immunology*, *167*(9), 5067–5076. https://doi.org/10.4049/jimmunol.167.9.5067

Rabe, H., Lundell, A. C., Sjöberg, F., Ljung, A., Strömbeck, A., Gio-Batta, M., … Rudin, A. (2020). Neonatal gut colonization by Bifidobacterium is associated with higher childhood cytokine responses. *Gut Microbes*, *12*(1), 1–14. https://doi.org/10.1080/19490976.2020.1847628

Raftar, S. K. A., Ashrafian, F., Abdollahiyan, S., Yadegar, A., Moradi, H. R., Masoumi, M., … Zali, M. R. (2022). The anti-inflammatory effects of Akkermansia muciniphila and its derivates in HFD/CCL4-induced murine model of liver injury. *Scientific Reports 2022 12:1*, *12*(1), 1–14. https://doi.org/10.1038/s41598-022-06414-1

Rakoff-Nahoum, S., Paglino, J., Eslami-Varzaneh, F., Edberg, S., & Medzhitov, R. (2004). Recognition of commensal microflora by toll-like receptors is required for intestinal homeostasis. *Cell*, *118*(2), 229–241. https://doi.org/10.1016/j.cell.2004.07.002

Randhawa, A. K., Shey, M. S., Keyser, A., Peixoto, B., Wells, R. D., de Kock, M., … Hawn, T. R. (2011). Association of Human TLR1 and TLR6 Deficiency with Altered Immune Responses to BCG Vaccination in South African Infants. *PLoS Pathogens*, *7*(8), e1002174. https://doi.org/10.1371/journal.ppat.1002174

Robak, O. H., Heimesaat, M. M., Kruglov, A. A., Prepens, S., Ninnemann, J., Gutbier, B., … Opitz, B. (2018). Antibiotic treatment–induced secondary IgA deficiency enhances susceptibility to Pseudomonas aeruginosa pneumonia. *The Journal of Clinical Investigation*, *128*(8), 3535–3545. https://doi.org/10.1172/JCI97065

Robbins, A., Bahuaud, M., Hentzien, M., Maestraggi, Q., Barbe, C., Giusti, D., … Servettaz, A. (2021). The 13-Valent Pneumococcal Conjugate Vaccine Elicits Serological Response and Lasting Protection in Selected Patients With Primary Humoral Immunodeficiency. *Frontiers in Immunology*, *12*, 2694. https://doi.org/10.3389/FIMMU.2021.697128/BIBTEX

Robertson, R. C., Church, J. A., Edens, T. J., Mutasa, K., Min Geum, H., Baharmand, I., … Manges, A. R. (2021). The fecal microbiome and rotavirus vaccine immunogenicity in rural Zimbabwean infants. *Vaccine*, *39*(38), 5391–5400. https://doi.org/10.1016/j.vaccine.2021.07.076

Robertson, R. C., Manges, A. R., Finlay, B. B., & Prendergast, A. J. (2019). The Human

Microbiome and Child Growth – First 1000 Days and Beyond. *Trends in Microbiology*, *27*(2), 131–147. https://doi.org/10.1016/j.tim.2018.09.008
Robertson, S. J., Lemire, P., Croitoru, K., Girardin, S. E., & Correspondence, D. J. P. (2019). Comparison of Co-housing and Littermate Methods for Microbiota Standardization in Mouse Models. *Cell Reports*, *27*. https://doi.org/10.1016/j.celrep.2019.04.023
Robinson, G. A., Peng, J., Peckham, H., Butler, G., Pineda-Torra, I., Ciurtin, C., & Jury, E. C. (2022). Investigating sex differences in T regulatory cells from cisgender and transgender healthy individuals and patients with autoimmune inflammatory disease: a cross-sectional study. *The Lancet Rheumatology*, *4*(10), e710–e724. https://doi.org/10.1016/S2665-9913(22)00198-9
Robinson, M. J., Dowling, M. R., Pitt, C., O'Donnell, K., Webster, R. H., Hill, D. L., … Tarlinton, D. M. (2022). Long-lived plasma cells accumulate in the bone marrow at a constant rate from early in an immune response. *Science Immunology*, *7*(76), eabm8389. https://doi.org/10.1126/sciimmunol.abm8389
Roca, A., Bojang, A., Bottomley, C., Gladstone, R. A., Adetifa, J. U., Egere, U., … Greenwood, B. (2015). Effect on nasopharyngeal pneumococcal carriage of replacing PCV7 with PCV13 in the Expanded Programme of Immunization in The Gambia. *Vaccine*, *33*(51), 7144–7151. https://doi.org/10.1016/j.vaccine.2015.11.012
Rolhion, N., Chassaing, B., Nahori, M. A., de Bodt, J., Moura, A., Lecuit, M., … Cossart, P. (2019). A Listeria monocytogenes Bacteriocin Can Target the Commensal Prevotella copri and Modulate Intestinal Infection. *Cell Host and Microbe*, *26*(5), 691–701.e5. https://doi.org/10.1016/j.chom.2019.10.016
Rolig, A. S., Parthasarathy, R., Burns, A. R., Bohannan, B. J. M., & Guillemin, K. (2015). Individual Members of the Microbiota Disproportionately Modulate Host Innate Immune Responses. *Cell Host & Microbe*, *18*(5), 613–620. https://doi.org/10.1016/J.CHOM.2015.10.009
Rosshart, S. P., Herz, J., Vassallo, B. G., Hunter, A., Wall, M. K., Badger, J. H., … Rehermann, B. (2019). Laboratory mice born to wild mice have natural microbiota and model human immune responses. *Science*, *365*(6452). https://doi.org/10.1126/SCIENCE.AAW4361/SUPPL_FILE/AAW4361-ROSSHART-SM.PDF
Rosshart, S. P., Vassallo, B. G., Angeletti, D., Hutchinson, D. S., Morgan, A. P., Takeda, K., … Rehermann, B. (2017). Wild Mouse Gut Microbiota Promotes Host Fitness and Improves Disease Resistance. *Cell*, *171*(5), 1015–1028.e13. https://doi.org/10.1016/j.cell.2017.09.016
Ruane, D., Chorny, A., Lee, H., Faith, J., Pandey, G., Shan, M., … Mehandru, S. (2016). Microbiota regulate the ability of lung dendritic cells to induce IgA class-switch recombination and generate protective gastrointestinal immune responses. *Journal of Experimental Medicine*, *213*(1), 53–73. https://doi.org/10.1084/JEM.20150567
Rusmil, K., Gunardi, H., Fadlyana, E., Soedjatmiko, Dhamayanti, M., Sekartini, R., … Sari, R. M. (2015). The immunogenicity, safety, and consistency of an Indonesia combined DTP-HB-Hib vaccine in expanded program on immunization schedule. *BMC Pediatrics*, *15*(1), 1–10. https://doi.org/10.1186/S12887-015-0525-2/FIGURES/3
Ryan, F. J., Norton, T. S., McCafferty, C., Blake, S. J., Stevens, N. E., James, J., … Lynn, D. J. (2023). A systems immunology study comparing innate and adaptive immune responses in adults to COVID-19 mRNA and adenovirus vectored vaccines. *Cell Reports Medicine*, *4*, 100971. https://doi.org/10.1016/J.XCRM.2023.100971
Salgado, V. R., Fukutani, K. F., Fukutani, E., Lima, J. V., Rossi, E. A., Barral, A., … Queiroz, A.

T. L. (2020). Effects of 10-valent pneumococcal conjugate (PCV10) vaccination on the nasopharyngeal microbiome. *Vaccine*, *38*(6), 1436–1443. https://doi.org/10.1016/J.VACCINE.2019.11.079

Salk, H. M., Simon, W. L., Lambert, N. D., Kennedy, R. B., Grill, D. E., Kabat, B. F., & Poland, G. A. (2016). Taxa of the Nasal Microbiome Are Associated with Influenza-Specific IgA Response to Live Attenuated Influenza Vaccine. https://doi.org/10.1371/journal.pone.0162803

Sánchez-Tarjuelo, R., Cortegano, I., Manosalva, J., Rodríguez, M., Ruíz, C., Alía, M., … de Andrés, B. (2020). The TLR4-MyD88 Signaling Axis Regulates Lung Monocyte Differentiation Pathways in Response to Streptococcus pneumoniae. *Frontiers in Immunology*, *11*, 2120. https://doi.org/10.3389/FIMMU.2020.02120/BIBTEX

Sanchez, H. N., Moroney, J. B., Gan, H., Shen, T., Im, J. L., Li, T., … Casali, P. (2020). B cell-intrinsic epigenetic modulation of antibody responses by dietary fiber-derived short-chain fatty acids. *Nature Communications 2020 11:1*, *11*(1), 1–19. https://doi.org/10.1038/s41467-019-13603-6

Sanders, M. E., Merenstein, D. J., Reid, G., Gibson, G. R., & Rastall, R. A. (2019). Probiotics and prebiotics in intestinal health and disease: from biology to the clinic. *Nature Reviews Gastroenterology & Hepatology 2019 16:10*, *16*(10), 605–616. https://doi.org/10.1038/s41575-019-0173-3

Sato, K., Yokoji, M., Yamada, M., Nakajima, T., & Yamazaki, K. (2018). An orally administered oral pathobiont and commensal have comparable and innocuous systemic effects in germ-free mice. *Journal of Periodontal Research*, *53*(6), 950–960. https://doi.org/10.1111/JRE.12593

Schaupp, L., Muth, S., Rogell, L., Kofoed-Branzk, M., Melchior, F., Lienenklaus, S., … Probst, H. C. (2020). Microbiota-Induced Type I Interferons Instruct a Poised Basal State of Dendritic Cells. *Cell*, *181*(5), 1080–1096.e19. https://doi.org/10.1016/j.cell.2020.04.022

Scott, S. A., Fu, J., & Chang, P. V. (2020). Microbial tryptophan metabolites regulate gut barrier function via the aryl hydrocarbon receptor. *Proceedings of the National Academy of Sciences of the United States of America*, *117*(32), 19376–19387. https://doi.org/10.1073/PNAS.2000047117/SUPPL_FILE/PNAS.2000047117.SAPP.PDF

Sen, G., Chen, Q., & Snapper, C. M. (2006). Immunization of aged mice with a pneumococcal conjugate vaccine combined with an unmethylated CpG-containing oligodeoxynucleotide restores defective immunoglobulin G antipolysaccharide responses and specific CD4 +-T-cell priming to young adult levels. *Infection and Immunity*, *74*(4), 2177–2186. https://doi.org/10.1128/IAI.74.4.2177-2186.2006

Sen, G., Khan, A. Q., Chen, Q., & Snapper, C. M. (2005). In Vivo Humoral Immune Responses to Isolated Pneumococcal Polysaccharides Are Dependent on the Presence of Associated TLR Ligands. *The Journal of Immunology*, *175*(5), 3084–3091. https://doi.org/10.4049/jimmunol.175.5.3084

Shao, Y., Forster, S. C., Tsaliki, E., Vervier, K., Strang, A., Simpson, N., … Lawley, T. D. (2019). Stunted microbiota and opportunistic pathogen colonization in caesarean-section birth. *Nature*, *574*(7776), 117–121. https://doi.org/10.1038/s41586-019-1560-1

Shekhar, S., & Petersen, F. C. (2020). The Dark Side of Antibiotics: Adverse Effects on the Infant Immune Defense Against Infection. *Frontiers in Pediatrics*, *8*(October), 1–7. https://doi.org/10.3389/fped.2020.544460

Sheridan, P. A., Paich, H. A., Handy, J., Karlsson, E. A., Hudgens, M. G., Sammon, A. B., …

Beck, M. A. (2012). Obesity is associated with impaired immune response to influenza vaccination in humans. *International Journal of Obesity (2005)*, *36*(8), 1072–1077. https://doi.org/10.1038/IJO.2011.208
Shi, J., Hou, S., Fang, Q., Liu, X., Liu, X., & Qi, H. (2018). PD-1 Controls Follicular T Helper Cell Positioning and Function. *Immunity*, *49*(2), 264. https://doi.org/10.1016/J.IMMUNI.2018.06.012
Siegrist, C.-A. (2008). Vaccine Immunology. *Vaccine*, 131–137. https://doi.org/10.1016/b978-0-323-55435-0.00008-2
Siegrist, C. A., & Aspinall, R. (2009). B-cell responses to vaccination at the extremes of age. *Nature Reviews Immunology 2009 9:3*, *9*(3), 185–194. https://doi.org/10.1038/nri2508
Siegrist, C. A. C.-A. (2008). Vaccine Immunology. *Vaccine*, 131–137. https://doi.org/10.1016/b978-0-323-55435-0.00008-2
Silva-Neta, H. L., Brelaz-De-Castro, M. C. A., Chagas, M. B. O., Mariz, H. A., Arruda, R. G. D., Vasconcelos, V. F. D., … Pitta, M. G. R. (2018). CD4+CD45RA-FOXP3low Regulatory T Cells as Potential Biomarkers of Disease Activity in Systemic Lupus Erythematosus Brazilian Patients. *BioMed Research International*, *2018*. https://doi.org/10.1155/2018/3419565
Silva, M., Nguyen, T. H., Philbrook, P., Chu, M., Sears, O., Hatfield, S., … Sitkovsky, M. V. (2017). Targeted Elimination of Immunodominant B Cells Drives the Germinal Center Reaction toward Subdominant Epitopes. *Cell Reports*, *21*(13), 3672–3680. https://doi.org/10.1016/j.celrep.2017.12.014
Singh, R., Chandrashekharappa, S., Bodduluri, S. R., Baby, B. V., Hegde, B., Kotla, N. G., … Jala, V. R. (2019). Enhancement of the gut barrier integrity by a microbial metabolite through the Nrf2 pathway. *Nature Communications 2019 10:1*, *10*(1), 1–18. https://doi.org/10.1038/s41467-018-07859-7
Sivan, A., Corrales, L., Hubert, N., Williams, J. B., Aquino-Michaels, K., Earley, Z. M., … Gajewski, T. F. (2015). Commensal Bifidobacterium promotes antitumor immunity and facilitates anti-PD-L1 efficacy. *Science*, *350*(6264), 1084–1089. https://doi.org/10.1126/SCIENCE.AAC4255
Sjögren, Y. M., Tomicic, S., Lundberg, A., Böttcher, M. F., Björkstén, B., Sverremark-Ekström, E., & Jenmalm, M. C. (2009). Influence of early gut microbiota on the maturation of childhood mucosal and systemic immune responses. *Clinical & Experimental Allergy*, *39*(12), 1842–1851. https://doi.org/10.1111/j.1365-2222.2009.03326.x
Slifka, M. K., Antia, R., Whitmire, J. K., & Ahmed, R. (1998). Humoral immunity due to long-lived plasma cells. *Immunity*, *8*(3), 363–372. https://doi.org/10.1016/S1074-7613(00)80541-5
Smith, M., Tourigny, M. R., Noakes, P., Thornton, C. A., Tulic, M. K., & Prescott, S. L. (2008). Children with egg allergy have evidence of reduced neonatal CD4(+)CD25(+)CD127(lo/-) regulatory T cell function. *The Journal of Allergy and Clinical Immunology*, *121*(6). https://doi.org/10.1016/J.JACI.2008.03.025
Soh, S. E., Ong, D. Q. R., Gerez, I., Zhang, X., Chollate, P., Shek, L. P. C., … Aw, M. (2010). Effect of probiotic supplementation in the first 6 months of life on specific antibody responses to infant Hepatitis B vaccination. *Vaccine*, *28*(14), 2577–2579. https://doi.org/10.1016/j.vaccine.2010.01.020
Sommer, F., & Bäckhed, F. (2013, April). The gut microbiota-masters of host development and physiology. *Nature Reviews Microbiology*. https://doi.org/10.1038/nrmicro2974

St Jean, D. T., Rogawski McQuade, E. T., Edwards, J. K., Thompson, P., Thomas, J., & Becker-Dreps, S. (2022). Effect of early life antibiotic use on serologic responses to oral rotavirus vaccine in the MAL-ED birth cohort study. *Vaccine*, *40*(18), 2580–2587. https://doi.org/10.1016/j.vaccine.2022.03.023

Stebegg, M., Kumar, S. D., Silva-Cayetano, A., Fonseca, V. R., Linterman, M. A., & Graca, L. (2018). Regulation of the Germinal Center Response. *Frontiers in Immunology*, *9*, 2469. https://doi.org/10.3389/fimmu.2018.02469

Stebegg, M., Silva-Cayetano, A., Innocentin, S., Jenkins, T. P., Cantacessi, C., Gilbert, C., & Linterman, M. A. (2019). Heterochronic faecal transplantation boosts gut germinal centres in aged mice. *Nature Communications*, *10*(1). https://doi.org/10.1038/S41467-019-10430-7

Stewart, C. J., Ajami, N. J., O'Brien, J. L., Hutchinson, D. S., Smith, D. P., Wong, M. C., … Petrosino, J. F. (2018, October 25). Temporal development of the gut microbiome in early childhood from the TEDDY study. *Nature*. Nature Publishing Group. https://doi.org/10.1038/s41586-018-0617-x

Stocker, M., Klingenberg, C., Navér, L., Nordberg, V., Berardi, A., el Helou, S., … Giannoni, E. (2023). Less is more: Antibiotics at the beginning of life. *Nature Communications 2023 14:1*, *14*(1), 1–9. https://doi.org/10.1038/s41467-023-38156-7

Strachan, D. P. (1989). Hay fever, hygiene, and household size. *BMJ : British Medical Journal*, *299*(6710), 1259. https://doi.org/10.1136/BMJ.299.6710.1259

Strugnell, R., Zepp, F., Cunningham, A., & Tantawichien, T. (2011). Vaccine antigens. *Perspectives in Vaccinology*, *1*(1), 61–88. https://doi.org/10.1016/j.pervac.2011.05.003

Su, L. F., Kidd, B. A., Han, A., Kotzin, J. J., & Davis, M. M. (2013). Virus-Specific CD4+ Memory-Phenotype T Cells Are Abundant in Unexposed Adults. *Immunity*, *38*(2), 373–383. https://doi.org/10.1016/j.immuni.2012.10.021

Subramanian, S., Huq, S., Yatsunenko, T., Haque, R., Mahfuz, M., Alam, M. A., … Gordon, J. I. (2014). Persistent gut microbiota immaturity in malnourished Bangladeshi children. *Nature*, *510*(7505), 417–421. https://doi.org/10.1038/nature13421

Suzuki, K., Maruya, M., Kawamoto, S., & Fagarasan, S. (2010). Roles of B-1 and B-2 cells in innate and acquired IgA-mediated immunity. *Immunological Reviews*, *237*(1), 180–190. https://doi.org/10.1111/J.1600-065X.2010.00941.X

Swarthout, T. D., Fronterre, C., Lourenço, J., Obolski, U., Gori, A., Bar-Zeev, N., … Heyderman, R. S. (2020a). High residual carriage of vaccine-serotype Streptococcus pneumoniae after introduction of pneumococcal conjugate vaccine in Malawi. *Nature Communications*, *11*(1). https://doi.org/10.1038/s41467-020-15786-9

Swarthout, T. D., Fronterre, C., Lourenço, J., Obolski, U., Gori, A., Bar-Zeev, N., … Heyderman, R. S. (2020b). High residual carriage of vaccine-serotype Streptococcus pneumoniae after introduction of pneumococcal conjugate vaccine in Malawi. *Nature Communications 2020 11:1*, *11*(1), 1–12. https://doi.org/10.1038/s41467-020-15786-9

Swarthout, T. D., Henrion, M. Y. R., Thindwa, D., Meiring, J. E., Mbewe, M., Kalizang'Oma, A., … Heyderman, R. S. (2022). Waning of antibody levels induced by a 13-valent pneumococcal conjugate vaccine, using a 3 + 0 schedule, within the first year of life among children younger than 5 years in Blantyre, Malawi: an observational, population-level, serosurveillance study. *The Lancet Infectious Diseases*, *22*(12), 1737–1747. https://doi.org/10.1016/S1473-3099(22)00438-8

Tanca, A., Manghina, V., Fraumene, C., Palomba, A., Abbondio, M., Deligios, M., … Uzzau, S. (2017). Metaproteogenomics reveals taxonomic and functional changes between

cecal and fecal microbiota in mouse. *Frontiers in Microbiology*, *8*(MAR), 391. https://doi.org/10.3389/FMICB.2017.00391/BIBTEX

Tang, B., Tang, L., He, W., Jiang, X., Hu, C., Li, Y., … Yang, S. (2022). Correlation of gut microbiota and metabolic functions with the antibody response to the BBIBP-CorV vaccine. *Cell Reports Medicine*, *3*(10), 100752. https://doi.org/10.1016/j.xcrm.2022.100752

Teng, F., Klinger, C. N., Felix, K. M., Bradley, C. P., Wu, E., Tran, N. L., … Wu, H. J. J. (2016). Gut Microbiota Drive Autoimmune Arthritis by Promoting Differentiation and Migration of Peyer's Patch T Follicular Helper Cells. *Immunity*, *44*(4), 875–888. https://doi.org/10.1016/J.IMMUNI.2016.03.013

The Lancet. (2022, October 1). Polio eradication: falling at the final hurdle? *The Lancet*. Elsevier B.V. https://doi.org/10.1016/S0140-6736(22)01875-X

Treffers, L. W., van Houdt, M., Bruggeman, C. W., Heineke, M. H., Zhao, X. W., van der Heijden, J., … van den Berg, T. K. (2019). FcγRIIIb Restricts Antibody-Dependent Destruction of Cancer Cells by Human Neutrophils. *Frontiers in Immunology*, *9*(JAN), 3124. https://doi.org/10.3389/fimmu.2018.03124

Tulic, M. K., Hodder, M., Forsberg, A., McCarthy, S., Richman, T., DVaz, N., … Prescott, S. L. (2011). Differences in innate immune function between allergic and nonallergic children: new insights into immune ontogeny. *The Journal of Allergy and Clinical Immunology*, *127*(2). https://doi.org/10.1016/J.JACI.2010.09.020

Turnbaugh, P. J., Ley, R. E., Hamady, M., Fraser-Liggett, C. M., Knight, R., & Gordon, J. I. (2007, October 18). The Human Microbiome Project. *Nature*. Nature Publishing Group. https://doi.org/10.1038/nature06244

Uchida, T., Pappenheimer, A. M., & Harper, A. A. (1972). Reconstitution of Diphtheria Toxin from Two Nontoxic Cross-Reacting Mutant Proteins. *Science*, *175*(4024), 901–903. https://doi.org/10.1126/SCIENCE.175.4024.901

Uppal, S. S., Verma, S., & Dhot, P. S. (2003). Normal values of CD4 and CD8 lymphocyte subsets in healthy indian adults and the effects of sex, age, ethnicity, and smoking. *Cytometry. Part B, Clinical Cytometry*, *52*(1), 32–36. https://doi.org/10.1002/CYTO.B.10011

Valdez, Y., Brown, E. M., & Finlay, B. B. (2014). Influence of the microbiota on vaccine effectiveness. *Trends in Immunology*. Elsevier Ltd. https://doi.org/10.1016/j.it.2014.07.003

Van Duin, D., Medzhitov, R., & Shaw, A. C. (2006, January). Triggering TLR signaling in vaccination. *Trends in Immunology*. https://doi.org/10.1016/j.it.2005.11.005

van Gent, R., van Tilburg, C. M., Nibbelke, E. E., Otto, S. A., Gaiser, J. F., Janssens-Korpela, P. L., … Tesselaar, K. (2009). Refined characterization and reference values of the pediatric T- and B-cell compartments. *Clinical Immunology*, *133*(1), 95–107. https://doi.org/10.1016/j.clim.2009.05.020

Van Hoek, A. J., Sheppard, C. L., Andrews, N. J., Waight, P. A., Slack, M. P. E., Harrison, T. G., … Miller, E. (2014). Pneumococcal carriage in children and adults two years after introduction of the thirteen valent pneumococcal conjugate vaccine in England. *Vaccine*, *32*(34), 4349–4355. https://doi.org/10.1016/j.vaccine.2014.03.017

Van Puyenbroeck, K., Hens, N., Coenen, S., Michiels, B., Beunckens, C., Molenberghs, G., … Verhoeven, V. (2012). Efficacy of daily intake of Lactobacillus casei Shirota on respiratory symptoms and influenza vaccination immune response: A randomized, double-blind, placebo-controlled trial in healthy elderly nursing home residents. *American Journal of Clinical Nutrition*, *95*(5), 1165–1171.

https://doi.org/10.3945/ajcn.111.026831
Vatanen, T., Kostic, A. D., D'Hennezel, E., Siljander, H., Franzosa, E. A., Yassour, M., … Xavier, R. J. (2016). Variation in Microbiome LPS Immunogenicity Contributes to Autoimmunity in Humans. *Cell*, *165*(4), 842–853. https://doi.org/10.1016/J.CELL.2016.04.007
Velazquez-Salinas, L., Verdugo-Rodriguez, A., Rodriguez, L. L., & Borca, M. V. (2019). The role of interleukin 6 during viral infections. *Frontiers in Microbiology*, *10*(MAY), 1057. https://doi.org/10.3389/FMICB.2019.01057/BIBTEX
Verma, R., Lee, C., Jeun, E. J., Yi, J., Kim, K. S., Ghosh, A., … Im, S. H. (2018). Cell surface polysaccharides of Bifidobacterium bifidum induce the generation of Foxp3+ regulatory T cells. *Science Immunology*, *3*(28). https://doi.org/10.1126/sciimmunol.aat6975
Vesikari, T., Karvonen, A., Prymula, R., Schuster, V., Tejedor, J., Cohen, R., … Bouckenooghe, A. (2007). Efficacy of human rotavirus vaccine against rotavirus gastroenteritis during the first 2 years of life in European infants: randomised, double-blind controlled study. *Lancet*, *370*(9601), 1757–1763. https://doi.org/10.1016/S0140-6736(07)61744-9
Wagner, C., & Hänsch, G. M. (2004). Genetic deficiency of CD 16, the low-affinity receptor for immunoglobulin G, has no impact on the functional capacity of polymorphonuclear neutrophils. *European Journal of Clinical Investigation*, *34*(2), 149–155. https://doi.org/10.1111/j.1365-2362.2004.01298.x
Waide, M. L., Polidoro, R., Powell, W. L., Denny, J. E., Kos, J., Tieri, D. A., … Schmidt, N. W. (2020). Gut Microbiota Composition Modulates the Magnitude and Quality of Germinal Centers during Plasmodium Infections. *Cell Reports*, *33*(11), 108503. https://doi.org/10.1016/j.celrep.2020.108503
Wang, Y., & Jönsson, F. (2019, August 27). Expression, role, and regulation of neutrophil Fcγ receptors. *Frontiers in Immunology*. Frontiers Media S.A. https://doi.org/10.3389/fimmu.2019.01958
Wargo, J. A. (2020). Modulating gut microbes. *Science*, *369*(6509), 1302–1303. https://doi.org/10.1126/SCIENCE.ABC3965
Watson, O. J., Barnsley, G., Toor, J., Hogan, A. B., Winskill, P., & Ghani, A. C. (2022). Global impact of the first year of COVID-19 vaccination: a mathematical modelling study. *The Lancet Infectious Diseases*, *22*(9), 1293–1302. https://doi.org/10.1016/S1473-3099(22)00320-6
Wei, C. M., Lee, J. H., Wang, L. C., Yang, Y. H., Chang, L. Y., & Chiang, B. L. (2008). Frequency and phenotypic analysis of CD4+CD25+ regulatory T cells in children with juvenile idiopathic arthritis. *Journal of Microbiology, Immunology and Infection*, *41*(1), 78–87. Retrieved from https://europepmc.org/article/med/18327431
Weller, S., Braun, M. C., Tan, B. K., Rosenwald, A., Cordier, C., Conley, M. E., … Weill, J. C. (2004). Human blood IgM "memory" B cells are circulating splenic marginal zone B cells harboring a prediversified immunoglobulin repertoire. *Blood*, *104*(12), 3647–3654. https://doi.org/10.1182/BLOOD-2004-01-0346
Weller, S., Sterlin, D., Fadeev, T., Coignard, E., Aires, A. V. de los, Goetz, C., … Reynaud, C.-A. (2023). T-independent responses to polysaccharides in humans mobilize marginal zone B cells prediversified against gut bacterial antigens. *Science Immunology*, *8*(79). https://doi.org/10.1126/SCIIMMUNOL.ADE1413
West, C. E., Gothefors, L., Granström, M., Käyhty, H., Hammarström, M. L. K. C., & Hernell, O. (2008). Effects of feeding probiotics during weaning on infections and antibody

responses to diphtheria, tetanus and Hib vaccines. *Pediatric Allergy and Immunology : Official Publication of the European Society of Pediatric Allergy and Immunology*, *19*(1), 53–60. https://doi.org/10.1111/J.1399-3038.2007.00583.X
White, M. B., Shen, A. L., Word, C. J., Tucker, P. W., & Blattner, F. R. (1985). Human immunoglobulin D: genomic sequence of the delta heavy chain. *Science (New York, N.Y.)*, *228*(4700), 733–737. https://doi.org/10.1126/SCIENCE.3922054
Wickham, H. (2016). ggplot2. https://doi.org/10.1007/978-3-319-24277-4
Wilkinson, T. M., Li, C. K. F., Chui, C. S. C., Huang, A. K. Y., Perkins, M., Liebner, J. C., … Xu, X. N. (2012). Preexisting influenza-specific CD4 + T cells correlate with disease protection against influenza challenge in humans. *Nature Medicine*, *18*(2), 274–280. https://doi.org/10.1038/nm.2612
Williams, W. B., Liao, H. X., Moody, M. A., Kepler, T. B., Alam, S. M., Gao, F., … Haynes, B. F. (2015). Diversion of HIV-1 vaccine-induced immunity by gp41-microbiota cross-reactive antibodies. *Science*, *349*(6249). https://doi.org/10.1126/science.aab1253
Wilmore, J. R., Jones, D. D., & Allman, D. (2017). Improved resolution of plasma cell subpopulations by flow cytometry. *European Journal of Immunology*, *47*(8), 1386. https://doi.org/10.1002/EJI.201746944
Woo, V., & Alenghat, T. (2022). Epigenetic regulation by gut microbiota. *Gut Microbes*, *14*. https://doi.org/10.1080/19490976.2021.2022407
Wood, D. E., & Salzberg, S. L. (2014). Kraken: ultrafast metagenomic sequence classification using exact alignments. *Genome Biology*, *15*(3), R46. https://doi.org/10.1186/gb-2014-15-3-r46
Wood, H., Acharjee, A., Pearce, H., Quraishi, M. N., Powell, R., Rossiter, A., … Toldi, G. (2021). Breastfeeding promotes early neonatal regulatory T-cell expansion and immune tolerance of non-inherited maternal antigens. *Allergy*, *76*(8), 2447–2460. https://doi.org/10.1111/ALL.14736
Wu, B. B., Yang, Y., Xu, X., & Wang, W. P. (2016). Effects of Bifidobacterium supplementation on intestinal microbiota composition and the immune response in healthy infants. *World Journal of Pediatrics*, *12*(2), 177–182. https://doi.org/10.1007/s12519-015-0025-3
Wuorimaa, T., & Käyhty, H. (2002). Current state of pneumococcal vaccines. *Scandinavian Journal of Immunology*, *56*(2), 111–129. https://doi.org/10.1046/J.1365-3083.2002.01124.X
Xiu, L., Zhang, H., Hu, Z., Liang, Y., Guo, S., Yang, M., … Wang, X. (2018). Immunostimulatory activity of exopolysaccharides from probiotic lactobacillus casei WXD030 strain as a novel adjuvant in vitro and in vivo. *Food and Agricultural Immunology*, *29*(1), 1086–1105. https://doi.org/10.1080/09540105.2018.1513994
Xu, J., Ren, Z., Cao, K., Li, X., Yang, J., Luo, X., … Xu, J. (2021). Boosting Vaccine-Elicited Respiratory Mucosal and Systemic COVID-19 Immunity in Mice With the Oral Lactobacillus plantarum. *Frontiers in Nutrition*, *8*(December). https://doi.org/10.3389/fnut.2021.789242
Yatsunenko, T., Rey, F. E., Manary, M. J., Trehan, I., Dominguez-Bello, M. G., Contreras, M., … Gordon, J. I. (2012, June 14). Human gut microbiome viewed across age and geography. *Nature*. https://doi.org/10.1038/nature11053
Yeh, S. H., Gurtman, A., Hurley, D. C., Block, S. L., Schwartz, R. H., Patterson, S., … Scott, D. A. (2010). Immunogenicity and safety of 13-Valent pneumococcal conjugate vaccine in infants and toddlers. *Pediatrics*, *126*(3), e493–e505. https://doi.org/10.1542/peds.2009-3027

Younge, N., McCann, J. R., Ballard, J., Plunkett, C., Akhtar, S., Araújo-Pérez, F., … Seed, P. C. (2019). Fetal exposure to the maternal microbiota in humans and mice. *JCI Insight*, *4*(19). https://doi.org/10.1172/jci.insight.127806

Youngster, I., Kozer, E., Lazarovitch, Z., Broide, E., & Goldman, M. (2011). Probiotics and the immunological response to infant vaccinations: A prospective, placebo controlled pilot study. *Archives of Disease in Childhood*, *96*(4), 345–349. https://doi.org/10.1136/adc.2010.197459

Yousefi, Z., Aria, H., Ghaedrahmati, F., Bakhtiari, T., Azizi, M., Bastan, R., … Eskandari, N. (2022). An Update on Human Papilloma Virus Vaccines: History, Types, Protection, and Efficacy. *Frontiers in Immunology*, *12*, 6036. https://doi.org/10.3389/FIMMU.2021.805695/BIBTEX

Zaghouani, H., Hoeman, C. M., & Adkins, B. (2009, December). Neonatal immunity: faulty T-helpers and the shortcomings of dendritic cells. *Trends in Immunology*. https://doi.org/10.1016/j.it.2009.09.002

Zehentmeier, S., Roth, K., Cseresnyes, Z., Sercan, Ö., Horn, K., Niesner, R. A., … Hauser, A. E. (2014). Static and dynamic components synergize to form a stable survival niche for bone marrow plasma cells. *European Journal of Immunology*, *44*(8), 2306–2317. https://doi.org/10.1002/eji.201344313

Zeng, M. Y., Cisalpino, D., Varadarajan, S., Hellman, J., Warren, H. S., Cascalho, M., … Núñez, G. (2016). Gut Microbiota-Induced Immunoglobulin G Controls Systemic Infection by Symbiotic Bacteria and Pathogens. *Immunity*, *44*(3), 647–658. https://doi.org/10.1016/j.immuni.2016.02.006

Zeng, M. Y., Inohara, N., & Nuñez, G. (2017). Mechanisms of inflammation-driven bacterial dysbiosis in the gut. *Mucosal Immunology*, *10*(1), 18–26. https://doi.org/10.1038/MI.2016.75/ATTACHMENT/21CAEEF4-FCD4-4CFE-AB97-19BA82F9849C/MMC1.PPT

Zhang, L., Li, Z., Wan, Z., Kilby, A., Kilby, J. M., & Jiang, W. (2015, August 26). Humoral immune responses to Streptococcus pneumoniae in the setting of HIV-1 infection. *Vaccine*. Elsevier Ltd. https://doi.org/10.1016/j.vaccine.2015.06.077

Zhang, X., Borbet, T. C., Fallegger, A., Wipperman, M. F., Blaser, M. J., & Müller, A. (2021). An Antibiotic-Impacted Microbiota Compromises the Development of Colonic Regulatory T Cells and Predisposes to Dysregulated Immune Responses. *MBio*, *12*(1). https://doi.org/10.1128/mbio.03335-20

Zhang, X., Li, L., Jung, J., Xiang, S., Hollmann, C., & Choi, Y. S. (2001). The distinct roles of T cell-derived cytokines and a novel follicular dendritic cell-signaling molecule 8D6 in germinal center-B cell differentiation. *Journal of Immunology (Baltimore, Md. : 1950)*, *167*(1), 49–56. Retrieved from http://www.ncbi.nlm.nih.gov/pubmed/11418631

Zhang, Y., Collier, F., Naselli, G., Saffery, R., Tang, M. L., Allen, K. J., … Dwyer, T. (2016). Cord blood monocyte-derived inflammatory cytokines suppress IL-2 and induce nonclassic "T(H)2-type" immunity associated with development of food allergy. *Science Translational Medicine*, *8*(321). https://doi.org/10.1126/SCITRANSLMED.AAD4322

Zhao, T., Li, J., Fu, Y., Ye, H., Liu, X., Li, G., … Yang, J. (2020a). Influence of gut microbiota on mucosal IgA antibody response to the polio vaccine. *NPJ Vaccines*, *5*(1). https://doi.org/10.1038/S41541-020-0194-5

Zhao, T., Li, J., Fu, Y., Ye, H., Liu, X., Li, G., … Yang, J. (2020b). Influence of gut microbiota on mucosal IgA antibody response to the polio vaccine. *Npj Vaccines*, *5*(1), 1–9. https://doi.org/10.1038/s41541-020-0194-5

Zimmermann, P., & Curtis, N. (2018, January 4). The influence of probiotics on vaccine responses – A systematic review. *Vaccine*. Elsevier Ltd. https://doi.org/10.1016/j.vaccine.2017.08.069

Zimmermann, P., & Curtis, N. (2019, April 1). Factors that influence the immune response to vaccination. *Clinical Microbiology Reviews*. American Society for Microbiology. https://doi.org/10.1128/CMR.00084-18

Zimmermann, P., Perrett, K. P., Ritz, N., Flanagan, K. L., Robins-Browne, R., van der Klis, F. R. M., … Vuillermin, P. (2020). Biological sex influences antibody responses to routine vaccinations in the first year of life. *Acta Paediatrica, International Journal of Paediatrics*, *109*(1), 147–157. https://doi.org/10.1111/apa.14932

Appendices

Appendix 1: Supplementary Material from Chapter 1

Removed due to copyright restriction.

Removed due to copyright restriction.

Removed due to copyright restriction.

Removed due to copyright restriction.

Removed due to copyright restriction.

Removed due to copyright restriction.

Removed due to copyright restriction.

Removed due to copyright restriction.

Removed due to copyright restriction.

Removed due to copyright restriction.

Removed due to copyright restriction.

Removed due to copyright restriction.

Removed due to copyright restriction.

Removed due to copyright restriction.

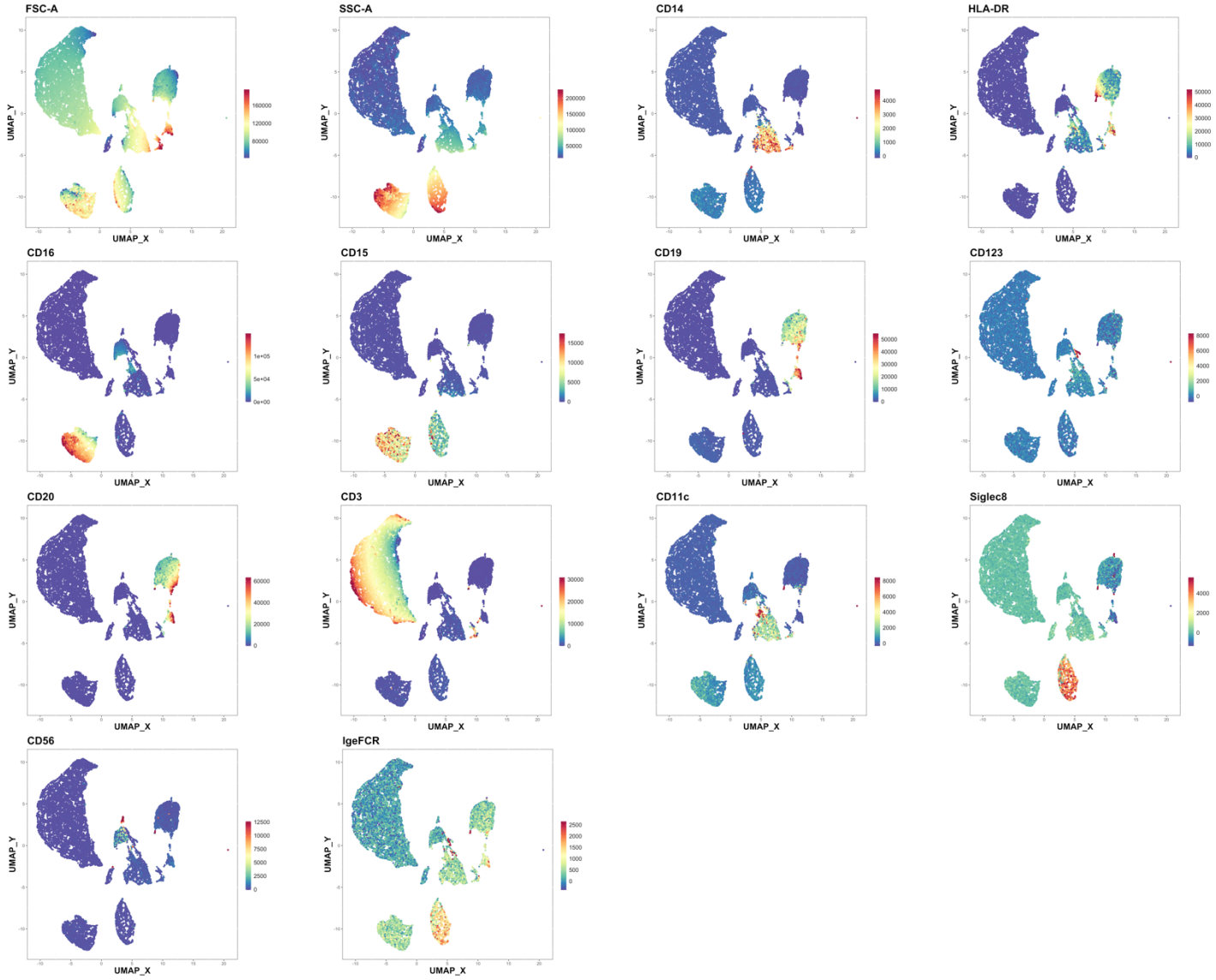

Figure S2.1| Unbiased clustering of markers identify unique cell populations. Multiplot UMAP using the Spectre discovery workflow on PBMCs assessed using the pan-leukocyte flow cytometry panel. UMAP generated from compensated CD45^{+} populations exported from a No ABX infant analysed using Flowjo. FSC-A, SSC-A, CD14, HLA-DR, CD16, CD15, CD19, CD123, CD20, CD3, CD11c, Siglec8, CD56 and IgE FCR (FcεRI) populations are shown.

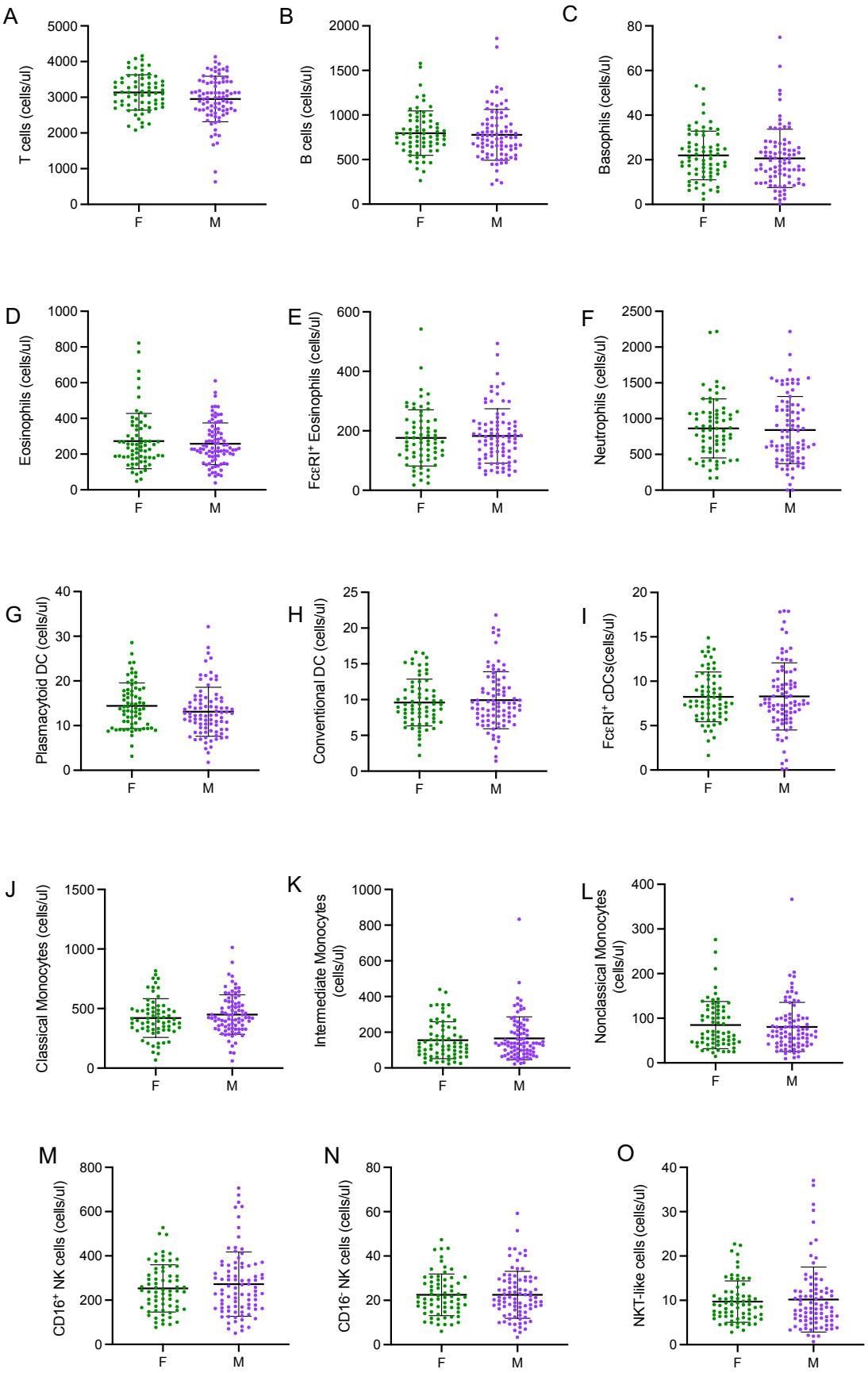
A
T cells (cells/ul)
5000
4000
3000
2000
1000
0
F
M
B
B cells (cells/ul)
2000
1500
1000
500
0
F
M
C
Basophils (cells/ul)
80
60
40
20
0
F
M
D
Eosinophils (cells/ul)
1000
800
600
400
200
0
F
M
E
FcεRI+ Eosinophils (cells/ul)
600
400
200
0
F
M
F
Neutrophils (cells/ul)
2500
2000
1500
1000
500
0
F
M
G
Plasmacytoid DC (cells/ul)
40
30
20
10
0
F
M
H
Conventional DC (cells/ul)
25
20
15
10
5
0
F
M
I
FcεRI+ cDCs(cells/ul)
20
15
10
5
0
F
M
J
Classical Monocytes (cells/ul)
1500
1000
500
0
F
M
K
Intermediate Monocytes (cells/ul)
1000
800
600
400
200
0
F
M
L
Nonclassical Monocytes (cells/ul)
400
300
200
100
0
F
M
M
CD16+ NK cells (cells/ul)
800
600
400
200
0
F
M
N
CD16- NK cells (cells/ul)
80
60
40
20
0
F
M
O
NKT-like cells (cells/ul)
40
30
20
10
0
F
M

Figure S2.2| No significant differences in the circulating immune cell populations defined using the pan-leukocyte when grouped by sex. The absolute number of **A|** T cells ($SSC^{lo}CD3^{+}$), **B|** B cells ($CD3^{-}CD56^{-}CD19^{+}$), **C|** Basophils ($SSC^{lo}CD3^{-}CD56^{-}CD14^{-}CD16^{-}CD19^{-}HLA\text{-}DR^{-}CD123^{+}$), **D|** Eosinophils ($SSC^{hi}CD16^{-}Siglec8^{+}$), **E|** $FcεRI^{+}$ eosinophils ($SSC^{hi}CD16^{-}Siglec8^{+}FcεRI^{+}$), **F|** Neutrophils ($SSC^{hi}CD16^{+}$), **G|** Plasmacytoid DC ($SSC^{lo}CD3^{-}CD56^{-}CD14^{-}CD16^{-}CD19^{-}HLA\text{-}DR^{+}CD11c^{-}CD123^{+}$), **H|** Conventional DCs ($SSC^{lo}CD3^{-}CD56^{-}CD14^{-}CD16^{-}CD19^{-}HLA\text{-}DR^{+}CD11c^{+}$), **I|** $FcεRI^{+}$ cDCs ($SSC^{lo}CD3^{-}CD56^{-}CD14^{-}CD16^{-}CD19^{-}HLA\text{-}DR^{+}CD11c^{+}FcεRI^{+}$), **J|** Classical Monocytes ($SSC^{lo}CD3^{-}CD56^{-}CD14^{++}CD16^{-}$), **K|** Intermediate Monocytes ($SSC^{lo}CD3^{-}CD56^{-}CD14^{+}CD16^{+}$), **L|** Nonclassical Monocytes ($SSC^{lo}CD3^{-}CD56^{-}CD14^{-}CD16^{+}$), **M|** $CD16^{+}$ NK cells ($SSC^{lo}CD3^{-}CD19^{-}CD56^{+}CD56^{+}CD16^{+}$), **N|** $CD16^{-}$ NK cells ($SSC^{lo}CD3^{-}CD19^{-}CD56^{+}CD56^{++}CD16^{-}$) and **O|** NKT-like cells ($CD3^{+}CD56^{+}$). Data are represented as the mean ± SEM. Statistical significance was assessed using a Mann-Whitney test as data were not normally distributed. F = Female, M= Male.

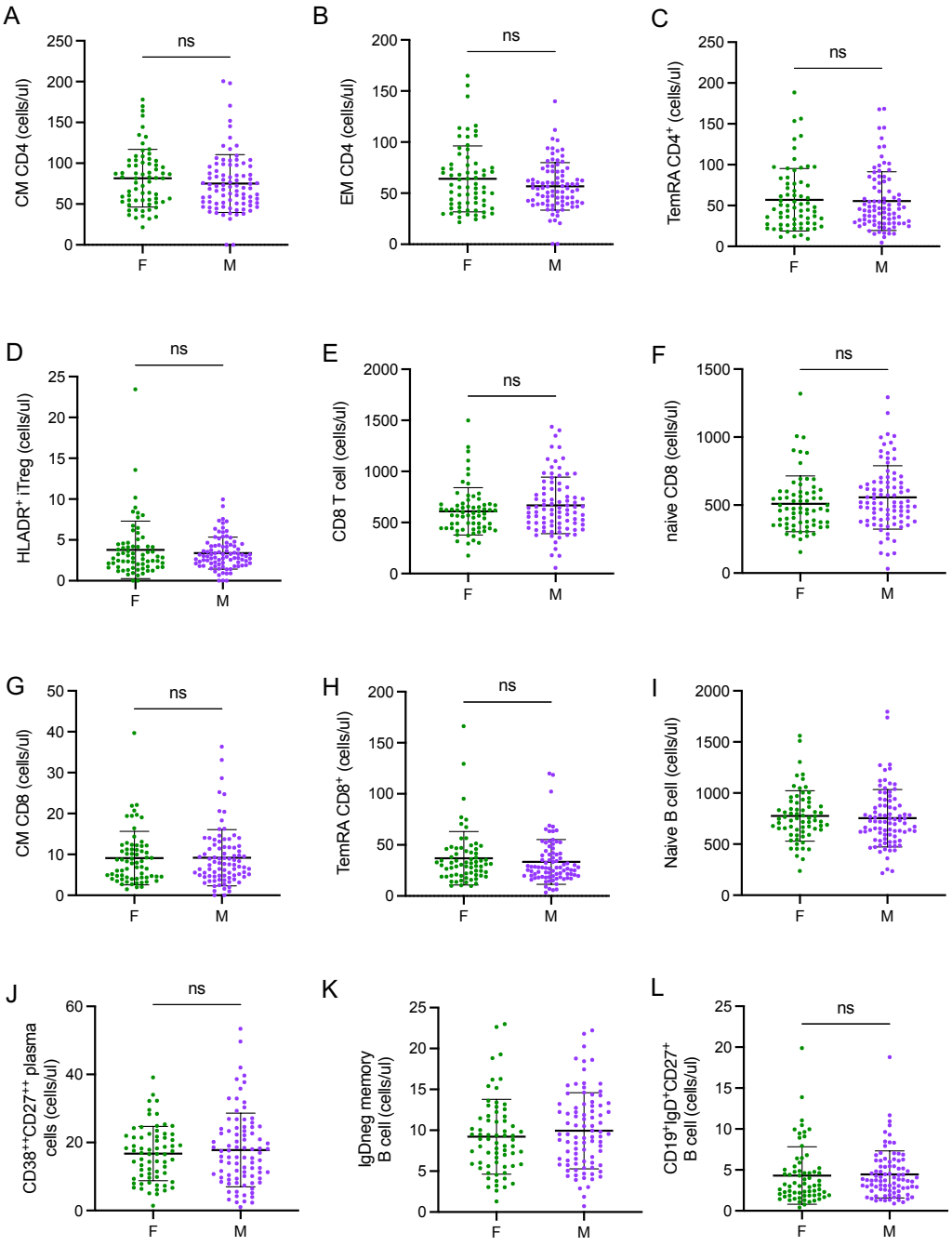

Figure S2.3| No significant differences in the majority of circulating B and T cell populations when grouped by sex. A| Central Memory CD4$^+$ T cell (T_{CM}) (CD3$^+$CD56$^-$ CD4$^+$CD45RA$^-$CCR7$^+$), **B|** Effector Memory CD4$^+$ T (T_{EM}) cell (CD3$^+$CD56$^-$CD4$^+$CD45RA$^-$ CCR7$^-$), **C|** TemRA CD4$^+$ T cells **(**CD3$^+$CD56CD4$^+$CD45RA$^+$CCR7$^-$), **D|** HLADR$^+$ iTreg cells (CD3$^+$CD4$^+$CD127$^-$CD25$^+$CD45RA$^-$HLADR$^+$), **E|** CD8$^+$ T cells (CD3$^+$CD56$^-$CD8$^+$), **F|** Naïve CD8$^+$ T cells (CD3$^+$CD56$^-$CD8$^+$CD45RA$^+$CD27$^+$) **G|** Central memory CD8$^+$ T cells (CD3$^+$CD56$^-$ CD8$^+$CD45RA$^-$CD27$^+$), **H|** TemRA CD8$^+$ T cells (CD3$^+$CD56$^-$CD8$^+$CD45RA$^+$CCR7$^-$), **I|** Naïve B cells (CD3$^-$CD56$^-$CD19$^+$CD27$^-$), **J|** CD38^{++}CD27^{++} plasma cells (CD3$^-$CD56$^-$CD19$^{+/-}$CD20$^-$ CD27^{++}CD38^{++}), **K|** Memory B cells (CD3$^-$CD56$^-$CD19$^+$IgD$^-$CD27$^+$) and **L|** IgD$^+$CD27$^+$ non-switched memory B cells/marginal zone B cells (CD3$^-$CD56$^-$CD19$^+$IgD$^+$CD27$^+$). Data are represented as the mean ± SEM. Statistical significance was assessed using a Mann-Whitney test as data were not normally distributed. F = Female, M= Male. ns = not significant.

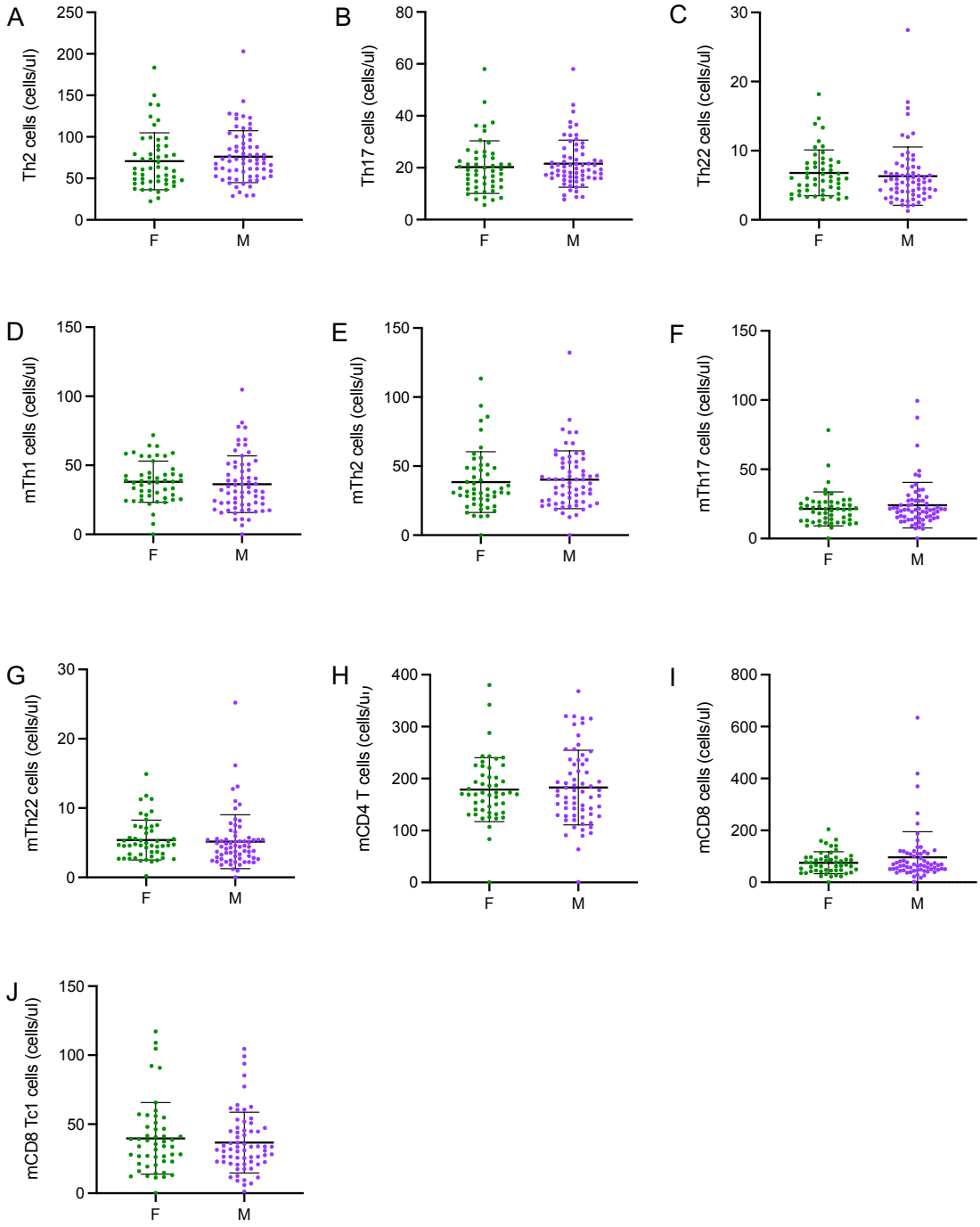

Figure S2.4| No significant differences in the circulating immune cell populations defined using the extended T cell panel when grouped by sex. The absolute number of **A|** Th2 cells ($CD3^+CD4^+CCR4^+CCR6^-$), **B|** Th17 cells ($CD3^+CD4^+CCR4^+CCR6^+CCR10^-CXCR3^-$), **C|** Th22 cells ($CD3^+CD4^+CCR4^+CCR6^+CCR10^+$), **D|** Th1 memory cells ($CD3^+CD4^+CD45RA^-CCR4^-CXCR3^+$), **E|** Th2 memory cells ($CD3^+CD4^+CCR4^+CCR6^-$), **F|** Th17 memory cells ($CD3^+CD4^+CCR4^+CCR6^+CCR10^-CXCR3^-$), **G|** Th22 memory cells ($CD3^+CD4^+CCR4^+CCR6^+CCR10^+$), **H|** $CD45RA^-$ $CD4^+$ T cells($CD3^+CD8^+CD45RA^-$), **I|** $CD45RA^-$ $CD8^+$ T cells ($CD3^+CD8^+CD45RA^-$) and **J|** $CD8^+$ Tc1 memory cells ($CD3^+CD8^+CD45RA^-CCR4^-CCR10^+$). Data are represented as the mean ± SEM. Statistical significance was assessed using a Mann-Whitney test as data were not normally distributed. F = Female, M= Male.

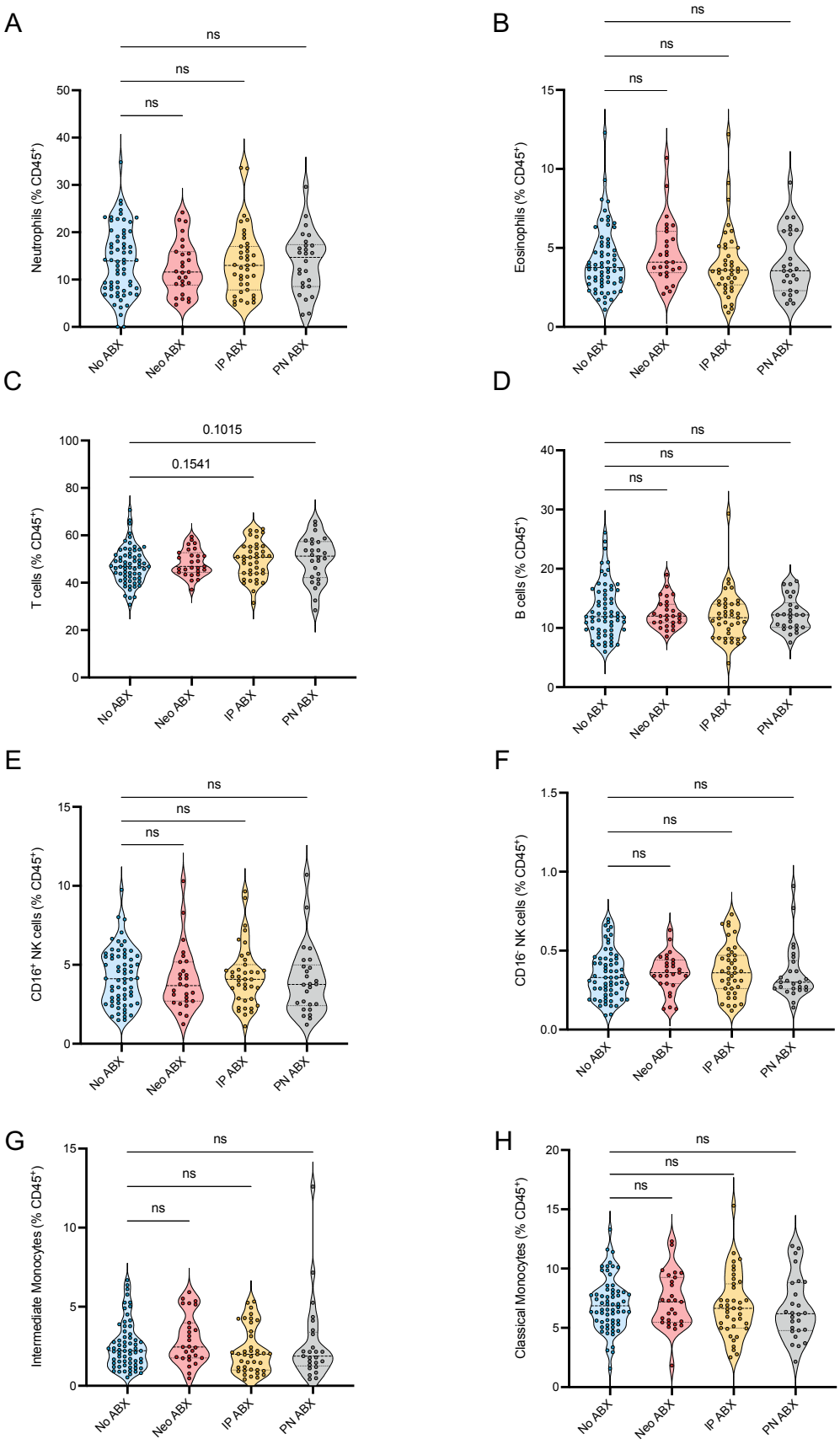
A
Neutrophils (% CD45+)
ns
ns
ns
No ABX
Neo ABX
IP ABX
PN ABX
B
Eosinophils (% CD45+)
C
T cells (% CD45+)
0.1015
0.1541
D
B cells (% CD45+)
E
CD16+ NK cells (% CD45+)
F
CD16- NK cells (% CD45+)
G
Intermediate Monocytes (% CD45+)
H
Classical Monocytes (% CD45+)

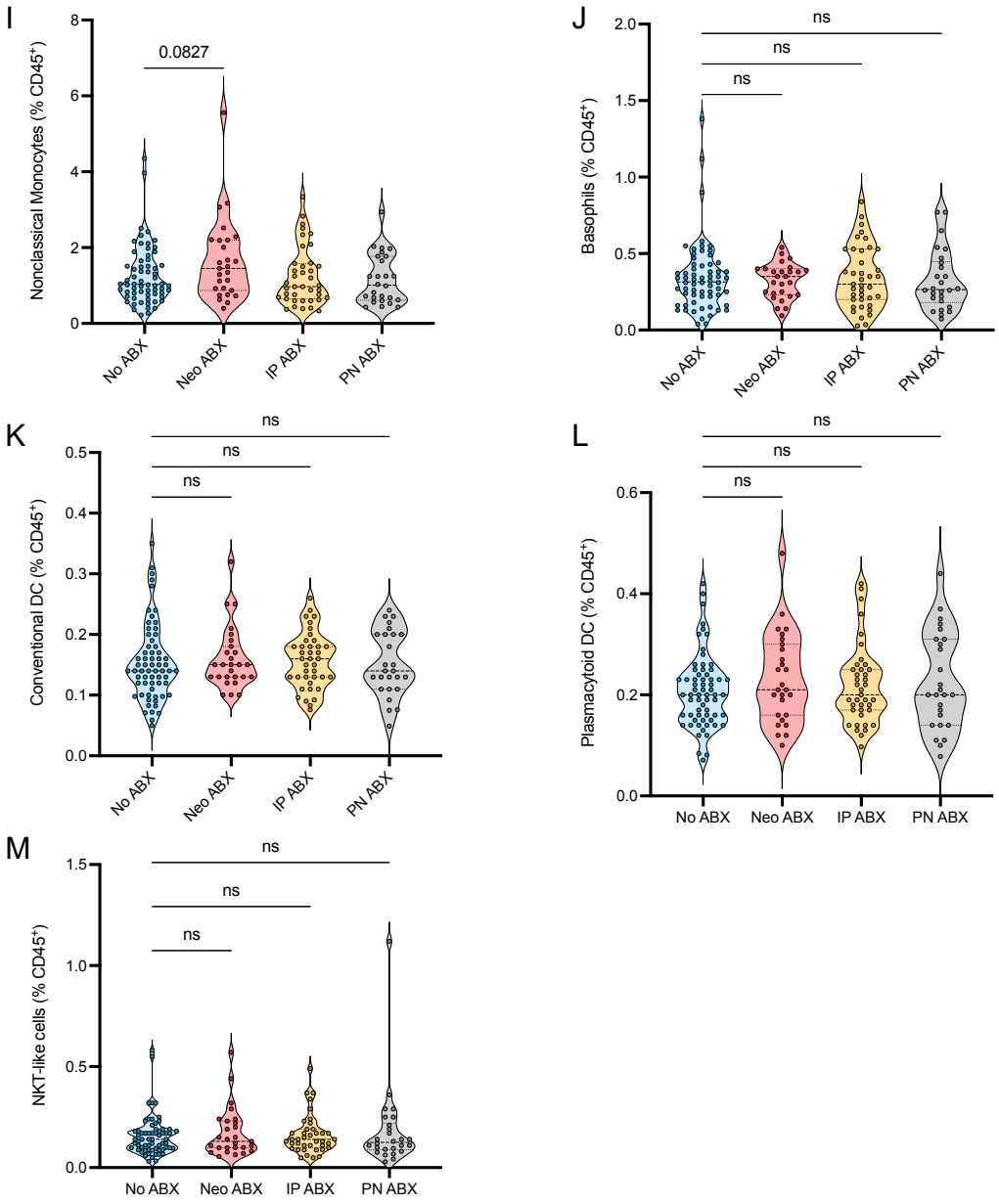

Figure S2.5| No significant differences in the pan-leukocyte panel as a frequency of total CD45$^+$ cells when grouped by ABX exposure group. The absolute number of **A|** Neutrophils (SSC^{hi}CD16$^+$), **B|** Eosinophils (SSC^{hi}CD16$^-$Siglec8$^+$), **C|** T cells (SSC^{lo}CD3$^+$), **D|** B cells (CD3$^-$CD56$^-$CD19$^+$), **E|** CD16$^+$ NK cells (SSC^{lo}CD3$^-$CD19$^-$CD56$^+$CD56$^+$CD16$^+$), **F|** CD16$^-$ NK cells (SSC^{lo}CD3$^-$CD19$^-$CD56$^+$CD56^{++}CD16$^-$), **G|** Intermediate Monocytes (SSC^{lo}CD3$^-$CD56$^-$CD14$^+$CD16$^+$), **H|** Classical Monocytes (SSC^{lo}CD3$^-$CD56$^-$CD14^{++}CD16$^-$), **I|** Nonclassical Monocytes (SSC^{lo}CD3$^-$CD56$^-$CD14$^-$CD16$^+$), **J|** Basophils (SSC^{lo}CD3$^-$CD56$^-$CD14$^-$CD16$^-$CD19$^-$HLA-DR$^-$CD123$^+$), **K|** Conventional DCs (SSC^{lo}CD3$^-$CD56$^-$CD14$^-$CD16$^-$CD19$^-$HLA-DR$^+$CD11c$^+$), **L|** Plasmacytoid DC (SSC^{lo}CD3$^-$CD56$^-$CD14$^-$CD16$^-$CD19$^-$HLA-DR$^+$CD11c$^-$CD123$^+$) and **M|** NKT-like cells (CD3$^+$CD56$^+$). Kruskal-Wallis tests were used to assess statistical significance. Dunn's multiple comparison tests was used to correct for multiple comparisons within each graph. Data are represented as a Violin plot, with the thick dashed representing the median and thinner dashed lines representing the quartiles. ns = not significant.

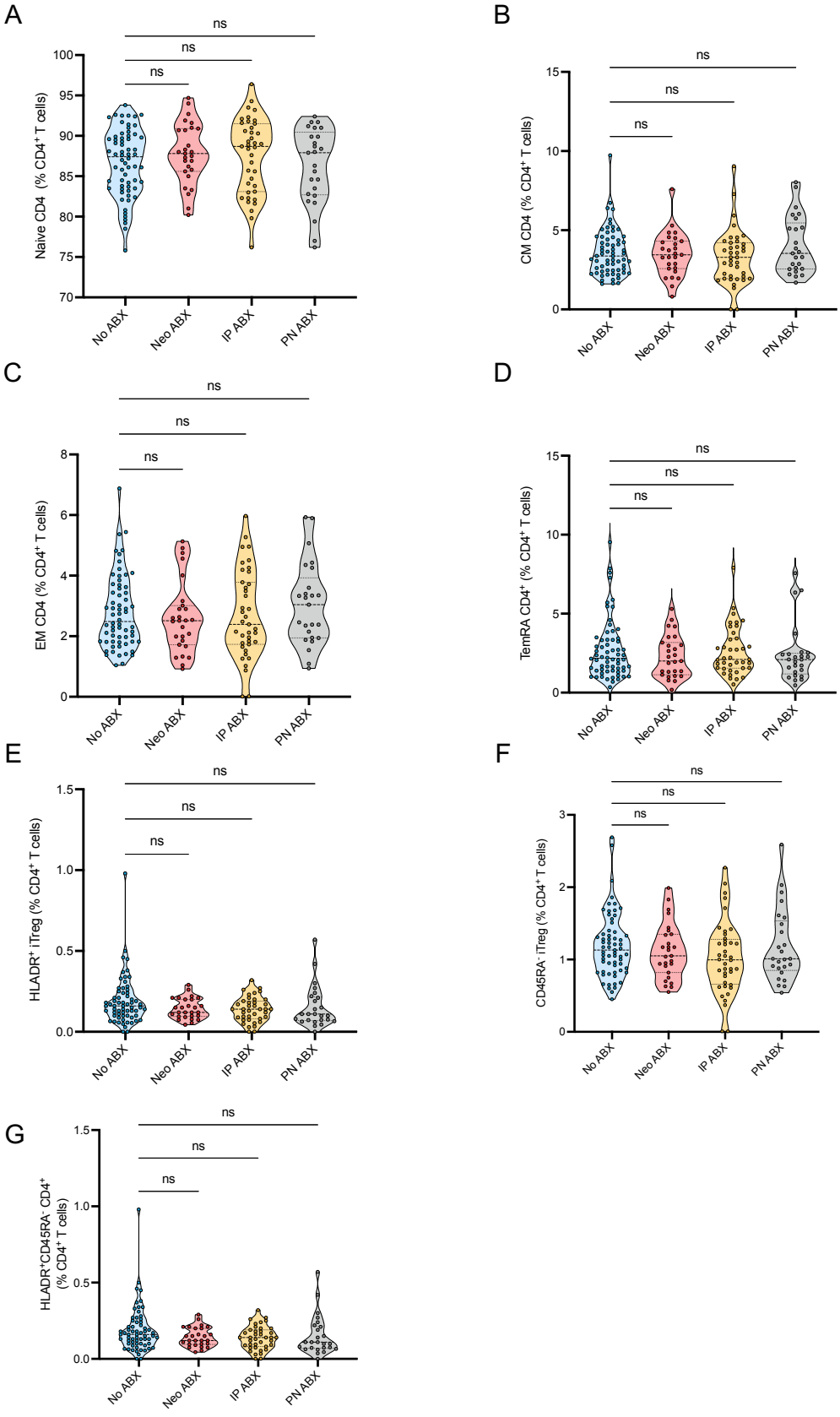
A
Naive CD4 (% CD4+ T cells)
B
CM CD4 (% CD4+ T cells)
C
EM CD4 (% CD4+ T cells)
D
TemRA CD4+ (% CD4+ T cells)
E
HLADR+ iTreg (% CD4+ T cells)
F
CD45RA- iTreg (% CD4+ T cells)
G
HLADR+CD45RA- CD4+ (% CD4+ T cells)
ns
No ABX
Neo ABX
IP ABX
PN ABX

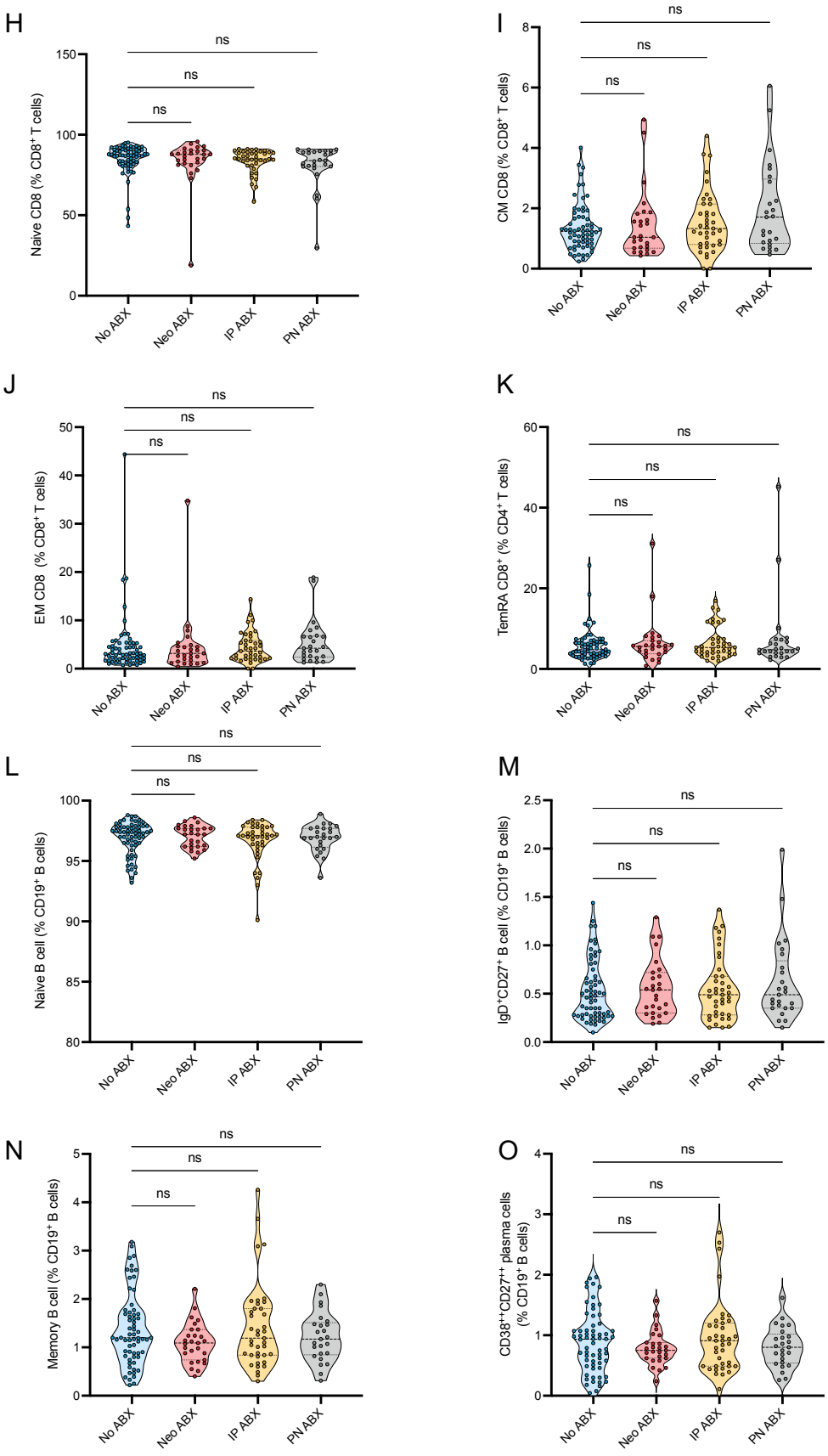

Figure S2.6| No significant differences in B and T cell panel % of CD4+ T cell, CD8+ T cell and CD19+ B cell subsets when grouped by ABX exposure group. The frequency of

of **A|** Naïve $CD4^+$ T cells ($CD3^+CD56^-CD4^+CD45RA^+CCR7^+$), **B|** Central Memory $CD4^+$ T cell (T_{CM}) ($CD3^+CD56^-CD4^+CD45RA^-CCR7^+$), **C|** Effector Memory $CD4^+$ T (T_{EM}) cell ($CD3^+CD56^-CD4^+CD45RA^-CCR7^-$), **D|** TemRA $CD4^+$ T cells (**(**$CD3^+CD56^-CD4^+CD45RA^+CCR7^-$) **F|** $CD3^+CD4^+CD127$-$CD25^+CD45RA^-$ **G|** $HLADR^+CD45RA^-$ $CD4^+$ T cells ($CD3^+CD4^+CD45RA^-HLADR^+$) **H|** Naïve $CD8^+$ T cells ($CD3^+CD56^-CD8^+CD45RA^+CD27^+$), **I|** Central memory $CD8^+$ T cells ($CD3^+CD56$-$CD8^+CD45RA^-CD27^+$), **J|** Effector Memory $CD8^+$ T cells ($CD3^+CD56^-CD8^+CD45RA^-CD27^-$), **K|** TemRA $CD8^+$ T cells ($CD3^+CD56^-CD8^+CD45RA^+CCR7^-$) **L|** Naïve B cells ($CD3^-CD56^-CD19^+CD27^-$), **M|** IgD^+CD27^+ non-switched memory B cells/marginal zone B cells ($CD3^-CD56^-CD19^+IgD^+CD27^+$), **N|** Memory B cells ($CD3^-CD56^-CD19^+IgD^-CD27^+$) and **O|** $CD38^{++}CD27^{++}$ plasma cells ($CD3^-CD56^-CD19^{+/-}CD20^-CD27^{++}CD38^{++}$). Kruskal-Wallis tests were used to assess statistical significance. Dunn's multiple comparison test was used to correct for multiple comparisons within each graph. Data are represented as a Violin plot, with the thick dashed representing the median and thinner dashed lines representing the quartiles. ns = not significant.

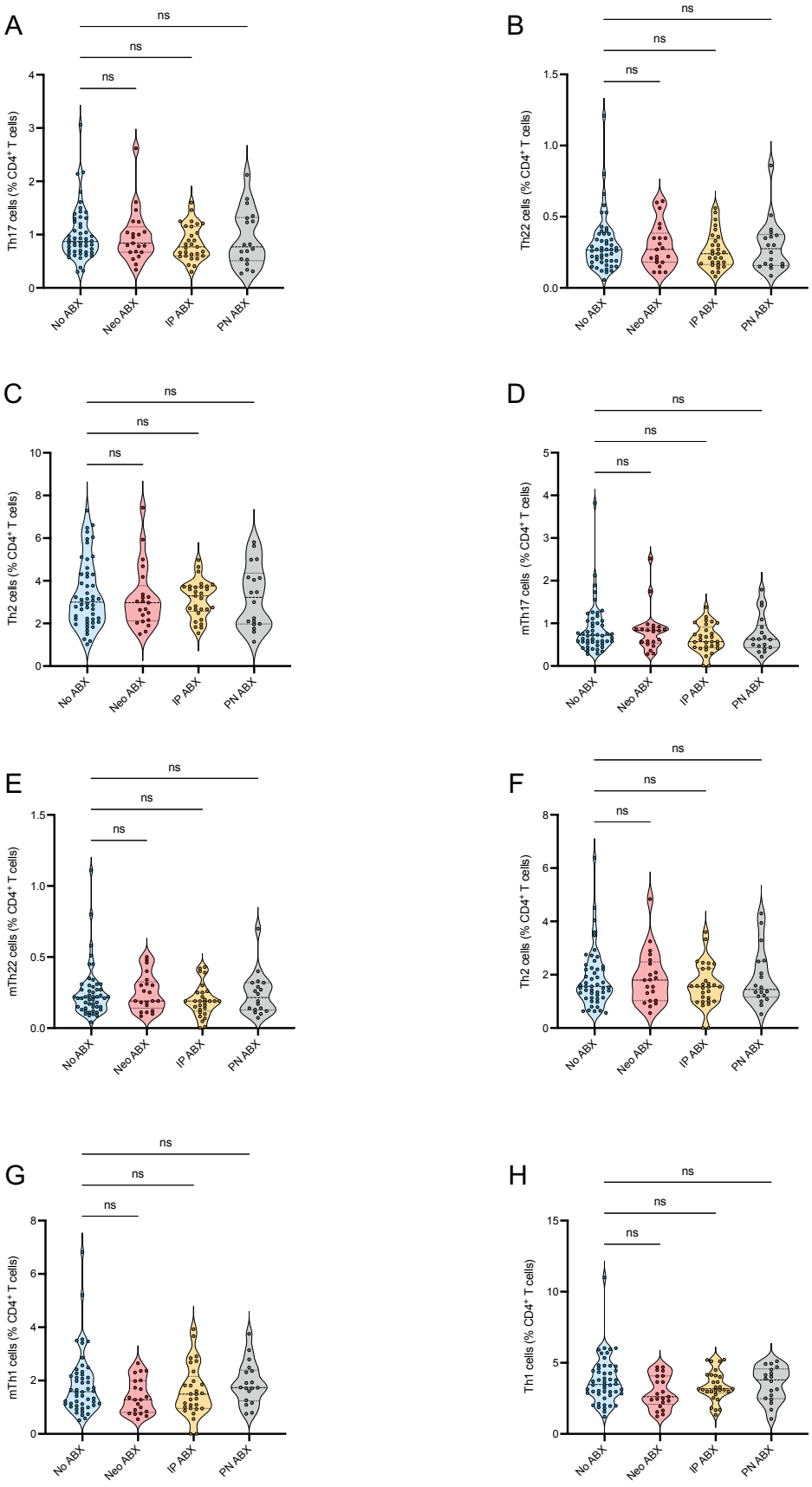
A
ns
ns
ns
Th17 cells (% CD4+ T cells)
No ABX
Neo ABX
IP ABX
PN ABX
B
ns
ns
ns
Th22 cells (% CD4+ T cells)
No ABX
Neo ABX
IP ABX
PN ABX
C
ns
ns
ns
Th2 cells (% CD4+ T cells)
No ABX
Neo ABX
IP ABX
PN ABX
D
ns
ns
ns
mTh17 cells (% CD4+ T cells)
No ABX
Neo ABX
IP ABX
PN ABX
E
ns
ns
ns
mTh22 cells (% CD4+ T cells)
No ABX
Neo ABX
IP ABX
PN ABX
F
ns
ns
ns
Th2 cells (% CD4+ T cells)
No ABX
Neo ABX
IP ABX
PN ABX
G
ns
ns
ns
mTh1 cells (% CD4+ T cells)
No ABX
Neo ABX
IP ABX
PN ABX
H
ns
ns
ns
Th1 cells (% CD4+ T cells)
No ABX
Neo ABX
IP ABX
PN ABX

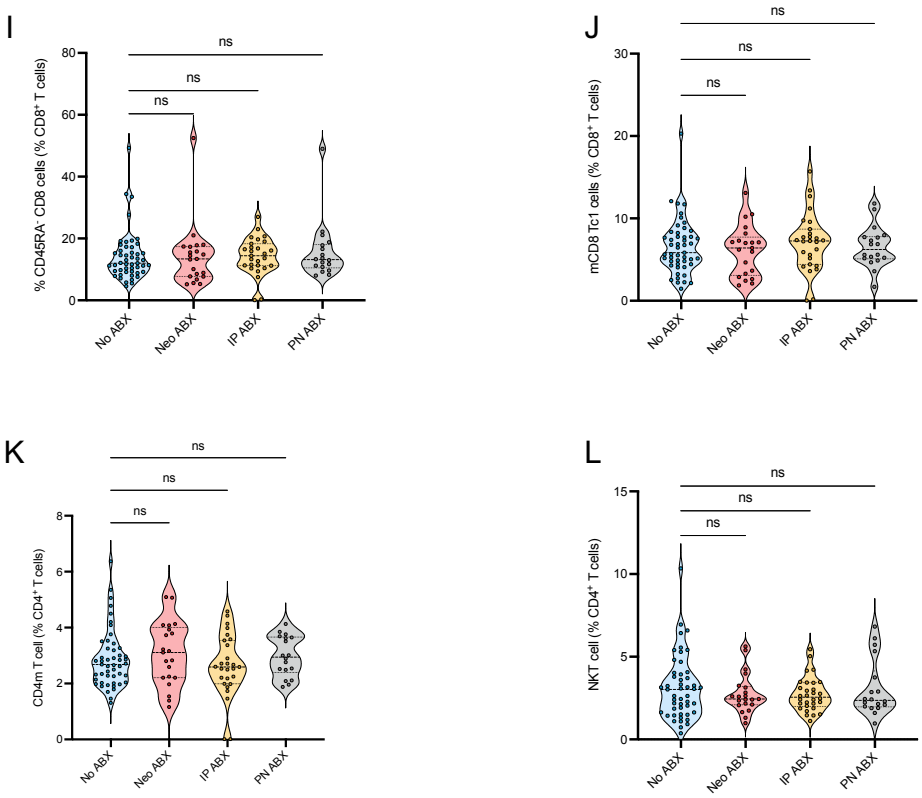

Figure S2.7| No significant differences in the extended B and T cell panel as a % of $CD4^+$ and $CD8^+$ T cell subsets when grouped by ABX exposure group. The frequency of **A|** Th17 cells ($CD3^+CD4^+CCR4^+CCR6^+CCR10^-CXCR3^-$), **B|** Th22 cells ($CD3^+CD4^+CCR4^+CCR6^+CCR10^+$), **C|** Th2 cells ($CD3^+CD4^+CCR4^+CCR6^-$), **D|** Th17 memory cells ($CD3^+CD4^+CCR4^+CCR6^+CCR10^-CXCR3^-$), **E|** Th22 memory cells ($CD3^+CD4^+CCR4^+CCR6^+CCR10^+$), **F|** Th2 cells ($CD3^+CD4^+CCR4^+CCR6^-$), **G|** Th1 memory cells ($CD3^+CD4^+CD45RA^-CCR4^-CXCR3^+$), **H|** Th1 cells ($CD3^+CD4^+CCR4^+CCR3^+$), **I|** $CD45RA^-$ $CD8^+$ T cells ($CD3^+CD8^+CD45RA^-$), **J|** $CD8^+$ Tc1 memory cells ($CD3^+CD8^+CD45RA^-CCR4^-CCR10^+$), **K|** $CD45RA^-$ $CD4^+$ T cells ($CD3^+CD8^+CD45RA^-$), and **L|** NKT cells ($CD3^+$CD1d-tet^+). Kruskal-Wallis test was used to assess statistical significance. Dunn's multiple comparison test was used to correct for multiple comparisons within each graph. Data are represented as a Violin plot, with the thick dashed representing the median and thinner dashed lines representing the quartiles. ns = not significant.

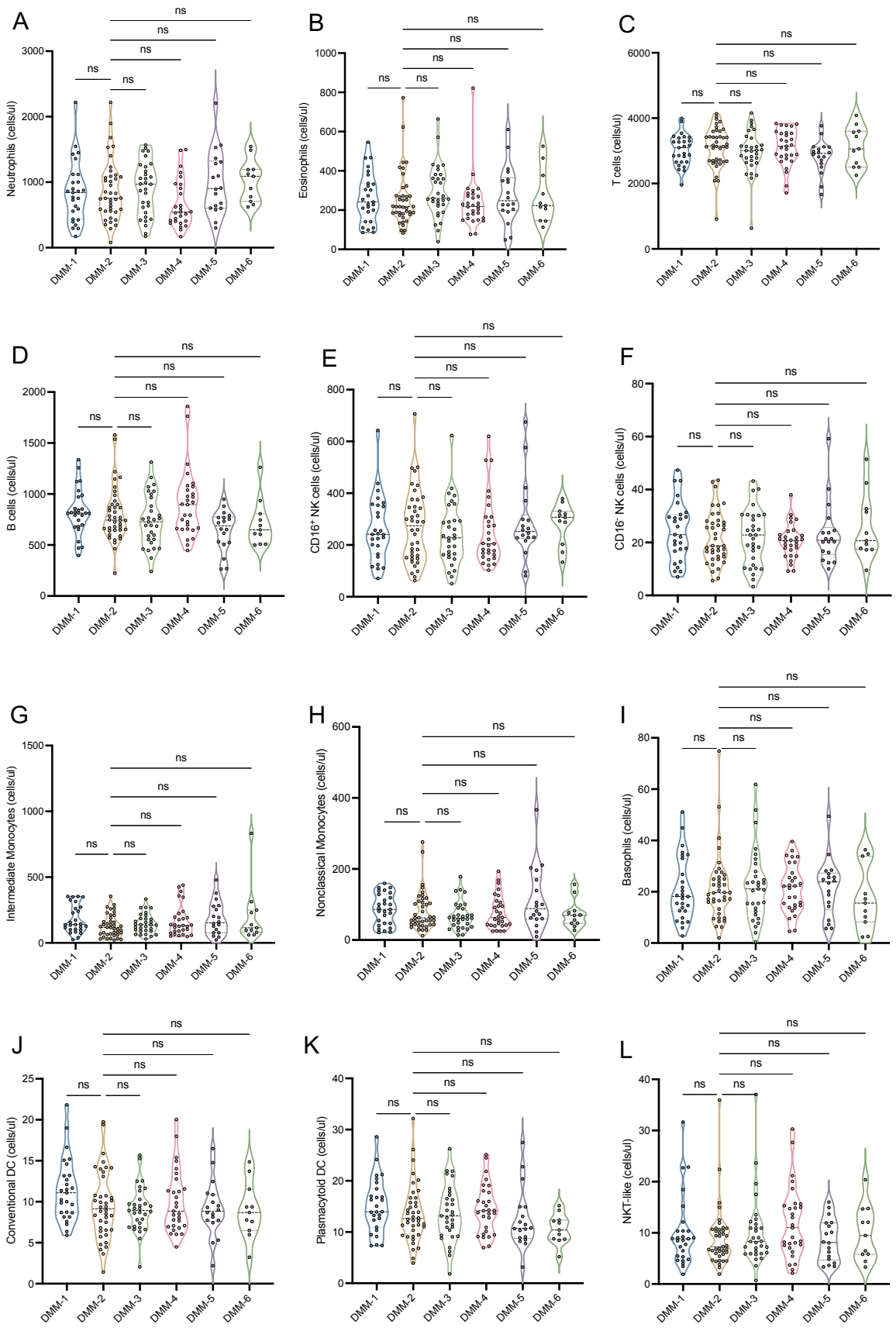
A
Neutrophils (cells/ul)
B
Eosinophils (cells/ul)
C
T cells (cells/ul)
D
B cells (cells/ul)
E
CD16+ NK cells (cells/ul)
F
CD16- NK cells (cells/ul)
G
Intermediate Monocytes (cells/ul)
H
Nonclassical Monocytes (cells/ul)
I
Basophils (cells/ul)
J
Conventional DC (cells/ul)
K
Plasmacytoid DC (cells/ul)
L
NKT-like (cells/ul)
ns
DMM-1
DMM-2
DMM-3
DMM-4
DMM-5
DMM-6

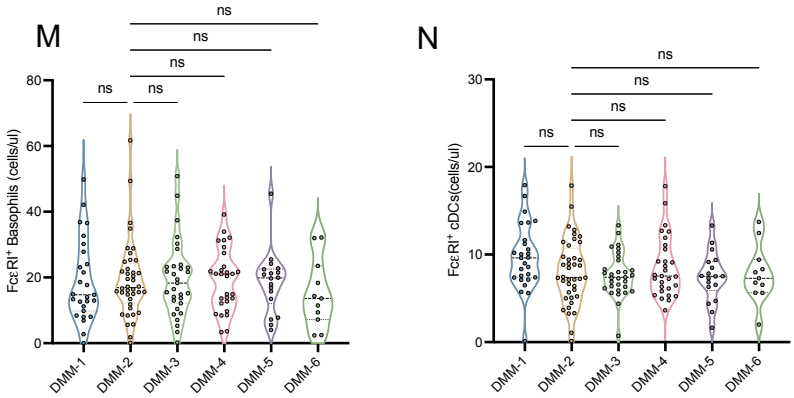

Figure S2.8| Pan-leukocyte panel cell numbers grouped by DMM cluster. The absolute number of **A|** Neutrophils ($SSC^{hi}CD16^{+}$), **B|** Eosinophils ($SSC^{hi}CD16^{-}Siglec8^{+}$), **C|** T cells ($SSC^{lo}CD3^{+}$), **D|** B cells ($CD3^{-}CD56^{-}CD19^{+}$), **E|** $CD16^{+}$ NK cells ($SSC^{lo}CD3^{-}CD19^{-}CD56^{+}CD56^{+}CD16^{+}$), **F|** $CD16^{-}$ NK cells ($SSC^{lo}CD3^{-}CD19^{-}CD56^{+}CD56^{++}CD16^{-}$), **G|** Intermediate Monocytes ($SSC^{lo}CD3^{-}CD56^{-}CD14^{+}CD16^{+}$), **H|** Nonclassical Monocytes ($SSC^{lo}CD3^{-}CD56^{-}CD14^{-}CD16^{+}$), **I|** Basophils ($SSC^{lo}CD3^{-}CD56^{-}CD14^{-}CD16^{-}CD19^{-}$HLA-$DR^{-}CD123^{+}$), **J|** Conventional DCs ($SSC^{lo}CD3^{-}CD56^{-}CD14^{-}CD16^{-}CD19^{-}$HLA-$DR^{+}CD11c^{+}$), **K|** Plasmacytoid DC ($SSC^{lo}CD3^{-}CD56^{-}CD14^{-}CD16^{-}CD19^{-}$HLA-$DR^{+}CD11c^{-}CD123^{+}$), **L|** NKT-like cells ($CD3^{+}CD56^{+}$), **M|** $FcεRI^{+}$ basophils ($SSC^{lo}CD3^{-}CD56^{-}CD14^{-}CD16^{-}CD19^{-}$HLA-$DR^{-}CD123^{+}FcεRI^{+}$) **N|** $FcεRI^{+}$ cDCs ($SSC^{lo}CD3^{-}CD56^{-}CD14^{-}CD16^{-}CD19^{-}$HLA-$DR^{+}CD11c^{+}FcεRI^{+}$). All cell populations are $CD45^{+}$. Kruskal-Wallis tests were used to assess statistical significance. Dunn's multiple comparison tests was used to correct for multiple comparisons within each graph. Data are represented as a Violin plot, with the thick dashed representing the median and thinner dashed lines representing the quartiles. ns = not significant.

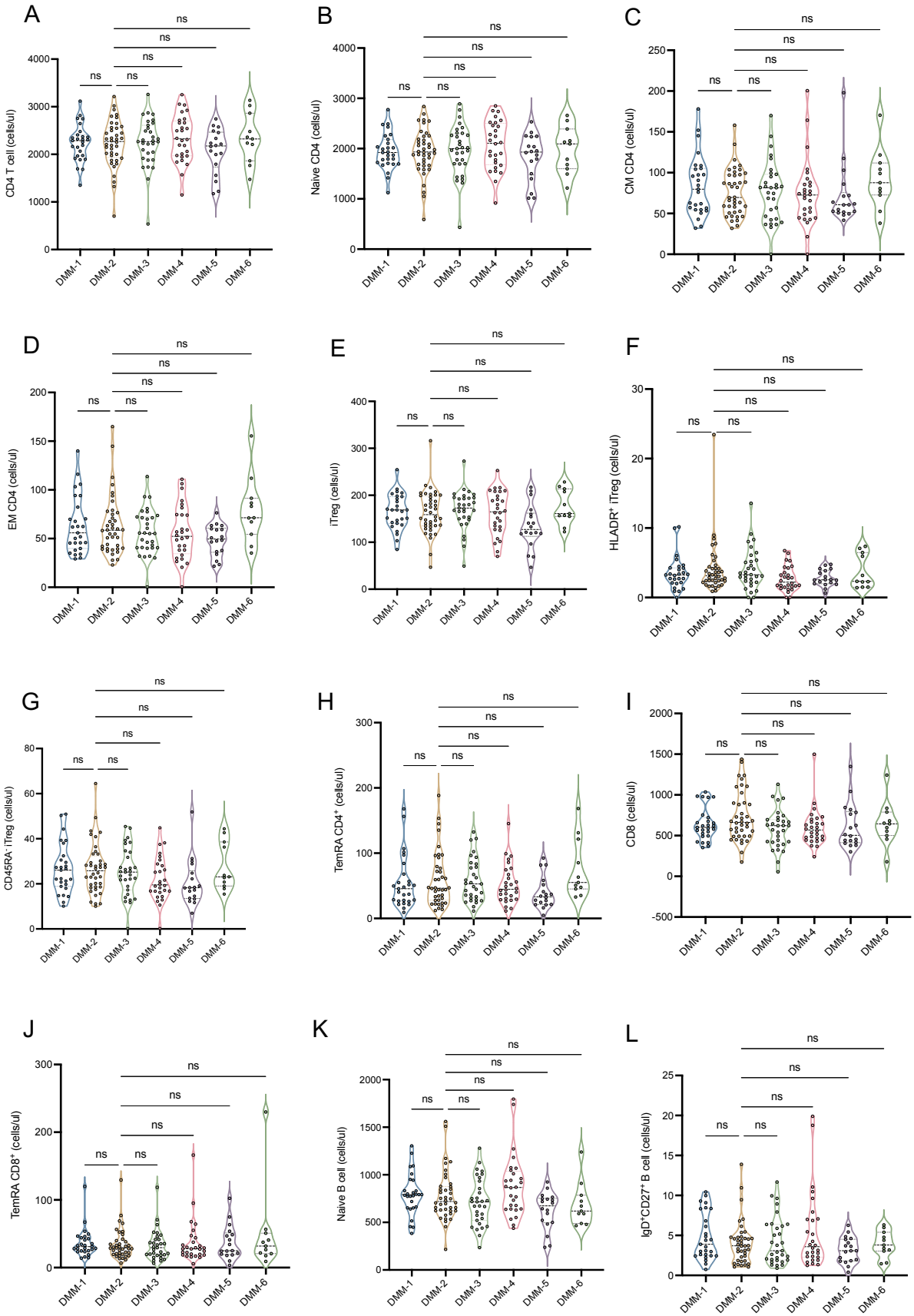
A
CD4 T cell (cells/ul)
B
Naive CD4 (cells/ul)
C
CM CD4 (cells/ul)
D
EM CD4 (cells/ul)
E
iTreg (cells/ul)
F
HLADR+ iTreg (cells/ul)
G
CD45RA- iTreg (cells/ul)
H
TemRA CD4+ (cells/ul)
I
CD8 (cells/ul)
J
TemRA CD8+ (cells/ul)
K
Naive B cell (cells/ul)
L
IgD+CD27+ B cell (cells/ul)
ns
DMM-1
DMM-2
DMM-3
DMM-4
DMM-5
DMM-6

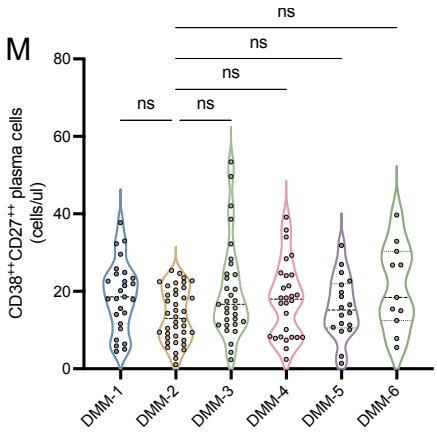

Figure S2.9| B and T cell panel cell numbers grouped by DMM cluster. The absolute number of **A|** $CD4^+$ T cells ($CD3^+CD56^-CD4^+$), **B|** Naïve $CD4^+$ T cells ($CD3^+CD56^-CD4^+CD45RA^+CCR7^+$), **C|** Central Memory $CD4^+$ T cell (T_{CM}) ($CD3^+CD56^-CD4^+CD45RA^-CCR7^+$), **D|** Effector Memory $CD4^+$ T (T_{EM}) cell ($CD3^+CD56^-CD4^+CD45RA^-CCR7^-$), **E|** iTregs **(**$CD3^+CD4^+CD127\text{-}CD25^+$) **F|** $HLADR^+$ iTreg cells ($CD3^+CD4^+CD127^-CD25^+CD45RA^-HLADR^+$) **G|** $CD45RA^-$ iTregs **(**$CD3^+CD4^+CD127\text{-}CD25^+CD45RA^-$), **H|** TemRA $CD4^+$ T cells **(**$CD3^+CD56^-CD4^+CD45RA^+CCR7^-$) **I|** $CD8^+$ T cells ($CD3^+CD56^-CD8^+$), **J|** TemRA $CD8^+$ T cells ($CD3^+CD56^-CD8^+CD45RA^+CCR7^-$), **K|** Naïve B cells ($CD3^-CD56^-CD19^+CD27^-$), **L|** IgD^+CD27^+ non-switched memory B cells/marginal zone B cells ($CD3^-CD56^-CD19^+IgD^+CD27^+$) and **M|** $CD38^{++}CD27^{++}$ plasma cells ($CD3^-CD56^-CD19^{+/-}CD20^-CD27^{++}CD38^{++}$). Kruskal-Wallis tests were used to assess statistical significance. Dunn's multiple comparison test was used to correct for multiple comparisons within each graph. Data are represented as a Violin plot, with the thick dashed representing the median and thinner dashed lines representing the quartiles. ns = not significant.

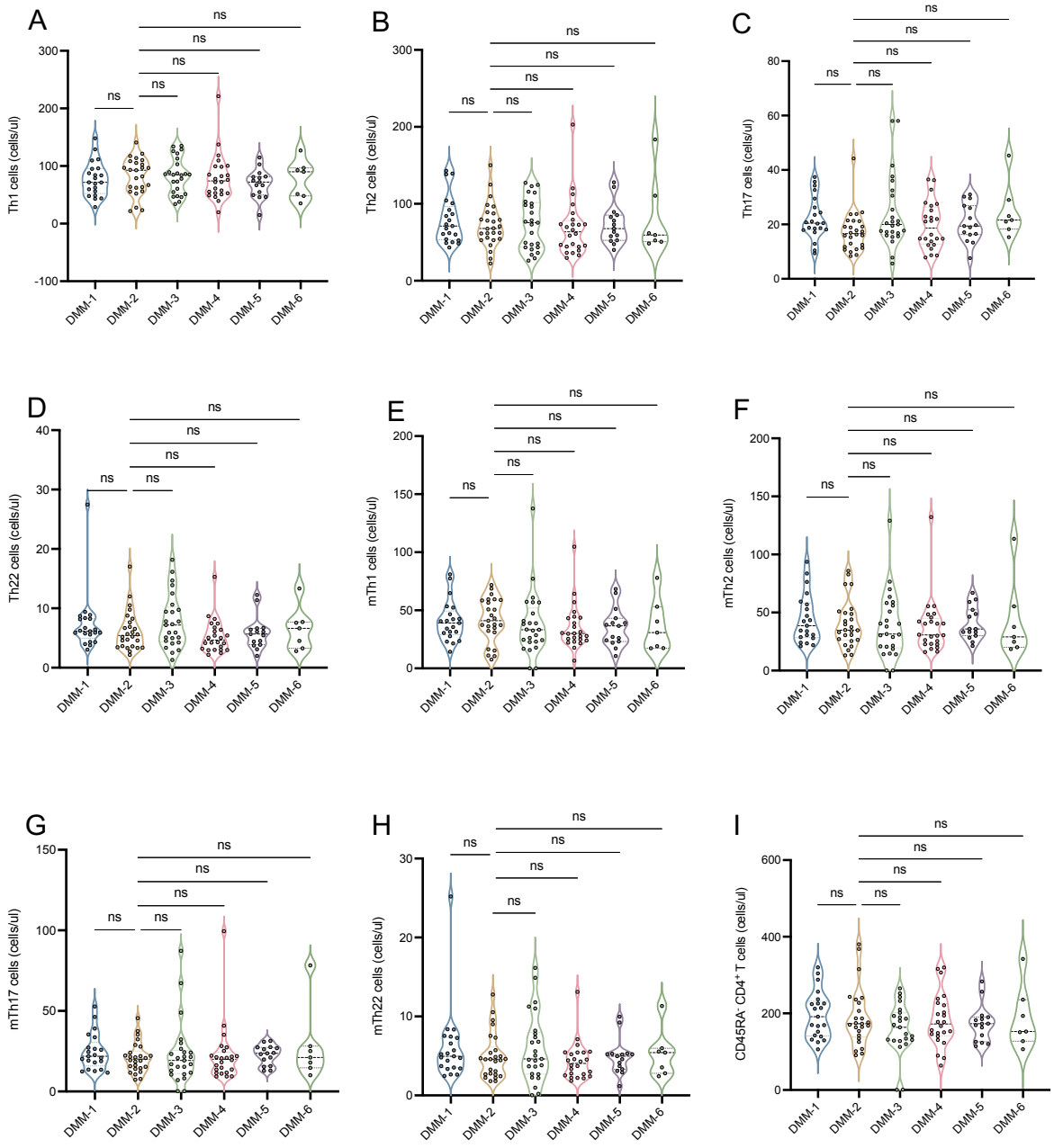

Figure S2.10| Extended T cell panel cell numbers grouped by DMM cluster. The absolute number of **A|** Th1 cells ($CD3^+CD4^+CCR4^+CCR3^+$), **B|** Th2 cells ($CD3^+CD4^+CCR4^+CCR6^-$), **C|** Th17 cells ($CD3^+CD4^+CCR4^+CCR6^+CCR10^-CXCR3^-$), **D|** Th22 cells ($CD3^+CD4^+CCR4^+CCR6^+CCR10^+$), E| Th1 memory cells ($CD3^+CD4^+CD45RA^-CCR4^-CXCR3^+$), **F|** Th2 memory cells ($CD3^+CD4^+CCR4^+CCR6^-$), **G|** Th17 memory cells ($CD3^+CD4^+CCR4^+CCR6^+CCR10^-CXCR3^-$), **H|** Th22 memory cells ($CD3^+CD4^+CCR4^+CCR6^+CCR10^+$) and **I|** $CD45RA^-$ $CD4^+$ T cells ($CD3^+CD8^+CD45RA^-$). ns = not significant.

Appendix 3: Supplementary Material from Chapter 4

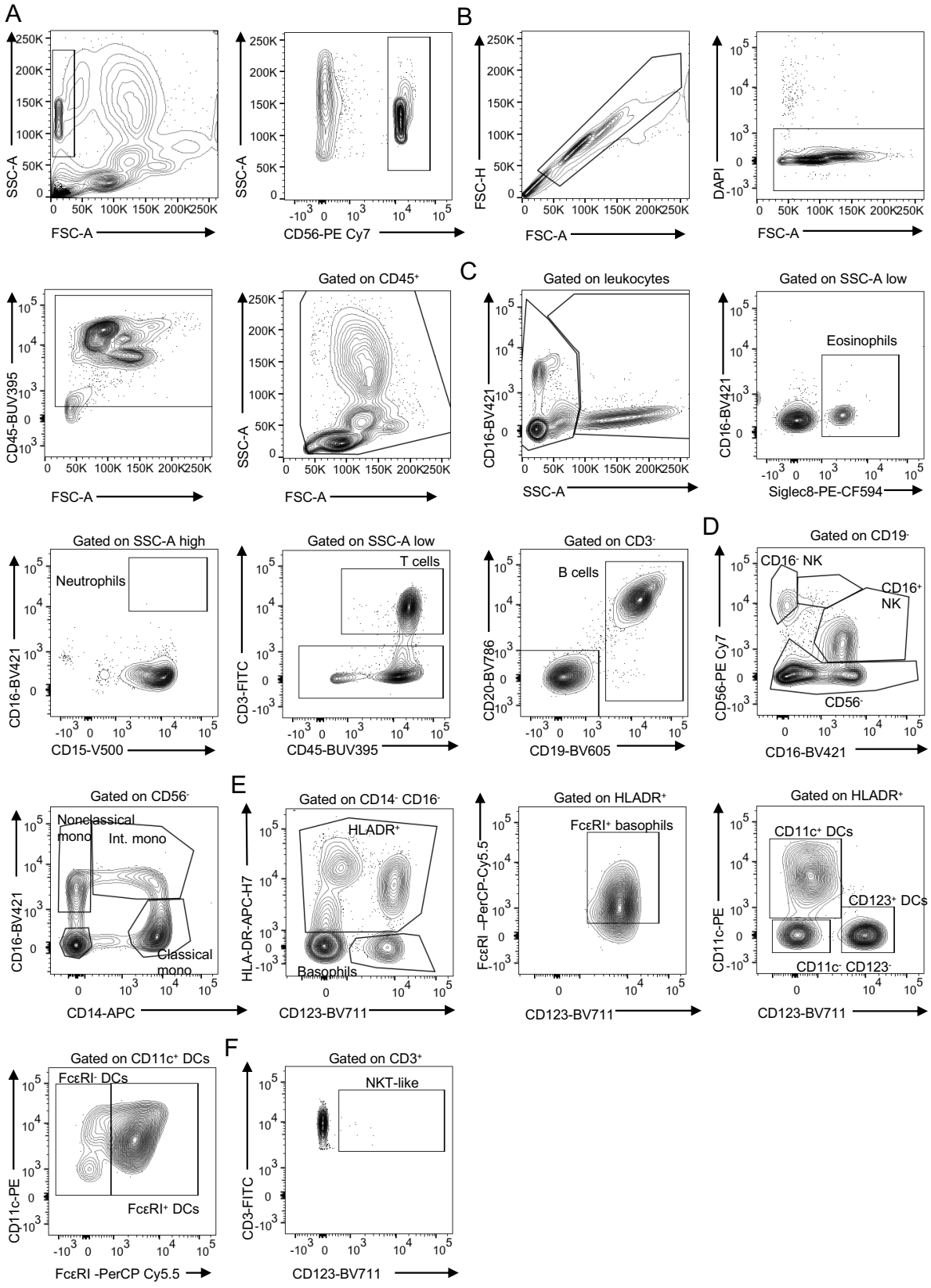

Figure S3.1| PAN panel illustrates CD16 absence in infant WCH-028 but no other obvious defects. A| Beads from each Trucount tube were recorded from the FSCxSSC gate

and then the PE^{hi} population. **B|** For all pan-leukocyte panel analyses, cells were gated by singlet discrimination, followed by live ($DAPI^-$), $CD45^+$ and $CD45^+$ leukocytes. **C|** Leukocytes were split into SSC high and low populations. Eosinophils and neutrophils were gated on SSC low and high populations, respectively. T cells were gated on SSC low $CD3^{hi}$, and $CD3^-$ cells were further defined as $CD19^+CD20^+$ B cells. **D|** The $CD19^-$ population was gated on to define $CD16^-CD56^+$ NK cells. $CD56^-$ cells were further gated on CD16 and CD14 expression identifying monocyte populations. **E|** Remaining $CD14^-CD16^-$ cells were further gated on HLA-DR and CD123 expression to identify $CD123^+$HLA-DR^- basophils. Basophils were further gated based positive expression of FcεRI. HLA-DR^+ cells were gated on CD11c and CD123 in order to identify various DC populations. Conventional $CD11c^+$ DCs were further gated based on their expression of FcεRI. **F|** $CD3^+$ T cells were gated further on their CD56 expression to identify $CD56^+CD3^+$ NKT-like cells. An additional $FcεRI^+$ population was also gated from the eosinophil gate.

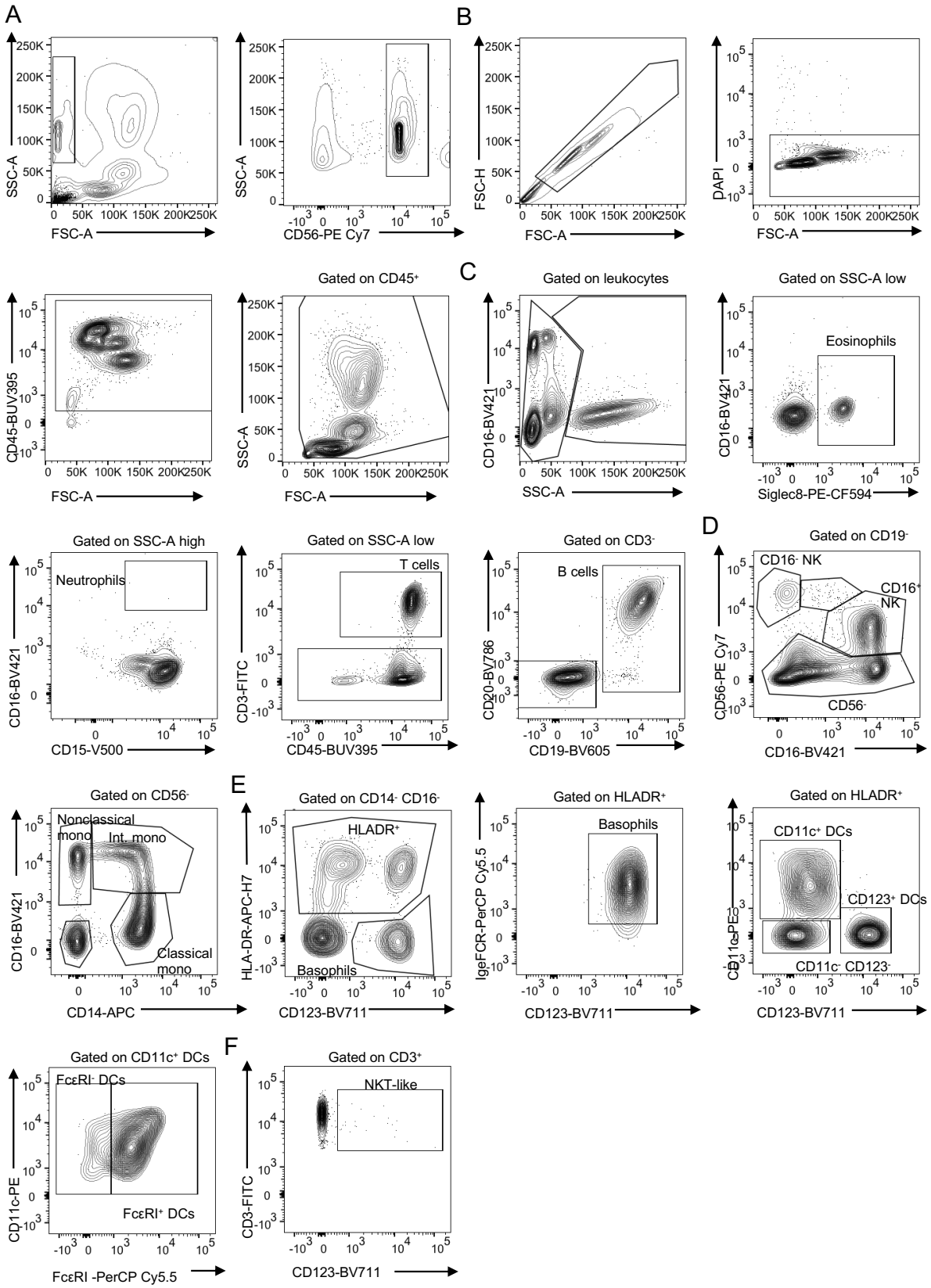

Figure S3.2| PAN panel illustrates CD16 absence in infant WCH-227 but no other obvious defects. A| Beads from each Trucount tube were recorded from the FSCxSSC gate and then the PE^{hi} population. **B|** For all pan-leukocyte panel analyses, cells were gated by singlet discrimination, followed by live ($DAPI^-$), $CD45^+$ and $CD45^+$ leukocytes. **C|** Leukocytes were split into SSC high and low populations. Eosinophils and neutrophils were gated on SSC

low and high populations, respectively. T cells were gated on SSC low $CD3^{hi}$, and $CD3^-$ cells were further defined as $CD19^+CD20^+$ B cells. **D|** The $CD19^-$ population was gated on to define $CD16^-CD56^+$ NK cells. $CD56^-$ cells were further gated on CD16 and CD14 expression identifying monocyte populations. **E|** Remaining $CD14^-CD16^-$ cells were further gated on HLA-DR and CD123 expression to identify $CD123^+$HLA-DR^- basophils. Basophils were further gated based positive expression of FcεRI. HLA-DR^+ cells were gated on CD11c and CD123 in order to identify various DC populations. Conventional $CD11c^+$ DCs were further gated based on their expression of FcεRI. **F|** $CD3^+$ T cells were gated further on their CD56 expression to identify $CD56^+CD3^+$ NKT-like cells. An additional $FcεRI^+$ population was also gated from the eosinophil gate.

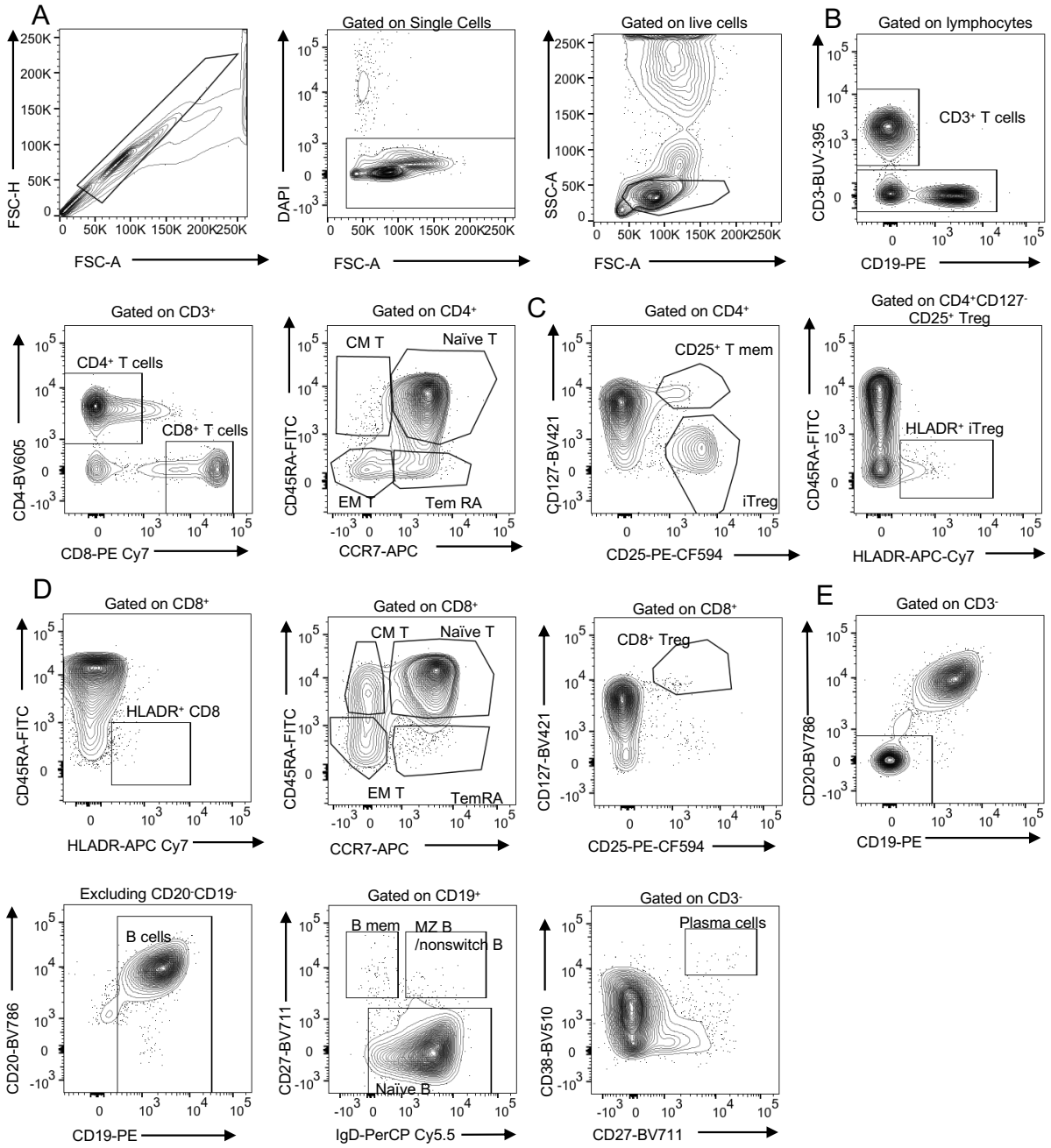

Figure S3.3| WCH-028 B and T cell populations show no obvious defects. A| For all B and T cell panel analyses, cells were gated by singlet discrimination, live ($DAPI^-$) and for leukocytes ($SSC\text{-}A^{lo}$) **B|** $CD3^+$ T cells were gated on $CD4^+$ and $CD8^+$ expression. $CD4^+$ T cells were then defined as $CD45RA^+HLADR^-$ TemRA $CD4^+$ T cells, $CCR7^+CD45RA^+$ Naïve $CD4^+$ T cells (naïve T), $CCR7^+CD45RA^-$ CD4 central memory T cells (CM T), $CCR7^-CD45RA^-$ $CD4^+$ effector memory T cells. **C|** $CD4^+$ T cells were also gated on CD127 and CD25 expression to identify $CD127^-CD25^+$ iTregs, further gated for CD45RA and HLADR expression to identify $CD45RA^-HLADR^+$ iTregs. **D|** $CD8^+$ T cells were then defined as $CD45RA^+HLADR^-$ $CD8^+$ TemRA T cells, $CCR7^+CD45RA^+$ Naïve CD8 T cells (naïve T), $CCR7^+CD45RA^-$ $CD8^+$ central memory T cells (CM T), $CCR7^-CD45RA^-$ $CD8^+$ effector memory T cells (EM T). A population of $CD8^+CD25^+CD127^+$ Tregs was also identified from the $CD8^+$ T cell gate. **E|** The $CD3^-$ population from B| was gated further on CD20 and CD19 so that $CD20^-CD19^-$ cells could be gated out and $CD19^+$ B cells could then be identified. These were further divided into a CD38 and CD20 gate to identify $CD38^+CD20^-$ plasma cells and an IgD and CD27 gate was applied

to identify IgD$^-$CD27$^+$ Memory B cells, IgD$^+$CD27$^+$ non-switched memory B cells/marginal zone-like B cells and IgD$^-$ naïve B cells.

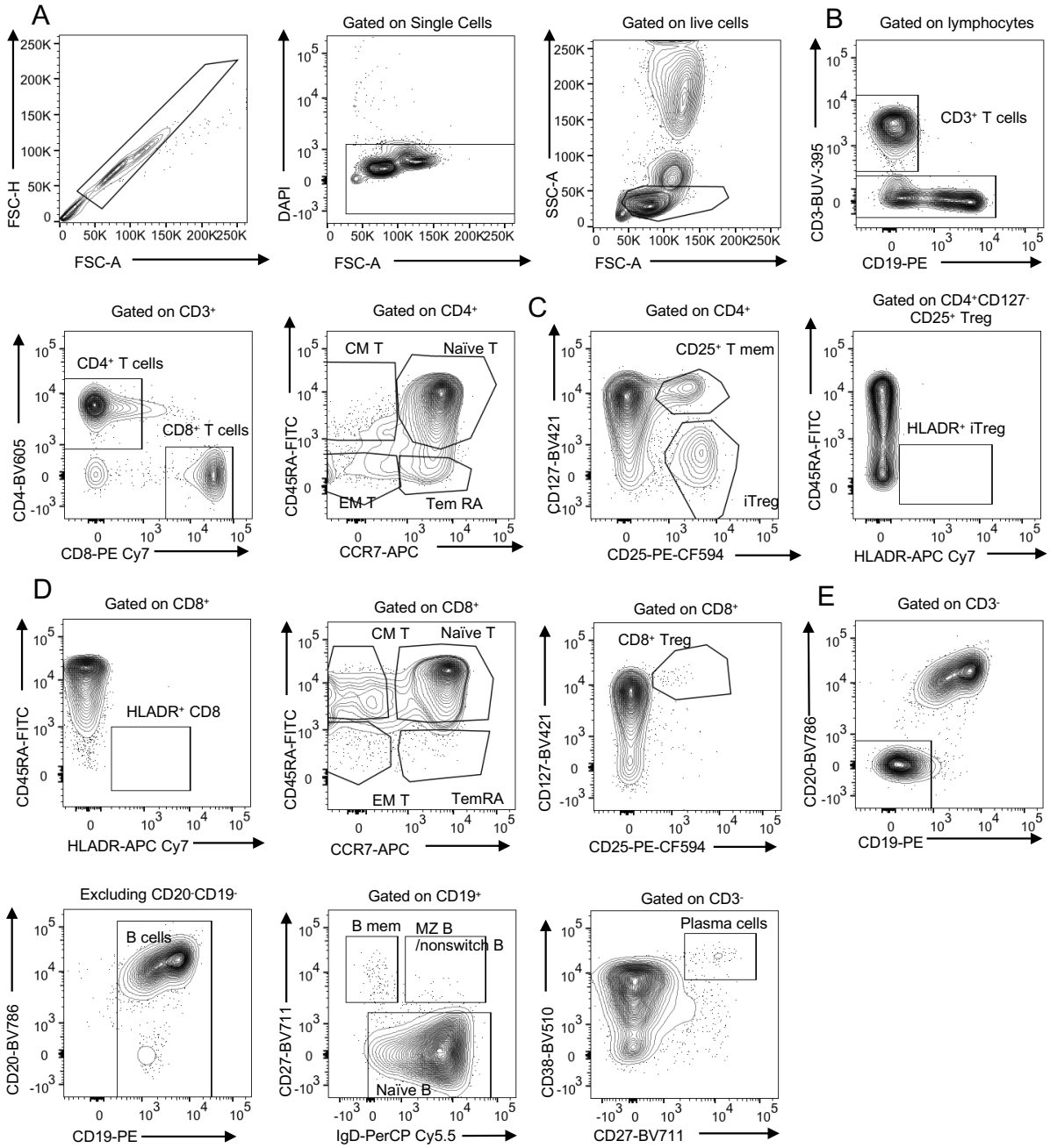

Figure S3.4| WCH-227 B and T cell populations show no obvious defects. A| For all B and T cell panel analyses, cells were gated by singlet discrimination, live (DAPI$^-$) and for leukocytes (SSC-A^{lo}) **B|** CD3$^+$ T cells were gated on CD4$^+$ and CD8$^+$ expression. CD4$^+$ T cells were then defined as CD45RA$^+$HLADR$^-$ TemRA CD4$^+$ T cells, CCR7$^+$CD45RA$^+$ Naïve CD4$^+$ T cells (naïve T), CCR7$^+$CD45RA$^-$ CD4 central memory T cells (CM T), CCR7$^-$CD45RA$^-$ CD4$^+$ effector memory T cells. **C|** CD4$^+$ T cells were also gated on CD127 and CD25 expression to identify CD127$^-$CD25$^+$ iTregs, further gated for CD45RA and HLADR expression to identify CD45RA$^-$HLADR$^+$ iTregs. **D|** CD8$^+$ T cells were then defined as CD45RA$^+$HLADR$^-$ CD8$^+$ TemRA T cells, CCR7$^+$CD45RA$^+$ Naïve CD8 T cells (naïve T), CCR7$^+$CD45RA$^-$ CD8$^+$ central memory T cells (CM T), CCR7$^-$CD45RA$^-$ CD8$^+$ effector memory T cells (EM T). A population of CD8$^+$CD25$^+$CD127$^+$ Tregs was also identified from the CD8$^+$ T cell gate. **E|** The CD3$^-$ population from B| was gated further on CD20 and CD19 so that CD20$^-$CD19$^-$ cells could be

gated out and CD19^{+} B cells could then be identified. These were further divided into a CD38 and CD20 gate to identify CD38^{+}CD20^{-} plasma cells and an IgD and CD27 gate was applied to identify IgD^{-}CD27^{+} Memory B cells, IgD^{+}CD27^{+} non-switched memory B cells/marginal zone-like B cells and IgD^{-} naïve B cells.

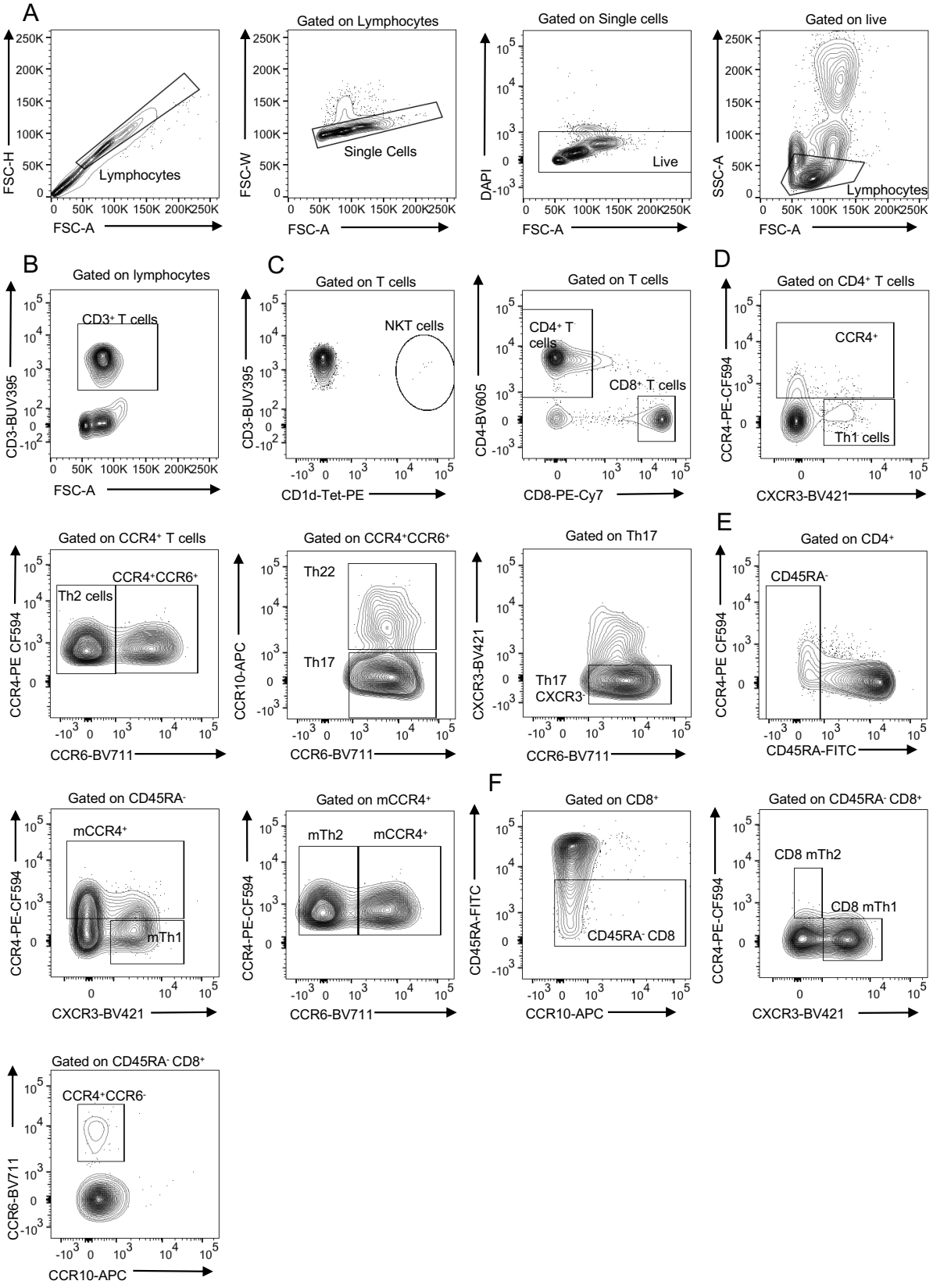

Figure S3.5| WCH-227 extended T cell panel gating strategy shows no obvious defects. **A|** For all extended T cell panel analyses, cells were gated by singlet discrimination, live ($DAPI^-$) and for leukocytes ($SSC\text{-}A^{lo}$). **B|** NKT cells were identified using a tetramer specific for CD1d. **C|** $CD3^+$ T cells were gated on $CD4^+$ and $CD8^+$ expression. **D|** $CD4^+$ T cells were then defined as $CCR4^+$ $CCR3^+$ Th1 cells and $CCR4^+$ $CD4^+$ T cells. This $CCR4^+$ gate was used to define $CCR4^+CCR6^-$ Th2 cells and $CCR4^+CCR6^+$ cells. The $CCR4^+CCR6^+$ cells were further gated to identify $CCR10^+CCR6^+$ Th22 cells and $CCR10^-CCR6^+$ Th17 cells. Th17 cells could be further distinguished by identifying the $CXCR3^-$ population of Th17 cells. **E|** $CD45^-$ T cells were identified using the $CD4^+$ T cell gate. This $CD45^-$ T cell gate was used to identify $CCR4^-$ $CXCR3^+$ Th1 memory cells (mTh1) and a $CCR4^+$ memory population that was further gated to identify $CCR4^+CCR6^-$ Th2 memory cells (mTh2). **F|** Finally the $CD8^+$ T cell gate was further gated on the $CD45^-$ population to identify $CD45RA^-$ $CD8^+$ cells. This population was further gated to identify $CCR4^+CCR10^-$ $CD8^+$ mTh2 cells and $CCR10^+CCR4^-$ $CD8^+$ mTh1 cells. Finally, the $CD45RA^-$ $CD8^+$ population was also gated on to identify a $CCR6^+CCR10^-$ population.

Table S3.1 Differences in gene expression between infants WCH-028 and WCH-227.

Immune Blood Transcriptional Module Activity Score	**Week 6**		**Week 7**	
Scaled to between -1 and 1. Calculated on each timepoint separately.	**WCH028**	**WCH227**	**WCH028**	**WCH227**
type.I.interferon.response M127.	-0.77	-0.34	0.92	-0.15
innate.antiviral.response M150.	-0.62	-0.12	0.85	0.21
RIG.1.like.receptor.signaling M68.	-0.73	0.08	0.84	-0.12
enriched.in.B.cells VI M69.	0.60	0.09	0.80	0.34
viral.sensing immunity IRF2.targets.network II M111.1.	-0.66	0.12	0.80	-0.19
antigen.processing.and.presentation M200.	0.58	0.66	0.79	0.68
enriched.in.B.cells I M47.0.	0.54	0.18	0.77	0.47
enriched.in.B.cells IV M47.3.	0.63	0.20	0.73	0.41
antiviral.IFN.signature M75.	-0.43	0.13	0.73	0.23
enriched.in.B.cells II M47.1.	0.40	0.09	0.72	0.47
activated.dendritic.cells M67.	-0.47	-0.26	0.71	0.17
enriched.in.naive.and.memory.B.cells M83.	0.46	0.35	0.70	0.39
B.cell.development.activation M58.	-0.23	0.18	0.69	0.14
enriched.in.B.cells III M47.2.	0.47	0.12	0.67	0.37
enriched.in.antigen.presentation III M95.1.	0.23	0.60	0.66	0.46
viral.sensing immunity IRF2.targets.network I M111.0.	-0.51	0.40	0.64	0.15
B.cell.surface.signature S2.	0.46	0.11	0.61	0.26
enriched.in.B.cells V M47.4.	0.46	-0.34	0.61	-0.24
antigen.presentation lipids.and.proteins M28.	0.14	0.56	0.60	0.43
Naive.B.cell.surface.signature S8.	0.44	0.25	0.59	0.32
enriched.in.activated.dendritic.cells II M165.	-0.45	0.31	0.56	0.31
enriched.in.activated.dendritic.cells I M119.	0.05	0.47	0.56	0.54
BCR.signaling M54.	-0.38	0.58	0.53	0.64
enriched.in.activated.dendritic.cells.monocytes M64.	-0.58	0.79	0.50	0.65
plasma.cells B.cells immunoglobulins M156.0.	0.22	0.15	0.48	0.37

innate.activation.by.cytosolic.DNA.sensing M13.	-0.35	0.20	0.48	0.20
inflammasome.receptors.and.signaling M53.	-0.28	0.39	0.47	0.31
chemokines.and.inflammatory.molecules.in.myeloid.cells M86.0.	-0.25	0.12	0.45	0.08
enriched.in.antigen.presentation I M71.	0.23	0.38	0.44	0.53
proinflammatory.dendritic.cell myeloid.cell.response M86.1.	0.02	0.07	0.41	0.16
immuregulation monocytes T.and.B.cells M57.	0.32	0.11	0.40	0.02
cell.activation IL15 IL23 TNF M24.	-0.08	0.31	0.38	0.14
regulation.of.antigen.presentation.and.immune.response M5.0.	0.04	0.32	0.36	0.28
enriched.in.antigen.presentation II M95.0.	0.14	0.58	0.33	0.55
Activated LPS dendritic.cell.surface.signature S11.	-0.50	0.45	0.30	0.34
T.cell.activation III M7.4.	0.33	-0.76	0.29	-0.68
enriched.in.B.cell.differentiation M123.	-0.25	0.12	0.29	0.38
MHC.TLR7.TLR8.cluster M146.	-0.22	0.45	0.28	0.43
enriched.in.monocytes III M73.	-0.27	0.67	0.27	0.62
T.cell.surface activation M36.	0.18	0.31	0.27	0.10
CD1.and.other.DC.receptors M50.	-0.09	0.57	0.23	0.55
chemokines.and.receptors M38.	0.10	0.35	0.21	0.58
myeloid.cell.enriched.receptors.and.transporters M4.3.	-0.34	0.67	0.20	0.67
enriched.in.monocytes surface M118.1.	-0.31	0.66	0.19	0.56
enriched.in.monocytes IV M118.0.	-0.36	0.61	0.18	0.54
B.cell.development M9.	-0.34	0.74	0.18	0.54
complement.activation I M112.0.	-0.05	0.67	0.17	0.52
T B.cell.development activation M62.0.	0.03	-0.25	0.16	0.15
CCR1 7.and.cell.signaling M59.	-0.57	0.59	0.14	0.48
enriched.in.monocytes I M4.15.	-0.50	0.71	0.13	0.68
myeloid.cell.cytokines metallopeptidases.and.laminins M78.	-0.42	0.21	0.12	-0.42
enriched.in.myeloid.cells.and.monocytes M81.	-0.56	0.34	0.12	0.24
lymphocyte.generic.cluster M60.	0.05	-0.17	0.11	0.23
enriched.in.monocytes II M11.0.	-0.43	0.64	0.07	0.56
TLR8.BAFF.network M25.	-0.33	0.59	0.06	0.32
recruitment.of.neutrophils M132.	-0.71	0.72	0.06	0.55
T.cell.activation IV M52.	-0.23	0.26	0.04	0.29
CD4.T.cell.surface.signature.Th1.stimulated S6.	-0.24	-0.59	0.03	-0.16
double.positive.thymocytes M126.	-0.46	-0.11	0.02	-0.34
myeloid dendritic.cell.activation.via.NFkB II M43.1.	-0.56	0.50	0.00	0.27
complement.and.other.receptors.in.DCs M40.	0.32	0.33	-0.01	0.13
chemokine.cluster II M27.1.	0.09	-0.09	-0.02	-0.09
plasma.cells immunoglobulins M156.1.	-0.10	0.37	-0.03	0.53
DC.surface.signature S5.	-0.17	0.30	-0.03	0.34
Monocyte.surface.signature S4.	-0.41	0.65	-0.04	0.56
enriched.in.T.cells II M223.	0.15	-0.59	-0.05	-0.51
cytokines recepters.cluster M115.	-0.16	-0.32	-0.07	-0.51

TLR.and.inflammatory.signaling M16.	-0.58	0.59	-0.08	0.44
enriched.in.NK.cells III M157.	0.35	-0.47	-0.09	-0.26
T.cell.differentiation M14.	-0.24	-0.68	-0.10	-0.60
Resting.dendritic.cell.surface.signature S10.	0.01	0.44	-0.11	0.49
enriched.in.neutrophils II M163.	-0.53	0.63	-0.11	0.40
enriched.in.NK.cells KIR.cluster M61.1.	0.70	0.05	-0.11	0.30
immune.activation generic.cluster M37.0.	-0.11	0.34	-0.11	0.29
T.cell.activation I M7.1.	0.04	-0.48	-0.12	-0.46
Plasma.cell.surface.signature S3.	-0.40	0.53	-0.14	0.24
enriched.in.dendritic.cells M168.	-0.06	0.63	-0.16	0.57
RA WNT CSF.receptors.network monocyte M23.	-0.40	0.81	-0.17	0.71
CD28.costimulation M12.	-0.23	-0.37	-0.18	-0.45
inflammatory.response M33.	-0.35	0.71	-0.19	0.57
T.cell.differentiation.via.ITK.and.PKC M18.	-0.12	-0.64	-0.19	-0.54
enriched.in.NK.cells receptor.activation M61.2.	0.46	-0.24	-0.19	0.01
enriched.in.neutrophils I M37.1.	-0.60	0.63	-0.19	0.38
IL2 IL7 TCR.network M65.	-0.57	-0.27	-0.20	-0.42
chemokine.cluster I M27.0.	-0.18	-0.18	-0.21	-0.34
signaling.in.T.cells I M35.0.	0.02	0.43	-0.24	0.45
enriched.in.NK.cells II M61.0.	0.62	-0.16	-0.24	0.04
Memory.B.cell.surface.signature S9.	-0.22	-0.29	-0.25	-0.34
NK.cell.surface.signature S1.	0.59	0.19	-0.29	0.26
myeloid dendritic.cell.activation.via.NFkB I M43.0.	-0.36	0.49	-0.33	0.24
enriched.in.T.cells I M7.0.	0.12	-0.52	-0.35	-0.47
CORO1A.DEF6.network I M32.2.	-0.64	0.66	-0.36	0.64
T.cell.activation II M7.3.	0.06	-0.47	-0.37	-0.38
T.cell.activation.and.signaling M5.1.	-0.17	-0.39	-0.37	-0.50
T.cell.signaling.and.costimulation M44.	-0.35	0.20	-0.39	0.09
proinflammatory.cytokines.and.chemokines M29.	-0.16	0.45	-0.39	0.47
T.cell.surface.signature S0.	-0.41	-0.52	-0.42	-0.58
T.cell.differentiation Th2 M19.	-0.37	-0.60	-0.43	-0.71
enriched.in.NK.cells I M7.2.	0.54	-0.35	-0.47	-0.08
CORO1A.DEF6.network II M32.4.	-0.61	0.54	-0.47	0.58
signaling.in.T.cells II M35.1.	0.05	0.33	-0.52	0.31
CD4.T.cell.surface.signature.Th2.stimulated S7.	-0.45	-0.65	-0.60	-0.68

Table S3.2 Antibody response data for infants WCH-028 and WCH-227

Timepoint	6 weeks		7 months		15 months	
Subject	WCH028	WCH227	WCH028	WCH227	WCH028	WCH227
Timepoint	6_wks	6_wks	7_M	7_M	15_M	15_M
PT	32845.14	852.69	42438.91	42859.01	2518.82	3235.3
PRN	141996.17	49002.07	17975.89	18082.56	1666.72	1117.57
FHA	71233.47	76339.51	334681.24	40064.79	23217.38	12077.82
FIM	67968.53	99532.74	4960.81	3381.02	0.355	0.355
TT	8371.05	3059.59	1120.46	661.77	343.96	1026.07
DT	1380.35	531.15	675.64	449.15	93.52	34.29
PCV13_1	457.16	20.15	1657.47	4792.67	450.8	654.26
PCV13_3	56.69	12.82	826.42	526.08	168.36	95.17
PCV13_5	75.49	51.15	8539.65	6373.83	1643.14	1399.96
PCV13_6B	83.87	19.01	3269	2942.33	520.66	1328.62
PCV13_7F	50.49	14.11	4889	3189.56	1615.75	721.24
PCV13_9V	34.92	16.99	3449.77	3693.82	808.76	639.12
NonVax_11A	360.72	62.78	48.59	61.11	28.45	142.42
PCV13_14	222.6	68.93	4186.54	5400.03	1093.23	1061.59
PCV13_18C	40.86	169.53	3577.09	4965.67	432.36	717.9
PCV13_19A	130.31	28.5	743	1821.84	71.29	297.07
PCV13_23F	33.75	703.75	1242.08	653.22	278.9	388.75
PCV13_4	113.9	8.64	3581.4	4836.57	417.38	812.45
PCV13_6A	196.96	35.79	8501.55	6580.7	1026.62	1429.37
PCV13_19F	337.1	310.91	4418.91	7315.99	723.05	1917.65
RV	7.5	7.5	467.0397	301.4928	38.359	100.7728
HiB	178.07	57.26	1475.53	903.56	175.78	624.72
HBs	323.79	831.96	2526.8	3872.21	313.15	208.9

Appendix 4: Supplementary Material from Chapter 5

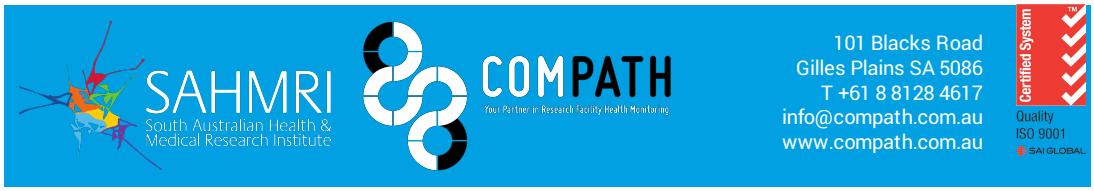

FINAL ANIMAL HEALTH MONITORING REPORT

Requested By	SAHMRI- Germ Free Mariah Turelli 101 Blacks Road Gilles Plains, SA, 5086	**Submission No** **Order No** **Date Received**	2821 Miriam Lynn DLBU 22-01-2020

GROUP 15825 - GERM FREE SWABS — SPECIES: MOUSE

SAMPLE REFERENCE

1	**Shipper 1**	3	**Shipper 3**
2	**Shipper 2**	4	**Shipper 4**

RESULTS SUMMARY

> All samples were Germ Free.

DISEASE INVESTIGATION

B-CULT results for sample: Shipper 2

> No growth was observed on both aerobic and anaerobic Blood Agar culture after 48 hours at 35 Degrees Celsius.
>
> No growth was observed after 6 days on Nutrient Agar at room temperature.

B-CULT results for sample: Shipper 4

> No growth was observed on both aerobic and anaerobic Blood Agar culture after 48 hours at 35 Degrees Celsius.
>
> No growth was observed after 6 days on Nutrient Agar at room temperature.

B-CULT results for sample: Shipper 1

> No growth was observed on both aerobic and anaerobic Blood Agar culture after 48 hours at 35 Degrees Celsius.

Figure S4.1| Example Compath report illustrating the GF status of the experimental mice. Reports like this were generated regularly by Compath.

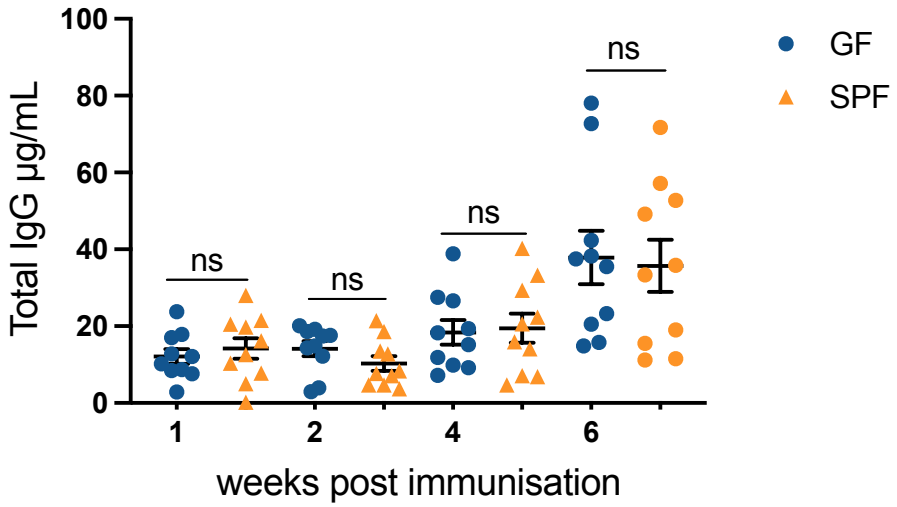

Figure S4.2| No differences in IgG_{total} between GF and SPF mice after immunization. The amount of unspecific IgG_{total} was assessed by ELISA in the serum of GF and SPF mice. ns = not significant.

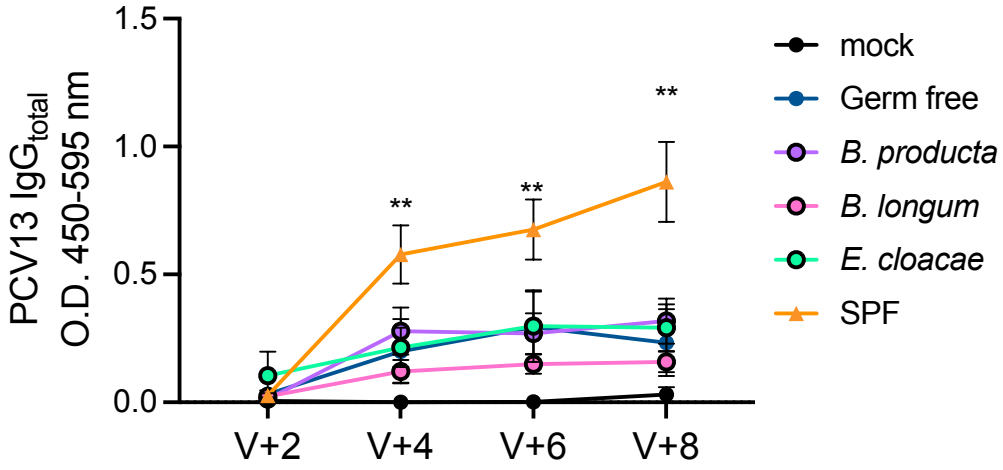

Figure S4.3| GF mice colonised with Blautia producta, Bifidobacterium longum or Enterobacter cloacae did not have improved antibody responses to PCV13. PCV13 specific IgGtotal responses in GF mice colonised with *Blautia producta, Bifidobacterium longum* or *Enterobacter cloacae* compared with SPF and GF controls.

SAHMRI South Australian Health & Medical Research Institute
COMPATH Your Partner in Research Facility Health Monitoring
101 Blacks Road
Gilles Plains SA 5086
T +61 8 8128 4617
info@compath.com.au
www.compath.com.au

FINAL ANIMAL HEALTH MONITORING REPORT

Requested By	SAHMRI- Germ Free Mariah De Virgilio 101 Blacks Road Gilles Plains, SA, 5086	**Submission No** **Order No** **Date Received**	4475 SBexp197 29-08-2022

GROUP 18856 - GERM FREE SWABS — SPECIES: MOUSE

SAMPLE REFERENCE

1	**Cage 1**	3	**Cage 3**
2	**Cage 2**	4	**Cage 4**

RESULTS SUMMARY

> All samples were Germ Free.

DISEASE INVESTIGATION

B-CULT results for sample: Cage 1

> No growth was observed on both aerobic and anaerobic Blood Agar culture after 48 hours at 35 Degrees Celsius.
>
> No growth was observed after 6 days on Nutrient Agar at room temperature.

B-CULT results for sample: Cage 2

> No growth was observed on both aerobic and anaerobic Blood Agar culture after 48 hours at 35 Degrees Celsius.
>
> No growth was observed after 6 days on Nutrient Agar at room temperature.

B-CULT results for sample: Cage 3

> No growth was observed on both aerobic and anaerobic Blood Agar culture after 48 hours at 35 Degrees Celsius.

Figure S4.4| Compath reports for GF vs colonisation experiments.

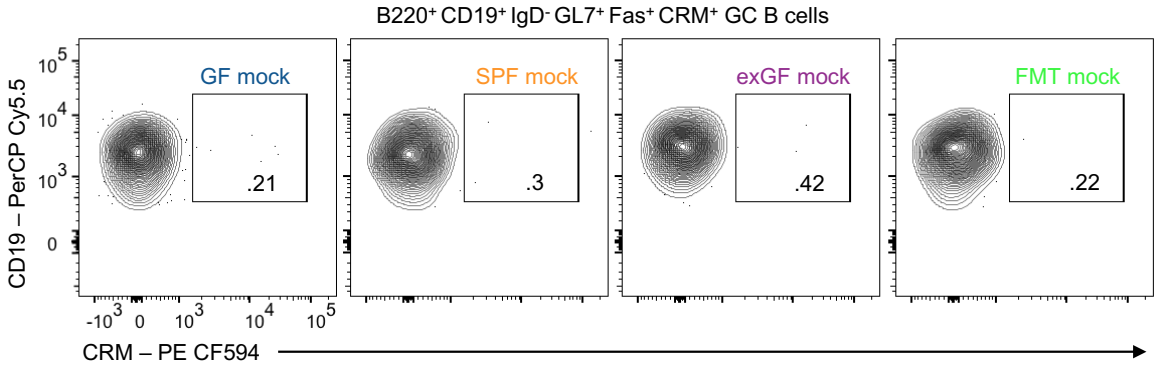

Figure S4.5| Absence of CRM_{197}^{+} GC B cells in mock vaccinated mice in the spleen illustrates specificity of probe. A| Representative flow cytometry of CRM_{197}^{+} GC B cells ($CRM_{197}^{+}GL7^{+}Fas^{+}$) in the spleen of mock GF, SPF, exGF and FMT mice. Cells were pre-gated on live $CD19^{+}B220^{+}IgD^{-}GL7^{+}Fas^{+}$ populations.

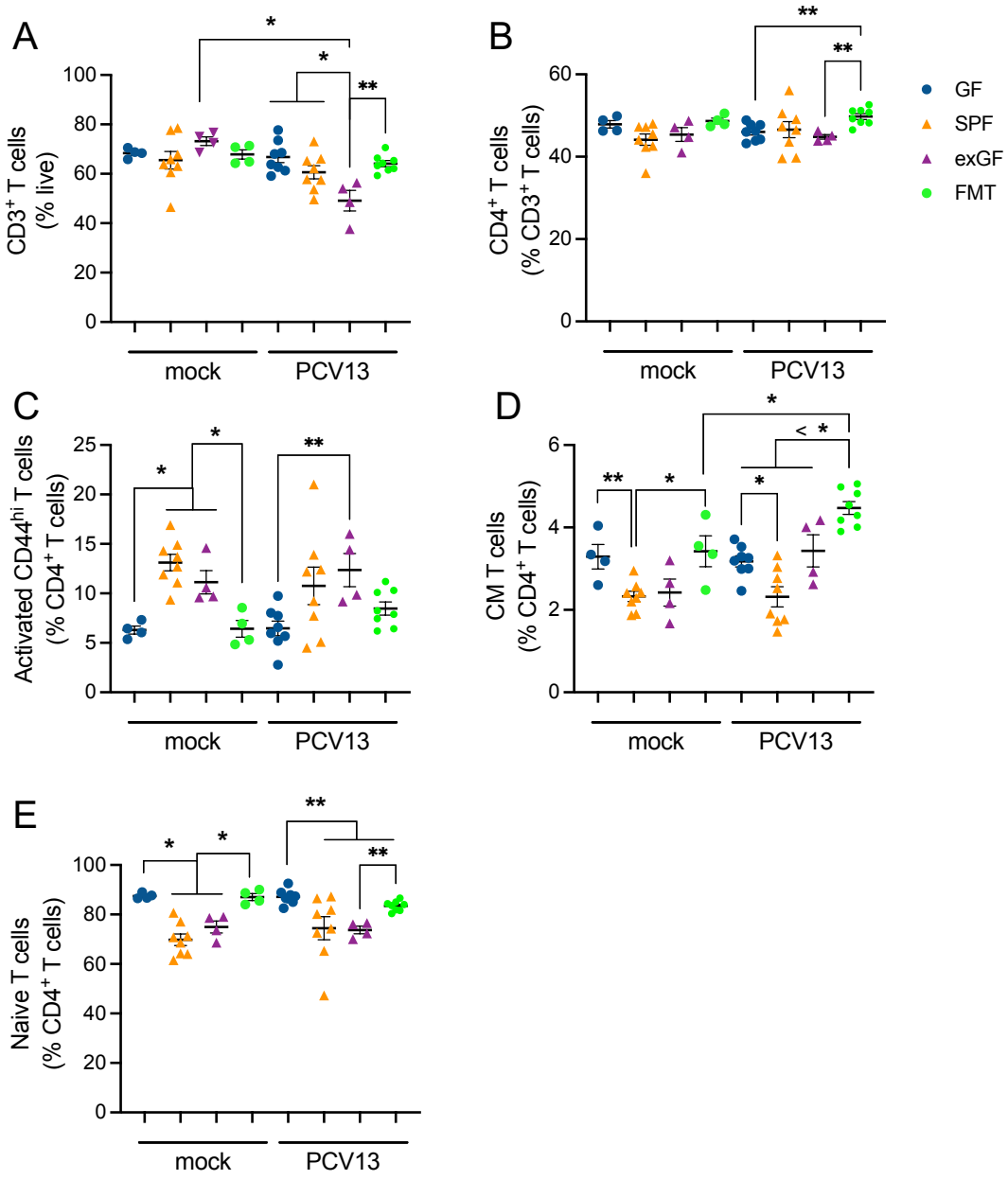

Figure S4.6| The frequency of T cell subsets the mediastinal lymph nodes . **A|** $CD3^+$ T cells ($CD3^+CD19^-$) as a frequency of CD3+ T cells as a frequency of live cells. **B|** $CD4^+$ T cells ($CD3^+CD19^-CD4^+$) as a frequency of CD3+ T cells. **C|** Activated $CD4^+$ T cells ($CD3^+CD19^-CD4^+CD44^{hi}CD62l^-$) as a frequency of CD4+ T cells. **D|** Central memory $CD4^+$ T cells ($CD3^+CD19^-CD4^+CD44^{hi}CD62l^+$) as a frequency of CD4+ T cells. **E|** naïve T cells ($CD3^+CD19^-CD4^+CD44^-CD62l^+$) as a frequency of CD4+ T cells.. Data are represented as mean ± SEM. One-way ANOVA was used to assess statistical significance.

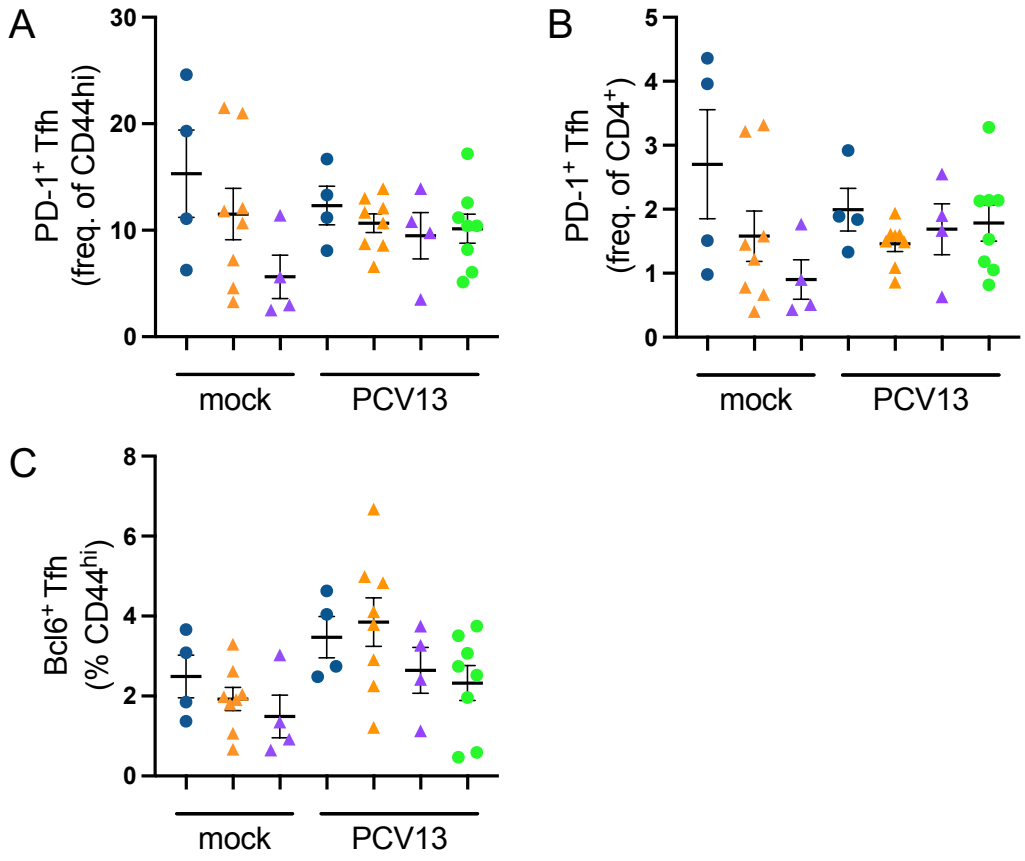

Figure S4.7| There were no significant differences in the frequency of Tfh cells in the spleen pf GF, SPF, exGF and FMT mice. Frequency of PD-1^{+} Tfh cells in the spleen as a proportion of **A|** CD44^{hi} T cells and **B|** CD4^{+} T cells. **C|** Frequency of Bcl6^{+} Tfh cells in the spleen as a proportion of CD44^{hi} T cells. Data are represented as mean ± SEM. One-way ANOVA was used to assess statistical significance.

Appendix 5: Supplementary Material from Chapter 6

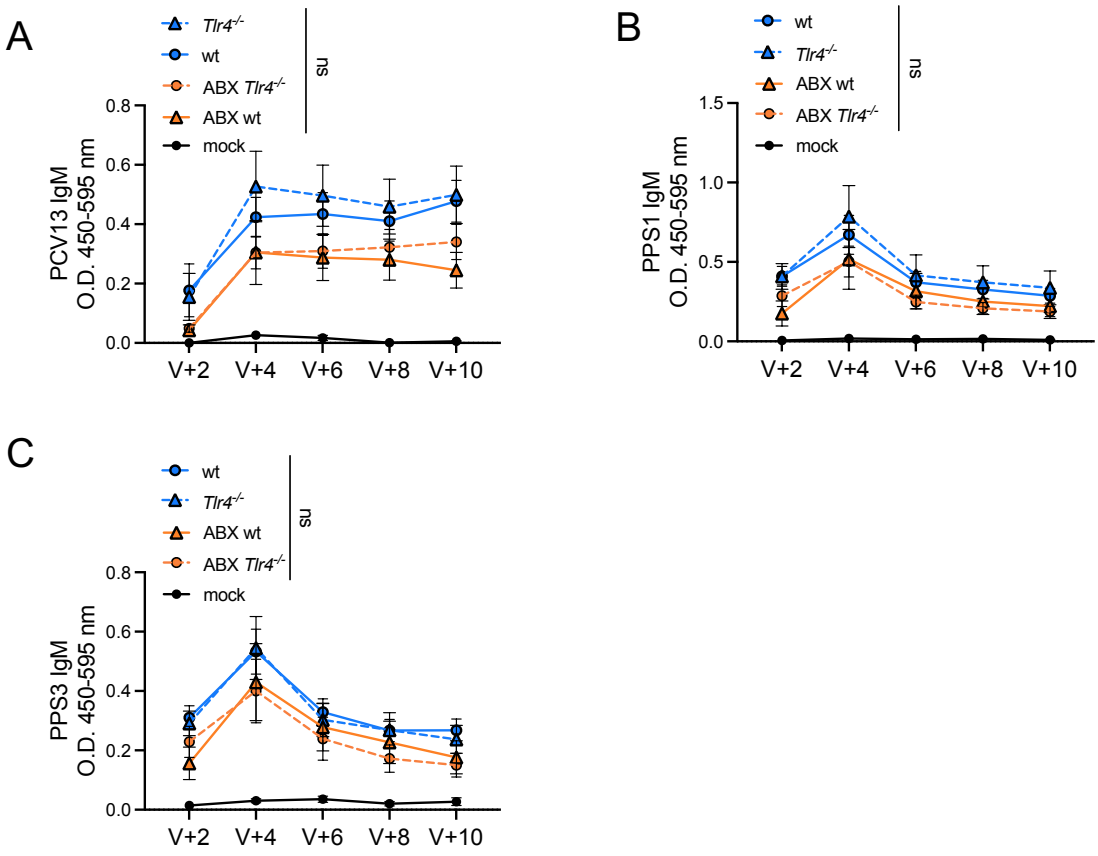

Figure S5.1| Antibody responses to the PCV13 vaccine were not significantly different between wildtype (+/+) and Tlr4$^{-/-}$ (-/-) mice after boost. IgM responses were measured against **A|** PCV13, **B|** PPS1 and **B|** PPS3. Raw O.D. values are shown. Data are represented as mean ± SEM. One-way ANOVA was used to assess statistical significance. ns = not significant.